2013

SYNTHESIS AND STABILITY STUDIES OF PRODRUGS AND CODRUGS OF NALTREXONE AND 6-β-NALTREXOL

Joshua A. Eldridge
University of Kentucky, j.adam.eldridge@gmail.com

STUDENT AGREEMENT:

I represent that my thesis or dissertation and abstract are my original work. Proper attribution has been given to all outside sources. I understand that I am solely responsible for obtaining any needed copyright permissions. I have obtained and attached hereto needed written permission statements(s) from the owner(s) of each third-party copyrighted matter to be included in my work, allowing electronic distribution (if such use is not permitted by the fair use doctrine).

I hereby grant to The University of Kentucky and its agents the non-exclusive license to archive and make accessible my work in whole or in part in all forms of media, now or hereafter known. I agree that the document mentioned above may be made available immediately for worldwide access unless a preapproved embargo applies.

I retain all other ownership rights to the copyright of my work. I also retain the right to use in future works (such as articles or books) all or part of my work. I understand that I am free to register the copyright to my work.

REVIEW, APPROVAL AND ACCEPTANCE

The document mentioned above has been reviewed and accepted by the student's advisor, on behalf of the advisory committee, and by the Director of Graduate Studies (DGS), on behalf of the program; we verify that this is the final, approved version of the student's dissertation including all changes required by the advisory committee. The undersigned agree to abide by the statements above.

Joshua A. Eldridge, Student

Dr. Peter A. Crooks, Major Professor

Dr. Jim Pauly, Director of Graduate Studies

SYNTHESIS AND STABILITY STUDIES OF PRODRUGS AND CODRUGS OF NALTREXONE AND 6-β-NALTREXOL

DISSERTATION

A dissertation submitted in partial fulfillment of the
requirements for the degree of Doctor of Philosophy in the
College of Pharmacy
at the University of Kentucky

By

Joshua A. Eldridge

Lexington, KY

Director: Dr. Peter A. Crooks, Professor and Chairman of Pharmaceutical Sciences

University of Arkansas for Medical Sciences

Little Rock, Arkansas

2013

ABSTRACT OF DISSERTATION

SYNTHESIS AND STABILITY STUDIES OF PRODRUGS AND CODRUGS OF NALTREXONE AND 6-β-NALTREXOL

The present study was divided between two different drug delivery goals, each involving naltrexone (NTX) or its active metabolite, 6-β-naltrexol (NTXOL). First, amino acid esters of NTX and NTXOL were prepared in order to test their candidacy for microneedle-enhanced transdermal delivery. Second, a 3-*O*-(-)-cytisine-naltrexone (CYT-NTX) codrug was prepared for screening as a potential oral delivery form of NTX and (-)-cytisine (CYT). The amino acid prodrugs were intended for the treatment of alcohol abuse, while the codrug was designed as a single agent for the treatment of alcoholism and tobacco-dependency co-morbidities. One hypothesis of this work was that prodrugs of NTX or NTXOL can be designed that possess superior skin transport properties through microneedle-treated skin compared to parent NTX or NTXOL. Nine amino acid ester prodrugs were prepared, and only three 6-*O* amino acid ester prodrugs of NTXOL were stable enough at skin pH (pH 5.0) to move forward to studies in 50% human plasma. 6-O-*β*-Ala-NTXOL, the lead compound, exhibited the most rapid bioconversion to NTXOL in human plasma ($t_{1/2}$ = 2.2 ± 0.1 h); however, this *in vitro* stability value indicates that the prodrug may require hepatic enzyme-mediated hydrolysis for sufficiently rapid bioconversion to NTXOL *in vivo*. A second hypothesis of this work was that a CYT-NTX codrug could be designed with appropriate stability characteristics for oral delivery. CYT-NTX was found to be stable over the time course of 24 h in buffer systems of pH 1.5, 5.0, 7.4 and 9.0, and in 80% rat plasma, 80% human plasma, simulated gastric fluid and simulated intestinal fluid. Six (3 rats/group) Sprague-Dawley male rats were dosed i.v. with 1 mg/kg CYT-NTX codrug, or 10 mg/kg, p.o. Oral administration of a 10 mg/kg dose of CYT-NTX codrug resulted in rapid absorption and distribution (5 min) of CYT-NTX codrug, and NTX was released from codrug with a peak plasma concentration of 6.8 ± 0.9 nmol/L reached within 65 minutes. Plasma CYT was not detected; however, NTX delivery was achieved with a fraction absorbed value of 13%. Thus, CYT-NTX may hold promise as a potential oral codrug for further optimization and development.

Keywords: naltrexone, amino acid prodrugs, codrugs, (-)-cytisine, microneedles

Joshua A. Eldridge
Signature of Student

4-29-13
Date

SYNTHESIS AND STABILITY STUDIES OF PRODRUGS AND CODRUGS OF NALTREXONE AND 6-β-NALTREXOL

By

Joshua A. Eldridge

Peter A. Crooks
Director of Dissertation

Jim Pauly
Director of Graduate Studies

4-29-13
Date

DEDICATION

This work is dedicated to my wife, parents, family and friends. Thank you for your patience and support.

ACKNOWLEDGEMENTS

The following dissertation arose through a combination of collaboration and personal effort. Without the expertise and guidance of Drs. Peter Crooks and Audra Stinchcomb, and the resources they worked hard to secure over many years of research, this dissertation would not have been possible. Synthesis advice was also provided by Dr. Greg Elliott, formerly of the University of Kentucky, and I am likewise thankful to him for the use of his resources (LC-MS, Biotage microwave reaction equipment, and a solvent drying system). Drs. Andrew J. Morris, Philip Breen, Zaineb Albayati and Manjula Sunkara were indispensible in the development of Chapter 7 of this dissertation. Special thanks are given within the introductory comments of Chapter 7 to emphasize the division of labor that culminated in the final write-up.

I am further thankful to the members of my committee for helping me stay on the right track throughout the course of this doctoral work. These members include Drs. Peter Crooks, Audra Stinchcomb, Abeer Al-Ghananeem, Susan Barron and Jim Pauly. Likewise, gratitude is warranted for the members of Peter Crooks' and Audra Stinchcomb's research groups (both past and present) who were involved directly or indirectly in the procurement of data and knowledge that lead to the end product presented within these pages. Especially of note are the following: Mikolaj Milewski, my collaborator and dear friend, who participated directly in this work and was always there to help me figure out problems with analytical assays; Dr. Guangrong Zheng, who was a constant source of great information regarding synthetic problems; John Culver, who was a true comrade

when it came time to fix laboratory equipment that did not wish to cooperate (especially Old Betsy, the 300 MHz NMR); Dana Hammell, who ordered so many reagents and vital pieces of lab equipment for me that she must have a list the size of Texas; Ujjwal Chakraborty and Harpreet Dhooper, who combined forces with me on HPLC method development work that proved to be anything but trivial; and Ashish, Sonny, Razi and many other post-docs who helped to keep me from making silly mistakes along the way.

Final thanks are to be paid to my wife, my family and my friends, who were all instrumental in providing me with the support and understanding that completion of this scientific endeavor required. Thanks to all of you for listening to me talk jargon or whine; whichever was required following lab work on a particular day…

TABLE OF CONTENTS

LIST OF TABLES

LIST OF SCHEMES

LIST OF FIGURES

Chapter 1

Goals of the study and literature review

1.1 Hypotheses

This study involved two central hypotheses. One hypothesis of this work was that prodrugs of NTX or NTXOL can be designed that possess superior skin transport properties through microneedle-treated skin compared to parent NTX or NTXOL. A second hypothesis of this work was that a CYT-NTX codrug could be designed with appropriate stability characteristics for oral delivery.

1.2 Overall Aims

There exists an ongoing need for new medications that can provide efficacy in the treatment of alcohol abuse and nicotine addiction with minimal side effects. This project has been designed to address two specific populations of drug-addicted individuals. The first target population is people who abuse alcohol, but who do not smoke cigarettes as well. The second target population is the group of individuals who smoke cigarettes and abuse alcohol simultaneously. For those who abuse alcohol but do not smoke, poorly bioavailable naltrexone (NTX) is often a medication that is prescribed. To circumvent the poor bioavailability and gastrointestinal side effects of NTX, it has been envisioned that highly water soluble prodrugs of NTX or its active metabolite 6-β-naltrexol (NTXOL) could possibly serve as dosage forms for microneedle-enhanced transdermal delivery (MNTD). Otherwise, for the second population of drug-dependent individuals who abuse alcohol and smoke cigarettes, a dual therapeutic strategy is indicated

since consumption of either drug serves as a cue for abuse of the other (comorbidity). In the case of patients belonging to population two, it has been envisioned that an oral codrug of NTX conjugated to (-)-cytisine, a smoking cessation agent, could be a plausible therapeutic agent to approach the treatment of both addictions with a single drug molecule (i.e. a codrug). Within the following dissertation, the design, synthesis, and stability characterization of a number of amino acid ester prodrugs of NTX and NTXOL is described. Also, the design, synthesis, stability, and pharmacokinetic evaluation of a codrug of NTX conjugated with (-)-cytisine is described.

1.3 Methodology to be utilized in this study

- To develop the chemistry to afford amino acid ester prodrugs of NTX and NTXOL.
- To investigate amino acid ester prodrug chemical stability at pH 5.0 and pH 7.4 to assess MNTD candidacy.
- To investigate amino acid ester prodrug enzymatic stability in 50% human plasma.
- To prepare a codrug of (-)-cytisine and NTX (CYT-NTX) in which (-)-cytisine and NTX are covalently linked by a secondary carbamate linker.
- To evaluate oral delivery candidacy of the CYT-NTX codrug by investigating its simple chemical stability over the pH range 1.2 – 9.0 and its enzymatic stability in simulated gastric and intestinal fluids using an HPLC-UV assay.

- To evaluate the enzymatic stability of CYT-NTX in 80% rat and 80% human plasma using an HPLC-UV assay.
- To investigate the hydrolytic profile and pharmacokinetics of the CYT-NTX codrug in the live Sprague-Dawley rat using LC-MS/MS.

1.4 Alcohol and tobacco abuse prevalence and treatment limitations

Abuse of alcohol and/or tobacco are worldwide problems with enormous societal and medical impact. In the United States, alcohol abuse is the third leading cause of preventable death, while tobacco use is the first. The scope of the American alcohol and tobacco abuse problem is perhaps best understood by inspection of the annual statistics published by the Substance Abuse and Mental Health Services Administration (SAMHSA 2011). The following data are quoted directly from the reference.

Alcohol Use

"In 2011, 133.4 million (51.8%) American citizens aged 12 years or older reported themselves to be drinkers of alcohol, which is similar to the number reported in 2010. A large percentage, 22.6% (58.3 million), of these individuals reported binge pattern drinking which is characterized by having five or more drinks on the same day on at least one day in the 30 days prior to the survey. Heavy drinking, as defined by at least five days of binge drinking in the 30 days prior to the study, was characteristic of 15.9 million people surveyed (6.2%). Among young adults aged 18 to 25 in 2011, the rate of binge drinking was 39.8

percent. The rate of heavy drinking was 12.1 percent, which was lower than the rate in 2010 (13.5 percent).”

Tobacco Use

“In 2011, an estimated 68.2 million Americans aged 12 or older were current (past month) users of a tobacco product. This represents 26.5 percent of the population in that age range. Also, 56.8 million persons (22.1 percent of the population) were current cigarette smokers; 12.9 million (5.0 percent) smoked cigars; 8.2 million (3.2 percent) used smokeless tobacco; and 2.1 million (0.8 percent) smoked tobacco in pipes.”

Alcohol Abuse Treatment

Currently, alcohol abuse is approached therapeutically with pharmaceuticals, psychotherapy and group counseling efforts. Medical programs often involve inpatient treatment during drug detoxification periods, with concomitant use of pharmaceutical regimens. Subsequently, outpatient group therapies are also often employed, with or without personal psychotherapy. Regardless of the effectiveness of such approaches for some individuals, often only limited success is realized. The limitations of these approaches could be related to the low number of available medicines indicated for alcohol addiction management. For instance, only four pharmaceutical options are currently FDA-indicated: NTX (ReVia®), NTX depot (Vivitrol®), acamprosate (Campral®), and disulfiram (Antabuse®). Likewise, each option has its own share of problems that often lead to poor patient compliance and/or poor effectiveness in the management of

alcohol addiction. Acamprosate has undesirable adverse-effects, including diarrhea and suicidality, and the therapy requires a large dosing regimen and pill burden (2 x 333 mg tablets 3 x daily) (Forest Pharmaceuticals, St. Louis, MO. 2004). Disulfiram is hepatotoxic, and requires patient compliance to take the drug, since nausea occurs if the patient drinks after drug administration (Bjoernsson, Nordlinder et al. 2006). Additionally, oral NTX delivery carries the burden of dose-dependent hepatotoxicity along with variable, poor bioavailability (5-40%) and gastrointestinal adverse-effects (Verebey 1981, Verebey and Mule 1986, Volpicelli, Rhines et al. 1997). The problems involved with oral administration of NTX have been addressed by the invention of Vivitrol®, a once-per month IM depot injection of NTX that does not exhibit the fluctuating plasma concentrations associated with daily oral dosing of NTX (Garbutt 2006, Swainston, Plosker et al. 2006). However, in emergency situations where pain management by opioid administration may be beneficial, Vivitrol® has the disadvantage that larger doses of agonist must be administered to a patient to overcome μ-receptor blockade. Another disadvantage of the depot form is the possibility of adverse reactions at the injection site (Covyeou, Atto et al. 2011). Clearly, oral and depot delivery forms of NTX cannot meet the needs of all alcoholic patients who could benefit from the use of the drug in their cessation and abstinence programs.

Tobacco abuse treatment

Tobacco abuse is facilitated by nicotine dependence. Indeed, some research has suggested that nicotine is akin to heroin or alcohol in its addiction potential,

but these claims have also been critiqued (Frenk and Dar 2011). Nonetheless, it is clear that the smoking process exposes the smoker to numerous toxic and carcinogenic chemicals that ultimately lead to chronic disorders such as COPD, emphysema and/or lung cancers (Rodgman, Smith et al. 2000, Starek and Podolak 2009). Smokeless tobacco has proven to be no better than smoked tobacco, because it also results in various cancers (Zhou, Michaud et al. , Roy, Chatterjee et al. 2011).

Since tobacco abuse is a pervasive health problem, numerous therapy regimens have emerged to aid nicotine addicts in their efforts to quit smoking or using smokeless tobacco products. For instance, psychotherapy is available for smokers who seek help to quit smoking. Nicotine replacement therapies are also available which include patches, lozenges, gums, nasal sprays and electronic cigarettes. Also, non-nicotine pharmaceuticals such as bupropion hydrochloride (Wellbutrin®, Zyban®) and varenicline tartrate (Chantix®) have shown promise in certain patient populations. However, all of these treatment options are met with high relapse rates and other unsavory limitations that render them sub-optimal as front line therapies for tobacco abuse (Dwoskin, Smith et al. 2009, Keating and Lyseng-Williamson 2010). In particular, none of these approaches address the co-abuse problem of simultaneous nicotinism and alcoholism. Therefore, within this body of work, we sought to explore a codrug design to approach the development of a dual therapeutic which could lead to management of tobacco abuse and alcoholism simultaneously.

Naltrexone

NTX (**Fig. 1.1**) is a long-acting synthetic competitive μ-/κ-, and to a lesser extent δ-opioid receptor antagonist used primarily in the management of alcohol and opioid dependence (Verebey 1981, Volpicelli, Rhines et al. 1997). Blockade of the aforementioned receptors prevents activation of the critical dopamine reward system and attenuates the desire for drug self-administration in opioid-dependent people. The mode of action of NTX in the treatment of alcohol dependence seems to involve blockade of endogenous opioid receptor binding that normally accompanies alcohol consumption (Jung and Namkoong 2006, Unterwald 2008). In this respect, alcoholic patients taking NTX are reported to have as much as a 50% reduction in the number of drinks they consume per day.

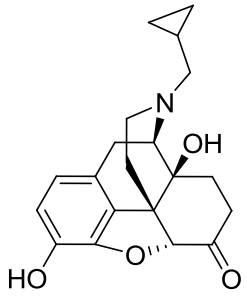

Figure 1.1 Structure of Naltrexone (NTX).

NTXOL

NTXOL (**Fig. 1.2**) is the major active metabolite of NTX that is present in higher concentration than NTX in blood samples following oral dosing in man,

and NTXOL could contribute significantly to the duration of the therapeutic effects of NTX (Verebey, Volavka et al. 1976, Volpicelli 1995).

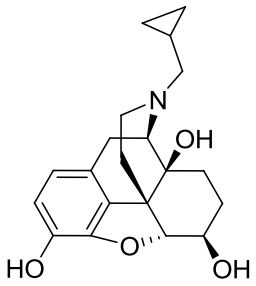

Figure 1.2 Structure of 6-β-Naltrexol (NTXOL).

1.5 Rationale for the transdermal delivery approach to dose NTX/NTXOL

Formulation of a drug into a transdermal delivery system is desirous when the effective dose of the drug is fairly low and the drug has side effects or extensive first pass metabolism or extraction via the oral route. As mentioned above, NTX exhibits variable interpatient bioavailabilty and extensive first pass side effects when dosed *per os*. Inasmuch, formulation of a transdermal NTX dosage form could potentially solve the problems associated with oral NTX therapy. Transdermal delivery of NTXOL could also be of potential clinical utility since NTX is extensively converted to NTXOL via first pass metabolism when the FDA-approved hydrochloride salt is given orally. Unfortunately, previous work in this area has demonstrated that neither NTX nor NTXOL can be delivered in therapeutically-relevant levels by traditional passive transdermal delivery (PTD) techniques (Paudel, Nalluri et al. 2005). Therefore, several NTX prodrugs with enhanced lipophilicity have been prepared and assayed for their potential as

PTD candidates (Stinchcomb, Swaan et al. 2002, Pillai, Hamad et al. 2004, Hammell, Stolarczyk et al. 2005, Vaddi, Hamad et al. 2005, Valiveti, Hammell et al. 2005). Straight-chain and branched-chain 3-*O*-NTX carboxylate and carbonate ester prodrugs were investigated in these studies. Although superior flux values were observed in the straight-chain 3-*O*-NTX ester series of prodrugs, plasma levels that would be adequate for therapeutic outcomes in man were not achieved.

Microneedle-enhanced transdermal delivery (MNTD) methods have been developed in recent years which have allowed expansion of the pool of molecules that can be delivered transdermally. Notably, the hydrochloride salt of NTX has been shown to be transdermally available in man in the lower levels of the therapeutic window when aqueous microchannels are first created to breech the barrier properties of the stratum corneum (SC) (Wermeling, Banks et al. 2008). Otherwise, a clear increase in the microneedle enhanced delivery of NTX or NTXOL as a function of increased water solubility due to ionic charge has been demonstrated (Banks, Pinninti et al. 2008). Nonetheless, to make NTX or NTXOL transdermally useful for alcoholic patients, further enhancements to these molecular skeletons is still necessary. Therefore, in keeping with the prodrug approach, it was envisioned in this body of work that amino acid ester prodrugs of NTX and NTXOL could be prepared that would impart additional charge at skin-relevant pH (~ pH 5.0). The goal of this part of the study was to prepare a prodrug with adequate solubility and stability at pH 5.0, which would also rapidly afford parent drug at pH 7.4 or in human plasma. A successful

MNTD prodrug could serve as a potential clinical addition to the currently limited pool of pharmaceuticals used to treat alcohol abuse, and its advantages would be as follows:

- Painless patient self-application
- Steady-state profiles of drug delivery (zero order)
- Avoidance of first pass effects
- Reduced gastrointestinal adverse-effects and hepatotoxicity
- Improved patient compliance
- Lower effective dose compared to oral formulations

The syntheses of amino acid ester prodrugs of NTX and NTXOL are summarized in **Chapters 2-4**, and their stability data are summarized in **Chapter 6**.

1.6 Rationale for oral delivery of a secondary carbamate codrug of NTX and (-)-cystisine

(-)-cytisine (CYT)

CYT (**Fig. 1.3**) is a natural product isolated from *Cytisus laborinum* which is marketed in Europe as a smoking cessation agent under the trade name Tabex (Etter 2006, Zatonski, Cedzynska et al. 2006). It is currently unavailable in the USA, and varenicline (Chantix®) is the synthetic analogue of CYT that has achieved FDA approval. Nonetheless, CYT has a long-standing record of efficacy in the treatment of nicotine addiction in Europe, and it could be far cheaper to produce and utilize than bupropion or varenicilne (Etter, Lukas et al. 2008). CYT is a selective partial agonist of human α4β2 nicotinic acetylcholine

receptors (Lukas 2007) and a full agonist of α7 receptors (LeSage, Shelley et al. 2009). In addition to its known efficacy in smoking cessation treatments (Hajek, McRobbie et al. 2013), CYT has also shown anti-depressant activity in male C57BL/6J mice (Mineur, Somenzi et al. 2007). In contrast, currently FDA-approved varenicline carries a black box warning for adverse effects that include depression and suicidality.

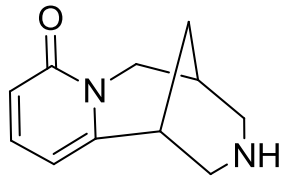

Figure 1.3 Structure of (-)-cytisine (CYT).

Codrug design is often undertaken to afford dual drug delivery from a single molecule. It is a type of prodrug strategy that has been widely investigated by many routes of administration (Crooks, Dhooper et al. 2011). The particular formulation and delivery method assigned to a given codrug generally depends on the target area for the two released agents and the stability profile of the codrug. It is known that the hydrolytic stability of carbamates over a large pH range is dependent upon the substitution of the carbamate, where secondary carbamates tend to show many orders of magnitude higher stability than primary carbamates (Hegarty and Frost 1972). One would expect that enzymatic systems could increase the rate of hydrolyses dramatically in the case of

carbamate esters; however, this need not be the case. The particular molecule in question must always be assayed individually.

Indeed, primary carbamates need not always degrade faster than secondary carbamates either. Recently, primary carbamate codrugs of opioids and ketamine or norketamine have been patented (Holtman, Crooks et al. 2009). Additionally, secondary carbamate codrugs of nornicotine and opioids have also been patented and prepared (Holtman, Crooks et al. 2009). However, these compounds proved to be stable over a pH 1.3 – 7.4 range, and they also did not degrade to parent drugs in simulated gastric fluid (SGF), in simulated intestinal fluid (SIF), in 80% rat plasma, or in rat brain homogenate (Chakraborty 2011). Previously, the synthesis of secondary carbamates of bupropion (BUP) and NTX or BUP and NTXOL were attempted, and it was found that *N*-acylated derivatives of the bupropion core moiety could not be isolated (Hamad, Kiptoo et al. 2006). Follow up efforts within the present body of work also failed to afford the desired secondary carbamate of bupropion and NTX (**Chapter 5**).

In order to continue pursuit of a potential co-therapeutic for alcohol and tobacco abuse, design efforts were switched toward alternative molecules that have been shown to be efficacious in the treatment of nicotine addiction, while maintaining NTX as the alcohol abuse agent. Since the secondary amine of bupropion is sterically hindered, we decided to pursue chemistry to afford a conjugate of (-)-cytisine (CYT) and NTX. The structure of CYT (**Fig. 1.3**) affords a sterically accessible secondary amine for acylation reactions, and synthesis of the CYT-NTX codrug proved to be facile with microwave chemistry (**Chapter 5**).

Overall, by switching attention to the study of CYT-NTX, three themes of the original BUP-NTX codrug work were maintained. First, the formulation stability advantages of a secondary carbamate were preserved in the CYT-NTX codrug structure. Second, The NTX moiety remained as the key FDA-approved alcohol abuse agent. Finally, the codrug thus designed should have potential as a co-therapeutic for alcohol and tobacco abuse since CYT is used commercially in Europe as a smoking cessation agent. One critical deviation of the CYT-NTX work was a change of course from the MNTD approach to oral delivery; a data-driven decision which was made during stability analyses.

During the course of the present study, it was found that CYT-NTX is stable over the pH 1.5 – 9.0 range. Stability studies in 80% human plasma, 80% rat plasma, SGF, and SIF also showed that the codrug was stable under a variety of physiologically-relevant conditions (**Chapter 6**). However, *in vivo* analysis of the codrug demonstrated that oral delivery in the live rat resulted in systemic hydrolysis of CYT-NTX to afford NTX more efficiently than intravenous delivery (**Chapter 7**), indicating that first-pass metabolism was a likely mechanism for increased systemic delivery of NTX. CYT was unfortunately not detected.

1.7 Prodrugs and Codrugs (What are they?)

Oftentimes in drug design and development, there are situations in which a given drug lacks optimal physiochemical properties or *in vivo* performance. For instance, the drug may have poor bioavailability if given as an oral delivery form. The latter situation can be subdivided into several undesirable physiochemical

features that ultimately cause the low systemic exposure. These include poor aqueous solubility, inadequate absorption or permeation, extensive first pass metabolism and extraction, and/or general instability in the variable pH environment of the gut or in the presence of the various gut enzymes. Otherwise the performance of a therapeutic agent may be limited by poor site activity or transport, or by general formulation difficulties. In many cases, these types of problems can be solved by converting the potential drug molecule into a delivery form called a prodrug. Various types of prodrugs have recently been widely reviewed (Yang, Aloysius et al. 2011, Imai 2012, Li, Dong et al. 2012, Wexselblatt and Gibson 2012, Zhang, Qu et al. 2012), and numerous books have been published on the subject (Higuchi and Stella 1975, Roche 1977, Bundgaard 1985, Reeves, Speller et al. 1989, Stella, Borchardt et al. 2007).

A prodrug can be a composite of the therapeutic agent of interest and a promoiety, such that exposure to physiological conditions results in release of the drug molecule and the promoiety as separate molecules. Otherwise, a compound can be a bioprecursor that has to undergo biotransformation *in vivo* to become pharmacologically active. In the latter case, no promoiety exists. Within this body of work, the use of a promoiety strategy was employed.

The critical defining features of a properly designed prodrug which contains a promoiety are as follows. First, the prodrug must possess a promoiety that is conjugated to the parent drug by a biologically labile linker. Second, the linker must cleave under physiological conditions to release the parent drug and the promoiety. Generally speaking, the promoiety needs to be a pharmacologically

inert or harmless endogenous chemical species so it does not present toxicity issues when it is generated following hydrolysis. The prodrug cleavage event that delivers the parent drug and promoiety may be facilitated by simple chemical means under various physiologically-relevant pH conditions or by enzymatically-accelerated processes, and the usual mode of conversion is a hydrolytic event. A third important feature of a properly designed prodrug of this class is that the prodrug must not have any biological activity of its own (i.e. it must not be a new drug entity).

An important deviation from these critical criteria is the case in which a prodrug is actually a codrug. In that case, there is no true promoiety, because the prodrug species is specifically designed to release more than one therapeutic agent, or more than one molar equivalent of the same therapeutic agent following systemic hydrolysis. Therefore, codrugs may be comprised of two different drugs conjugated by a hydrolyzable linker moiety in a one-to-one molar ratio, or they may be comprised of two molar equivalents of the same drug conjugated similarly. Otherwise, some codrugs are designed in molar ratios other than one-to-one, depending on the particular design. Codrugs have also been widely reviewed (Bryskier 1997, Bryskier 2005, Al-Ghananeem and Crooks 2007, Cynkowski, Cynkowska et al. 2008, Lau, White et al. 2008, Strasinger, Scheff et al. 2008, Das, Dhanawat et al. 2010, Das, Dhanawat et al. 2010, Crooks, Dhooper et al. 2011)

Within this dissertation, prodrugs and codrugs will both be covered, so it is important to understand their differences now. **Figure 1.4(A)** shows a bipartate

conjugate of NTX and β-alanine with an ester linker. **Figure 1.4 (B)** depicts a tripartate codrug of NTX in which the co-therapeutic entity is (-)-cytisine, and the linker is a secondary carbamate.

In **Fig 1.4 (A)**, the ester linker can theoretically be cleaved by enzyme-assisted or simple chemical hydrolysis. The same can be said of the secondary carbamate in **Fig. 1.4 (B)**. The defining difference is that in (**A**), hydrolytic cleavage of the ester results in the release of two separate chemical species, NTX and β-alanine, while in (**B**), hydrolytic cleavage of the secondary carbamate linker leads to the release of (-)-cytisine, NTX and a molar equivalent of carbonic acid or carbon dioxide, depending on pH. Thus, bipartate prodrugs cleave into two parts while tripartate prodrugs cleave into three parts.

The bonds that are cleaved by a molar equivalent of water are shown in **Figure 1.4** as indicated by the wavy lines, and the resultant cleavage products are identified as well. In the codrug, there are two possible cleavage points that are plausible, although it is far more likely that the carbon-oxygen bond of the NTX side of the carbamate linker is cleaved since the phenolate leaving group that would emerge is resonance stabilized and a far better leaving group than a nucleophilic secondary amine.

There is currently a rich body of literature surrounding the idea of amino acid conjugation to drugs, especially in the recent prodrugs literature. The resultant prodrug design affords bipartate prodrugs with improved physiochemical properties that solve one or more of the typical drug performance problems

mentioned above. Indeed, the recent surge in prodrug design that is aimed at the development of amino acid prodrugs of various drug molecules is in keeping with the bulk of the work presented in this dissertation, and a thorough review is presented. Amino acids as promoieties in prodrug design are also the subject of an excellent, recent review (Vig, Huttunen et al. 2012).

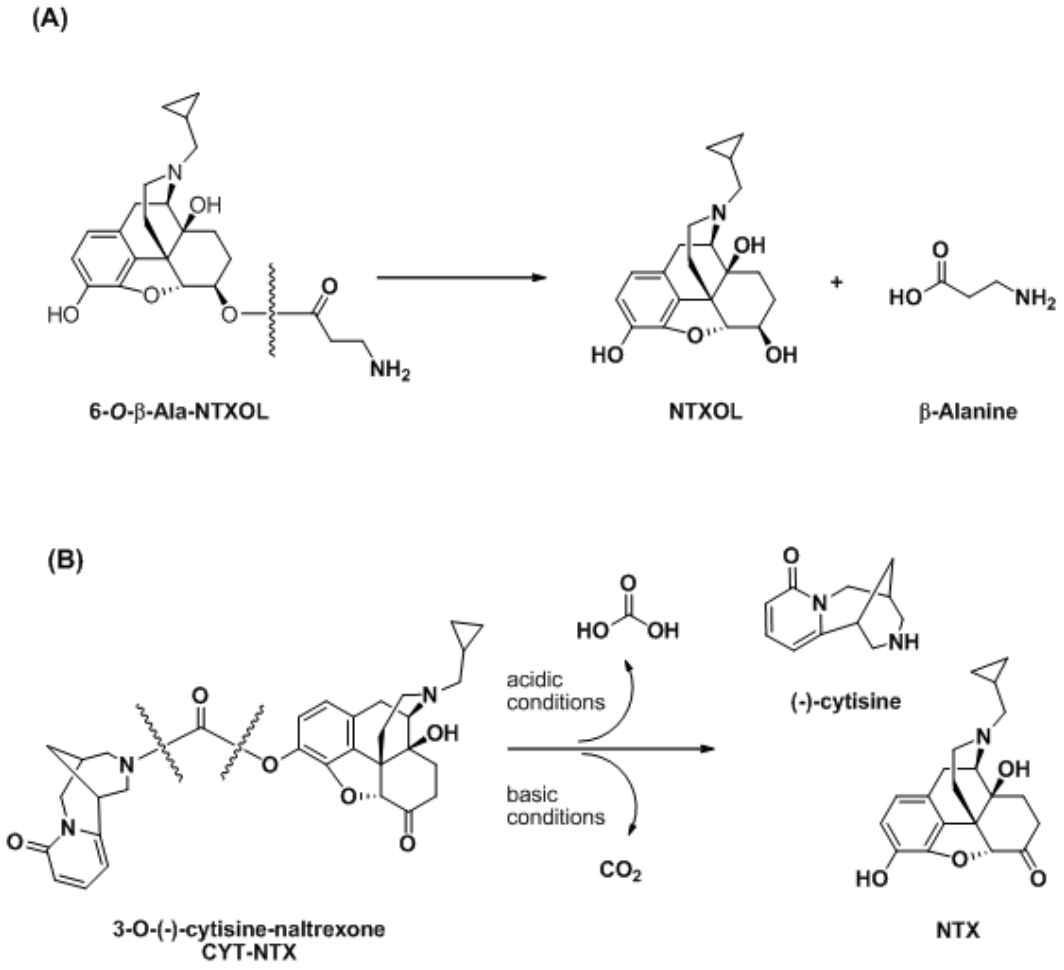

Figure 1.4 (A) A bipartate conjugate of NTX and β-alanine. (B) A tripartate codrug of NTX and (-)-cytisine.

1.8 Amino acid prodrugs

Throughout recent decades, a hot area of drug delivery research has focused on the development of amino acid prodrugs for various active transporter-targeted delivery goals. In this section, a review of many of these research efforts and their various delivery contexts is presented (i.e. oral, intraocular, and intranasal). Indeed, L-Valine ester prodrugs of the antiviral nucleoside analogues acyclovir (ACV) and ganciclovir (GCV) have been developed and have progressed to the market. Of these two, the richest body of literature exists for ACV, and **Figure 1.5** illustrates the best prodrug structures that have been prepared and assayed along with their references.

Valacylovir

One of the most extensively studied amino acid prodrugs is the antiviral agent valacyclovir (Valtrex®), an FDA-approved L-valine ester prodrug of acyclovir. As with many amino acid prodrugs, D- and L- forms of the prodrug have been prepared and assayed (Beauchamp, Orr et al. 1992). For the purpose of this review, VACV denotes specifically the L-isomer of valacyclovir as shown in **Figure 1.5,** unless stated otherwise.

Acyclovir (ACV) is an antiherpetic drug which suffers from poor bioavailability of 15-21% (Blum 1983). Varicella zoster (VSZ) and human cytomegalovirus (HCMV) belong to the herpes family along with herpes simplex virus types 1 and 2 (HSV-1 and HSV-2), and VSV and HCMV have been shown to be less sensitive to acyclovir treatment (O'Brien and Campoli-Richards 1989).

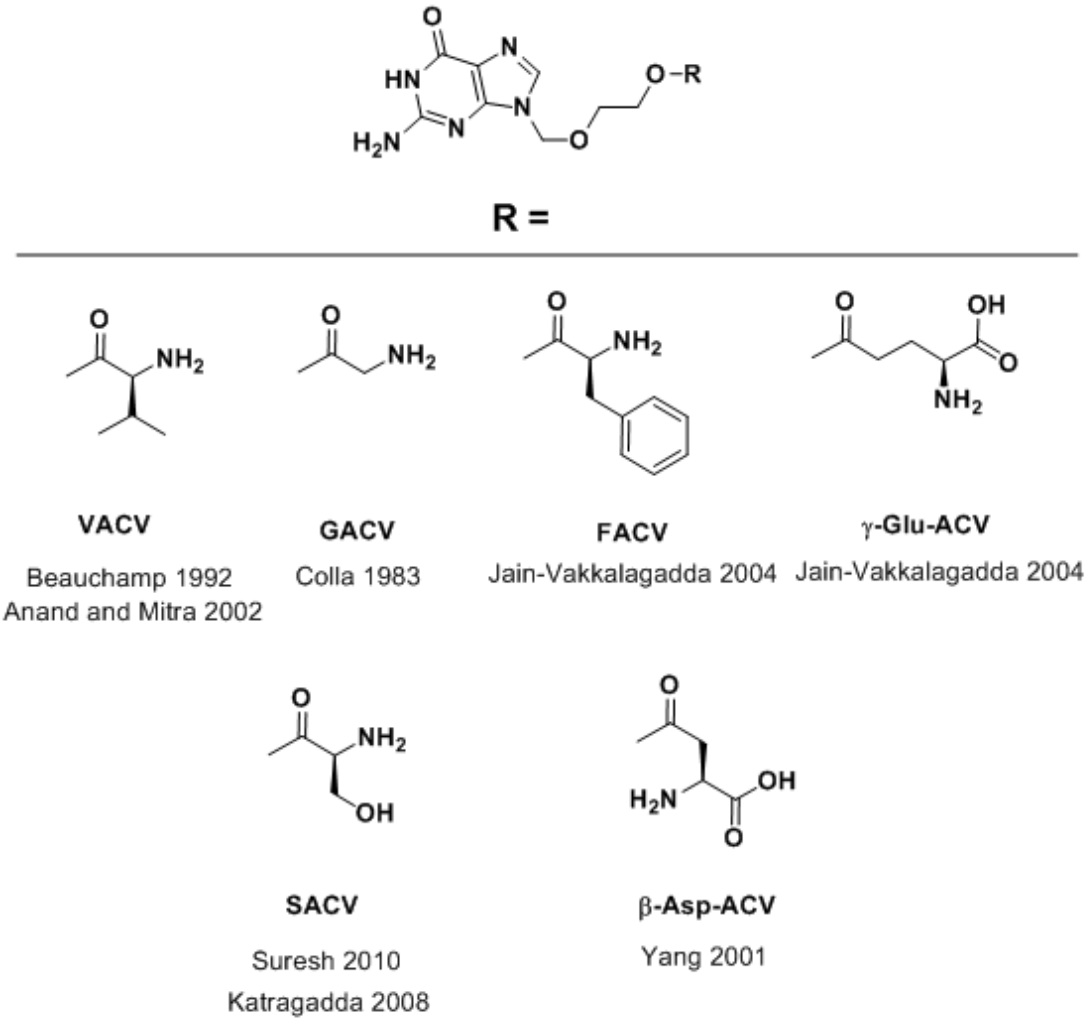

Figure 1.5 Structures of the most successful amino acid ester prodrugs of ACV (R = H).

In order to approach an improved oral drug delivery profile of acyclovir to avoid the need for parenteral administration to treat VSV and HCMV, Beauchamp *et al*. synthesized and bioassayed 18 amino acid ester prodrugs of ACV (Beauchamp, Orr et al. 1992). In this work, D-, L-, and racemic forms of amino acid esters of acyclovir were tested for stability, bioavailability and antiviral activity against HSV-1. The L-Val prodrug, valacyclovir (VACV) was found to be

the best candidate. Indeed, the findings of this work ultimately led to clinical trials and the eventual market approval of VACV (Valtrex®) by the FDA. Valtrex® has since reached blockbuster status.

To assay bioavailabilities of the prodrugs, Long Evans rats were dosed by oral gavage using solutions of the amino acid ester prodrugs (Beauchamp, Orr et al. 1992). The amount of ACV present in urine filtrates was analyzed by HPLC over a 40 hour time course. ACV is known to be excreted virtually unchanged following oral dosing (Krasny, Page et al. 1981).

None of the amino acid esters were detected in urine, indicating a probable 100% hydrolytic conversion of the prodrugs to parent acyclovir in the biophase. Also, VACV demonstrated the best oral bioavailability (63%). Of all the prodrugs tested, D-forms of the promoieties afforded less enhancement in bioavailability compared to their L-isomers, which suggested the involvement of a stereospecific transport system. It is interesting to note that most of the prodrugs tested improved bioavailability of ACV compared to parent ACV.

A significant solubility enhancement in water at room temperature was also afforded by VACV. An approximate 134-fold increase in solubility was observed (174 mg/mL VACV compared to 1.3 mg/mL ACV), which also favored improved oral dosing. The aqueous stability of VACV was also acceptable for oral delivery ($t_{1/2}$ = 95 h @ pH 6, 13 h @ pH 7.4, and 9.5 h @ pH 9.5).

In a much later body of work, the stability of VACV was investigated in buffer, in dog gastrointestinal fluids, and in the gastrointestinal fluids of man (Granero and Amidon 2006). At acidic pH (below pH 4), VACV was adequately stable ($t_{1/2}$

= 1386 h in human gastric fluid (pH 1.22), 111.77 h in dog gastric fluid, and 39.60 h (pH 4.11) in phosphate buffer). The results in dog and human intestinal fluids, and in buffers which mimic GI pH gradients suggest that VACV is stable enough to be dosed orally, but some hydrolysis in the gut lumen is to be expected, which limits bioavailability. Nonetheless, the approximate 54.5% bioavailability of VACV in man represents a 3-5-fold increase in bioavailability over orally administered ACV, and VACV is 99% converted to ACV by first pass metabolism.

In terms of antiviral activity against HSV-1 SC 16 strain in Vero Cells, VACV again showed the best activity; IC_{50VACV} = 0.84 µM compared to 10.5 µM for the 3-aminopropionate ester. ACV demonstrated the highest IC_{50} value (0.1 µM), indicating that the antiviral activity of VACV required a hydrolytic event, and the observed plaque reduction in Vero Cells was most likely due to regenerated ACV (Beauchamp, Orr et al. 1992).

In a separate study of amino acid ester prodrugs of ACV, similar antiviral activities against various HSV-1 and HSV-2 strains were observed in infected primary rabbit kidney cells (Colla, Busson et al. 1983). The prodrugs were synthesized as hydrochloride salts, and the observed IC_{50} = 0.04 – 0.5 µg/mL values for Gly, L-Ala, and β-Ala prodrugs of ACV compared to 0.04 – 0.1 µg/mL values for ACV also suggested that the antiviral activity of the prodrugs was due to parent ACV. Here, the goal was to design a water soluble prodrug of ACV that could be formulated as an IM injectable dosage form, or as an eye drop formulation for the treatment of ocular HSV-1 keratitis. It was found that HSV-1

induced epithelial and stromal keratitis and irititis were suppressed in rabbits when the Gly prodrug of ACV (GACV) was formulated into a 1% eye drop solution in pH 5.7 isotonic borate buffer. ACV could not be dissolved in a sufficient quantity to prepare a 1% eye drop. Importantly, GACV was stable for 6 days at room temperature in the borate buffer as compared to pH 7.4. These data suggest that eye drops containing an amino acid ester prodrug of ACV can be prepared and administered to treat ocular HSV-1 infections. The structure of GACV is given in **Figure 1.5**.

Given these encouraging results, it is no surprise that significant research efforts have been applied to establish the utility of active transporters as targets for enhanced drug absorption. Indeed, several studies have provided evidence for the human peptide transporter (hPEPT-1) as the critical absorption enhancer of VACV following oral administration (Balimane, Tamai et al. 1998, Han, Oh et al. 1998, Smith and Lee 1998). Further amino acid prodrug designs to target hPEPT-1 are covered under specific prodrugs later in this review.

Amino acid esters of acyclovir for ocular drug delivery

Ocular drug delivery can also benefit from an amino acid prodrug approach. Evidence of a rabbit corneal oligopeptide transport system has been obtained (Anand and Mitra 2002). Threefold enhancement of corneal permeation of VACV was observed compared to ACV. Moreover, known substrates of a peptide transporter (glycylsarcosine, glycylproline, captopril, and others) inhibited the transport of VACV, and the transport of VACV was pH/concentration-dependent

and saturable. Also, Ouabain, a Na^+/K^+ ATPase inhibitor, significantly decreased the permeability of VACV across rabbit cornea. Taken together, these data suggest the role of an active oligopeptide transport system in the corneal permeation of VACV. On the other hand, ACV corneal transport is limited by passive diffusion and poor lipophilicity among other physiochemical shortcomings (Anand and Mitra 2002).

In addition to an active oligopeptide transport system on the rabbit cornea, an Na^+-dependent cationic and neutral amino acid transporter ($B^{0,+}$) has been identified (Jain-Vakkalagadda, Pal et al. 2004). L-Arg transport across rabbit cornea was concentration-dependent, saturable, and involved a single carrier system. Inhibition of L-Arg permeation by ouabain or sodium and chloride free buffers suggested the involvement of an active carrier transport process. Neutral amino acids L-Phe, L-Cys, and Gly significantly inhibited the transport of [^{3}H]-L-Arg, as did L-Arg itself, suggesting substrate recognition of neutral and cationic amino acids. L-Glu, an anionic amino acid did not inhibit the transport of L-Arg while 2-aminobicyclo[2,2,1]heptane-2-carboxylic acid (BCH) did. BCH is a known specific inhibitor of the $B^{0,+}$ system, and this further suggests that transport of L-Arg is enhanced by $B^{0,+}$ carrier-mediated processes. The amino acid transporter was further characterized by reverse transcription-polymerase chain reaction (RT-PCR) utilizing total RNA from rabbit cornea, human cornea, and rabbit corneal epithelium samples.

In this same work, three amino acid prodrugs of acyclovir were prepared (γ-Glu-ACV, Phe-ACV, and Gly-ACV). Inhibition studies in Dulbecco's phosphate

buffered saline (PBS) at a concentration of 1mM prodrug demonstrated that only γ-Glu-ACV (EACV) and Phe-ACV (FACV) had a significant inhibition of [^{3}H]-L-Arg. The Gly-ACV prodrug did not inhibit the transport, although the amino acid Gly was found to be an inhibitor in the same study. Obviously, there is no guarantee of substrate recognition by a given transporter in prodrug design if one simply prepares a conjugate of a drug and a known transporter substrate. All prodrugs must be tested in a biological context to unveil their utility in clinical applications.

A Na^+-independent large neutral amino acid transporter (LAT1) has also been identified in human and rabbit cornea (Jain-Vakkalagadda, Dey et al. 2003) which is responsible for the transport of L-forms of Leu, Ile, Val, Phe, Tyr, Trp, Met, and His. Using RT-PCR and various inhibition studies, the authors investigated [^{3}H]-L-Phe transport across rabbit cornea and uptake in SIRC rabbit corneal cells. Uptake was concentration-dependent and saturable. Transport was saturable, sodium buffer-independent, energy-independent, and significantly inhibited in the presence of L-Phe, L-Tyr, L-Leu, L-Ile, and L-dopa. Gly and L-Ala had a negligible effect on transport. Also, D-forms of Leu, Phe, and Met are known substrates of LAT1, and D-Phe and D-Leu inhibited [^{3}H]-L-Phe uptake in SIRC cells. No amino acid esters of ACV were assayed in this study.

An Na+-dependant neutral amino acid transporter (ASCT1), has also been characterized in rabbit primary corneal epithelial cell culture and rabbit cornea using the same type of inhibition studies and RT-PCR techniques (Katragadda, Talluri et al. 2005). [^{3}H]-L-Ala uptake in rabbit primary corneal epithelial culture

and [^{3}H]-L-Ala transport across rabbit cornea were found to be saturable, sodium-dependent, energy and pH- independent, and inhibited in the presence of L-Ser, L-Thr, L-Cys, and L-Glu. The transporter was not inhibited in the presence of BCH or α-methylaminoisobutyric acid, which sets it apart as the ASC system, rather than the A system which is known to be inhibited by those species.

In follow up efforts to exploit the $B^{0,+}$ amino acid transporter as an ocular bioavailability enhancer, Anand *et al.* synthesized and assayed the transcorneal flux of L-γ-Glu-ACV (EACV) and L-Tyr-ACV (YACV) (Anand, Katragadda et al. 2004). In PBS buffers held at pH 5.0, 6.0, and 7.4, half lives of the two prodrugs covered a large rang (5.5 – 654.5 h). Maximum stability for both prodrugs was observed at pH 5.0. In cornea, YACV was much more labile to hydrolysis than EACV; however, EACV was converted to ACV more rapidly in aqueous humor and in the Iris-cilliary body.

Noncompetitive inhibition of [^{3}H]-L-Arg was observed in the presence of 1mM EACV but not in the presence of an equivalent concentration of YACV. Accordingly, EACV and ACV had similar transport while YACV transport was significantly less than either EACV or ACV. The affinity of EACV for the $B^{0,+}$ transporter was low (2.66 ± 0.28 mM), which accounts for a similar transport profile to ACV. Further experiments revealed that EACV transport was pH-independent, Na^+-dependent, and energy-dependent. These data suggest the involvement of $B^{0,+}$ in the transport of EACV. However, in this case the delivery was not sufficient to constitute an advantage in corneal dosing with EACV over

ACV. Still, the antiviral activities of both prodrugs against HSV-1, HSV-2, HCMV, and VZV were quite similar to commercial VACV and ACV, so these prodrugs could still be good oral delivery candidates since hPEPT-1 was not targeted in these delivery efforts.

L-serine-succinate (SSACV), L-cysteine (CACV), L-alanine (AACV), and L-serine (SACV) prodrugs have also been assayed as potential ocular drug delivery candidates (Suresh, Zhu et al. 2010). The drug target for these candidates was the Na^+-dependent neutral amino acid transporter (ASCT1) where ASC refers to the Alanine-, Serine-, and Cysteine-preferring nature of the nutrient transporter. Additionally, these prodrugs were also tested for their affinity at the other known corneal nutrient transporters. A 51% inhibition of transcorneal flux of SACV was observed in the presence of 5 mM arginine and a 38% inhibition was noted in the presence of BCH. CACV transport was uninhibited by alanine or gly-sar. AACV transport was unaffected by alanine, gly-sar, or BCH, and the prodrug was found to be unstable in transport medium. On the other hand, [^{3}H]-L-Alanine transport was significantly inhibited in the presence of 10 mM SSACV, and the uptake of [^{3}H]-L-Alanine into rPCEC cells was likewise inhibited in the presence of SSACV. Taken together, these results indicate that CACV and SACV are not substrates for ASCT1, while AACV was too unstable, and its permeability data were statistically identical to parent ACV. Inhibition of [^{3}H]-L-Alanine in the presence of SSACV indicates that SSACV is the only substrate for ASCT1 in this series of prodrugs, and it is likely that the

free carboxylate is necessary for transporter recognition. In every case, the prodrugs were converted to ACV in ocular tissues.

Permeability of the prodrugs was best for SACV; however, despite recognition by ASCT1, SSACV showed permeability no better than CACV, and both SSACV and CACV were less permeable than ACV control. SACV proved to be a substrate for multiple nutrient transporters. SACV also showed the best antiviral activity against HSV-1 and VZV (HSV-1 EC_{50} (SACV/ACV) = (6.3/7.1)μM, VZV EC_{50} (SACV/ACV) = (1.7/2) μM). AACV and CACV had similar acitivities against HSV-1 compared to ACV. Otherwise, antiviral activity data suggest that none of the prodrugs was as effective against HSV-2 as ACV, and only SACV was similar in affinity for VZV compared to control. SSACV, the only ASCT1 substrate, demonstrated poor affinity for HSV-1 and HSV-2 compared to ACV, and a nearly 4-fold lower affinity for VZV. Overall, SACV was the best prodrug discovered in this series of compounds.

A recent study was conducted to assess the pharmacokinetics of amino acid ester prodrugs of acyclovir (ACV) following oral administration (Katragadda, Jain et al. 2008). The prodrugs studied were AACV, SACV, L-isoleucinyl-ACV (IACV), EACV, and VACV.

The *in vitro* enzymatic stability data that were obtained in this study are very interesting. AACV was observed to be too unstable in liver homogenate to measure residual prodrug, while EACV showed the longest half life (223 ± 8.8 h). VACV was rapidly hydrolyzed in intestinal and liver homogenate with half lives of 0.6 ± 0.02 h and 0.07 ± 0.004 h respectively. On the other hand, the rat plasma

half life of VACV was 226 ± 67 h. These data suggest that systemic exposure to ACV from VACV occurs via a combination of intestinal and hepatic metabolism. Interestingly, the plasma half lives of all of the acyclovir amino acid ester prodrugs except AACV were found to be rather long, ranging from a low of 4.8 ± 0.7 h for AACV to a maximum of 226 ± 67 h for VACV. Overall, the study suggests that the in vitro stability of amino acid ester prodrugs of acyclovir is highly dependent upon the tissue used in the stability studies.

A number of transporter affinity studies were carried out in this work; however, the pharmacokinetics data best speak to the ability of these prodrugs to act as bioavailability enhancers in the live Sprague-Dawley rat. In that regard, SACV and VACV showed the best bioavailability enhancements compared to control, as determined by $AUC_{Inf(T)}$. An approximately 7.2-fold increase was observed for SACV, and a roughly 5-fold increase was observed for VACV. The C_{max} for SACV (39 ± 2 µM) was also significantly higher than that of VACV (22 ± 0.3 µM), the commercial prodrug. C_{max} for ACV was fifteen times less than SACV. These data, and data from the previous study, suggest that SACV should be strongly considered as a candidate for further study in oral and ocular treatment of HSV infections.

Amino acid ester prodrugs of acyclovir for intranasal drug delivery

ACV cannot be delivered by nasal drug delivery without a prodrug approach (Shao and Mitra 1994). L-Phe and L-Tyr are absorbed nasally by an active transport process (Tengamnuay and Mitra 1988). As a natural parallel to oral

and ocular drug delivery efforts involving amino acid prodrugs of acyclovir which target nutrient transporters, the nasal drug delivery route has also been investigated (Yang, Gao et al. 2001). Utilizing L-amino acids, Phe-ACV, Lys-ACV, and β-Asp-ACV were synthesized and assayed for stability and nasal uptake compared to parent ACV. The animal model used in this work was the adult male Sprague-Dawley rat. Stability studies were conducted in phosphate buffers held at pH 3.0, 5.0 and 7.4 containing a minimal amount of acetonitrile for complete prodrug dissolution. Samples of rat nasal washings and rat plasma were utilized as the enzymatic hydrolysis media.

The prodrugs were very stable with measured degradation values of less than 10 – 15% in one week at pH 3.0 or pH 5.0 and 25 °C, with the exception of Phe-ACV which had a half life of 136.6 ± 3.7 h at pH 5.0 and 25 °C. A significant rate enhancement in prodrug hydrolysis to roughly $t_{1/2}$ = 4 hours was observed in buffer held at pH 7.4 and 37 °C for Lys-ACV and Phe-ACV (approximately four times faster than β-Asp-ACV). β-Asp-ACV showed no significant increase in hydrolysis rate in rat nasal washings but demonstrated nearly 1/13th the apparent buffer stability in rat plasma which indicates that the β-Asp-ACV prodrug could likely be a good nasal delivery candidate for ACV with sustained stability at the nasal mucosa absorption barrier ($t_{1/2}$ = 16.6 ± 0.3 h) and rapid systemic hydrolysis ($t_{1/2}$ = 77.5 min) to ACV following absorption. Stability of the Phe-ACV and Lys-ACV prodrugs in nasal washings suggested that these prodrugs would not be the best candidates for intranasal drug delivery ($t_{1/2}$ = 0.80 h and 2.93 h respectively). Furthermore, the nasal absoprtion of Phe-ACV and Lys-ACV were

found to be immeasurable, which certainly excludes these compounds as nasal delivery candidates. On the other hand, 8% absoprtion of β-Asp-ACV at a concentration of 100 µM was observed over 90 minutes perfusion. As would be expected, the transport of β-Asp-ACV appears to be carrier-mediated in that 2 mM L-asparagine significantly inhibited the nasal uptake of the prodrug.

Model L-tyrosine derivatives for intranasal drug delivery

In order to explore the carrier-mediated drug delivery of L-tyrosine derivatives and their nasal absorption, Yang *et al. (*Yang and Mitra 2001*)* prepared three model L-tyrosine-linked benzyl alcohol conjugates with a variable R-substitution in the 4-position (**Figure 1.6**). The ether linkage utilized in this model compound design evades systemic cleavage by hydrolytic enzymes so the nasal absorption data need not be convoluted by concurrent metabolism during barrier transport.

From this work, it can be appreciated in general that an active transport system does exist on the nasal mucosa that can significantly increase the bioavailability of L-tyrosine-linked model test compounds. For instance, when R = COOH versus R = NO_2 an expected increase in nasal absorption was seen for the parent benzylic alcohols. In this case, the nitro compound absorbed while the carboxylic acid did not. This was due to the ionic nature of the carboxylate in the isotonic phosphate buffer vehicle which was held at pH 7.4. Also, the nitro compound showed a linear correlation between initial drug concentration and absorption rate which was maintained over a concentration range of two orders of magnitude.

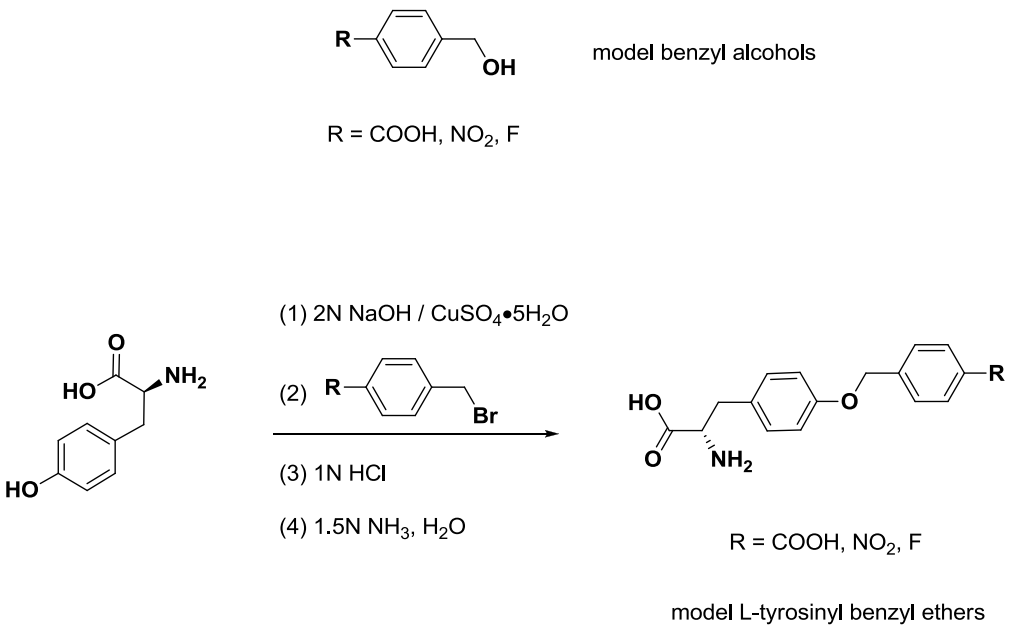

Figure 1.6 Structures of model benzyl alcohols and their L-tyrosinyl ether conjugates/ synthesis of the conjugates. Adapted from (Yang and Mitra 2001).

The latter suggests a passive permeation mechanism of absorption. On the other hand, each of the L-tryosinyl conjugates, along with L-tyrosine, exhibited Michaelis-Menten kinetics, and a clear dependance of the apparent first order rate constant on initial drug concentration was observed. Also, each of the conjugates showed higher affinity for the carrier system than L-tyrosine, and they were transport-inhibited in the presence of L-tyrosine. The nitro and fluoro dervatives in particular showed an order of magnitude increase in transporter affinity. These affinity data also correlated positively with the absorption rate data in which the nitro conjugate showed the best affinity and fastest absorption rate. Importantly, the impermable parent 4-carboxylic benzyl alcohol moiety did

not inhibit absorption rate enhancement of the carboxylate conjugate model compound, which further suggests the presence of an active transport system that recognizes the L-tyrosine moiety as a substrate. These data provide good evidence that amino acid ester prodrugs may be a suitable drug design strategy for intranasal drug delivery.

Amino Acid esters of Danazol for oral drug delivery

Danazol (D) (**Figure 1.7**) is an oral therapeutic approved for the treatment of endometriosis. It is also used in fibrocystic breast disease and angioedema. Several dosage strengths of the drug are avaiable in capsule form. As may be expected, the neutral nature of danazol, and its sterol core structure impart little water solubility to the compound (5 mg/mL), and its solubility is not variable as a function of pH (Simmons, Portmann et al. 1995). Inasmuch, dose doubling of D does not result in a compensatory doubling of systemic drug concentration due to the bioavailability limitations of poor aqueous solubility. At best, approximately 35 – 45% increases in blood levels have been noted. Therefore, the amino acid ester prodrug approach has been applied to D with some very interesting results.

A study by Simmons *et al*. (Simmons, Portmann et al. 1995) has demonstrated that L-Lysine, Glycine, and sarcosine conjugates of D (DL, DG, and DS respectively) (**Figure 1.7**) improve systemic exporsure to D. Also, whithin this study, significant differences were observed in enzymatic activities between different species and different biological fluids. For instance, upon rat intraduodenal bolus dosing of prodrug, DL and DS were completley hydrolyzed to

D, while DG could be measured in portal plasma in a ratio of 2:1 D:DG. In contrast, DL did not hydrolyze at all in rat liver perfusion studies while DG could be measured along with D and DS was not present (i.e. hydrolyzed completely). In rat intestinal fluid, DG did not hydrolyze at all while DL hydrolyzed rapidly and DS hydrolyzed slowly.

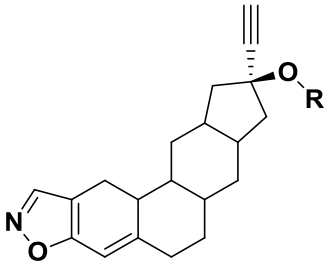

Danazol (R = H)
Danazol lysinate (R = $COCHNH_2(CH_2)_4NH_2$
Danazol glycinate (R = $COCH_2NH_2$)
Danazol sarcosinate (R = $COCH_2NHCH_3$)

Figure 1.7 Structures of danazol and its amino acid ester conjugates. Adapted from (Simmons, Portmann et al. 1995).

In human gastric and intestinal fluids, DG was not a substrate for esterase enzymes. DS hydrolyzed slowly in human intestinal fluid, similar to its behavior in rat intestinal fluid, and DL hydrolyzed rapidly in human intestinal fluid just like its behavior in rat intestinal fluid.

Porcine liver esterase rapidly cleaved the DG and DS prodrugs, but did not hydrolyze DL at all, and a completely opposite rate enhancement effect was observed in porcine pancreatin.

Comparing rat, human and dog plasma, DL hydrolyzed slowly in dog plasma and not at all in rat and human media. The other two prodrugs were not substrates for esterase activity in human and dog media, but they were rapidly converted to D in rat plasma.

These data demonstrate a very important point in prodrug design. The different biological fluids that the prodrug will encounter in transport to its target represent variegated barriers whose specific effects on the prodrug must be individually studied. It is not possible a priori to determine what the specificity of a prodrug will be for the enzymatic mileau of a particular biological matrix, and interspecies differences must also be considered. In this case, each of the prodrugs tested increased systemic exposure to parent D by the oral route as compared to control; however, their manner of doing so must clearly abide by different mechanisms.

Amino acid amide prodrugs of antitumor benzothiazoles

2-(4-aminophenyl)benzothiazoles (**Figure 1.8**) have been shown to possess potent activity against numerous cancer cell lines, and they also exhibit activity against a unique subset of human cancer cell lines that are part of the National Cancer Institute's *in vitro* anticancer drug screen (Bradshaw, Wrigley et al. 1998, Bradshaw, Chua et al. 2002).

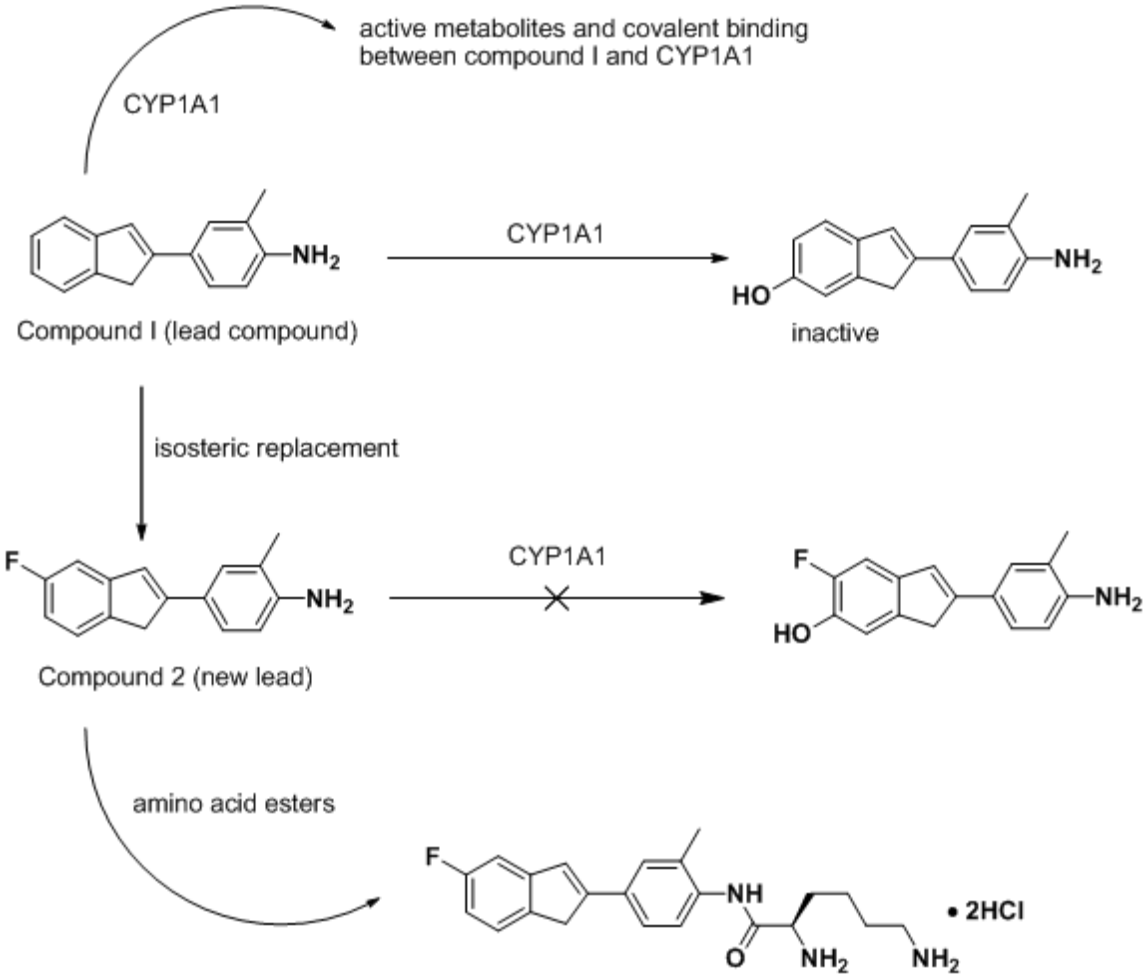

Figure 1.8 Rational design of *N*-lysyl-2-(4-amino-3-methylphenyl)-5-fluorobenzothiazole. Adapted from (Bradshaw, Bibby et al. 2002, Bradshaw, Chua et al. 2002, Hutchinson, Jennings et al. 2002).

Compund I has been pursued as an anticancer agent due to its activity against breast MCF-7, MDA-468 and other sensitive cell lines; however, its utility has been truncated by problems associated with its hydroxy metabolites. In particular the *C*-6 oxidation product of compound I causes sensitive cells to not

sequester the therapeutic parent compound I, and the *C*-6 metabolite is itself inactive as an antitumor agent (Kashiyama, Hutchinson et al. 1999).

In efforts to circumvent these untoward characteristics of the hydroxy metabolites, flourine isosteric replacement of the hydrogen atoms on the benzothiazole core has been investigated. As a result, compound 2 was found to be the best compound for further drug development due to its performance against human breast and ovarian tumor xenografts in nude mice. Also, compound 2 exhibits superior performance in blocking the *C*-6 oxidation on the benzothiazole core which in the case of compound I effectively thwarts CYP1A1 induction and suicide inhibition. Respectively, the latter two events result in the formation of active metabolites and the tumor growth-inhibiting CYP1A1-benzothiazole covalent binding complex (Hutchinson, Chua et al. 2001).

In order to develop a clinical candidate with adequate water solubility for parenteral administration, Bradshaw et al. (Bradshaw, Chua et al. 2002) synthesized a series of amino acid amide prodrugs of 2-(4-amino-3-methylphenyl)-5-fluorobenzothiazole (compound 2) along with other homologous isosteres of the fluorobenzothiazole class. Though promising results were obtained with L-alanyl and L-lysyl promoieties when they were conjugated to many of the fluoro-isostere positional isomers, the *N*-lysyl-5-F dihydrochloride prodrug (5-FBL) of compound 2 (**Figure 1.8**) has emerged as the most promising candidate for clinical development (Bradshaw, Wrigley et al. 1998, Bradshaw, Bibby et al. 2002, Hutchinson, Jennings et al. 2002).

In terms of pH-dependent stability, at pH 4.5 and 25 °C, 5-FBL was stable for 45 days. At pH 7.4 and 25 °C, 5-FBL exhibited t_{90} = 45 days. These data suggest that 5-FBL is best stored in mildly acidic solution as a dosage form with acceptable shelf life. Furthermore, 5-FBL showed 136.4-fold better solubility at pH 5.0 than at pH 7.4, as expected of an amine-containing compound (Hutchinson, Jennings et al. 2002). In general, the stability of 5-FBL is as should be expected for an amide prodrug.

In the presence of senstitive cancer cell lines, 5-FBL was converted to parent compound 2 in detectable amounts within 24 hours, and levels of compond 2 significantly increased over seven days of the experiment. Furthermre, 5-FBL was observed to be stable for greater than seven days at 37 °C in cell culture medium not containing cells, indicating that conversion of prodrug 5-FBL to active compound 2 was facilitated by cellular metabolic machinery. Western Blot analysis of CYP1A1 induction in lysates of MCF-7 (sensitive) cells exposed to 5-FBL compared to those untreated with 5-FBL revealed selective induction of CYP1A1, which is required for anticancer activity. Insensitive HCT 116 cells did not present evidence of CYP1A1 induction when treated with 5-FBL or parent compound 2. Maximum CYP1A1 induction occurred at 1 µM 5-FBL concentration (Bradshaw, Chua et al. 2002).

In a further study, the pharmacokinetics of 5-FBL in mice and dogs were determined (Bradshaw, Bibby et al. 2002). The $t_{1/2}\beta$ values indicate that in mice and both male and female dogs, 5-FBL is rapidly converted to parent compound 2 (2, 17, and 30 minutes respectively). However, these data were obtained at a

dose level of 32.2 mg/kg i.v. in mice and 14.3 mg/kg in the dogs. Significant gastrointestinal toxicity was observed in the dogs at the 14.3 mg/kg dose level, and 4 mg/kg was found to be a more suitable dose with an associated peak plasma concentration of compound 2 of 0.9 μM. The latter exposure level is within the range of efficacy in terms of sensitive breast cancer cell *in vitro* data.

Amino acid prodrugs of 5-aminosalacylic acid for colonic delivery

Figure 1.9 shows the structures of the compounds which are relevant for the following discussion. Lialda® (mesalamine) is the trade name for 5-aminosalicylic acid (5-ASA) which is an effective clinical agent for the treatment of inflammatory bowel diseases such as Crohn's Disease and ulcerative colitis. In order to effectively deliver 5-ASA to the colon, the azo prodrug (actually a codrug type of prodrug) sulfasalazine (Azulfidine®, SASP) has been designed. 70% of SASP is available to the distal intestine and colon upon oral dosing of SASP (Das, Chowdhury et al. 1979), and aza reductase enzymes that are present in the colonic region of the gut readily cleave the azo bond to liberate 5-ASA and sulfapyridine (SP). The prodrug approach is necessary in this case in order to prevent rapid pre-colonic absorption and acetylation of 5-ASA, both of which eliminate the drug from its desired target location. Though SASP is efficient in its delivery of 5-ASA, the SP moiety is known to cause hypersensitivity reactions in the majority of patients who receive therapy with SASP (Das, Eastwood et al. 1973, Taffet and Das 1983, Peppercorn 1984).

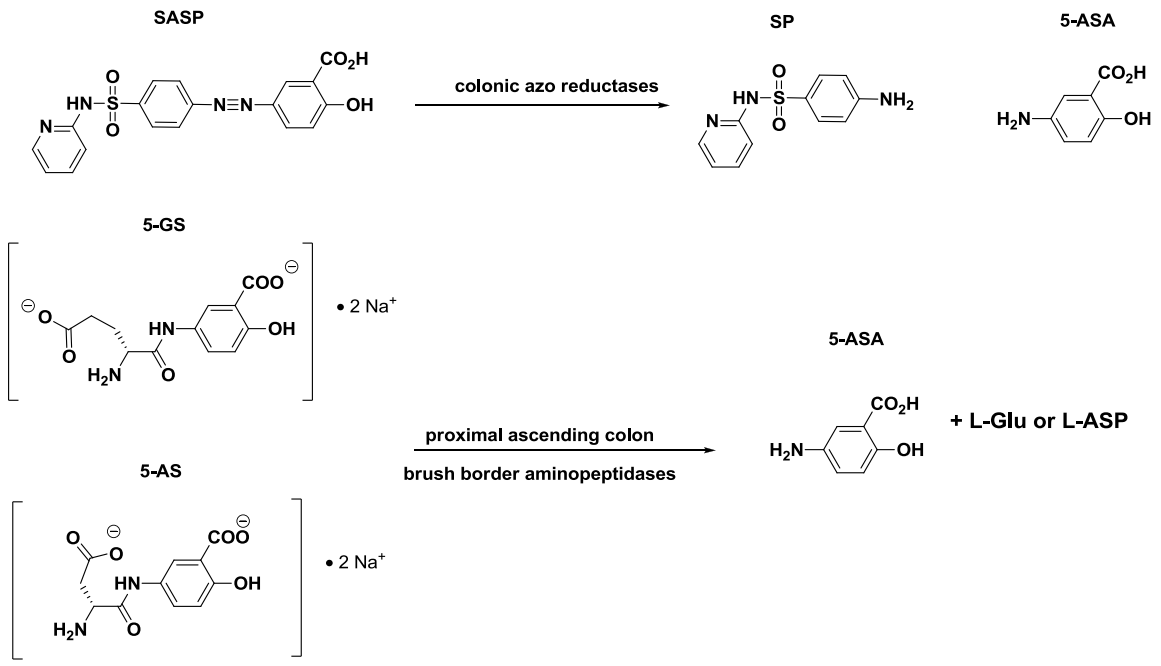

Figure 1.9 Structures of 5-aminosalicylic acid prodrugs and their mechanism of drug delivery. Adapted from (Pellicciari, Garzon-Aburbeh et al. 1993).

The amino acid prodrug approach has been utilized to afford amino acid amide prodrugs of 5-ASA for potential colonic delivery (Pellicciari, Garzon-Aburbeh et al. 1993). L-Glutamate and L-Aspartate moieties were conjugated to 5-ASA at the aryl amine moiety to prepare 5-(*N*-L-Glutamylamino)salicylic acid (5-GS) and 5-(*N*-L-Aspartylamino)salicylic acid (5-AS) as their disodium salts. In vitro experiments revealed that 5-GS did not cleave to release 5-ASA in human gastric juice, human feces suspension, human pancreatic juice, or bovine protease hydrolysis media; however, porcine peptidases cleaved the prodrug following first order kinetics, resulting in the liberation of 5-ASA ($t_{1/2}$ = 81 minutes).

Subsequently, 5-GS and 5-AS were orally dosed in colostomized and noncolostomized male Fisher rats and compared to 5-ASA and SASP to assess the effectiveness of brush border aminopeptidase-assisted release of 5-ASA from prodrug. The largest level of urinary recovery of 5-ASA and its metabolite, 5-*N*-acetyl-ASA was observed with oral dosing of 5-ASA, which substantiates early absorption in the first tract of the small intestine when 5-ASA is administered as parent drug. In contrast, the amino acid amide prodrugs exhibited lower urinary recovery levels of 5-ASA and the *N*-acetyl metabolite compared to oral dosing with 5-ASA, and fecal levels for 5-ASA and metabolite were far greater with orally dosed prodrug than with orally dosed 5-ASA. In all cases, there were no significant differences in recovery levels between the colostomized and noncolostomized rats. Collectively, these data suggest that an amino acid amide prodrug design can be advantageous for the delivery of 5-ASA to the proximal part of the ascending colon, which is a key area for the treatment of Crohn's Disease and ulcerative colitis. The activating enzymes in this case appear to be brush border aminopeptidases.

5'-Isoleucinyl-zidovudine for brain delivery

Zidovudine (AZT) is an antiviral agent used to treat HIV infection. However, AZT does not penetrate the blood brain barrier to an extent that is therapeutically relevant to treat brain infection of HIV-1. In order to improve brain delivery of AZT, the 5'-Isoleucinyl ester of zidovudine (IAZT, **Figure 1.10**) has been

prepared. Promising pharmacokinetic results have been observed in rabbits dosed by intravenous infusion (Lupia, Ferencz et al. 1993).

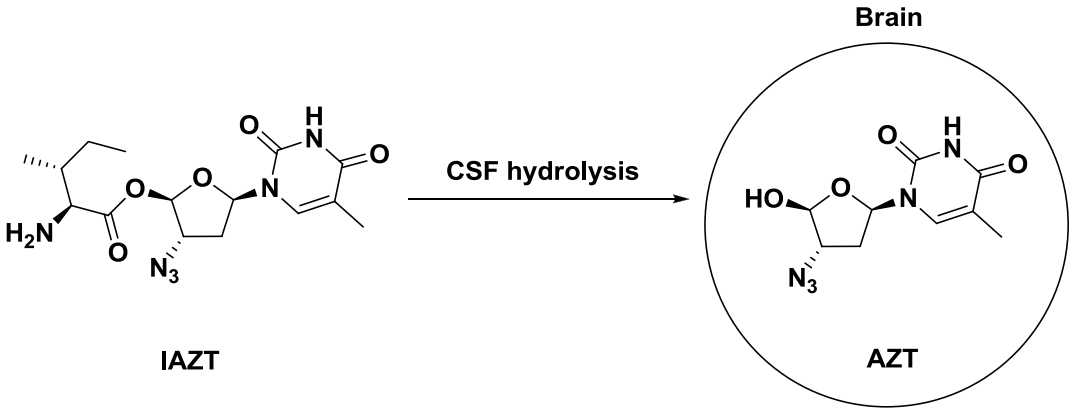

Figure 1.10 Brain delivery of AZT from IAZT prodrug. Adapted from (Lupia, Ferencz et al. 1993).

In the live rabbit, IAZT was rapidly converted to parent AZT (90% in 5 minutes) while *in vitro* plasma hydrolysis samples showed slower rates of conversion (22.5% in 5 minutes). Within 120 minutes, significantly higher levels of AZT were obtained from animals treated with IAZT compared to animals treated with AZT. However, at 120 minutes, IAZT could still be detected. The AUC for IAZT was approximately 1.5 times higher than that for AZT based on extrapolation to infinity for data points covering the time course to 120 minutes. Furthermore, a mean brain/CSF ratio of 0.64 corresponding to AZT from IAZT was observed, which is approximately twice the value observed following AZT dosing (0.32). IAZT was found to be completely hydrolyzed by plasma

esterases within 240 minutes, and by hepatic microsomes within 60 minutes. These data suggest that IAZT is a potential therapeutic agent for improved brain delivery of AZT.

Amino acid prodrugs of propofol for IV dosing

Propofol (PF) has become a staple in surgical anesthesia; however, a quick look at the molecule (**Figure 1.11**) reveals that it is quite lipophilic in nature and very water insoluble. To circumvent the solubility problems associated with PF, formulation design has been employed (Diprivan® 1% w/v oil/water emulsion). Also, the prodrug approach has resulted in an FDA-approved drug delivery system as well (Lusdera®, Fospropofol disodium). However, it has also been shown that the amino acid ester prodrug approach is likely to be a useful strategy for improved water solubility and IV delivery of PF (Trapani, Latrofa et al. 1998, Altomare, Trapani et al. 2003).

Figure 1.11 summarizes the amino acid ester prodrug structures as synthesized and tested by Trapani, Latrofa, Altomare and others. In every case racemic precursors were used to install the promoieties except for the L-prolinyl prodrug which was enantiopure. Compounds 1 – 8 were studied separately from compounds 9 – 12.

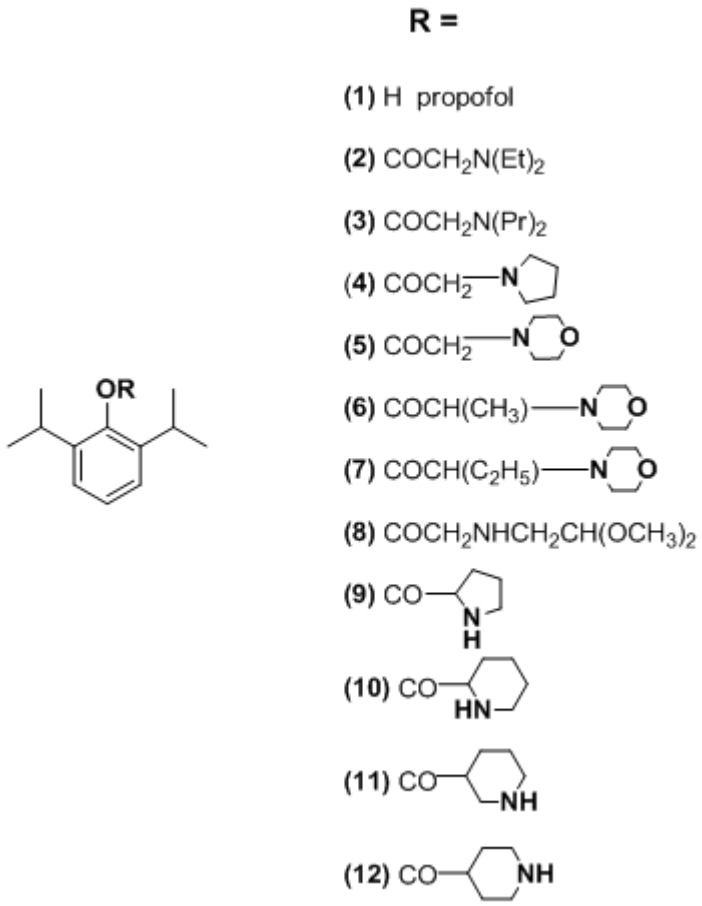

Figure 1.11 Amino acid ester prodrugs of propofol. Adapted from (Trapani, Latrofa et al. 1998, Altomare, Trapani et al. 2003).

Solubility studies in pH 7.4 phosphate buffer revealed that compound 8 had the greatest solubility (mg/mL) out of compounds 1-8; however, approximately 0.6 mg/mL is not highly soluble either. Hydrochloride salts of compounds 2 – 7 had better solubility than their free bases in phosphate buffer, with the exception of compound 5 in which no significant solubility difference was observed between the hydrochloride and free base at pH 7.4. The hydrochloride of compound 4 was significantly more soluble than the free base of compound 8, but none of the

materials (compounds 1 – 8) achieved even 1.0 mg/mL solubility regardless of ionic charge. Comparatively, the promoieties depicted in compounds 1 – 8 afforded an approximately 4.8-fold increase in solubility over propofol at best, and some prodrugs were far less soluble than propofol itself. Compound 3 had the worst solubility.

Amino acid esters 9 – 12 were prepared as hydrochloride salts only and tested for solubility in deionized water at room temperature (pH not reported). It is worth noting that this solubility testing procedure is in no way equivalent to that which was done on compounds 1 – 8 in which a controlled pH of 7.4 was maintained. IV injectable prodrugs should be assayed for solubility at pH 7.4. Nonetheless, the data are interesting. Ironically, compounds 9 and 11 exhibited log orders greater solubility (mmol/mL) as compared to the other isomers of 11. As expected, all of the amino acid ester hydrochloride prodrugs in the series of compounds 9 – 12 afforded at least 50-fold greater solubility than propofol in DI water. However, as a general critique, this may not be the case at all at pH 7.4.

In terms of stability, compounds 2, 4 and 5 were far too stable at pH 7.4 in buffer and in biological media to be considered viable prodrugs of propofol. This was true regardless of free base or salt form. Compounds 3 and 6 – 8 were not tested due to poor solubility.

Compounds 9 and 10 had half lives of 6 and 7 hours respectively in pH 7.4 buffer with large rates of acceleration in 50% rat plasma (17 and 2.5 minutes respectively). Similarly, in porcine liver esterase media, compound 9 hydrolyzed with a half life of 17 minutes, and compound 10 hydrolyzed with a half life of 13

minutes. These data provide clear evidence that compounds 9 and 10 are suitable prodrugs to consider as potential intravenous delivery systems of propofol. From this series of prodrugs, the L-prolinyl ester arises as the best candidate for further development given its greatly enhanced water solubility compared to propofol and its rapid conversion to propofol in biological media.

One important feature of compounds 2-12 must be addressed. In the definition of prodrugs, there is a requisite criterion that no prodrug can have pharmacological activity of its own. Within these studies, it was shown that the prodrugs do in fact have pharmacological activity at $GABA_A$ receptors in that many of them are able to reduce the binding of [^{3}S]*tert*-butylbicyclophosphorothionate ([^{3}S]TBPS) in a dose-dependent manner like propofol despite clear evidence of slow hydrolysis of most of the esters. Those esters are therefore behaving as analogues of propofol in the case where hydrolysis to propofol is too slow for prodrug behavior. Even the L-prolinyl prodrug exhibited some analogue activity in addition to its propofol drug delivery mechanism of action. Therefore, by definition, these agents are more appropriately viewed as analogues of propofol rather than prodrugs.

Amino acid esters of Penciclovir

Penciclovir (PCV), like acyclovir, is an acylnucleoside derivative of guanine that has potent and selective antiviral activity toward various herpes viruses in man. HSV-1, HSV-2, Epstein-Barr virus, and varicella-zoster viruses have each shown inhibited replication in the presence of PCV, both in cell cultures and in

animals (Harnden, Jarvest et al. 1987, Kim, Lee et al. 1996). Due to its poor oral bioavailability, which is akin to acyclovir, PCV is generally dosed as a topical formulation that is designed to treat cold sores of the HSV-1 variety. In the united states, PCV is supplied as a sodium salt in a 1% topical cream under the trade name Denavir®, and several strengths of the PCV prodrug famciclovir (FCV) are also available as oral delivery forms. In either case, PCV is available only by prescription. Systemic exposure to PCV following oral dosing of FCV requires two key steps (**Figure 1.12**). The terminal acetyl groups must be cleaved hydrolytically to afford the free hydroxyl groups of PCV, and the 6-position of the 6-deoxyguanine core structure of FCV must undergo oxidative bioconversion by xanthine oxidase to afford the true guanine skeleton of PCV.

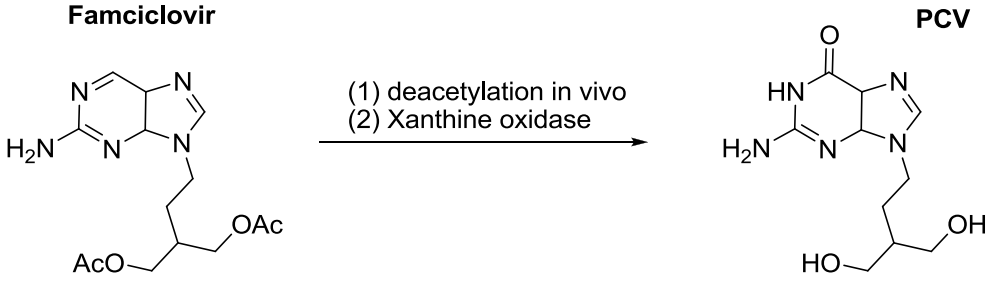

Figure 1.12 Bioconversion of famciclovir to penciclovir.

Notwithstanding the fact that famciclovir is orally well absorbed and extensively bioconverted to the desired PCV drug molecule, the bioconversion is not complete, and 60% PCV along with 5% 6-deoxy-PCV is observed in urine samples (Harnden, Jarvest et al. 1989, Vere, Sutton et al. 1989, Pue and Benet

1993). The 6-deoxy-PCV species represents a loss of PCV bioavailability, and it is of probable toxicological importance in that a similar 6-deoxy-ACV species has shown a chronic toxicity profile in animal models that is less favorable than the 6-oxy ACV compound (Beauchamp, Orr et al. 1992).

In order to investigate the utility of the PCV scaffold in a prodrug approach that does not require oxidation by xanthine oxidase at the 6-position of the guanine core structure, the amino acid ester approach was utilized on PCV itself (Kim, Lee et al. 1996). Again, it was expected that prodrugs of this structural design would be targets for the PEPT-1 and PEPT-2 transporters in the gut which are responsible for the increased absorption of VACV and VGCV by active transport.

Figure 1.13 illustrates the prodrug design and the intended outcome of prodrug exposure to physiological conditions. In this work, two forms of prodrug were assayed. In one design, the hydroxyl groups were substituted differently such that a simple alkyl ester was formed by acylation on one of the available hydroxyl groups while the other hydroxyl group was converted to an amino acid ester. In the second prodrug design, both available hydroxyl groups on PCV were substituted as amino acid esters using the same amino acid promoiety on both sides.

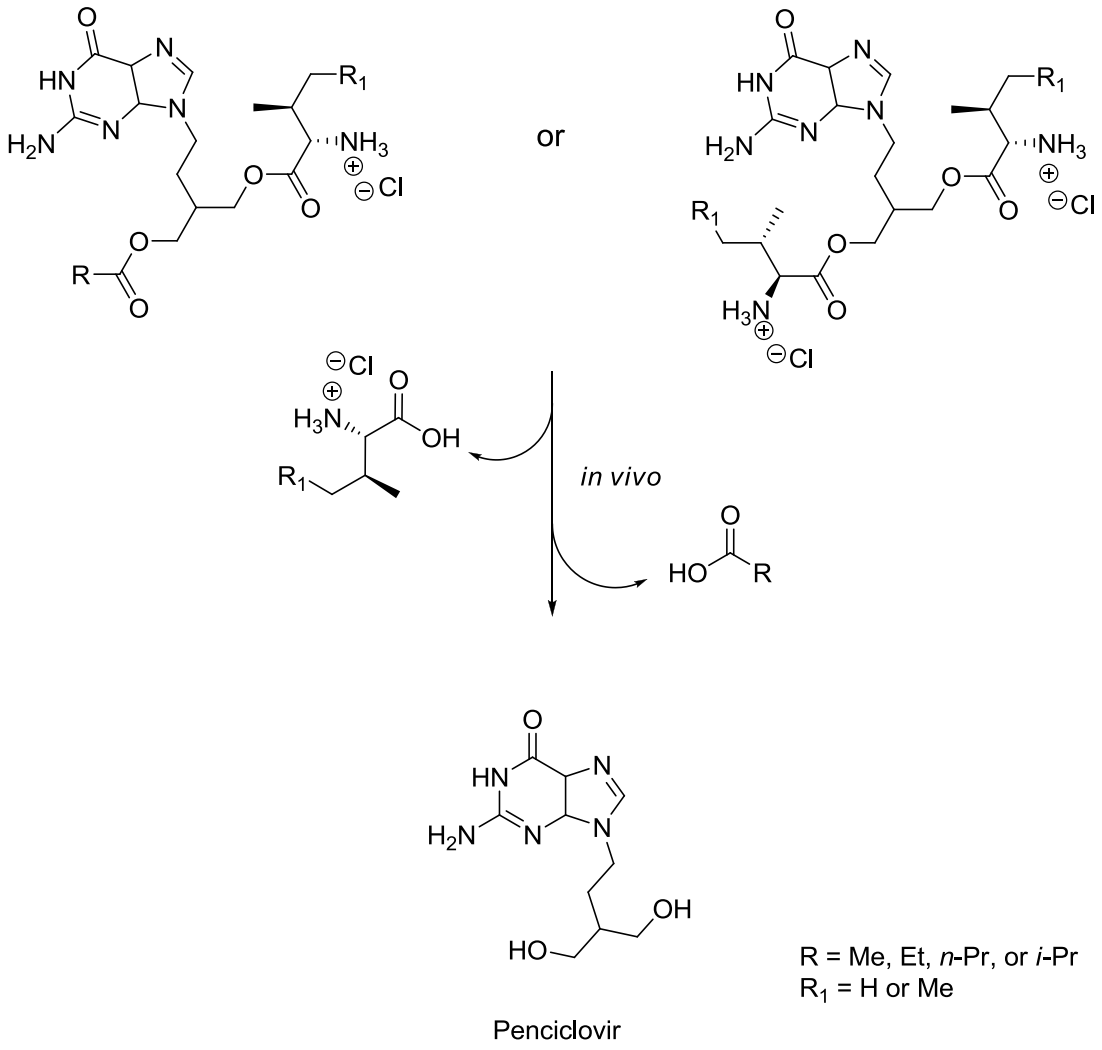

Figure 1.13 Generation of Penciclovir from amino acid/alkyl ester and di-amino acid ester prodrugs. Adapted from (Kim, Lee et al. 1996).

Since the PCV molecule is symmetric about the carbon connecting the free hydroxyl groups, this chemistry was easily achieved with traditional coupling methods to afford the desired compounds; however, unexpected racemization of the α-carbon was encountered in the Cbz-approach for reasons that are not very clear. Each of the prodrugs was found to be highly water soluble and to have a stability profile that was suitable for oral delivery at physiologically-relevant pH

values (pH 1.0, 6.0, 7.4, and 8.0). The oral bioavailability of the prodrugs was compared to that of PCV in ICR mice following 48 hours of urine collection, and it was observed that *O*-acetyl-*O*-L-valylpenciclovir achieved the highest systemic exposure of PCV with a fourfold increase over PCV. Importantly, the bioavailability of PCV from the *O*-acetyl-*O*-L-valylpenciclovir prodrug was not significantly different than that observed for the FDA-approved FCV, which bodes well for the amino acid ester approach in the case of PCV. The other prodrugs also afforded improved bioavailability of PCV as compared to the parent compound; however, none of them showed delivery comparable to that of FCV. In vitro anti-HSV-1 activity assays were less encouraging with EC_{50} values for prodrugs spanning a range of fourfold less than PCV to more than tenfold less; however, the authors note that partial hydrolysis in the test system could have been the problem. Overall, the L-valinyl promoiety theme for acylnucleoside antiviral medications is also applicable to PCV.

Amino acid esters of floxuridine

Floxuridine (FU) is a fluorinated nucleoside anticancer drug derived from a pyrimidine scaffold that is used in the treatment of colorectal and metastatic cancers (Kemeny, Huang et al. 1999). Like other nucleoside anticancer agents, FU exhibits considerable oral bioavailability problems. Therefore, it is dosed as an intravenous infusion.

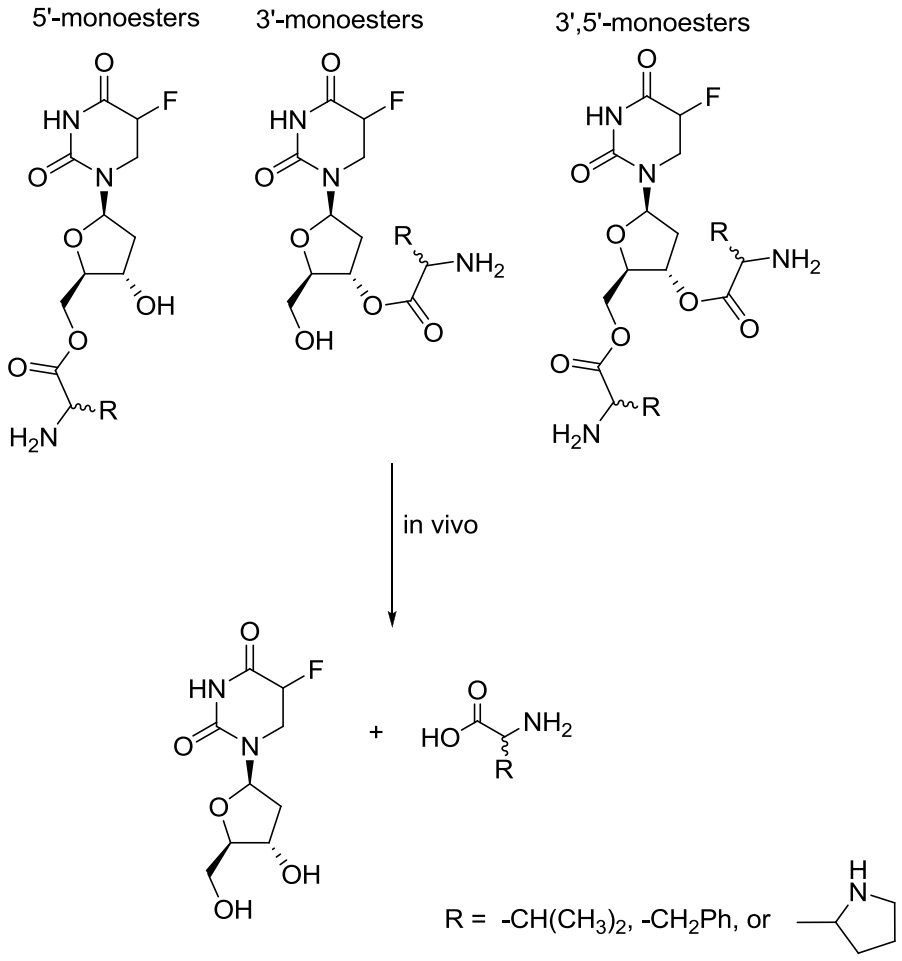

Figure 1.14 Generation of floxuridine and an amino acid from amino acid esters of floxuridine. Adapted from (Vig, Lorenzi et al. 2003).

In terms of prodrug design, FU has two available and nonequivalent hydroxyl functional groups which can be exploited as acylation handles (**Figure 1.14**). Accordingly, in a recent publication, both of these positions were derivatized into amino acid esters to determine the rate of prodrug hydrolysis in Caco-2 cell homogenates (Vig, Lorenzi et al. 2003). First, the effect of amino acid promoiety structure on hydrolysis rate was assayed using phenylalanine (Phe), valine (Val),

and proline (Pro). Second, D- and L-forms of Phe and Val were prepared and assayed to determine the effect of stereochemistry on hydrolysis rate. Finally, the authors determined the effect of esterification site on hydrolysis rate using 3'-monesters, 5'-monoesters, and 3',5'-diester prodrugs of FU. In all cases, the rate of prodrug hydrolysis in Caco-2 cell homogenates was compared to a pH 7.4 phosphate buffer to appreciate the rate acceleration afforded by enzymatic catalysis in the Caco-2 biological medium.

The structure of the promoiety had a big impact on hydrolysis rate in buffer. At pH 7.4, monoesters of Pro hydrolyzed approximately fourteen times faster than monoesters of Val and nearly ten times faster than monoesters of Phe. However, in buffer there was no significant effect of stereochemistry or site of esterification on the rate of hydrolysis, as expected.

The enzymatic environment of Caco-2 cell homogenates unveiled a significant effect on the rate of prodrug hydrolysis from all three of the variables tested, which is right in line with what should be observed. L-Val monoesters exhibited the longest half lives compared to L-Phe and L-Pro, and the L-forms of the promoieties imparted eleven to seventy-five times faster rates of hydrolysis over D-forms, depending on the site of esterification. There was no particular advantage to be realized by 3',5'-diester prodrug strategy, as these compounds were generally less stable in buffer than their monoester counterparts. Overall, it was found that the 5'-Valyl ester prodrug of FU is comparable in stability to the two commercial antiviral prodrugs VACV and VGCV which were tested under the

same conditions. Again, the L-Valyl promoiety is of probable utility in the design of an amino acid ester prodrug of FU.

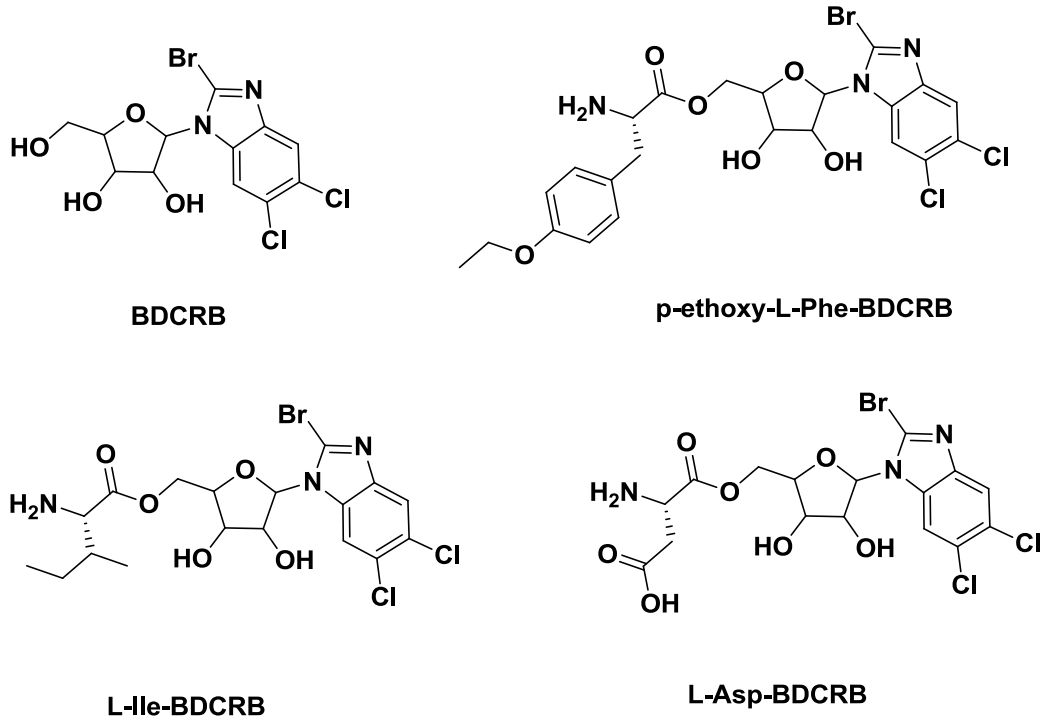

Figure 1.15 Structures of most promising BDCRB amino acid prodrugs. Adapted from (Lorenzi, Landowski et al. 2005, Song, Vig et al. 2005).

2-Bromo-5,6-dichloro-1-(*β*-D-ribofuranasyl)-benzimidazole (BDCRB, **Figure 1.15**) is a member of a class of compounds designed to target human cytomegalovirus (HCMV) replication. This particular ribonucleoside suffers from poor oral bioavailability due to hydrophilicity and metabolic instability of the *N*-glycosidic

bond. Accordingly, the compound is rapidly destroyed upon IV administration by *N*-glycosidic bond cleavage. Through analogues synthesis and testing, it has been demonstrated that this bond can be stabilized *in vivo* when the 2-Bromo substitutent is replaced by an isopropyl amino group (maribavir). Also, two of the enzymes responsible for the catalytic cleavage of the *N*-glycoside have been identified as 8-oxoguanine DNA glycosylase (OGG1) and *N*-methylpurine DNA glycosylase (MPG) (Lorenzi, Landowski et al. 2006). "Bioevasion" prodrug design has therefore been a key focus with this compound (Lorenzi, Landowski et al. 2005).

Since hPEPT1 has been shown to increase absorption of amino acid ester prodrugs via facilitated diffusion, recent work was aimed at investigating amino acid promoiety derivitization at the 5'-hydroxy position of the ribose sugar moiety of BDCRB to determine if enhanced hPEPT1 substrate affinity could be achieved (Song, Vig et al. 2005). In a follow up study, stabilization of the glycosidic bond *in vivo* by amino acid ester prodrug design was also investigated (Lorenzi, Landowski et al. 2005).

With regard to hPEPT1, the prodrugs were assayed for their ability to inhibit [^{3}H]Gly-Sar uptake in HeLa cells that overexpress hPEPT1, and it was found that amino acid promoieties with aromatic, aliphatic, and acidic side chains showed the best affinity for hPEPT1 compared to BDCRB and VACV. The lysinyl and prolinyl prodrugs had worse affinity for the hPEPT1 transporter than BDCRB alone or VACV. Of the D-amino acid forms that were tested, none of them showed enhanced affinity compared to BDCRB itself (which is oddly a good

substarte for hPEPT1), and the best prodrug in this series was actually *p*-ethoxy-L-Phe-BDCRB (**Fig. 1.15**). The latter material possesses a non-standard amino acid promoiety, so it could possibly have toxicity issues associated with its clinical use. The second best affinity for hPEPT1 was observed with L-Ile-BDCRB (**Fig. 1.15**).

In later experiments, the *in vitro* and *in vivo* stabilities of the amino acid ester prodrugs were assayed, and the hPEPT1 affinity studies were expanded to functional Caco-2 uptake studies (Lorenzi, Landowski et al. 2005). In the presence of human OGG1 (hOGG1) and murine MPG (mMPG), the glycosidic bond of all the BDCRB amino acid esters was significantly more stable than that of parent BDCRB. With the exception of the L-lys and L-Pro prodrugs, the amino acid esters were not substrates for the DNA repair enzymes.

In the enzymatic milieu of mouse liver and intestine homogenates, the prodrugs showed *N*-glycoside metabolic stability that was rate-limited by hydrolytic conversion of prodrugs to BDCRB. Therefore, further evidence was observed to suggest a protective role of amino acid ester derivatization on the parent drug.

Functional Caco-2 uptake studies were also conducted to give meaning to the original observations made in hPEPT1 affinity assays. The L-Ile prodrug performed the best. However, none of the prodrugs performed as good as BDCRB itself, which is oddly enough a good substrate for hPEPT1.

Tests for antiviral activity and cytotoxicity, when combined with the Caco-2 cellular uptake studies, hOGG1 and mMPG stability studies, and liver and

intestinal homogenate stability studies led to the discovery that the most promising “bioevasive prodrug” for pharmacokinetic analysis was L-Asp-BDCRB (**Fig 1.15**). When dosed in mice by oral gavage, and compared to BDCRB, the L-aspartyl prodrug exhibited five-fold enhancement in half-life, which confirmed a bioevasive mechanism of *N*-glycoside protection. Both the C_{max} and AUC of BDCRB following dosing with the L-aspartyl prodrug increased by a factor of approximately 1.5 as compared to dosing with the parent drug. Overall, these data suggest the potential for increased bioavailability and prolonged delivery of BDCRB via the L-Asp-BDCRB prodrug. It is also worth noting that the free carboxylate side chain of aspartic acid is situated in perfect position for a kinetically-favored 5-membered cyclization on the ester bond of this prodrug. The latter can lead to kinetic instability of the prodrug in various pH environments in the body; however, in the case of L-Asp-BDCRB, this appears to be a non-issue. To make a direct correlation to the work detailed in this dissertation, the aspartic acid prodrug of NTXOL coupled at the 6-OH position was extremely unstable (**see Chapter 3**), and it could not be isolated in pure form. Clearly, the stability of amino acid esters depends just as greatly on the drug moiety as it does the promoiety. These disparate stability profiles are of particular interest to medicinal chemists who will design amino acid ester prodrugs of other promising drug molecules in the future.

Amino acid amide prodrugs of 1-aryl-3,3-dimethyltriazene antitumor agents

Dacarbazine (**Figure 1.16**) is an anticancer drug that is typically employed for the treatment of malignant melanoma. It is supplied by IV injection under the supervision of a physician. In the United States, dacarbazine is available as the generic, or under the trade name DTIC-Dome®. The mode of action of dacarbazine involves a biotransformation process which dealkylates the 3-*N,N*-dimethyltriazene moiety to the monomethyltriazene. The latter is an alkylating agent that can methylate DNA and RNA. Referring to **Figure 1.17**, 1-Aryl-3,3-dimethyltriazenes (**1**) also possess antitumor activity due to their ability to alkylate DNA (Carvalho, Iley et al. 1998, Perry, Carvalho et al. 2009). Upon presentation to cytochrome P450 enzymes, phase I metabolism at the 3-methyl position of the triazene moiety results in the formation of a hydroxymethyltriazene intermediate (**2**) that is unstable under aqueous physiological conditions. Following the loss of the hydroxyl proton, a molar equivalent of formaldehyde is liberated from the molecule with the resultant formation of a molar equivalent of the 3-desmethyl triazene (**3**).

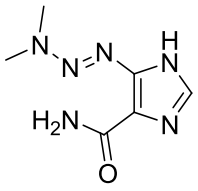

dacarbazine

Figure 1.16 Structure of dacarbazine.

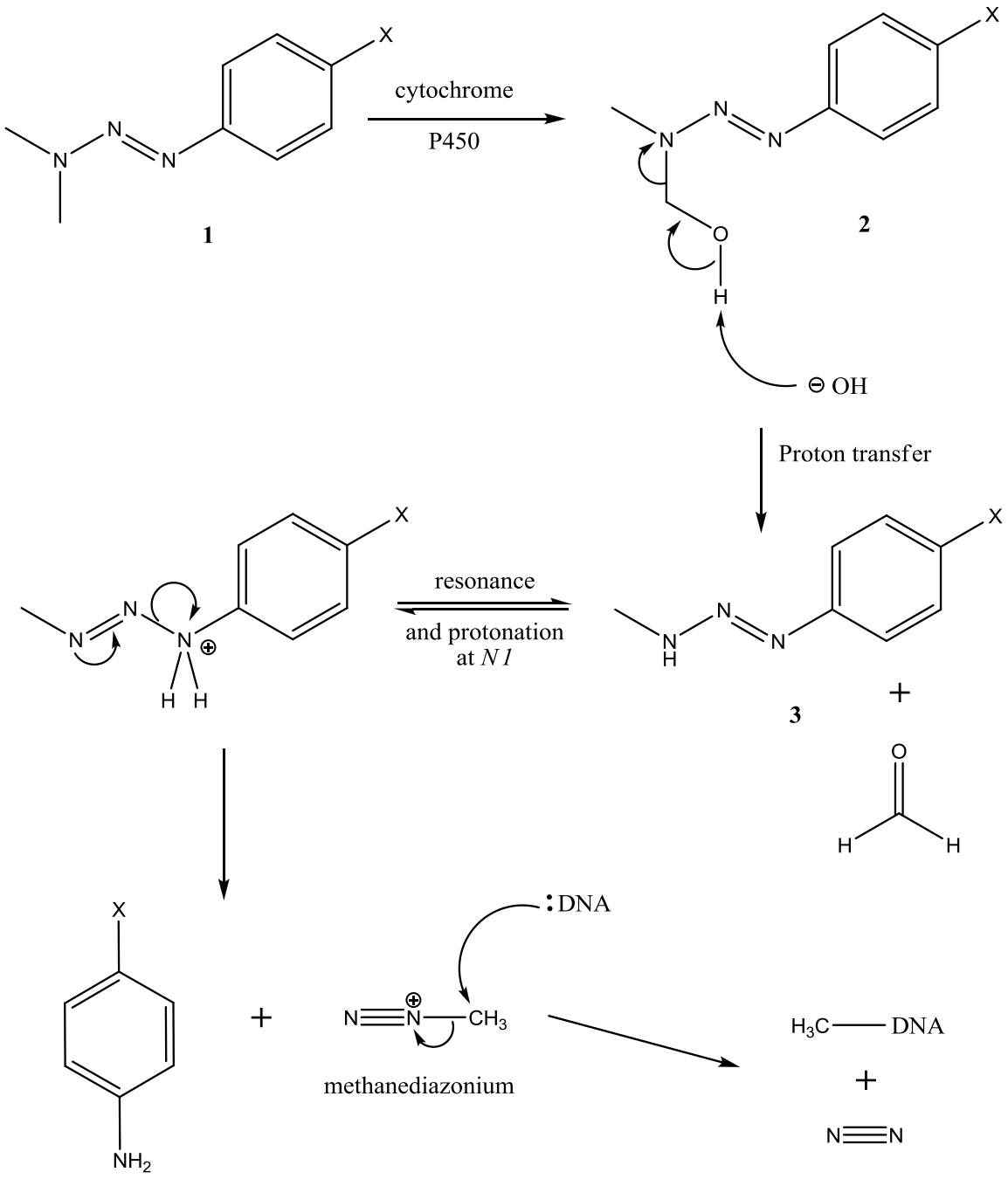

Figure 1.17 Mode of DNA alkylation by 1-aryl-3,3-dimethyltriazenes. Adapted from (Perry, Carvalho et al. 2009).

Subsequent protonation of the 1-nitrogen of the triazene moiety sets up the elimination of an aniline leaving group, and the remaining methanediazonium ion alkylates DNA following nucleophilic attack on the methyl group by DNA. Nitrogen gas that is liberated in the alkylation step ensures that the reaction is entropically driven to completion.

For the following discussion, refer to **Figure 1.18**. The CYP450 biotransformation is not always efficient. Indeed, dacarbazine is known to suffer from poor metabolic conversion of less than 20%. Therefore, along with the investigation of new derivatives that lack the imidazole core, prodrug strategies have been employed on triazenes in order to afford functional monomethyltriazene alkylating agents. With regard to amino acid promoieties, aminoacyltriazenes have shown promise as a means to avoid the oxidation step that normally affords the functional therapeutic agents in vivo (Carvalho, Iley et al. 1998).

Kinetics studies of the aminoacyltriazene prodrugs in isotonic phosphate buffer (pH 7.7) revealed hydrolysis rates on the order of 26 – 180 minutes when the amino acid moiety was not derivatized as an *N*-acetamide. Acetylation of the amino functional group of alanine in the compound R,R' = CH_3, X = CN led to a 3.4-fold increase in stability compared to the free amine. In terms of 80% human plasma hydrolysis (pH 7.7), when R = CH3 and X = Br or CH_3, the free amine prodrugs had 3 – 4 times greater stability than in buffer, suggesting that plasma protein binding protected these compounds from enzymatic hydrolysis.

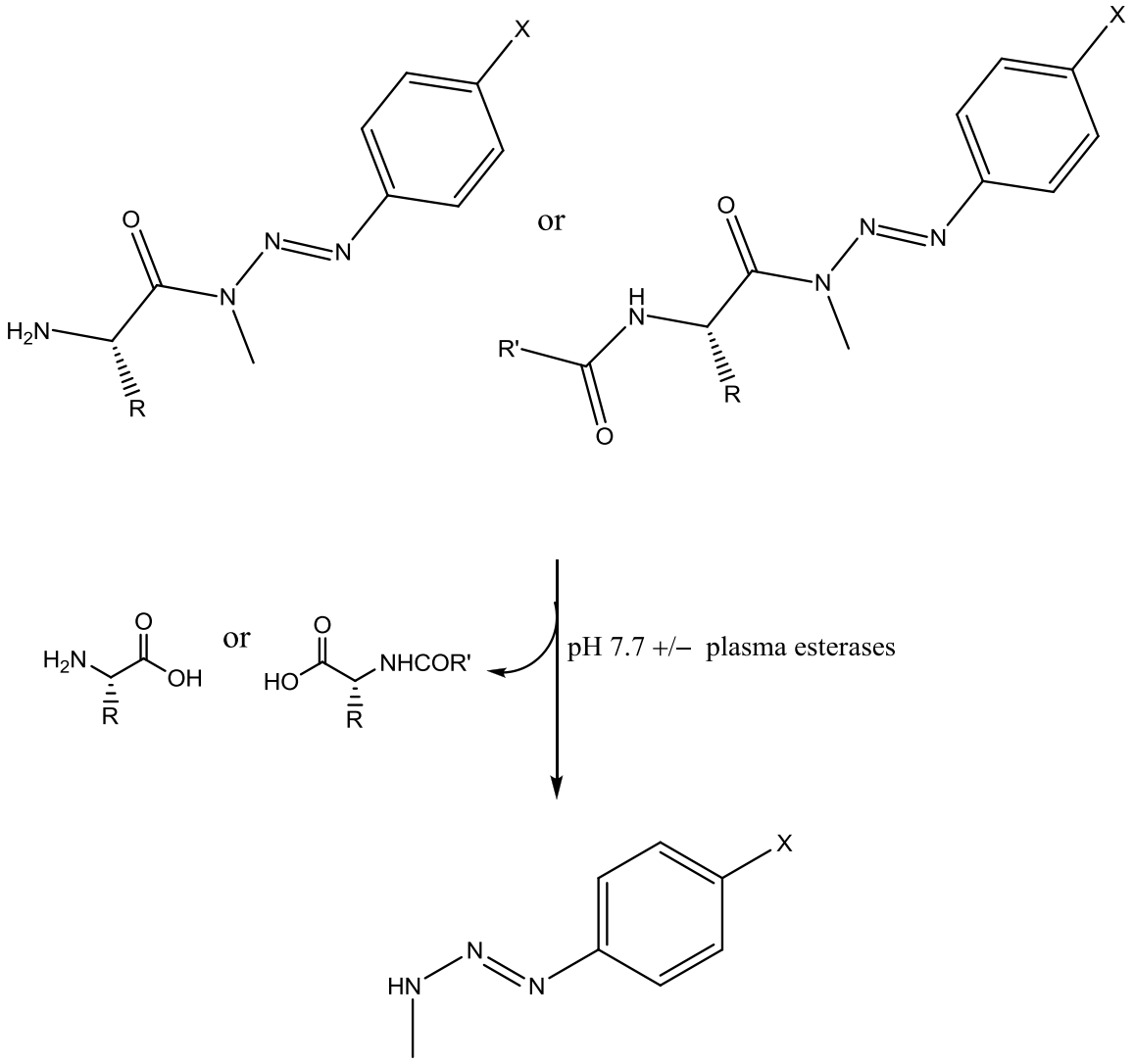

monomethyltriazene alkylating agent

R = H, CH_3 except for β-ala which is N_3-$COCH_2CH_2NH_2$
R' = CH_3, CH_2CH_3, $CH_2CH_2CH_3$, Ph
X = CN, $COCH_3$, COOEt, $CONH_2$, Br, or CH_3

Figure 1.18 Bioconversion of aminoacyl-1-aryl-3,3-triazene and 3-[α-(acylamino)acyl]-1-aryl-3-methyltriazene prodrugs to monomethyltriazene alkylating agents. Adapted from (Carvalho, Iley et al. 1998) and (Perry, Carvalho et al. 2009).

In the case of the free amine compound R,X = CH_3, the magnitude of hydrolytic protection was definitely found to depend on the concentration of human serum albumin spiked to working isotonic phosphate buffer solutions, which supports a plasma protein binding mode of hydrolytic protection. For the most part, the differences in phosphate buffer hydrolysis and plasma hydrolysis within this series of compounds were not extreme (i.e. the prodrugs were not good substrates for plasma esterases). However, the free amine compound where X = CN and the promoiety was β-alanine showed a 3.4 –fold fatser rate of 80% human plasma hydrolysis as compared to phosphate buffer, and the *N*-acetyl compound where R,R' = CH3 and X = CN was 15.1 times more stable in phosphate buffer than in 80% human plasma. Therefore, within this series of potential antitumor prodrugs, β-alanine and *N*-acetylalanine proved to be the best promoieties, and the *N*-acetylalanine prodrug had the best bioconversion of all prodrugs tested ($t_{1/2}$ = 41 minutes in human plasma compared to 53 minutes for the β-alanine prodrug). This preliminary work showed that an acylated amino acid promoiety was a better substrate for hydrolytic plasma enzymes than the natural free amino acid congeners tested.

To note some interesting parallels to these findings, the reader is referred to **Chapter 6** of this dissertation, in which β-alanine was found to be the best promoiety to use in order to prepare a prodrug of NTXOL. Within the NTXOL prodrugs series, there was also evidence of possible plasma protein binding that protected the valanyl and isoleucinyl prodrugs from enzymatic hydrolysis. Again, it is not possible to determine *a priori* which molecular features will ultimately

result in the best prodrug-like behavior under physiological conditions. Therefore, a structure-reactivity study is always called for in prodrug design.

Following the observation that *N*-acylation of the amino acid promoiety can afford better plasma enzyme targeting, more 3-[α-(acylamino)acyl]-1-aryl-3-methyltriazenes were also assayed (Perry, Carvalho et al. 2009). The goal was to investigate the utility of these potential prodrugs as compounds that are more formulation stable, but still adequately unstable in human plasma to be considered prodrugs. Each of the *N*-acylated compounds showed kinetics in human plasma 3-15 times faster than in buffer, which is in contrast to the free amino acid materials from the previous study. Apparently, the *N*-acylated compounds were substrates for esterase enzymes while the free amino compounds were not. With regard to simple chemical hydrolytic stability in pH 7.7 buffer, where the X substituent was electron withdrawing (i.e. –CN) the rate of hydrolysis was accelerated, and where the R-group of the *N*-acyl amino acid carrier was bulky (i.e. valine), the reaction rate was up to greater than ten times slower. The substitution R' of the *N*-acyl moiety contributed significant, but small reaction rate effects. In most cases, the rate enhancement obtained by plasma enzymes was good enough to impart prodrug-like character to the compounds, regardless of substitution; however, where R,R',X = CH_3, the compound was too stable to be a useful prodrug.

The triazene moiety is an interesting functional group. When it is acylated, as in amino acid prodrugs, an amide is generated. Normally, amides have very different stability characteristics as prodrugs than do esters; however, it has been

adequately shown that amino acid amide and *N*-acyl amino acid amide prodrugs of triazenes exhibit stability characteristics that are more characteristic of amino acid ester prodrugs (Carvalho, Iley et al. 1993), (Carvalho, Iley et al. 1998), (Iley, Ruecroft et al. 1989). Overall, these compounds show the promise of a potentially bright future as possible therapeutic agents in the war on cancer.

Amino acid ester prodrugs of benzocaine

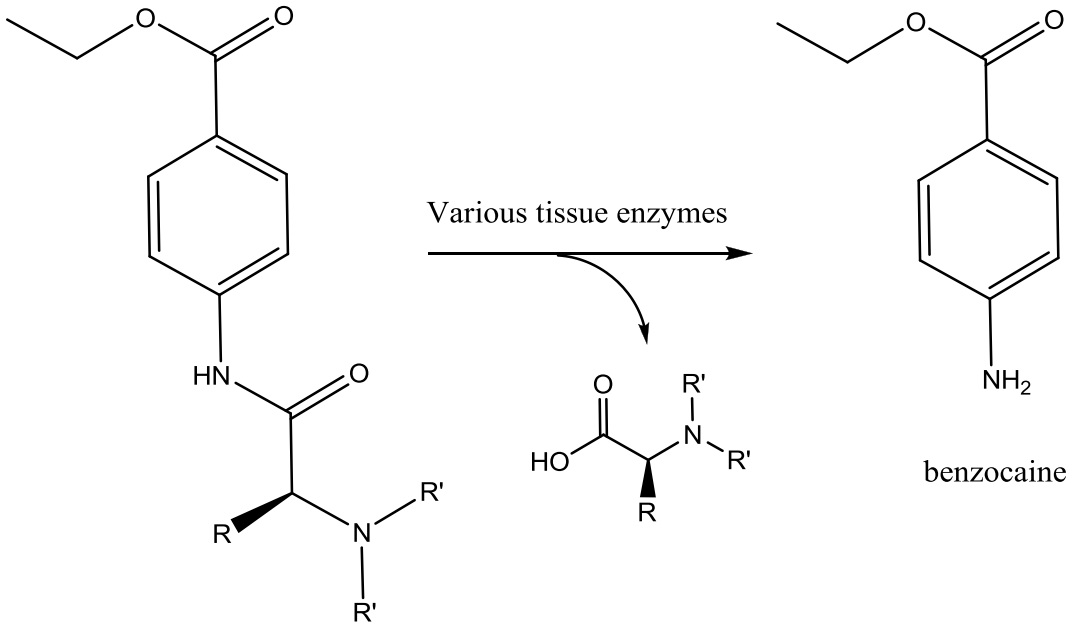

R,R' = H; R = H, R' = CH_3; R,R' = CH_3; R = H, R' = $CH(CH_3)_2$; R = H, R' = $CH_2CH(CH_3)_2$, R = H, R' = $CH_2CH_2COOCH_3$

Figure 1.19 Generation of benzocaine from amino acid amide prodrugs. Adapted from (Slojkowska, Krasuska et al. 1982).

Benzocaine (**Figure 1.19**) is a local anesthetic medication that is used in multiple over the counter medications in the United States. As one might expect from the structure, benzocaine is very water insoluble. The water insolubility of benzocaine limits its delivery to certain tissues, so an amino acid amide prodrug strategy has been investigated to determine if prodrugs of benzocaine may be designed as water soluble agents (Slojkowska, Krasuska et al. 1982). In this study, the authors prepared a number of prodrugs using the promoieties glycine, alanine, valine, leucine, dimethylglycine, dimethylalanine, and γ-methylglutamic acid. Each prodrug was assayed for hydrolytic rate in the presence of specific rat tissues, gastric and duodenal juices, pronase and other purified enzymes, and human serum. As would be expected, the rates of hydrolysis were found to vary widely depending on the specific tissue or biological fluid employed due to the different expression of enzymes between these various biological media. However, important insights can be gleaned from a study this thorough, as most prodrug analyses are done with buffer and plasma samples alone.

Adult male albino rats were sacrificed to obtain homogenates of various tissues, and a summary of the results follows. In rat kidney the leucine prodrug hydrolyzed the fastest with approximately 1.3 – 22 times the rate of any other prodrug; however, this trend did not hold in liver where the prodrugs were mostly similar in their rates of hydrolysis. Significant, but not dramatic, differences in hydrolysis rates were noted in other tissues (i.e. brain, heart, lung, stomach, small intestine, spleen, and duodenum) and in plasma, but the differences in rate were not higher than a factor of about 2 in most cases. Indeed, for all the

prodrugs, the rate of hydrolysis in kidney was much enhanced compared to the other tissues (1.72±0.02 – 38.17±0.98 nmol/min per mg of protein).

The prodrugs were fairly stable in duodenal juice. There was no degradation of any prodrug in gastric juice or in the presence of pepsin, trypsin, and chymotrypsin. However, pronase hydrolyzed the prodrugs remarkably faster than any of the tissue homogenates (340±50 – 19,900± 800 nmol/min per mg protein). In this case, the valine and alanine prodrugs were the best substrates for pronase. Alanylbenzocaine also showed the fastest rate of conversion to parent benzocaine in human serum while valylbenzocaine was only one third as rapid in conversion to the parent drug. The leucine, valine, alanine, and γ-methlyglutamic acid prdrugs all showed similar rates of hydrolysis in rat muscle homogenates which could be of potential therapeutic value (21 – 67 pmol/min per mg of protein). Leucinylbenzocaine exhibited the fastest muscular tissue release of benzocaine. Dimethylglycylbenzocaine was not a very good substrate for the enzymatic conditions in any case other than pronase, but dimethylalanylbenzocaine was the best substrate for enzymatic conversion in the lungs. Again, the theme is noted that structure means everything in prodrugs design, and that it is not possible to determine without thorough study which promoieties will result in the best prodrugs between different parent drugs and different target sites of delivery.

Amino acid esters of Quercetin

Quercetin is one of a number of plant polyphenols implicated in an antioxidant protective role against cellular reactive oxygen and reactive nitrogen oxide species. One major problem with polyphenols is their poor bioavailability which results from phase II metabolism by enterocytic transferases. In order to maintain intestinal absorption and solubility while simultaneously exploring the ability of prodrugs to avoid phase II conversion, amino acid esters of quercetin have been prepared and assayed (Biasutto, Marotta et al. 2007). Referring to **Firgure 1.20**, the 3'-position of quercetin was selected for amino acid ester derivitization; however, the authors note that some 4'-substitution was unavoidable, and the two acylated products could not be separated. Nonetheless, stability studies were conducted on the compounds in order to find suitable substrates for MDCK-1, MDCK-2, and Caco-2 transport studies.

As might be expected, the unprotected amino acid ester salts were too unstable for transport studies at pH values that would support cell function (except for where X = -Ph-). This was observed regardless of the substitution on the remaining phenolic hydroxyl groups of quercetin (R = H or $COCH_3$). Also, the Boc-protected amino acid esters of quercetin that had unacylated phenol groups were rapidly degraded in buffer. These compounds all showed hydrolysis half lives on the order of (0.07 – 119) x 10^{-2} s! Only Boc-protected amino acid esters with fully acylated phenols on quercetin proved to be stable enough for the transport studies, as would be expected for phenolic amino acid esters that are

known to be unstable (see **Chapter 6** on amino acid esters of 3-*O*-NTX for further evidence of instability of phenolic esters).

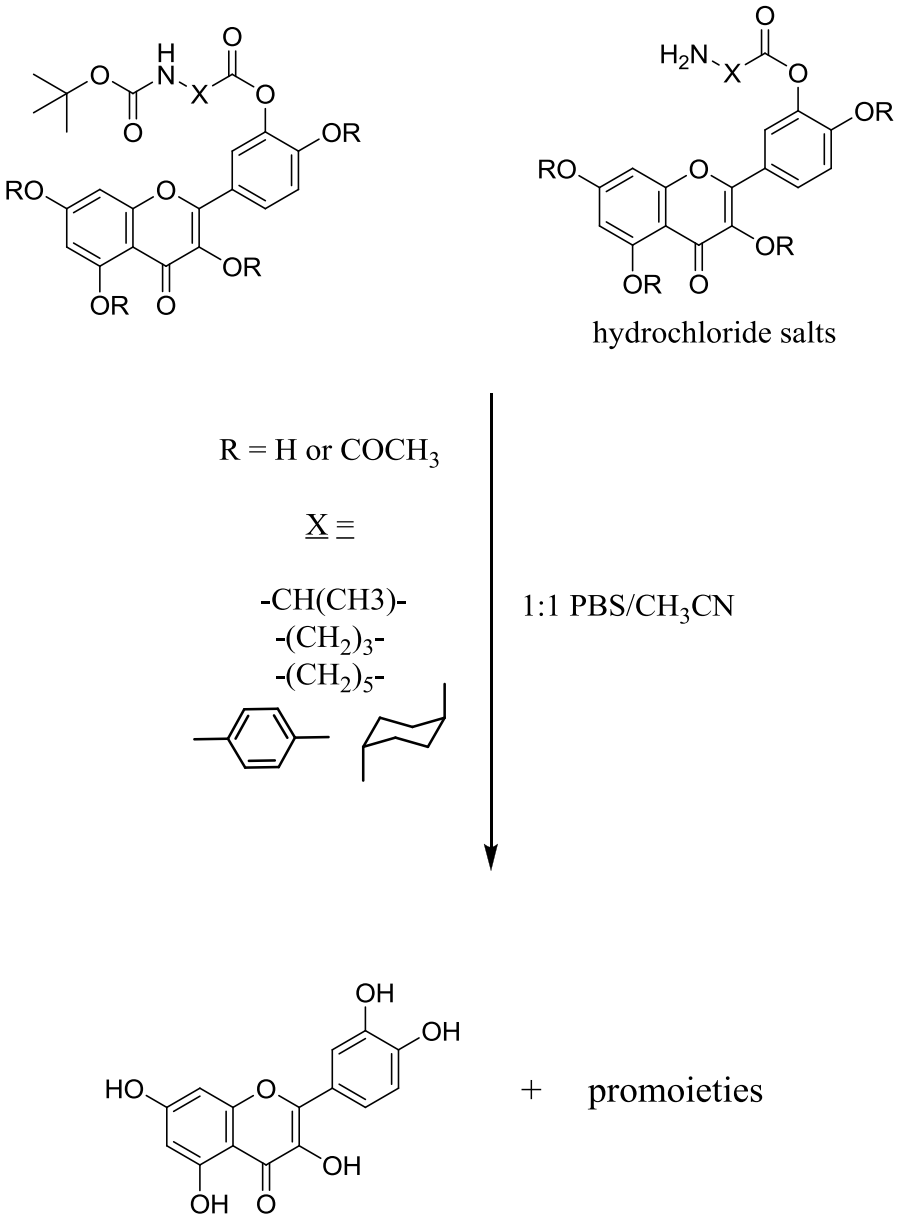

Figure 1.20 Generation of quercetin from quercetin prodrugs in 1:1 PBS/CH_3CN. Adapted from (Biasutto, Marotta et al. 2007).

Of the compounds found to be stable enough for cellular transport studies, only those with R = $COCH_3$ and X = $-CH(CH_3)-$, $-(CH_2)_3-$, or $-(CH_2)_5-$ were more soluble in Hank's salt buffer than quercetin itself, so these prodrugs were examined for phase II conversions in cellular media. The fully acetylated 3'-*O*-Boc-alanyl quercetin prodrug was found to contain 4.2% more quercetin on the basolateral side of Caco-2 monolayers compared to 1.0% that was observed following transport of quercetin itself. The Boc-γ-aminobutryic acid prodrug and the X = $-(CH_2)_5-$ homologue (both fully acetylated) showed less phase II protection in Caco-2 cells in terms of basolateral quercetin observed after 6 hours (2.6 & 2.5% respectively). Quercetin sulfate and quercetin methylsulfate were significantly reduced in every case. In MDCK-1 and MDCK-2 cells, the basolateral concentrations of quercetin from apically loaded prodrugs were generally less than that observed from apically loaded quercetin; however, significant concentrations of diacetylated and monoacetylated quercetins were found in the basolateral compartment after 6 hours, and it is to be assumed that the prodrug intermediates would further degrade to quercetin over time. Indeed, they may represent slow-release forms of the parent drug in these cell lines. Also, in the MDCK-1 and MDCK-2 cell lines where mono- and diacetylated quercetins were observed, no phase II quercetin sulfate and quercetin methylsulfate was detected. Overall, these data suggest that esterification of polyphenols with Boc-amino acids and acetate blocking groups can lead to improved bioavailability by protecting phenols from phase II conjugation during enterocytic translocation.

Amino acid esters of metronidazole

Metronidazole is an antimicrobial agent that is often used to treat anaerobic bacterial infections. The drug is marketed in the United States under numerous trade names (i.e. Flagyl®) and as generic as well. In terms of formulations, the drug is supplied orally, as a lotion, as a vaginal gel, and in intravenous applications. It is dosed either as free base or as the hydrochloride salt, depending on the particular delivery form.

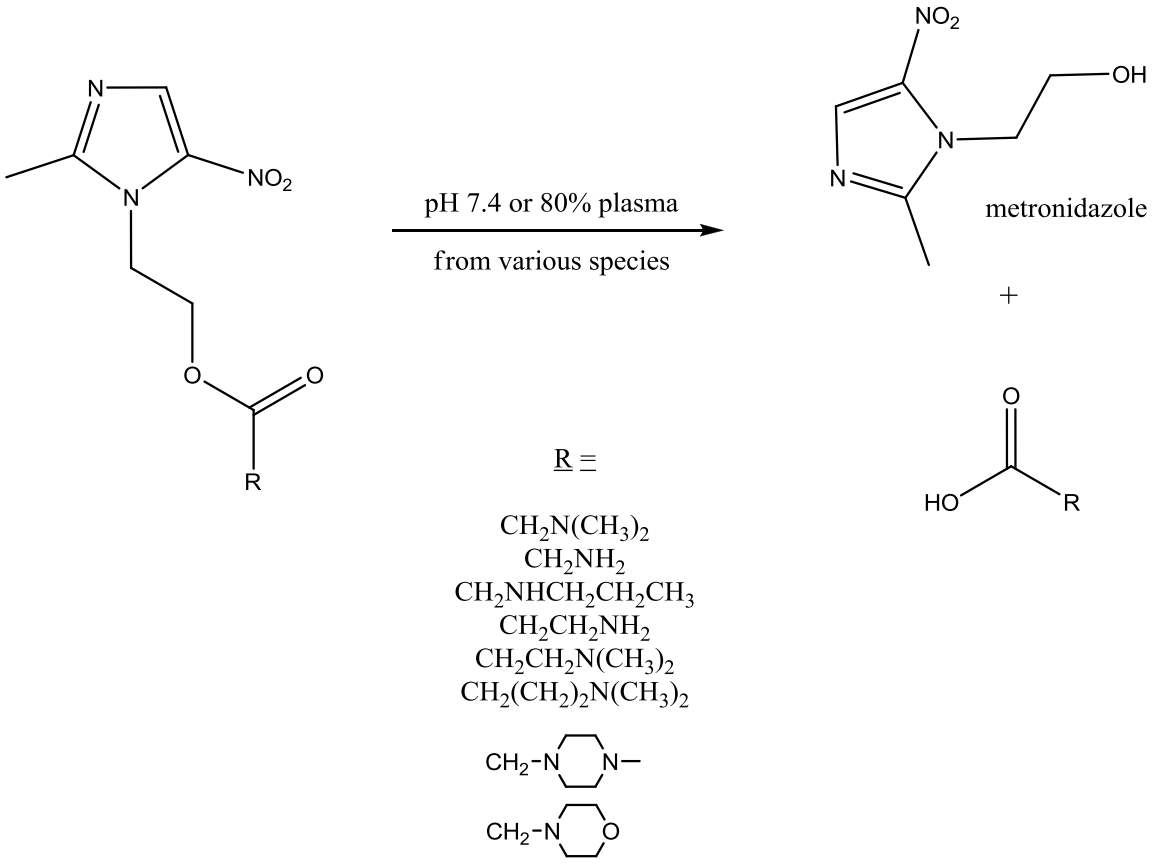

Figure 1.21 Generation of metronidazole from amino acid ester prodrugs under physiological conditions. Adapted from (Bundgaard, Larsen et al. 1984).

In the early days of amino acid ester prodrug design, Bundgaard and others looked at metronidazole as a potential drug for prodrug development, because intravenous delivery of the drug was hampered by poor aqueous solubility (roughly 1% w/v @ 25°C). Indeed, parenteral injection of the compound was not possible at the time, and only large volume infusions were available (Bundgaard, Larsen et al. 1984). Referring to **Figure 1.21**, it can be seen that Bundgaard *et al*. chose to use amino acid residues, with the exception of glycine, that are not members of the 20 endogenous examples. To a large extent, this was done for basic structure-reactivity analysis, and to avoid protecting group chemistry. At the time, little work had been done with amino acid prodrugs, and this is one of the pioneer works in the area.

The results obtained are very interesting. All of the compounds were hydrochloride end products with solubilities > 20% w/v at 20°C; however, the *N,N*-dimethylglycinate prodrug had the best combination of solubility (> 50% w/v @ 20°C) and pH 7.4 stability (250 min) with a rapid hydrolytic conversion to metronidazole in 80% human plasma (12 min). For the remainder of the prodrugs, these values varied by a large degree.

For instance, removal of the protonated amino group away from the ester carbonyl by one methylene unit, as in the dimethylaminopropionate prodrug, actually resulted in one fifth the pH 7.4 stability, but a nearly 4-fold increase in plasma stability as compared to the dimethylglycinate prodrug. In buffer alone, this is a bit counterintuitive. At pH 7.4, the dimethylamino moiety in both the dimethylglycinate and the dimethylaminopropionate (pKa ~ 9) prodrugs is

protonated like other amino acids, and one would expect a methylene spacer to diminish the electron withdrawing effect at the carbonyl of the ester, which would impart greater stability. Indeed, the pH 7.4 stability data of the primary amine prodrugs, glycinate and aminopropionate, were 115 min and 315 min respectively, accounting for a 2.7-fold increase in stability by comparison. One could posit a sterics argument here and suggest that the greater degrees of freedom obtained from moving the bulky methyl groups away from the center of nucleophilic attack in dimethylaminopropionate afforded accelerated access to the electrophilic carbon as compared to the dimethylglycinate prodrug. No matter the case, this is another example of why prodrugs have to be carefully assayed for their behavior under physiological conditions in order to find the best balance of stability and physiochemical properties.

The other prodrugs were either too stable in plasma or too unstable in buffer to be considered for further study. However, the 4-morpholinoacetate prodrug could be considered a promising candidate with only 2.5-fold greater stability than the dimethylglycinate prodrug in 80% human plasma ($t_{1/2}$ = 30 min vs. 12 min) and approximately 7.5-fold greater stability at pH 7.4. Nonetheless, metronidazole dimethylglycinate (MDMG) was found to be the best prodrug in this work.

MDMG hydrolysis kinetics studies in 80% plasma samples prepared from dog, rat, mouse, rabbit, and guinea pig revealed large differences in interspecies hydrolysis rates ($t_{1/2}$ = 1.9 min – 25 min) which is to be expected given the difference in genetics between these species. More importantly, this suggests

that a prodrug intended for human use should be assayed for hydrolysis kinetics in human plasma.

In a follow up cross-over study using two beagle dogs, metronidazole and MDMG were administered by IV injection in order to examine the *in vivo* prodrug behavior of MDMG as an injectable dosage form (Bundgaard, Larsen et al. 1984). The half-lives of MDMG in the two dogs were 3 and 7 minutes compared to 25 minutes in 80% dog plasma. MDMG was quantitatively converted to metronidazole within 37 minutes, and the metabolism and elimination profiles for metronidazole were similar whether dosed as parent drug or as prodrug. These data taken together suggest that MDMG could be a potential intravenous prodrug of metronidazole with greater than 50-fold increased solubility over parent drug.

In vitro antimicrobial activities of metronidazole esters containing glycine (R = CH_2NH_2), phenyalanine (R = CH-(CH_2Ph)-NH_2), leucine (R = CH-(CH_2 (CH_3)$_2$)-NH_2), and glycine-glycine (R = $CH_2NHCOCH_2NH_2$) spacers bound to a dextran carrier moiety have been conducted using *Trichomonas vaginalis* in Kupferberg medium (Vermeersch, Remon et al. 1990). The phenylalanyl metronidazole ester (M-Phe) and the leucinyl metronidazole ester (M-Leu) were found to exhibit similar behaviors to parent drug in terms of end point viability (in hours) of *T. vaginalis* at drug concentrations equivalent to 1-30 µg/mL metronidazole. However, it is interesting to note that 4 hours was the end point of viability for all of the prodrugs and metronidazole at 30 µg/mL concentration, but the M-Gly and M-GlyGly prodrugs showed twice the time to inhibit cell growth at 10 and 20 µg/mL concentrations. Since the half lives of the prodrugs were very similar, it is

tempting to assume that the cell growth was stopped by evolved metronidazole; however, the M-GlyGly ester degraded at roughly twice the rate of the other prodrugs with the evolution of a diketopiperazine (as expected). These data are also complicated by the fact that several kinetic phenomena are involved in the end result. For instance, the diffusion of metronidazole into the trichomonad cells is one variable. Increase in the number of viable cells that can absorb drug over time is also a variable. Diffusion of prodrug into the cells is yet a third variable. Cellular-level hydrolysis of the prodrugs supplies another variable. Culture medium level hydrolysis of the prodrugs over time is a fourth variable (pH ~ 6). Finally, whether or not the diketopiperazine of the GlyGly moiety is also cytotoxic is a variable too. Clearly, one must proceed with caution in the interpretation of these data. It appears as though the two most lipophilic prodrugs may have permeated the cells in a similar fashion to metronidazole, while the M-Gly and M-GlyGly compounds did not. However, it cannot be concluded that the prodrugs were actually converted to free metronidazole inside the cells in the manner that this study was done, and the authors note that the mode of action of metronidazole is mainly due to an enzymatic reduction of the nitro group and the access of the nitro group to electron transport proteins in the microbial cell. Since this blocking strategy only serves to enhance water solubility for improved metronidazole delivery, and the nitro group is free, it is just as likely that the prodrugs have intrinsic antimicrobial activity as it is that the end points of viability were caused by metronidazole itself. Clearly, a more thorough investigation would be needed to sort out the shortcomings of this experimental design.

Amino acid prodrugs of sulfonamides

Prodrugs of carbonic anhydrase inhibitors (CAIs) were examined several decades ago before the advent of ophthalmic solutions like Trusopt® (dorzolamide, FDA approved in 1994) and Azopt® (brinzolamide, FDA approved in 1998). The CAIs originally were dosed in an oral or parenteral fashion, and they showed little utility in topical eye delivery for the treatment of glaucoma. As part of a program to investigate the potential of amino acid conjugated sulfonamides as prodrugs, the model compound *N*-methyl-*p*-toluenesulfonamide was exploited as a sulfonamide material for in vitro stability studies (Larsen, Bundgaard et al. 1988).

The substituted sulfonamide amine moiety as depicted in **Figure 1.22** is a dual prodrug design. The aminoacyl portion is degraded by simple chemical or enzyme-assisted hydrolysis to liberate the *N*-methylsulfonamide and a molar equivalent of the amino acid promoeity. Then the *N*-methylsulfonamide is expected to undergo demethylation in the biophase to release the parent sulfonamide (Maren 1956, Duffel, Ing et al. 1986).

The aminoacyl carrier instills hydrophilicity to the molecule that increases aqueous solubility in the ionized form. Otherwise, when unionized, lipophilicity of the compound is improved over the primary amine form. The methyl group also increases lipophilicity. These physiochemical properties in unison were thought to be a reasonable approach to improve permeation of the cornea for intraocular delivery which would in turn have possible therapeutic use in the treatment of glaucoma.

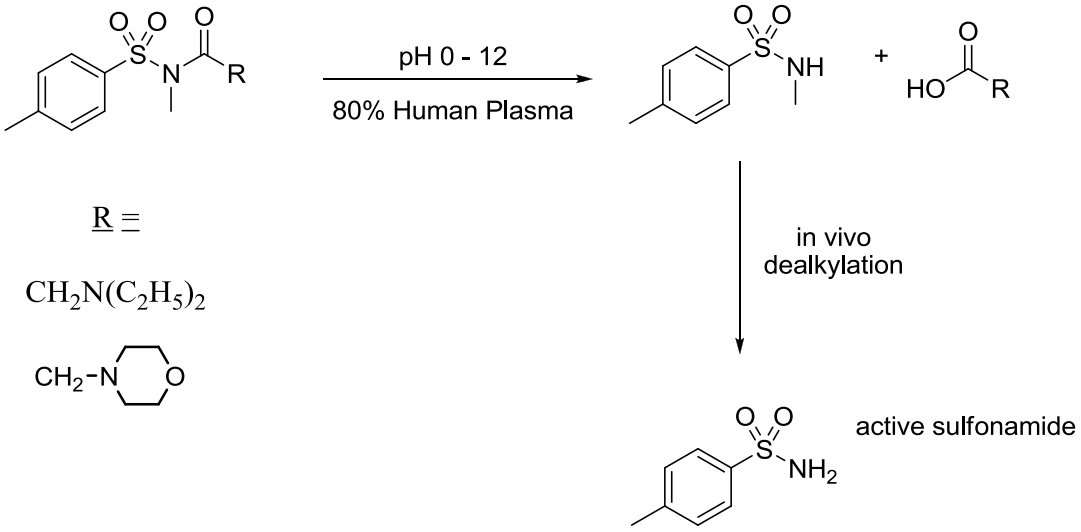

Figure 1.22 Generation of sulfonamides from *N*-methyl-*N*-aminoacylsulfonamide carriers. Adapted from (Larsen, Bundgaard et al. 1988).

The diethylglycine prodrug had a half-life at pH 4.0 of 4.3 days and 3.2 hours at pH 7.4. 80% human plasma enzymes cleaved the prodrug 3.2-fold faster than pH 7.4 buffer ($t_{1/2}$ = 1.0 h), indicating that the compound was a substrate for esterase enzymes. The 4-morpholinoacetate prodrug was much more stable, and unlikely to be a good prodrug candidate owing to its 6.8 hour half-life in 80% human plasma. Of course, since these prodrugs were intended for intraocular delivery, hydrolysis rates in aqueous humor would be of particular interest as well, and these values were not obtained in the study. Apparently, there was

also no follow up animal work to determine if these prodrugs actually improve corneal permeation over parent drug, and the authors note that the stability characteristics of these compounds, much like other amino acid-based prodrugs, warrant the possible need to use polymeric matrices or ophthalmic rods in order to achieve a formulation with a good shelf-life.

Amino acid prodrugs of saquinavir, indinavir, and nelfinavir

Saquinavir (Saq), indinavir (Ind), and nelfinavir (Nelf) are HIV protease inhibitors that are used in combination with HIV reverse transcriptase inhibitors. Saquinavir currently comes in two dosage forms. Invirase® is the mesylate salt, and it is supplied as a capsule or tablet and in different strengths depending on the prescription. Ritonavir (Norvir®) is often added to Invirase to improve its bioavailability. Another formulation of saquinavir (Fortovase®) has been discontinued. Indinavir (Crixivan®) is indinavir sulfate, and it comes as a capsule form in various strengths. Viracept® (nelfinavir mesylate) comes in several approved dosage forms (powder and tablet) of various strengths, and it is also taken orally. Any of the three drugs can be used in HAART (highly active retroviral therapy) as a means to battle HIV infection and AIDS. However, these compounds suffer from some pharmacokinetic shortcomings that limit their utility for absolute management of the HIV virus. For instance, viral replication has been observed to continue in the presence of these therapies, and the polytherapy regimens that include them, because poor penetration into the CNS and the lymphatic system allows a “sanctuary” reservoir for the HIV virus to be

established. Otherwise, resistance issues associated with the HIV virus also come into play. These problems are summarized in the references listed below.

It has been suggested that a prodrug approach may afford a solution to the CNS permeation problem. To approach this hypothesis, amino acid prodrugs have been synthesized and evaluated for their chemical stability, antiviral activity, Caco-2 cell transport, and P-gp transport. (Farese-Di, Rouquayrol et al. 2000, Rouquayrol, Gaucher et al. 2002, Gaucher, Rouquayrol et al. 2004).

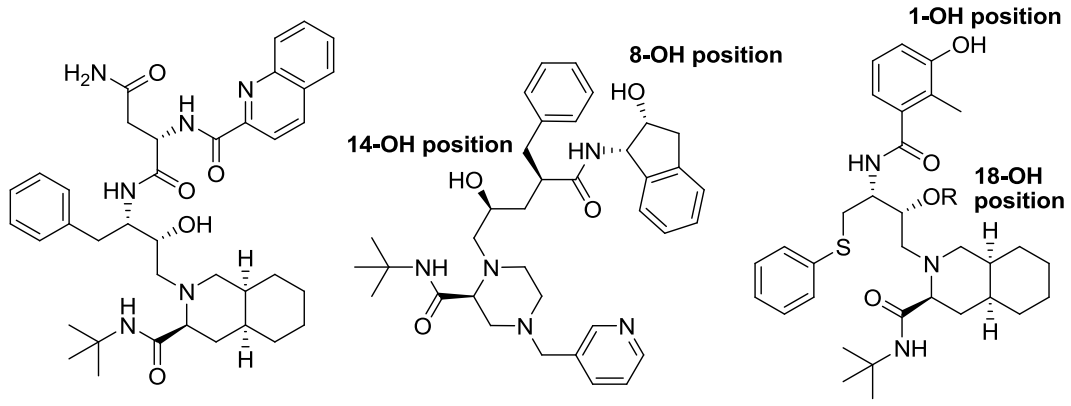

saquinavir (Saq) **indinavir (Ind)** **Nelfinavir (Nelf)**

Synthesis of amino acid prodrugs:

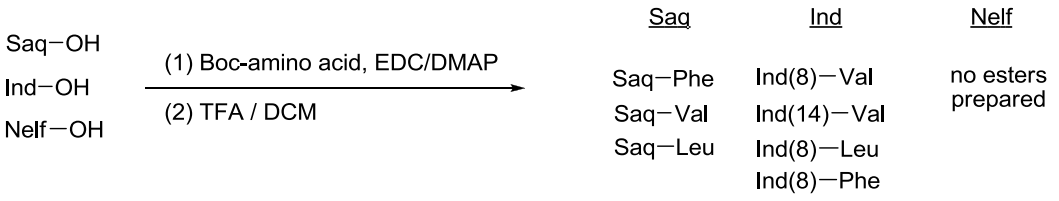

Figure 1.23 Synthesis of amino acid esters of saquinavir and indinavir. Adapted from (Gaucher, Rouquayrol et al. 2004).

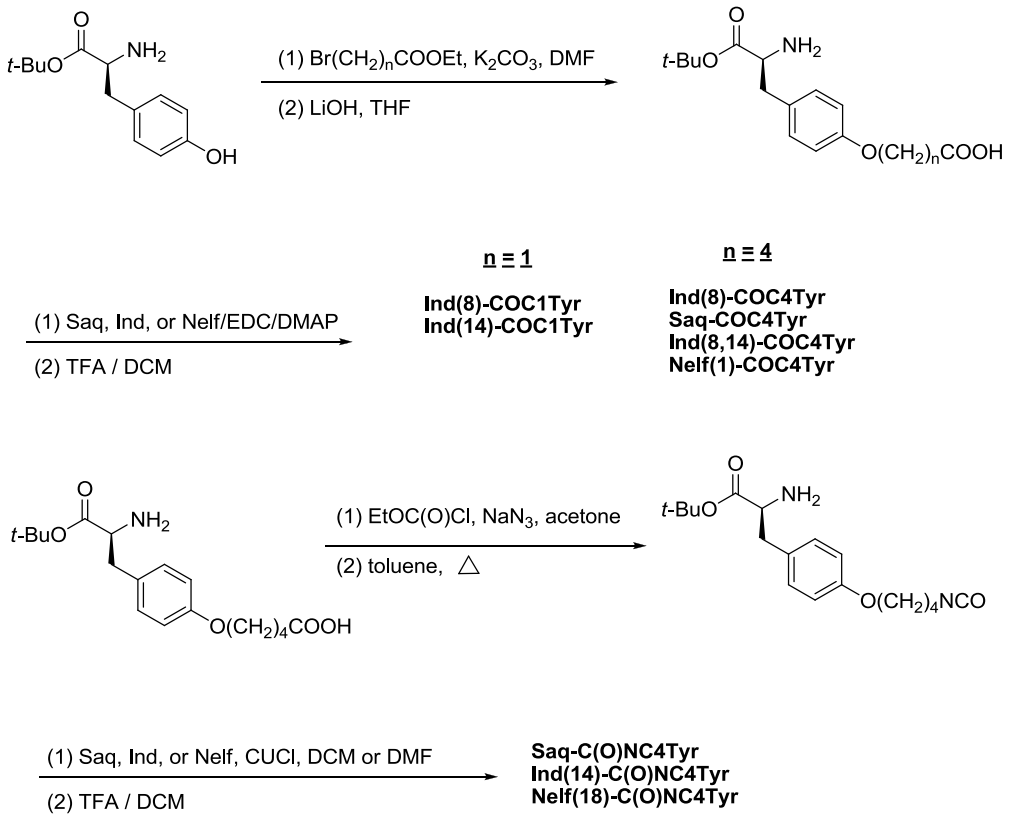

Figure 1.24 Synthesis of tyrosinyl derivative carbonates and carbamates of saquinavir, indinavir, and nelfinavir with spacer linkers n_{CH2} = 1-4. Adapted from (Gaucher, Rouquayrol et al. 2004).

The amino acid esters (**Fig. 1.23**) hydrolysis studies were conducted in buffer at pH 7.3 and 37 °C. The Phe and Leu esters had the shortest half-lives ($t_{1/2} \leq$ 4h) while Val esters exhibited up to 68h half-lives. In regard to esters containing the tyrosine derivative side chains (**Figure 1.24**), half-life values ranged from 1.5 – 60h. The n=1 homologues were far more labile to hydrolysis than were n=4 longer chain homologues. The carbamate prodrugs with tyrosine derivative side

chains were very stable with half lives longer than 7 days (Gaucher, Rouquayrol et al. 2004)! The tyrosinyl side chain design in this work was intended to target the amino acid transporter system of the blood brain barrier, which is known to actively transport tyrosine and tyrosinyl compounds (Walker, Nicholls et al. 1994).

Transport of the prodrugs in the apical-to-basolateral (AP to BL) and basolateral-to-apical (BL to AP) directions was carried out to determine the best candidates for active transport in the small intestine. The AP to BL transport relies on substrate recognition by hPEPT1 while the BL to AP transport relies on P-gp substrate recognition. A proper prodrug candidate should increase the transport of parent drug in the AP to BL direction, either by better carrier-mediated transport via hPEPT1, by worse transport by P-gp, or by a combination of the two transport events (Rouquayrol, Gaucher et al. 2002).

Using Caco-2 cell monolayers 14-27 days post-seeding, the parent drugs were found to favor BL to AP transport approximately 3 to 15 times better than AP to BL transport based on apparent permeability coefficients and percent of drug in the receiver reservoir. These data indicate that P-gp substrate recognition is high in the case of all three parent drugs, which limits bioavailability and, quite likely, blood brain barrier permeation. Significantly imporved transport in the AP to BL direction of approximately 3 to 6-fold was observed for the L-Val, L-Phe, and L-leu prodrugs of Ind and Saq. Also, compared to parent drug, efflux was approximately one half for the Ind amino acid prodrugs. However, it is important to note that BL to AP transport was still significantly higher for these

prodrugs compared to their AP to BL transport, and over time, the Saq prodrugs in particular were susceptible to hydrolysis. Saq-Phe also had greater transport in both directions compared to Saq, which suggests a passive diffusion enhancement from the lipophilic Phe moiety. Still, these data indicate that better systemic exposure is probably possible through the amino acid prodrug strategy on Saq and Ind. Unfortunately, the perfectly rational design of the tyrosinyl side chains to target amino acid transporters appears to have failed. In all cases, this derivatization resulted in a loss of transport in both directions. Only the Ind(14)-C(O)C1Tyr prodrug could be detected in the receiver chamber, and it exhibited less than half the transport of Ind in the absorptive direction and about 9 times less transport in the secretory direction (Rouquayrol, Gaucher et al. 2002).

Concluding Remarks

An extensive literature regarding the design and testing of amino acid prodrugs has been presented. The overarching theme throughout many studies is that amino acid prodrug design can result in substantial improvements in drug delivery, depending on the drug in question and its target location. Also, the necessity for appropriate stability studies has been illustrated. For the purposes of our study, the amino acid ester design was chosen as a water-solubilizing modification for MNTD, and the approach is much like that used by Bundgaard and others to enhance water solubility of metronidazole for parenteral delivery.

1.9 PTD prodrug design to treat alcoholism

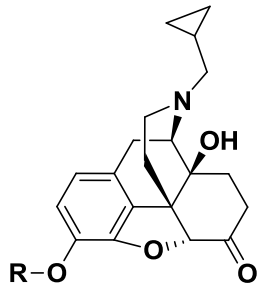

R =

ACE-ESTER $—COCH_3$	ME-CARBONATE $—COOCH_3$	PIV-ESTER $—COC(CH_3)_3$
PORP-ESTER $—COCH_2CH_3$	ETH-CARBONATE $—COOCH_2CH_3$	ISOVAL-ESTER $—COCH_2CH(CH_3)_2$
BUT-ESTER $—CO(CH_2)_2CH_3$	PROP-CARBONATE $—COO(CH_2)_2CH_3$	ETBUT-ESTER $—COCH(CH_2CH_3)_2$
VAL-ESTER $—CO(CH_2)_3CH_3$	BUT-CARBONATE $—COO(CH_2)_3CH_3$	ISOBUTYRL-ESTER $—COCH(CH_3)_2$
HEX-ESTER $—CO(CH_2)_4CH_3$	PENT-CARBONATE $—COO(CH_2)_4CH_3$	ISOPROP-CARBONATE $—COOCH(CH_3)_2$
HEP-ESTER $—CO(CH_2)_5CH_3$	ISOPROP-CARBONATE $—COCH(CH_3)_2$	t-BUT-CARBONATE $—COOC(CH_3)_3$

Figure 1.25 Straight-chain and branched-chain alkyl esters of NTX for PTD. Adapted from (Stinchcomb, Swaan et al. 2002, Pillai, Hamad et al. 2004, Vaddi, Hamad et al. 2005).

This section discusses the history of the transdermal NTX and NTXOL prodrugs project as it relates to passive transdermal delivery (PTD), and MNTD delivery is discussed as the final entry to this introductory chapter.

Figure 1.25 shows the structures of the straight-chain and branched-chain alkyl esters and carbonates that were prepared and tested (Stinchcomb, Swaan et al. 2002, Pillai, Hamad et al. 2004, Vaddi, Hamad et al. 2005).

In this PTD paradigm, the straight-chain alkyl ester prodrugs of NTX and NTX base were dissolved in light mineral oil, and human skin diffusion studies were carried out (Stinchcomb, Swaan et al. 2002). Prodrugs showed increased flux compared to NTX base, with the exception of the BUT-ESTER compound. ACE-ESTER, PROP-ESTER, and HEX-ESTER gave the best flux-enhancement compared to NTX base. All of the prodrugs were found to extensively bioconvert to parent NTX during a diffusion experiment, which resulted in rapid systemic delivery of NTX after the SC permeation event. ACE-ESTER showed the best mean molar percentage of regenerated NTX to total drug extracted from the skin (91%) out of the six esters studied. Prodrug stability in buffer was not assayed in this study.

ACE, PROP, and HEX esters were also formulated into PTD patches and applied to the dorsal region of hairless guinea pigs. In vivo evaluation of plasma NTX, NTXOL and prodrug levels was carried out using LC-MS (Valiveti, Hammell et al. 2005). All of the prodrugs rapidly cleaved to form parent drug in the plasma following i.v. dosing, and sustained levels of NTXOL were observed throughout all bolus experiments. The transdermal delivery experiments revealed several

critical observations. ACE-ESTER delivered greater amounts of NTX systemically to guinea pigs compared to NTX base, PROP-ESTER and HEX-ESTER. During 48 hours of PTD the greatest $C_{max,}$ $C_{ss,}$ $AUC_{0\text{-}48}$, and enhancement factor measurements were observed with ACE-ESTER formulated patches. These data indicate that higher plasma levels of NTX are achieved over 48 hours of patch placement, and that greater steady state concentrations of NTX can be delivered systemically by ACE-ESTER as compared to NTX base and the other two straight-chain alkyl ester prodrugs. Trace amounts of NTXOL and prodrug were recovered in some plasma samples, but these levels had no significant impact on total drug plasma concentrations. Also, fold-enhancement factors of flux were similar in these *in vivo* studies as compared to *in vitro* human skin diffusion data which suggests that the hairless guinea pig is an appropriate animal model for *in vitro-in vivo* comparison of transdermal NTX prodrugs.

A follow up *in vitro* study of the straight-chain promoiety theme was undertaken with modification of the linker from an ester design to a carbonate design (Pillai, Hamad et al. 2004). In the straight-chain carbonate series, pH 7.4 stabilities ranged from 73 to 315 hours in the usual manner one would expect based on alkyl chain length. Every prodrug showed evidence of bioconversion in the skin during diffusion experiments; however, the amount of intact prodrug found in the receiver compartment at the end of diffusion experiments ranged from 11-51%. This is in contrast to the trace amounts of intact prodrug found in receiver solutions in the straight-chain ester series. It is especially noteworthy that straight-chain esters showed better flux behaviors compared to their

carbonate cohorts. Therefore, further evidence was accumulated to suggest that the rate of skin transport to the systemic circulation following SC permeation is partly dependent on the rate of bioconversion of lipophilic prodrug to the more hydrophilic parent NTX. Skin disposition studies corroborated these findings since more NTX was extracted from skin samples in the alkyl ester series than the carbonate series. ME-CARBONATE (named ME-NTX in the original paper) was the only prodrug in this series that showed statistically significant increases in transdermal flux compared to NTX control, and it also was responsible for the greatest concentration of NTX extracted from skin in the drug disposition studies that were conducted following diffusion experiments. These date collectively suggest that short straight-chain alkyl esters outperform higher alkyl homologues or their carbonate counterparts in *in vitro* PTD transport studies.

Branched-chain alkyl esters and carbonates of NTX have also been prepared and analyzed for physiochemical characteristics and human *in vitro* skin diffusion behaviors (Vaddi, Hamad et al. 2005). These studies were done for direct comparison with the straight-chain cousins reviewed above. Overall, it was observed that chain branching affords no particular advantage in PTD of NTX esters or carbonates, although increased stability in aqueous media (enzymatic and non-enzymatic) was an outcome of the design. Decreased skin permeability coefficients were observed along with lower transdermal flux rates. Also, the skin bioconversion rates suffered as compared to compounds designed with straight-chain promoieties. The latter effect of the branched-chain structural modification on the promoiety likely contributed greatly to reduced transdermal flux rates,

which provides further evidence for the role of prodrug bioconversion in viable skin tissue as a contributing factor in parent drug delivery rate enhancement. None of these prodrugs significantly outperformed NTX base in terms of transdermal flux.

Bioconversion rates of VAL-ESTER and ETBUT-ESTER prodrugs were compared between a human skin epidermis models and fresh human skin surgical waste samples (Hammell, Stolarczyk et al. 2005). This study also characterized the metabolic formation of NTXOL from NTX in the human epidermis models and fresh surgical waste samples.

Metabolic conversion of NTX to NTXOL in human waste skin was not significantly different than that observed in intact EpiDerm^{TM} human skin equivalent. Disposition studies showed that the same behavior was also observed in extracted skin samples following diffusion experiments. Flux and bioconversion data were comparable between the human skin samples and the human skin models. VAL-ESTER was again established as a more appropriate prodrug than ETBUT-ESTER. Compared to human skin samples, VAL-ESTER flux data were some 30-fold higher in EpiDerm 606 as measured in NTX equivalents (NTX + Prodrug in receiver); however, the percent of NTX found in receiver solution and the fold-increase of flux enhancement was comparable to human skin. Disposition data were also comparable in human skin and human skin model for both prodrugs. These data suggest that the Epiderm human skin models can be predictive substitutes for actual human skin if one takes care not

to overestimate rate data. In the absence of available human skin surgical waste samples, these models may be useful for PTD studies.

1.10 MNTD prodrug design to treat alcoholism

Previously in our labs, various pegylated 3-*O*-carboxylate and 3-*O*-carbamate ester prodrugs of NTX (**Fig. 1.26**) were prepared and tested (Yerramreddy, Milewski et al. 2010). All of the prodrugs demonstrated adequate stability at pH 5.0 to be considered candidates for skin diffusion studies. Also, the prodrugs had pH 7.4 stability profiles that suggested rapid conversion of prodrug to parent drug at physiological pH. Prodrug solubilities in 0.3 M acetate buffer (pH 5.0) were typically 2-fold or 3-fold higher compared to NTX. However, the carboxylate ester prodrug where R = H (YTR-NTX-20) was advanced to skin diffusion studies, and it was found that micro-channel fluxes of the prodrug were not superior to NTX at any concentration (Milewski, Yerramreddy et al. 2010). A more thorough review of the latter study is given in **Section 1.12** on MNTD. Apparently, the large increases in donor vehicle viscosity resulting from saturated solutions of the pegylated prodrug were sufficient to retard prodrug traversal of aqueous microchannels, regardless of increased water-solubility over NTX.

It is particularly interesting to note that the YTR series of pegylated prodrugs in **Fig. 1.26** all share a common diethylene glycol (DEG) arrangement of atoms on the pro-moieties. The viscosity of diethylene glycol itself is roughly 36 times that of pure water at 20 °C (ME Global 2005). The exact concentration-dependent viscosities (n=3) of YTR-NTX-20 in 0.3 M acetate donor vehicle at

32°C were measured, and it was found that the average viscosity of 0.3 M acetate donor with no prodrug present was 0.83 cP. However, at 952 mM, YTR-NTX-20 concentration in the same vehicle, n_{avg} = 6.35 cP, a nearly 8-fold increase in donor viscosity was observed (data unpublished).

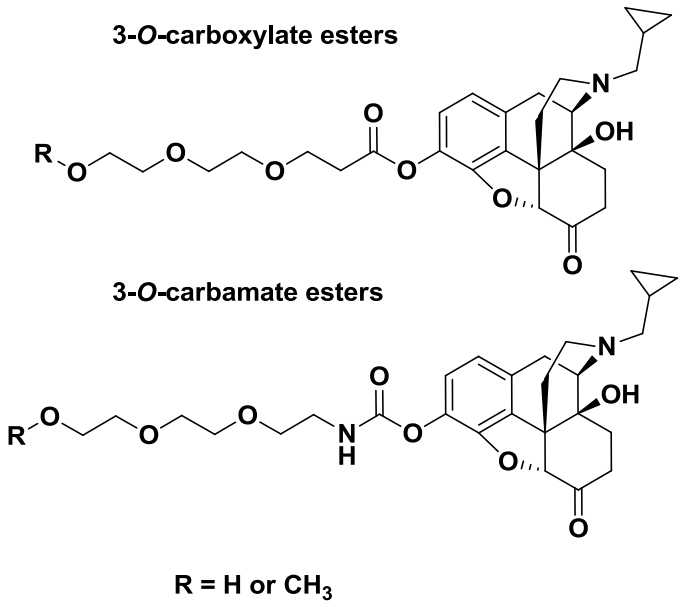

Figure 1.26 Novel Pegylated 3-*O*-carboxylate and 3-*O*-carbamate prodrugs of NTX. Adapted from (Yerramreddy, Milewski et al. 2010).

As a general defense of the amino acid ester prodrug design detailed in the current body of work, it is not possible to predict *a priori* what viscosity behaviors can be expected for non-pegylated prodrugs. One study of amino acid viscosities in water and $MgCl_2$ solution is of particular value in analyzing inherent viscosity properties of Gly, Ala, and Leu promoieties (Lark, Patyar et al. 2007). The data are presented in **Table 1.1**, where $[mM]_{water}$ refers to the concentration

of amino acid in pure water and $[mM]_{electrolyte}$ denotes amino acid concentration in 50.1 mM $MgCl_2$. The n-values are expressed as relative viscosities of amino acid solutions compared to blank solvent at 35°C.

Amino Acid	$[mM]_{water}$	η_{water} (cP)	$[mM]_{electrolyte}$	$\eta_{electrolyte}$ (cP)
Glycine	420.1	1.062	492.7	1.074
L-Alanine	484.8	1.123	493.5	1.128
L-Leucine	96.5	1.046	95.9	1.044

Table 1.1 Viscosity of amino acids (35°C). Adapted from (Lark, Patyar et al. 2007).

1.11 Codrugs

The bulk of the present study was focused on synthesis and stability studies of NXT and NTXOL amino acid ester prodrugs for MNTD. Only one prodrug that was prepared and assayed in this work can be classified as a codrug (CYT-NTX). Due to space limitations, the following section will only cover commercial codrugs, and those codrugs that have previously been explored in transdermal delivery efforts within our labs. The reader should access the recent book chapter by Crooks, *et al*. for a detailed discussion of other codrugs and their utility in various drug delivery situations (Crooks, Dhooper et al. 2011). Other reviews have also been noted in **Section 1.7.** A discussion about the defining features of codrugs was also given above in **Section 1.7.**

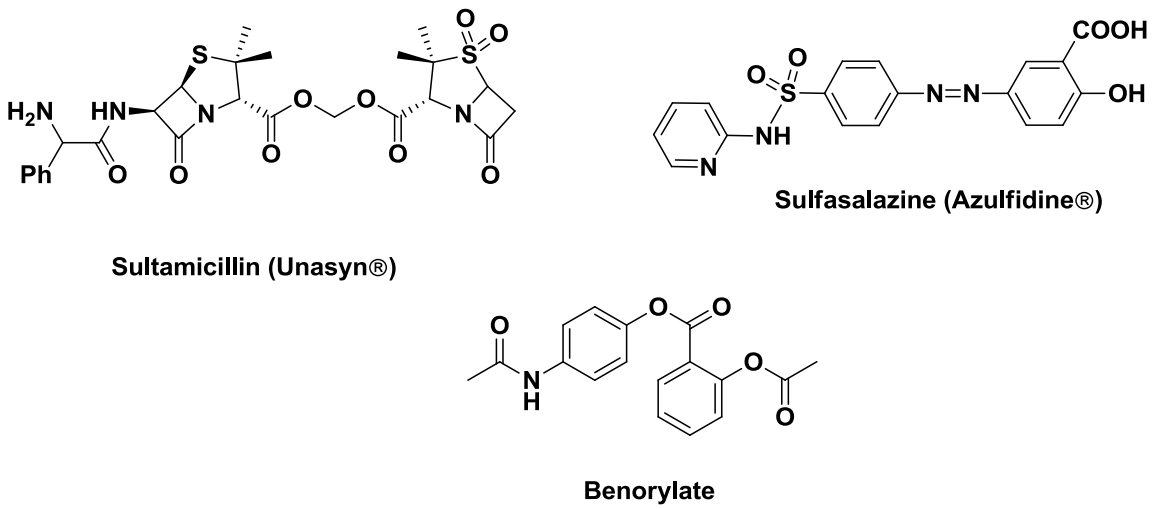

Figure 1.27 Marketed Codrugs. Adapted from (Baltzer, Binderup et al. 1980, Peppercorn 1984, Crooks, Dhooper et al. 2011).

Sultamicillin (SA, Unasyn®, **Fig 1.27**) is a codrug comprised of the antibiotic ampicillin (AMP) and the β-lactamase inhibitor penicillanic acid sulfone (PAS). This successful codrug (or mutual prodrug) design was approached by Baltzer *et al*. (Baltzer, Binderup et al. 1980), because AMP and PAS exhibit the following features: (1) poor oral absorption; (2) similar volumes of distribution and elimination rates; (3) appropriate 1:1 optimal synergy, and (4) PAS prevents bacterial β-lactamase from hydrolyzing the β-lactam ring of ampicillin, which would render it inactive. Under challenge in various enzymatic media, SA showed desirous instability with a half life range on the order of approximately one to nine minutes. The codrug is a tripartite species that releases the two parent carboxylic acids and a molar equivalent of formaldehyde upon hydrolysis. In healthy human volunteers, the codrug was found to be well absorbed and

rapidly bioconverted to the two parent drugs with symmetric plasma concentration profiles that indicated 1:1 drug delivery. These are the ideal behaviors that a codrug should possess, and SA has made it all the way to the clinic as a result of this mutual prodrug design effort.

Sulfasalazine (SASP, Azulfidine®, **Fig. 1.27**) is a marketed codrug of sulfapyridine (SP) and 5-aminosalicylic acid (5-ASA, mesalamine, Lialda®). The codrug is used in the treatment of ulcerative colitis (Peppercorn 1984). Bacterial enzymes cleave the azo bond in the colon which results in the release of the two therapeutic agents (Das, Eastwood et al. 1973, Das, Chowdhury et al. 1979). 5-ASA is an anti-inflammatory agent while the SP moiety has antibacterial properties. The advantages and drawbacks of the SASP design were discussed above in the amino acid prodrugs section entitled **Amino acid prodrugs of 5-aminosalacylic acid for colonic delivery.** Though SASP is a marketed codrug, some patients suffer from hypersensitivity to the SP moiety when it is released as free drug (Das, Eastwood et al. 1973, Taffet and Das 1983, Peppercorn 1984). Therefore, amino acid prodrugs of 5-ASA have also been prepared and tested (Pellicciari, Garzon-Aburbeh et al. 1993). Nonetheless, the SASP codrug design avoids pre-colonic absorption and elimination of 5-ASA, and the codrug also affords the advantage of colonic delivery of an anti-inflammatory agent and an antibacterial agent simultaneously. These features have rendered SASP a successful clinical agent for many years.

Benorylate is another example of a marketed codrug compound; however, it is not available in the USA. The codrug is a bipartate ester conjugate of acetylsalicylic acid (aspirin) and paracetamol (acetaminophen). The mutual prodrug is rapidly cleaved systemically such that oral dosing in man results in plasma detection of only the parent drugs (Robertson, Glynn et al. 1972). Another attractive feature of this drug design is that the ester formed from conjugation masks the free carboxylic acid that is present when aspirin is dosed alone. Free carboxylic acids are suspect as the cause of gastric irritation that accompanies NSAID therapy. In turn, the latter side effect limits the therapeutic utility of NSAIDs (Mahdi and Alsaad 2012). Benorylate is an effective analgesic and anti-inflammatory agent for use in the treatment of rheumatoid arthritis. Indeed, it has been shown that its analgesia and its anti-inflammatory properties are similar to aspirin and paracetamol (Beales, Burry et al. 1972). However, one limitation of the drug is that it does not demonstrate superior antipyretic effects compared to a physical mixture of aspirin and acetaminophen in children between 4 months and 12 years of age (Simila, Keinanen et al. 1975).

PTD Codrugs of NTX, bupropion and hydroxybupropion for alcohol abuse or alcohol-tobacco co-abuse

The codrugs in **Figure 1.28** have been prepared and tested in a PTD paradigm. The original idea surrounding this research is well-founded in that alcohol and tobacco co-abuse is a pervasive problem (Mello, Mendelson et al. 1987, Frosch, Shoptaw et al. 2000). During the course of research efforts to

prepare codrugs of bupropion and hydroxybupropion with NTX and NTXOL, the three compounds in **Figure 1.28** were afforded for study (Hamad, Kiptoo et al. 2006). Each molecule is conjugated by a carbonate linker.

Bupropion (BUP) is FDA-approved as a smoking cessation agent, and it has been shown to permeate human skin at rates sufficient to achieve therapeutic PTD (Kiptoo, Paudel et al. 2009). On the other hand, hydroxybupropion (BUPOH), an active metabolite of BUP, was found to need modification to a butyl carbamate prodrug in order to achieve acceptable transdermal flux rates (Kiptoo, Paudel et al. 2009). These observations taken together suggest that BUP and BUPOH could possibly improve the poor PTD profiles of NTX and NTXOL if lipophilic codrugs containing them were designed and synthesized. Furthermore, such codrugs could be of great clinical utility in the treatment of comorbid alcohol and tobacco abuse.

Although BUP is effective as a PTD agent, it is extremely unstable in the free base form required for PTD formulation. Furthermore, attempts to conjugate BUP to NTX or NTXOL by phosgenation chemistry failed due to rapid intramolecular cyclization to a product with no available handle for acylation. On the other hand, reaction of BUPOH with phosgene in toluene resulted in a BUPOH carbamate intermediate with a free terminal hydroxyl group available for further acylation chemistry. Reaction of the cyclized BUPOH intermediate first with phosgene, and then with NTX or NTXOL in the presence of triethylamine afforded CB-NTX-BUPOH and CB-NTXOL-BUPOH respectively.

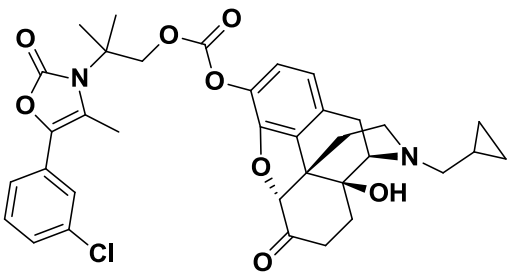

Hydroxybupropion-NTX codrug
CB-NTX-BUPOH

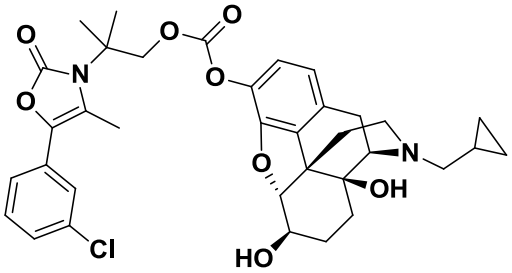

Hydroxybupropion-NTXOL codrug
CB-NTXOL-BUPOH

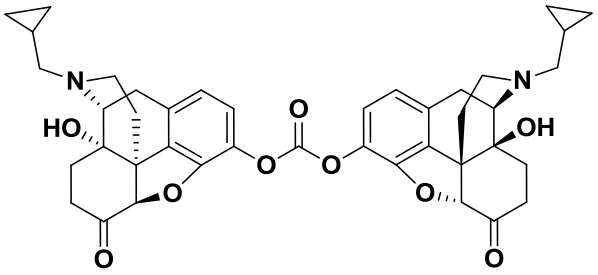

Gemini Duplex Codrug

Figure 1.28 PTD codrugs for alcohol abuse or alcohol-tobacco co-abuse. Adapted from (Hammell, Hamad et al. 2004, Hamad, Kiptoo et al. 2006, Kiptoo, Hamad et al. 2006, Kiptoo, Paudel et al. 2008).

The Gemini prodrug was afforded as an accidental product when phosgenation of NTX was approached as an alternate first step in efforts to prepare a codrug of BUP and NTX. Each of these reactions, and their proposed mechanisms, is detailed in Hamad et al. (Hamad, Kiptoo et al. 2006). At this writing, synthesis of the BUP-NTX codrug itself has never been achieved (see further efforts in **Chapter 5**).

Stability studies of CB-NTX-BUPOH and CB-NTXOL-BUPOH were carried out in isotonic phosphate buffer (pH 7.4) (Hamad, Kiptoo et al. 2006, Kiptoo, Hamad et al. 2006). These studies showed that the rate of codrug disappearance corresponded to the rate of NTX appearance, while the rate of appearance of BUPOH relied on the degradation of the 2,4-oxazolidine ring of the BUPOH intermediate, as expected. Further evidence of hydrolysis of the BUPOH 2,4-oxazolidine species was confirmed by summation of molar equivalents of BUPOH and its intermediate over the course of time, which coincided with molar equivalents of released NTX. The same behaviors were observed for both codrugs, and the authors noted that the delayed conversion of the BUPOH 2,4-oxazolidine intermediate to BUPOH could likely be dramatically accelerated *in vivo* by enzymatic activity. In the latter case, delivery of NTX and BUPOH might be expected to be more symmetric. *In vitro* enzymatic rate enhancement studies in GP plasma confirmed a much enhanced rate of hydrolysis in the presence of esterases; however, the same two-step kinetics for BUPOH formation were observed (Kiptoo, Paudel et al. 2008).

In vitro (Kiptoo, Hamad et al. 2006) and *in vivo* (Kiptoo, Paudel et al. 2008) characterization of CB-NTXOL-BUPOH as a PTD codrug has also been performed. In the *in vitro* work, J_{max} values of the codrug were measured in NTXOL equivalents and found to be four-fold greater than NTXOL control. BUPOH delivery was statistically the same as NTXOL, indicating that the codrug was responsible for the presence of NTXOL in receiver solution. Disposition studies confirmed extensive codrug bioconversion to BUPOH and NTXOL in the

skin, which was likely responsible in part for the four-fold increase in PTD of NTXOL by this method. Nonetheless, the calculated therapeutic window for NTXOL delivery based on NTX (11 – 197 nmol•cm^{-2}•hr^{-1}) was not reached in the *in vitro* studies.

In vivo studies in GPs showed that approximately five-fold higher steady state plasma levels were maintained for 48 hours following application of CB-NTXOL-BUPOH compared to NTXOL control. The AUC_{0-48} of NTXOL was also significantly higher than NTXOL control by about 4.2-fold following topical gel administration of codrug. Only trace amounts of codrug and the BUPOH intermediate were observed in the plasma samples, and these were not quantified. The enhancement factor for the codrug was found to be 5.3, and these data suggest that the codrug does significantly improve the delivery of NTXOL *in vivo* and that the BUPOH intermediate 2,4-oxazolidine may be an insignificant and rapidly cleaved species in the live GP. Unfortunately, NTXOL delivery did not reach therapeutic levels in these studies either.

The duplex Gemini codrug of NTX (**Fig. 1.28**) was also tested in a PTD paradigm (Hammell, Hamad et al. 2004). The codrug hydrolyzed extensively in the skin and small quantities of intact codrug were observed in receiver solution. Flux of NTX equivalents was about two-fold for codrug compared to NTX base. Human skin homogenate studies revealed a half-life of 31 minutes for the codrug, which supported rapid skin bioconversion as a likely permeation enhancer of the codrug. In further studies, skin bioconversion was also supported as the key permeation enhancer. For instance, the SC partition

coefficients of NTX and the codrug were not significantly different. Light mineral oil solubilities between NTX and the codrug were also not significantly different (when expressed as equivalents of NTX). Therefore, no concentration gradient differences due to light mineral oil solubilities could have contributed to the two-fold enhanced flux of NTX due to codrug. Overall, therapeutic levels of NTX delivery were not obtainable by the duplex NTX codrug approach either, but this study does provide further evidence that rapid skin bioconversion of codrugs and prodrugs is desirous for percutaneous delivery of prodrugs.

In **Sections 1.7 – 1.11**, prodrugs and codrugs have been introduced, and an extensive literature regarding their design and their uses in multiple drug delivery goals has been presented. The amino acid prodrugs that were prepared in this body of work were intended for MNTD, whereas the codrug (CYT-NTX) proved to be a more appropriate candidate for oral delivery studies. A section regarding the relatively new drug delivery area of MNTD is presented next. Collectively, a rationale for switching to MNTD for percutaneous delivery of NTX prodrugs can be appreciated from **Sections 1.9 – 1.12.**

1.12 Microneedle-enhanced transdermal delivery (MNTD)

Transdermal delivery of xenobiotics is an attractive route of drug delivery for compounds that have considerable first-pass metabolism, gastric instability or side effects, or poor oral bioavailability. Compounds that can be delivered by passive transdermal delivery (PTD) methods must be able to diffuse across the outermost protective layer of the skin; the stratum corneum (SC). Several key

physiochemical features are typically considered as guidelines for predicting which compounds can surmount the barrier properties of the SC. Among them are the following: logP ($logK_{O/W}$) of approximately 2; low melting point; and molecular weight < 500 g/mol (Bos and Meinardi 2000). As previously reviewed, NTX and NTXOL have been shown to lack sufficient transdermal flux to achieve therapeutic blood levels when they are exposed to intact SC. Therefore, the barrier properties of the SC must be compromised in order to deliver them in sufficient quantities to affect a therapeutic outcome.

Microneedle-enhanced transdermal delivery (MNTD) is a method that briefly compromises the barrier properties of SC through the creation of aqueous micropores in the SC. There are a number of different permutations of MNTD which are applicable in different cases depending on the nature of the molecules which are intended for delivery. The different methods, compounds which are best suited for them, and the specifics of formulation techniques that best optimize delivery by these techniques have been reviewed (Prausnitz 2004, Milewski, Brogden et al. 2010). For the purposes of the present study, only solid microneedles were employed in a paradigm variously described as “poke with patch” or “poke and patch” which simply denotes two separate steps that are involved in the MNTD patch application process. Specifically, in the poke and patch paradigm, an array of solid microneedles is inserted into the SC to create aqueous microchannels. Subsequently, a gel, or an occlusive patch formulation containing the drug of interest, is placed atop the aqueous microchannels in order to assay the delivery profile of the drug over the course of time. Since no

other MNTD paradigm was employed in the present work, the reader is referred to the cited reviews for information on MNTD techniques other than poke and patch.

Silicon wafers and stainless steel solid microneedle arrays are typically used in MNTD studies (Gill and Prausnitz 2007). Utilizing a deep plasma etching technique to prepare microneedles from silicon wafers, Henry et al. created 20-by-20 microneedle arrays measuring 80 µm at the base with a 150 µm length and demonstrated that calcein (**Fig. 1.29**) delivery through cadaver skin could be enhanced by three to four orders of magnitude following SC compromise (Henry, McAllister et al. 1998). The extent of increased calcein delivery was found to be dependent on the amount of time the microneedle array was applied to the skin, and whether or not the array was left in place during delivery. The best increase over intact skin, 25000-fold, was achieved with one hour microneedle insertion and removal of the array before skin exposure to the model compound. It is noteworthy that calcein is a fairly large compound in terms of transdermal delivery candidates (622.55 g/mol) and that it should be significantly ionic at skin relevant ~pH 5.0 with its multiple carboxylic acid groups and a couple of tertiary amine moieties present too. Indeed, permeability of calcein through intact SC was found to be poor and on the order of 10^{-6} cm/h. This study was the first study to demonstrate that the delivery profile of a large and fairly hydrophilic compound can be dramatically improved with MNTD.

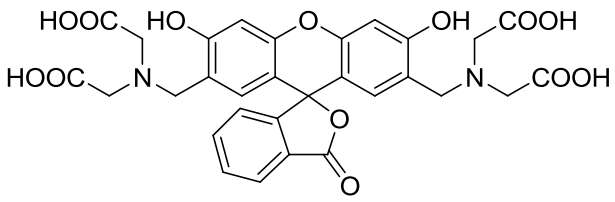

Figure 1.29 Structure of Calcein.

In a follow-up study by McAllister *et al*., the scope of molecules that can be delivered by MNTD was demonstrated (McAllister, Wang et al. 2003). In this study, macromolecules and nanoparticles of up to 100 nm diameter were found to be transported across microchannels following insertion of microneedles. Insulin and bovine serum albumin (BSA) are large proteins which do not traverse the skin without SC compromise. Using the same 20-by-20 microneedle arrays as Henry *et al*., it was confirmed in this study that insulin and BSA permeability increased by orders of magnitude with microneedle insertion if the array was left in place, and by an additional order of magnitude if the array was removed following microneedle insertion.

The MNTD transport of compounds which cover a molecular weight range of 538 Da – 72 kDa has been confirmed (Verbaan, Bal et al. 2007). 4 x 4 arrays were prepared from commercial 30G stainless steel hypodermic needles at lengths of 300, 550, 700 and 900 µm. Using human dermatomed skin treated with microneedles compared to no microneedle treatment as a control, Cascade Blue (538 Da) and Cascade Blue-Dextran (10 kDa) greatly out-performed FTIC-Dextran (72 kDa) transport by the MNTD route, and both the kDa molecular weight dyes showed some decrease in flux at approximately 5 hours which

increased again later after about 13 hours for 10 kDa and 16 hours for 72 kDa. The flux profile over time for Cascade Blue had smooth increase toward steady state over a 20 hour time course. In all cases, flux values were far greater with microneedle treatment over the course of 20 hours of the experiments. With regard to microneedle length, no significant difference in total accumulated amount was observed as a function of microneedle length, although a trend could be seen that suggested increased transport with longer needle length in the case of Cascade Blue and Cascade Blue-Dextran.

Collectively, these studies suggest that the pool of compounds which can use MNTD as a transport vehicle is much larger than that which can be delivered by classic PTD. Hydrophilic compounds with large molecular weights and ionic charge have been shown to have far greater permeability by the MNTD route than they do in the presence of uncompromised SC. Inasmuch, it is expected that small molecules with poor transdermal permeation due to hydrophilic character can be formulated in vehicles that can utilize MNTD as a means of improved systemic exposure via the skin. NTX and its active metabolite NTXOL serve as a case-in-point.

To test the hypothesis that percutaneous delivery of NTX can be improved by the use of a salt form of the drug and microneedle pretreatment of the skin, Wermeling *et al.* tested NTX hydrochloride on nine male and female volunteers (Wermeling, Banks et al. 2008). Four 6.7 cm^2 NTX•HCl patches were used per patient. Six patients were treated with four 5X10 arrays of solid stainless steel microneedle of 620 µm length, and three control subjects were left untreated with

microneedles. In patients who were treated with microneedle arrays, detectable blood plasma levels were observed within 15 to 30 minutes, and approximate zero order delivery of 2.5 ng/mL blood plasma concentrations was maintained for 48 hours. Inter-patient differences in maximum concentration values were observed; however, it is important to note that 2.5 ng/mL blood plasma concentrations of NTX are consistent with the lower level of the therapeutic window of the FDA-approved depot formulation, Vivitrol ®. Subjects who were untreated with microneedles had undetectable blood plasma levels of NTX, which is consistent with previous studies that clearly show that NTX is not permeable in sufficient quanitities for therapeutic outcomes when applied to intact SC.

In order to expound further on the effect of molecular charge versus MNTD skin transport, Banks *et al*. investigated the charge-dependent flux of NTX and NTXOL *in vitro* (Banks, Pinninti et al. 2008). Stainless steel microneedles were applied as a row of 5 with 750 µm length. NTX base exhibited roughly 4-fold better flux than the corresponding hydrochloride salt with intact hairless guinea pig (GP) skin; however, when microneedles were applied to the GP skin, the hydrochloride salt had approximately 2.3-fold greater flux. In the case of intact skin, lag times between NTX base and hydrochloride were not statistically different. However, when microneedle treatment was used, lag times for the hydrochloride salt were less than those observed for the free base. The free base itself showed no difference in steady state flux or lag time between intact and microneedle-treated GP skin, which indicates that there is no difference in

the permeation pathway that the free base follows under these two very different structural states of the SC. In contrast, the hydrochloride salt had about an order of magnitude increase in steady state flux under microneedle treatment as compared to the intact SC case, and the lag time under microneedle treatment was also roughly 1/10th the time necessary to achieve steady state flux in untreated GP skin samples. With regard to human skin samples treated under the same conditions, the hydrochloride salt had about 8-fold better flux in microneedle treated skin and approximately half the lag time to reach steady state. NTXOL held at pH 4.5 showed 1.3-fold increased flux over NTX•HCl in microneedle-treated GP skin; albeit, with similar permeability values between the two. Microneedle treatment also resulted in reduced lag times for samples of NTXOL held at pH 4.5 as compared to samples held at pH 8.5.

Overall, it was determined that charge does not influence the driving force across skin; rather, the effect of charge on solubility is responsible for flux enhancement of NTX and NTXOL across microneedle-treated skin. Diffusion studies of the compounds revealed this by demonstrating that at low equimolar concentrations of NTX held at pH 4.5 and at pH 8.5, enhanced flux and decreased lag time are still observed. Yet, there was no significant difference in permeability between the two charged states of the molecule in intact GP skin or microneedle-treated GP skin. Therefore, significant increases in permeability of drug only occur at higher concentrations where increases in solubility provide a driving force of diffusion across the aqueous microchannels.

A follow up pharmacokinetics study was conducted to assess the transdermal delivery of NTXOL free base and its hydrochloride salt from 2% hydroxyethylcellulose gel formulations. Along with transdermal delivery, skin permeability lifetime following microneedle treatment of GP skin was also investigated (Banks, Pinninti et al. 2010). Again, stainless steel microneedles were applied as a row of 5 with 750 µm length. GPs who were not treated with microneedles before occlusive patch placement showed very small levels of NTXOL or its hydrochloride salt in plasma samples while those treated with microneedles before patch placement showed increased steady state concentrations of both the free base and the salt. About a 5-fold increase was observed for free base, and the salt had a steady state concentration of 4 times the free base (about 20 times higher than hydrochloride control animals). Seemingly, solubility was the limiting factor in these results; the hydrochloride being more hydrophilic and able to create a greater diffusion gradient across aqueous microchannels. Further, it was found that transepidermal water loss (TEWL) measurements increased at 24 and 48 hours, but not at 72 hours on occluded skin samples versus control. These findings correlated well with the observed profiles of drug delivery since the most consistent plasma levels were measured up to 48 hours. These data suggest that a 48 hour time course of drug delivery was obtained by a poke and patch paradigm.

So far, the studies covered in this section have suggested that increased water solubility of a compound can have the most dramatic effect on improved percutaneous delivery via MNTD. In order to investigate the dependence of

permeation on concentration, Milewski *et al*. conducted MNTD skin transport experiments on a pegylated prodrug of naltrexone over a wide concentration range. Polyethyleneglycol-NTX (PEG-NTX, **Figure 1.26**) is approximately two times as soluble as parent NTX in 0.3M acetate buffer held at pH 5.0 (629 mM compared to 338 mM). Six concentrations of PEG-NTX from 10 mM up to saturation were assayed in diffusion cells containing microneedle-pretreated Yucatan minipig skin samples. In the concentration range from 63-252 mM, a linear relationship was observed between increase in flux versus increase in prodrug concentration. However, this relationship did not hold at higher concentration values (440-629 mM) where a curvilinear relationship was observed. Furthermore NTX•HCl actually out-performed the PEG-NTX prodrug with higher flux values obtained at every corresponding concentration tested. Overall, it was found that changes in the viscosity of the donor solution as a function of prodrug concentration accounted for the nonlinear behavior of prodrug flux values.

In a separate study involving NTX•HCl, binary mixtures of propylene glycol (PG) and water were prepared with varying amounts of PG (Milewski and Stinchcomb 2011). In 25:75 PG:water, steady state levels of NTX•HCl were rapidly obtained with MN-treated skin as opposed to untreated skin. In terms of flux, the greatest flux enhancement with MN-treatment was observed in pure water, and the least was observed in pure PG; however, the decrease in flux with increased concentrations of PG was nonlinear in nature. Surprisingly, the greatest changes in flux occurred in water rich solutions rather than PG rich

solutions. Approximately 40-fold difference in flux magnitude was observed, indicating that donor solution viscosity has a dramatic effect on the transport of NTX•HCl through aqueous microchannels. The difference in flux values in untreated skin samples were nowhere near as large as those observed in MN-treated skin samples. The ratio of flux through MN-treated skin to that through untreated skin revealed an enhancement factor of 17 in 100% water compared to 3 in PG rich donors (40 – 100% PG). Therefore, flux enhancement varies considerably as a function of donor composition. Furthermore, an inverse relationship between donor solution viscosity and transdermal flux through microchannels was observed. In this work, the vehicle composition itself was tested, and PEG influenced drug flux values. Moreover, viscosity issues also affected microchannel transport rates of pegylated NTX prodrugs compared to NTX•HCl. These data suggest that microchannel transport is not totally reliant on drug solubility alone, and that the MNTD prodrug approach may be most appropriate for highly lipophilic drugs with virtually no water solubility or microneedle transport capabilities. Nonetheless, the amino acids that we employed in our later generation prodrugs do not have the same viscosity enhancing properties as PEG chains, and we decided to pursue the amino acid prodrugs for stability evaluation and possible MNTD studies (**Chapter 6**)

1.13 Concluding Remarks

Within this introductory chapter, the overall aims of the present study have been summarized and rationalized with an extensive background literature. The group of prodrugs intended for MNTD was designed with amino acid promoieties to

enhance ionization at pH 5.0, and, thus, solubility of the prodrugs compared to NTX•HCl or NTXOL•HCl. This drug design is in contrast to the typical strategy that is desired with amino acid prodrug design. Our compounds were not meant to be dosed orally, although some of them may well be candidates for that drug delivery approach. Rather, our prodrugs were meant for MNTD, and this represents a novel approach to transdermal prodrug design using well-documented amino acid prodrug strategies. On the other hand, CYT-NTX was prepared with the sole intention of oral drug delivery, and it is an extension of the work that was done on transdermal codrugs for alcohol and tobacco co-abuse. The following data chapters tell the story of the challenges and successes that we encountered in our pursuit to find new potential clinical candidates for the treatment of alcohol and/or nicotine addictions; two of the most pervasive causes of preventable death in our society.

Chapter 2

Synthesis of 3-*O*-NTX amino acid esters

2.1 Synthetic design considerations

The phenolic hydroxyl group is by far the best nucleophile available for prodrug derivitization on NTX or NTXOL. Indeed, access to all the other hydroxyl groups on NTX or NTXOL requires more sophisticated protection and deprotection strategies to afford regioselctive promoiety derivitization on the oxymorphinan scaffold. Without protective group strategies one would expect reaction to first occur on the phenolic hydroxyl group. Of course, protecting group chemistry is always the last option to pursue since it is well known that such strategies are executed at the expense of synthetic step economy and yield. Even in the case of preparing 3-*O*-NTX/NTXOL amino acid ester conjugates, at least one protecting group has to be present on the amino acid nitrogen to suppress undesired side-reactions in the coupling procedures and to avoid purification problems. Access to the 6-*O* position of NTXOL requires an additional protective strategy, and the 14-*O* position of NTX or NTXOL is accessible only through the introduction of yet a third protecting group. The complexities of 6-*O* and 14-*O* coupling are the subject of **Chapters 3 and 4**. Returning to 3-*O* conjugation, though it was expected that there could be some stability issues in 0.3 M acetate (pH 5.0) donor solution, the development of 3-*O*-amino acid ester chemistry was approached first, because it was the simplest case of prodrug synthesis on NTX or NTXOL. **Schemes 2.1** and **2.2** show the best possibilities that could be used to prepare 3-*O*-amino acid ester end products from commercially available

protected amino acids. Both methods had their own unique set of potential advantages and drawbacks that were critical to consider in the synthetic design, and they are mentioned here for the sake of completeness. Referring to **Scheme 2.1**, the *t*-butyloxycarbonyl (BOC) method of prodrug synthesis is depicted; whereas **Scheme 2.2** shows the carbobenzyloxy (Cbz) method of prodrug synthesis. In both cases, it was envisioned that carbodiimide coupling strategies would work well to form the ester linkers; however, from a mechanistic point of view, carbodiimide coupling is not simple, and there are side products that must be considered in the synthetic design. **Figure 2.1** details a mechanism of carbodiimide coupling to illustrate the species that are involved. As the mechanism shows, the common side products that form in carbodiimide coupling strategies are ureas and *N*-acylureas, each of which is specific to the particular cabodiimide reagent employed in the synthesis. Consideration of these side products is very important because they add complexity to the purification process that is required to afford analytically pure prodrug precursors. Throughout the course of the experimental work involved in forming any NTX or NTXOL amino acid ester prodrug, all of the commercially available carbodiimide coupling reagents were employed at one time or another, and it was found that the ureas formed from dicyclohexylcarbodiimide (DCC) and diisopropylcarbodiimide (DIC) were the most difficult to remove from prodrug precursor samples, whereas the EDC urea was removed by workup and chromatography. In every case, there was no evidence of the formation of *N*-acylureas when dichloromethane (DCM) was used as the solvent. Referring

back to **Scheme 2.1**, it was expected that there could be some problems with the BOC approach in terms of the acidic nature of reagents that are needed to remove the BOC group and the possibility of hydrolysis of the prodrug ester bond. **Scheme 2.2** was expected to have a possible drawback in the form of reduction of the 6-*O* ketone to some extent. In **Scheme 2.1**, the final product is a dihydrochloride salt, and in **Scheme 2.2**, the end product is a free base. It was decided that the BOC strategy should be employed first on the amino terminus since the salt end products would be more water soluble than free base esters. It was also decided that trifunctional protected amino acid starting materials should be used first as a means to investigate the utility of BOC and Cbz methodologies simultaneously. Three protected amino acid materials were used for these initial investigations. BOC-Thr(Bzl)-OH, BOC-Lys(Cbz)-OH, and BOC-Asp(OBzl)-OH were materials that had protective groups that were labile under acidic conditions (BOC), and under the conditions of hydrogenolysis (Bzl and Cbz). All three protected amino acid starting materials were used to develop the carbodiimide coupling procedures; however, the material that was first selected to investigate deblocking methods was 3-*O*-Thr(Bzl)-NTX.

2.2 Synthesis of trifunctional amino acid ester prodrugs

The general synthetic strategy depicted in **Scheme 2.1** was utilized first to afford 3-*O*-NTX-amino acid esters. EDC•HCl coupling was established as the carbodiimide coupling procedure of choice due to the relative ease of purification of the EDC side products compared to those of DCC and DIC; however, the isolation yield of precursors was less with EDC (80-87% with EDC and ~ 90%

with DIC). It was found by trial and error that 1.7 equivalents of EDC•HCl coupling reagent and 1.7 equivalents of BOC-protected amino acid were required to drive the coupling reaction to completion. EDC•HCl did add one dimension of difficulty to the chemistry in that its HCl salt apparently also protonated NTX in an exchange equilibrium. This was apparent since workup with deionized water first to attempt to remove excess EDC•HCl and its associated products reduced the yield of isolated prodrug precursors by about ten percent. Five percent aqueous sodium bicarbonate was employed instead to remove some of the excess Boc-protected amino acid, leaving some deprotonated EDC and its urea behind in the organic phase. Luckily, column chromatography proved to be successful in removing the EDC products such that good yields (80 – 87%) of prodrug precursors could be obtained. The first prodrug precursors that were prepared were trifunctional amino acid ester conjugates with hydrophilic R-groups since MNTD was the target method of drug delivery. More hydrophilic compounds are indicated for use in MNTD, and the needed protected amino acid starting materials with hydrophilic side groups were available commercially at a reasonable price. The structures of the three prodrug precursors and their Electrospray ionization mass spectra (ESI-MS) are provided in **Figures 2.2-2.4.**

After successful development of the coupling chemistry to afford the 3-*O*-amino acid ester precursors of NTX in good yield, it was decided that the benzyl group of the threonyl prodrug should be targeted first for removal. The debenzylation step also served as a model reaction to determine if the Cbz method shown in **Scheme 2.2** would likely be of any merit in forming free base 3-*O* amino acid

esters. It was expected that the aliphatic benzyl ether substitution of threonine might be fairly resistant to the normal conditions that are generally employed for palladium-catalyzed hydrogenolysis, and that is exactly what turned out to be the case. Under a balloon atmosphere of hydrogen gas, and with palladium on carbon (Pd-C) as the catalyst, the benzyl ether showed no deprotection after 48 hours. The latter result was observed regardless of the solvent that was used to attempt the deblocking procedure. The conditions that were attempted are summarized in **Scheme 2.3.** The results were disappointing, because it was expected that a change to a stronger catalyst such as palladium black or palladium hydroxide would result in non-stereoselective reduction of the 6-keto position of NTX to form the 6-α/β-NTXOL scaffold. Of course, only the 6-β-NTXOL isomer would be an acceptable product, and the formation of either a diastereomeric mixture of the 6-α/β-NTXOL or an enantiopure 6-β-NTXOL product would ruin the possibility of obtaining a 3-*O*-threonyl prodrug of NTX—the FDA approved parent drug. It was therefore determined that the strongest hydrogenolysis solvent should be maintained (MeOH), and the compound should be subjected to hydrogenolysis with Pd-C under a 50 psi atmosphere of hydrogen using a Parr hydrogenator. This reaction led to some disappointing and important discoveries.

First, even under these conditions, the major peak shown at rt =12.99 min in the LC-UV chromatogram of **Figures 2.5 or 2.6** gave a mass for the parent benzylated derivative (See **Figure 2.4** for the mass spectrum). Therefore, stronger palladium catalysts like palladium black appeared to be necessary to

cleave the aliphatic benzyl ether of the threonine side chain. The latter observation also suggested that a keto-protection protocol would have to be devised to make use of hydrogenolysis of aliphatic benzyl ether-protected amino acid side chains in general (threonine and serine side chains). A second critical observation is shown in **Figure 2.6**. Following 48 hours of hydrogenolysis, there was a small peak in the LC-UV at rt=10.21 minutes that gave the expected mass for the desired debenzylated product (542.9 peak / MW = 542.62). The small amount of conversion also reinforced the possibility that stronger palladium catalysts would be needed for successful debenzylation of the threonine side chain. A third observation was that the small peak at rt=13.43 minutes in the LC-UV gave a mass of 636.9. The interpretation of this result is not so straight forward since the main peak of the reaction mixture chromatogram shows a parent mass of 632.9 (MW = 632.74 for the fully protected compound) along with other mass peaks of 633.9 and 634.9 m/z. However, it is noteworthy to say, qualitatively, that the largest intensity of these peaks corresponds to the expected 632.9 m/z for the fully protected compound and the M+H peak appears to be the second largest in intensity. Following up, the 636.9 m/z may correspond to a keto-reduced material. All things remaining equal with the other mass spectra, 634.9 m/z would correspond to the parent ion mass of the reduced ketone species, and 636.9 could be the same compound as well since this M+2H behavior was seen for the parent compound. Alternatively, another possibility is that the 634.9 m/z found under the major peak actually does result from the reduced ketone material that co-elutes with the original keto species. At any

rate, no evidence of keto reduction could be seen in the crude ^{1}H NMR spectrum (data not shown), so the reduced species would have been present in less than 5% of the material yield. The total ion count associated with these masses is shown in **Figure 2.7** along with arrows to indicate the peaks that correspond to the various species in solution. It was discovered by another colleague nearly simultaneously in a different prodrug synthesis that keto-reduction was indeed a problem on the NTX scaffold when attempts were made to employ hydrogenolytically labile protective groups (Reddy, unpublished). Therefore, these data led to the conclusion that this type of strategy, while viable in terms of retention of the critical ester linker, would not be amenable to the formation of 3-*O*-amino acid ester prodrugs with R-hydroxyl substitution on the pro-moiety (threonyl and serinyl prodrugs) since extensive reduction of the ketone would be likely before a suitable amount of the benzyl ether side chain could be deblocked. Use of stronger catalysts would have accelerated the unwanted reduction side reaction. Therefore, a keto-protection protocol would be necessary to access the desired prodrugs.

An attempt to deblock the benzyl ester of 3-*O*-BOC-Asp(OBzl)-NTX was conducted, but the ester linker was labile to intramolecular cyclization of the carboxylate side chain. The Cbz carbamate of 3-*O*-BOC-Lys(Cbz)-OH was not deblocked since reduction of the ketone would have been a universal problem. Therefore, attention was turned to the removal of the BOC group to see if it could at least be maintained as the amino protecting group.

In attempting to deblock the Boc group, small quantities of the Boc-protected precursors were divided up between separate flasks to investigate different deblocking conditions. It was found that TFA in DCM, $SnCl_4$ in DCM, H_3PO_4 in THF, and 2M HCl in diethyl ether or ethyl acetate were not viable methods for the removal of BOC in any case. HCl in ether or ethyl acetate simply led to immediate precipitation of a salt. Otherwise, with the other methods, the spots that emerged on the triethylamine-deactivated TLC plates were identical in R_f value to naltrexone starting material, and isolation of the "NTX-like" spot in each system with 1% sodium bicarbonate workup and TEA-deactivated silica gel chromatography proved that the material was always identical to NTX (as judged by ^{1}H NMR). These deblocking failures occurred, presumably because the TFA, $SnCl_4$, and H_3PO_4 reagents were appreciably hygroscopic, and none of them were supplied by the manufacturer in septa-sealed bottles. This was the first evidence that strongly acidic solutions with appreciable water content would prove to be detrimental to the preservation of the prodrug ester bond of 3-*O*-phenolic prodrugs. Furthermore, the TFA, $SnCl_4$, and H_3PO_4 reagents were all found to cleave the ester bonds in any useful dilution that could remove BOC, and it became obvious that an anhydrous deblocking reagent or a different protecting strategy would be necessary for further progress to be realized.

2.3 Synthesis of bifunctional amino acid ester prodrugs (R=alkyl)

In order to simplify matters to investigate the stability of 3-*O*-amino acid esters of NTX, the original lysine, threonine, and aspartic acid pro-moieties were replaced with valine, leucine, and alanine. The rationale for this approach was that hydrogenolysis of the side group protecting moieties had been identified as a problem, and the side groups of lysine and aspartic acid could participate in intramolecular degradation of the final prodrugs by cyclization. Also, as discussed in the introduction to this dissertation, valine is known to stabilize the ester bond in multiple prodrugs that have been prepared, including the commercial blockbusters valacyclovir and valganciclovir (see **Chapter 1** for references). Leucine and alanine were logical pro-moieties for stability comparison to valine, because they are also aliphatic in nature, but with different R-substitution. For instance, an extra methylene unit is present in the R-group of leucine compared to valine. In contrast, a simple methyl group is present as the R-group in the case of alanine. Therefore, it was expected that we may see some interesting differences in the simple chemical hydrolysis rates of 3-*O*-Val-NTX, 3-*O*-Leu-NTX, and 3-*O*-Ala-NTX in accord with steric and field-releasing factors associated with R-substitution on the amino acid side chains.

The coupling reagent of choice to form the three new 3-*O*-amino acid esters actually turned out to be DIC. It was chosen because EDC has a tertiary amine present, and it was an attractive idea to simply salt out the final prodrugs as dihydrochloride esters by deblocking the BOC group with anhydrous 4N HCl in dioxane that was available at modest cost. Residual DIC side products from the

coupling step were expected to wash out of the final prodrug salts with ether or acetonitrile. The isolation yield of DIC-coupled precursors was also a bit higher than what was observed in EDC coupling (~ 90%). The general synthetic strategy that was used to prepare 3-*O*-Val-NTX, 3-*O*-Leu-NTX, and 3-*O*-Ala-NTX dihydrochlorides is shown in **Scheme 2.4**. Pleasingly, the DIC urea side products were removed completely by the trituration procedure and cold acetonitrile washes that followed BOC removal. 4N HCl in dioxane was used as the sole solvent of the deblocking reaction, and it afforded the final prodrug products as dihydrochloride salts in 40-60% overall yields following flooding with ether and trituration. A significant material loss was incurred by incomplete precipitation in each case, and better yields could have quite likely been realized by the total removal of the dioxane. However, such a procedure was not to be as easy as simple solvent removal under vacuum due to the high concentration of toxic HCl gas dissolved in solution. Moreover, dioxane is high-boiling and problematic to remove without heating, so it was expected that the prodrugs might degrade with elevated temperature. Overall, the yields were sufficient for analytical purposes, and it was thought that optimization could be approached at a later time if in fact the 3-*O*-amino acid conjugates of valine, leucine, and alanine proved to show stability characteristics that were desirable for future skin diffusion and solubility studies ($t_{90} \geq 48$ hours). The specific details of the reactions to afford the three 3-*O*-amino acid esters of NTX are summarized below. LC-UV/ESI-MS, ^{1}H NMR, and ^{13}C NMR spectra are included for each prodrug. The t_{90} values that are specific to the three final dihydrochloride

prodrugs where R=alkyl are shown in **Figure 2.8** along with the prodrug structures. These data were determined using pH 5.0 acetate buffer held at 32 °C.

It turns out that the decision to accept an unoptimized yield and move forward with the 3-*O*-amino acid esters of NTX was an appropriate decision, as it can be seen in **Fig. 2.8** that none of the three 3-*O*-amino acid ester prodrugs that was prepared came even close to being stable enough for future MNTD work (t_{90}<<48 hours). Therefore, it was determined that no more phenolic amino acid ester conjugates should be prepared for assay, since valine is the pilot promoiety for stability comparisons in this class of prodrugs, and even 3-*O*-Val-NTX dihydrochloride was too unstable for future MNTD work (t_{90} = 1.5 h).

2.4 Future Directions

Some possible modifications can be made to the 3-*O*-coupling chemistry presented herein. For instance, a tripartate prodrug design could possibly be utilized to solve the problem of phenolic amino acid prodrug instability. It has been shown that phenolic alkyloxycarbonyloxymethyl (AOCOM) linkers can be installed under phase transfer synthesis conditions to form prodrugs that are more stabile to biological challenge compared to phenolic esters (Thomas and Sloan 2007). These linkers release a molar equivalent of formaldehyde during hydrolytic cleavage, but that has proven to be of no concern in prodrug design. A commercial example of a prodrug that releases a molar equivalent of

formaldehyde systemically is fosphenytoin (Kai, Tapani et al. 2009). One drawback to this suggested design is the possibility of increased viscosity due to the AOCOM arrangement of atoms. It is somewhat similar to a short chain polyethylene glycol linker, and PEG linkers definitely have a negative effect on MNTD prodrug flux at high prodrug concentrations (Milewski, Yerramreddy et al. 2010). Therefore, the AOCOM approach may be useful for MNTD prodrug design if, and only if, a critical balance between phenolic prodrug stability enhancement and viscosity levels can be realized. We decided to proceed with the 6-*O*-NTXOL prodrug design detailed in Chapter 3 to afford greater prodrug stability, because we were also interested in MNTD experiments involving NTXOL.

2.5 Experimental Section

Materials: All reagents were purchased from, Acros Organics, Sigma-Aldrich, and Advanced Chemtech, and were used without further purification. Naltrexone was a gift from Mallinckrodt-Covidien. All solvents were dried and stored over molecular sieves prior to use.

LC-ESI-MS characterization: Mass spectral data were obtained using an Agilent 1200 series HPLC system coupled to an Agilent 6120 LC-ESI-MS electrospray ionization detector. A Zorbax Eclipse XDB-C18 column was employed, and the mobile phase was 0.1% formic acid:acetonitrile set on a gradient elution program 95:5 to 5:95 over the course of 12 min.

NMR: All NMR spectra were obtained on a Varian 300 MHz or a Varian 500 mHz instrument. Line data and integral values for ^{1}H NMR spectra were acquired with Mestrenova Lite (Mesterlab Research Chemistry Software Solutions, Escondido, CA) using 500 MHz spectra. ^{13}C NMR frequencies were obtained from Varian Mercury 300 MHz NMR software. TMS was used as an internal standard.

General synthesis of 3-*O*-BOC-amino acid-NTX precursors (R=alkyl)

100.0 mg of naltrexone (0.2930 mmol) was weighed and dissolved in dichloromethane (DCM) with vigorous stirring. The NTX solution was set aside. In a separate flask, 0.498 mmol (1.70 eq.) of the BOC-L-amino acid starting material was also dissolved in DCM with rapid stirring. The latter solution was treated dropwise over the course of 10 minutes at room temperature with a mixture of 62.8 mg (0.498 mmol, 1.70 eq.) of diisopropylcarbodiimide (DIC) that was slightly diluted in DCM. The BOC-L-amino acid and DIC mixture was then allowed to stir for 15 minutes after which time needle-like crystals of DIC-urea began to form. The crystals were filtered through a cotton filter as the activated anhydride solution of the protected amino acid and DIC coupling reagent was delivered slowly at room temperature to the flask containing NTX. No base was added, because phenolic coupling is easier to achieve than aliphatic hydroxyl coupling, and the excess of carbodiimide was expected to provide sufficient excess base. The reaction was followed by thin layer chromatography (TLC) using 1:1 hexanes and ethyl acetate containing 1 drop of triethylamine (TEA) base. After 24-36 hours, no spot for NTX could be detected on the TLC plate (36 hours required for BOC-Val-OH coupling only). The reaction mixture was

poured into a 125 mL separatory funnel and worked up with 5% sodium bicarbonate solution (15 mL x 3). The aqueous fraction was washed with DCM, and the organic fractions were collected and washed once with 15 mL of deionized water and twice with 15 mL portions of brine. The solvent was reduced in vacuo, and the mixture was chromatographed over silica which had previously been deactivated by a mixture of 1% TEA in hexanes. The BOC protected prodrug precursor was obtained by elution with 20% ethyl acetate in hexanes following several column washes with 100% hexanes to remove DIC and some of its associated urea. The isolated precursor was further washed with a mixture of 1:1 diethyl ether and hexanes to remove more of the DIC and its urea. Removal of the DIC urea was a challenge. The final material was dried to a constant weight to afford crude material that was mostly the desired 3-*O*-BOC-amino acid-NTX prodrug precursor. Since the DIC associated side products were not fully removed by this method, all intermediate materials were used without further purification. The DIC side products were removed in the final step when the prodrugs were salted out as dihydrochlorides.

Synthesis of 3-*O*-amino acid-NTX dihydrochloride prodrugs (R=alkyl)

For each prodrug, the crude material enriched in the desired 3-*O*-BOC-L-amino acid-NTX prodrug precursor was placed into a 25 mL round bottom flask and flooded with 4N HCl in dioxane. The material initially went into solution sluggishly until dissolution was complete. After ten minutes of reaction time, a gummy material began to precipitate out and bind to the glass. The reaction was continued with vigorous stirring for one hour, after which time the dioxane

solution was charged with diethyl ether. There was an immediate formation of copious white precipitate. The gummy material on the bottom of the flask also became uniform as a white precipitate in the dioxane/diethyl ether solution following trituration with a spatula for fifteen minutes. The precipitated amorphous white powder was collected via filtration over a cotton plug, and the material was washed with a lot of chilled diethyl ether to remove all traces of dioxane and HCl. The powder was allowed to air dry. Subsequently, it was transferred to another round bottom flask and washed 3 times with chilled acetonitrile to remove all DIC urea. The acetonitrile was washed out with more chilled ether, and the final salt was stripped of solvent to a constant weight. The yields were moderate to good in all cases (40-60%), and the materials were characterized by ^{1}H NMR and ^{13}C NMR spectrometry, and LC-UV/ESI-MS analysis (**Figures 2.9-2.17**). The end yields are tabulated in **Table 2.1.** The ^{1}H NMR spectra were acquired after the ^{13}C NMR experiments were conducted, and it can be seen that some degradation of the prodrugs to parent NTX•HCl took place in d6-DMSO within the time frame of the experiments (compare the prodrug and NTX•HCl proton NMR spectra provided). LC-UV/ESI-MS data did not show peaks for NTX, because the chromatograms were obtained before the prodrugs were dissolved in d6-DMSO for NMR spectral analysis. These data further demonstrate the instability of phenolic amino acid ester prodrugs of NTX.

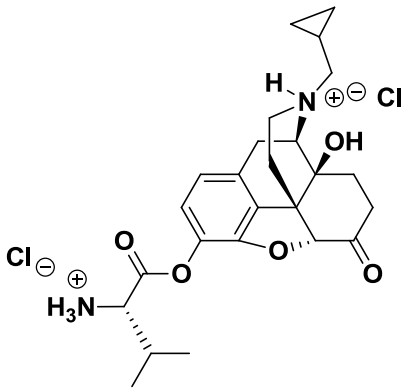

3-*O*-Val-NTX

^{1}H NMR (d_6-DMSO) 500 MHz: δ 9.14 (s, 1H, broad), 8.84 (s, 3H, broad), 7.20 (s, 1H, broad), 7.07 (d, 1H, *J*=10 Hz), 6.89 (d, 1H, *J*=10 Hz), 5.25 (s, 1H), 4.17 (m, 1H), 4.10 (d *J*=5.0 Hz, 1H), 3.5 (d, *J*=18 Hz, 1H), 3.34 (DMSO water peak), 3.21-3.08(m, 2H), 3.08-2.99(m, 1H), 2.99-2.92 (m, 1H), 2.83-2.63 (m, 2H), 2.50 (DMSO, overlap), 2.40-2.31 (m, 1H), 2.18-1.96 (m, 3H), 1.55-1.42 (m, 2H), 1.16 (d, *J*=5Hz, 3H), 1.12 (d, *J*=5Hz, 3H), 0.74-0.67 (m, 1H), 0.66-0.59 (m, 1H), 0.58-0.51 (m, 1H), 0.46-0.38 (m,1H) ppm.

^{13}C NMR (d_6-DMSO) 300 MHz: δ 205.97 (C=O, 6-*O* ketone), 166.61, (C=O, ester), 147.08, 131.02, 129.54, 128.94, 123.38, 120.31, 89.82, 69.56, 60.54, 57.16, 56.70, 48.65, 45.69, 34.92, 30.58, 29.72, 27.16, 23.40, 18.52, 17.42, 5.80, 5.25, 2.79 ppm.

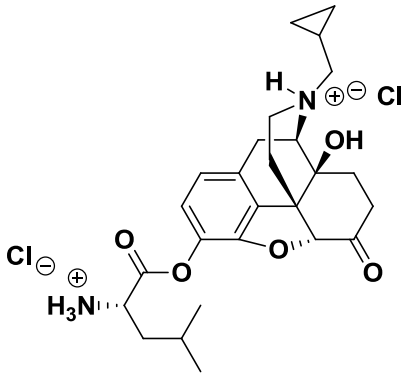

3-*O*-Leu-NTX

^{1}H NMR (d_6-DMSO) 500 MHz: δ 9.17 (s, 1H, broad), 8.88 (s, 3H, broad), 7.24 (s, < 1H, broad), 7.08 (d, 1H, *J*=10 Hz), 6.88 (d, 1H, *J*=10 Hz), 5.26 (s, 1H), 4.25 (m, 1H), 4.10 (d *J*=5.0 Hz, 1H), 3.56 (d, *J*=5 Hz, 2H), 3.50 (DMSO water peak), 3.40-3.30 (m, 1H), 3.21-2.99(m, 3H), 2.99-2.92 (m, 1H), 2.83-2.63 (m, 1H), 2.50 (DMSO, overlap), 2.17-2.06 (m, 2H), 1.97-1.89 (m, 1H), 1.86-1.80 (m, 2H), 1.55-1.44 (d, *J*=5 Hz, 2H), 1.20-1.07(m, 1H), 1.0 (s, 1H), 0.99-0.94 (overlap, doublets, 6H), 0.74-0.66 (m, 1H), 0.65-0.58 (m, 1H), 0.58-0.51 (m, 1H), 0.45-0.38 (m,1H) ppm.

^{13}C NMR (d_6-DMSO) 300 MHz: δ 206.08 (C=O, 6-*O* ketone), 167.67 (C=O, ester), 147.01, 131.05, 129.47, 128.91, 123.20, 120.22, 89.71, 69.53, 66.30, 60.48, 56.67, 50.50, 48.62, 45.65, 34.94, 30.60, 27.18, 23.79, 23.34, 22.31, 22.12, 5.78, 5.23, 2.79 ppm.

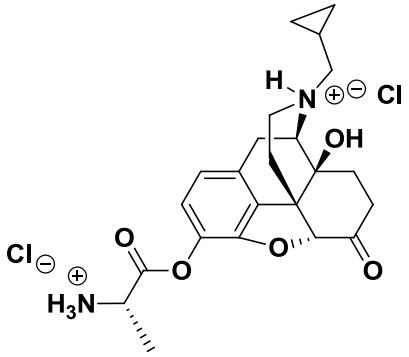

3-*O*-Ala-NTX

^{1}H NMR (d_6-DMSO) 500 MHz: δ 9.17 (s, broad, 1H), 8.81 (s, broad, 3H), 7.21 (s, broad, <1H), 7.07 (d, *J*=10 Hz, 1H), 6.88 (d, *J*=10 Hz, 1H), 5.76 (d, *J*=5Hz, <1H), 5.25 (s, 1H), 4.42 (m, 1H), 4.10 (d, *J*=5 Hz, 1H), 3.49 (DMSO water peak), 3.41-3.30 (m, 2H), 3.20-2.99 (m, 4H), 2.98-2.90 (m, 1H), 2.80-2.71 (m, 1H), 2.54 (m, <1H), 2.52-2.41 (DMSO overlap region), 2.18-2.06 (m, 2H), 1.60 (d, *J*=5 Hz, 3H), 1.55-1.44 (m, 2H), 1.17-1.06 (m, 1H), 0.73-0.66 (m, 1H), 0.66-0.58 (m, 1H), 0.58-0.50 (m, 1H), 0.46-0.38 (m, 1H) ppm.

13C NMR (d_6-DMSO) 300 MHz: δ 206.09 (C=O, 6-*O* ketone), 167.90 (C=O, ester), 146.98, 131.11, 129.48, 128.88, 123.21, 120.25, 89.67, 69.55, 60.51, 56.70, 48.62, 47.79, 45.65, 34.92, 30.60, 27.21, 23.38, 15.94, 5.78, 5.22, 2.80 ppm.

Table 2.1 3-*O*-NTX amino acid dihydrochlorides material recovery.

	3-*O*-Val-NTX	**3-*O*-Leu-NTX**	**3-*O*-Ala-NTX**
MW base (g mol^{-1})	440.53	454.56	412.48
MW salt (g mol^{-1})	513.45	527.48	485.40
mg isolated	90.2	81.3	56.8
Theoretical yield	150.4	154.5	142.2
% yield	60.0	52.6	40.0

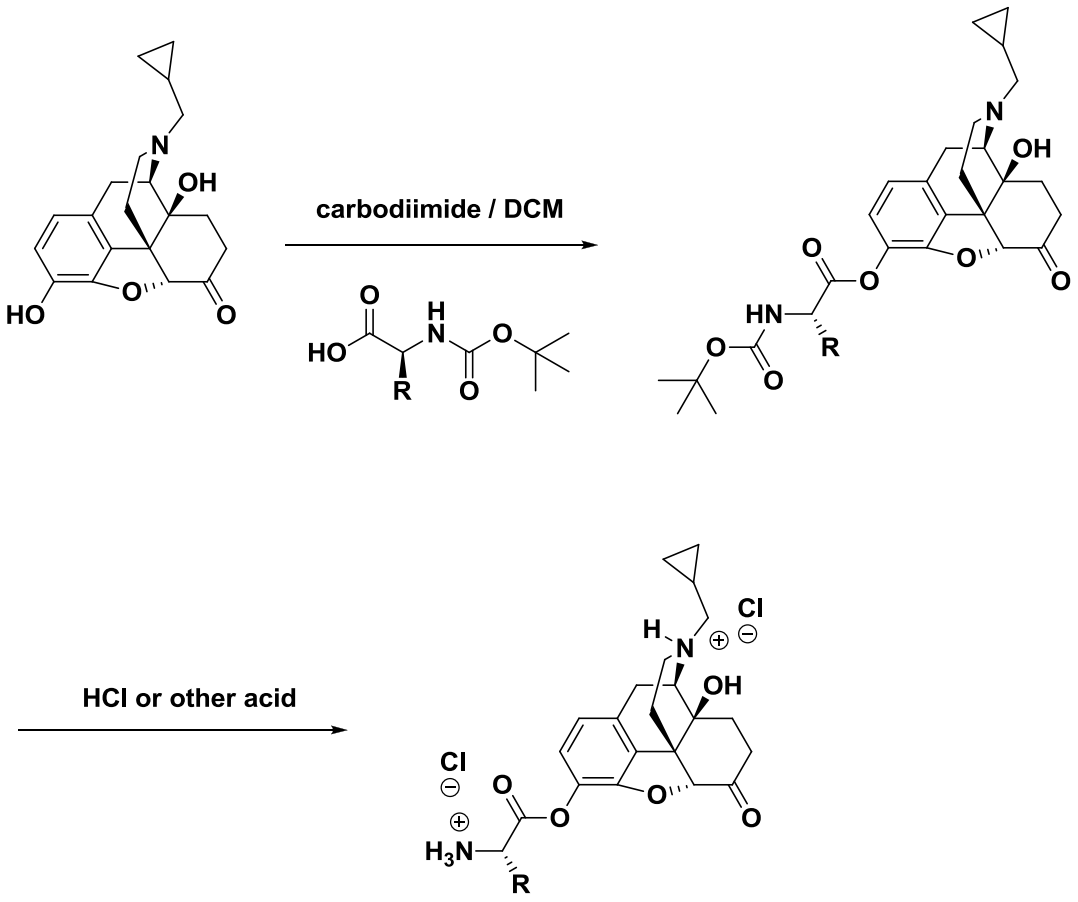

Scheme 2.1 BOC method to form 3-*O*-NTX amino acid ester prodrugs.

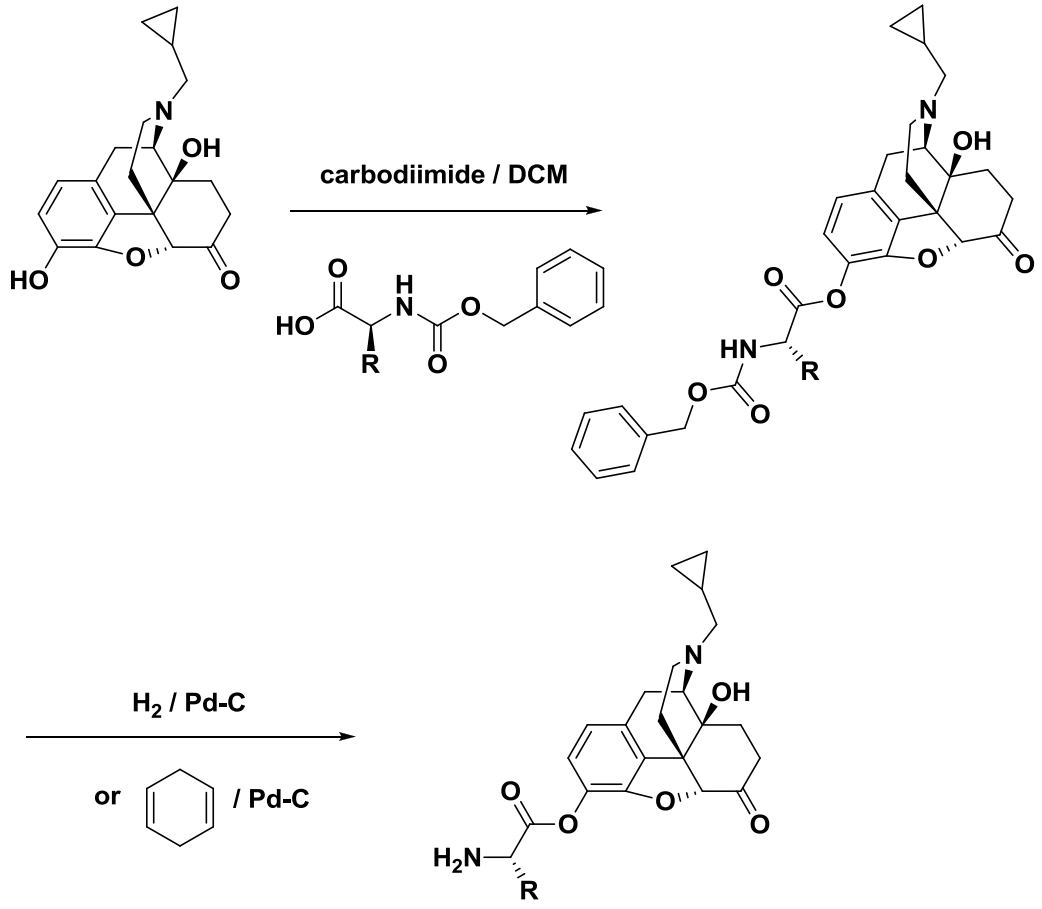

Scheme 2.2 Cbz method to form 3-*O*-NTX amino acid ester prodrugs.

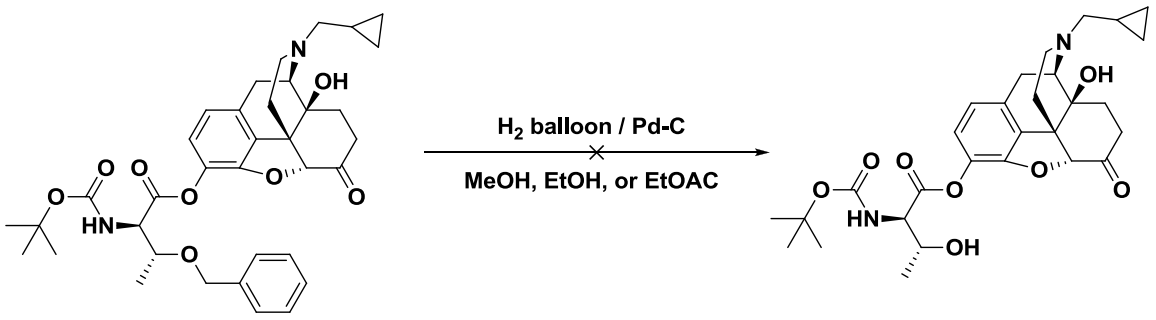

Scheme 2.3 First attempted debenzylations of 3-*O*-Boc-Thr(Bzl)-NTX.

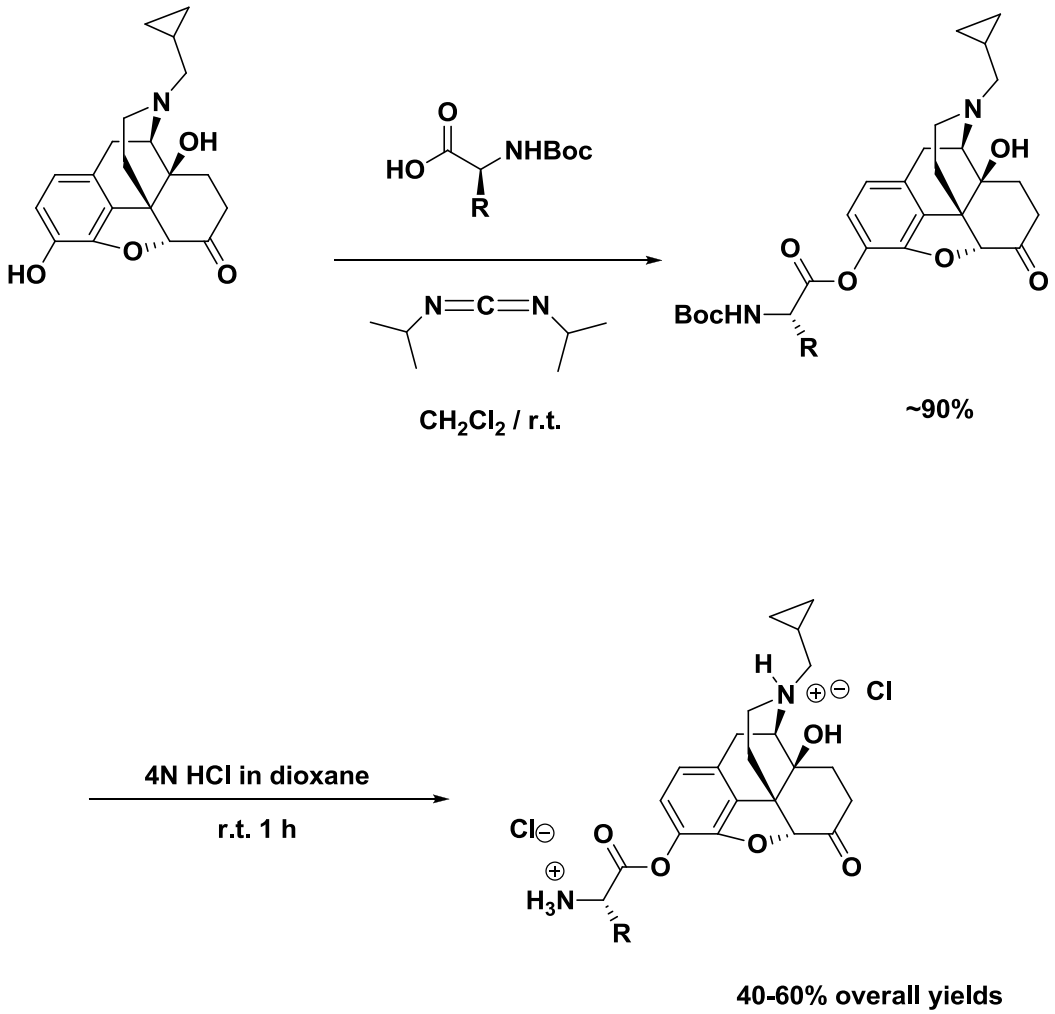

Scheme 2.4 Synthesis of 3-*O*-NTX amino acid dihydrochlorides.

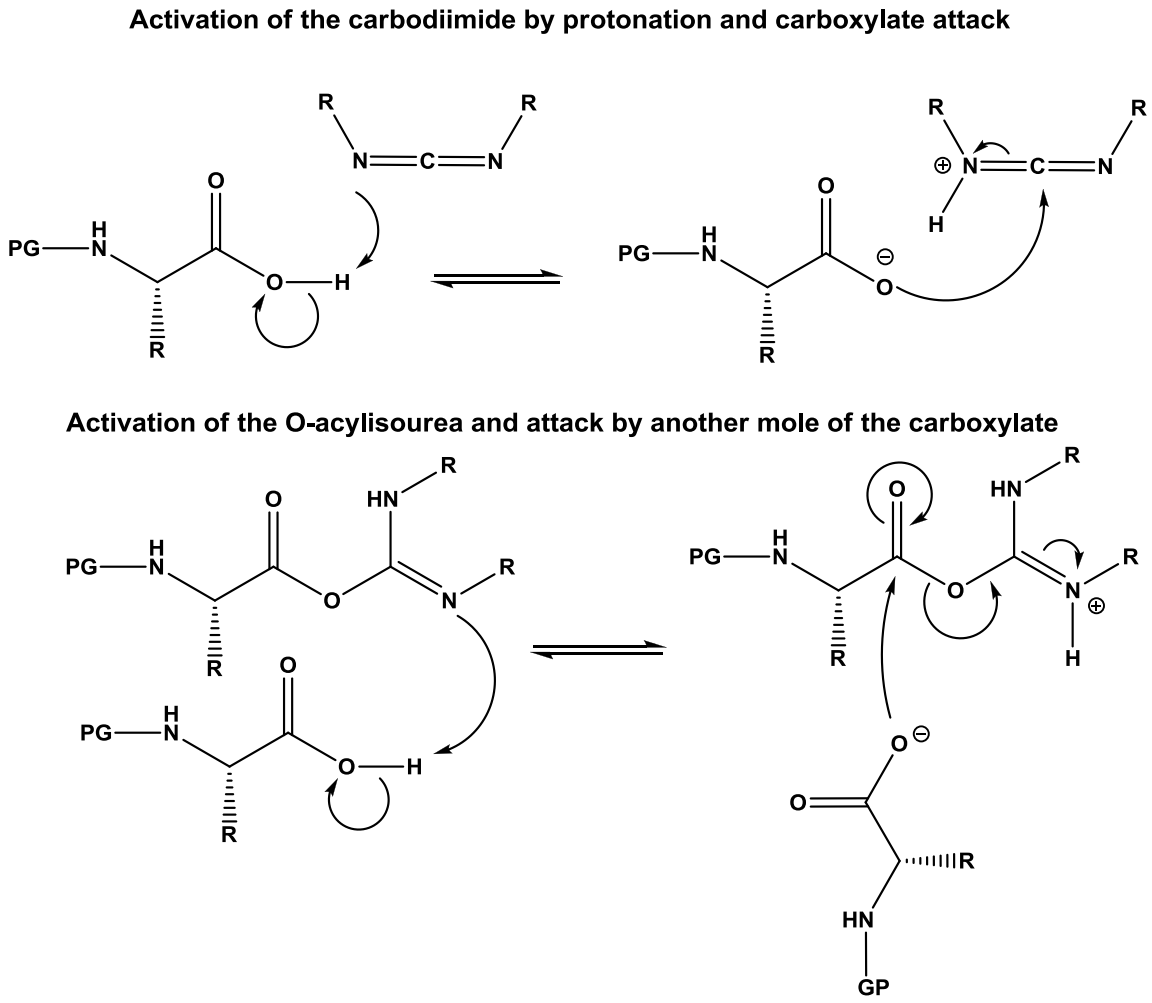

Figure 2.1 Mechanism of carbodiimide coupling (PG = protecting group).

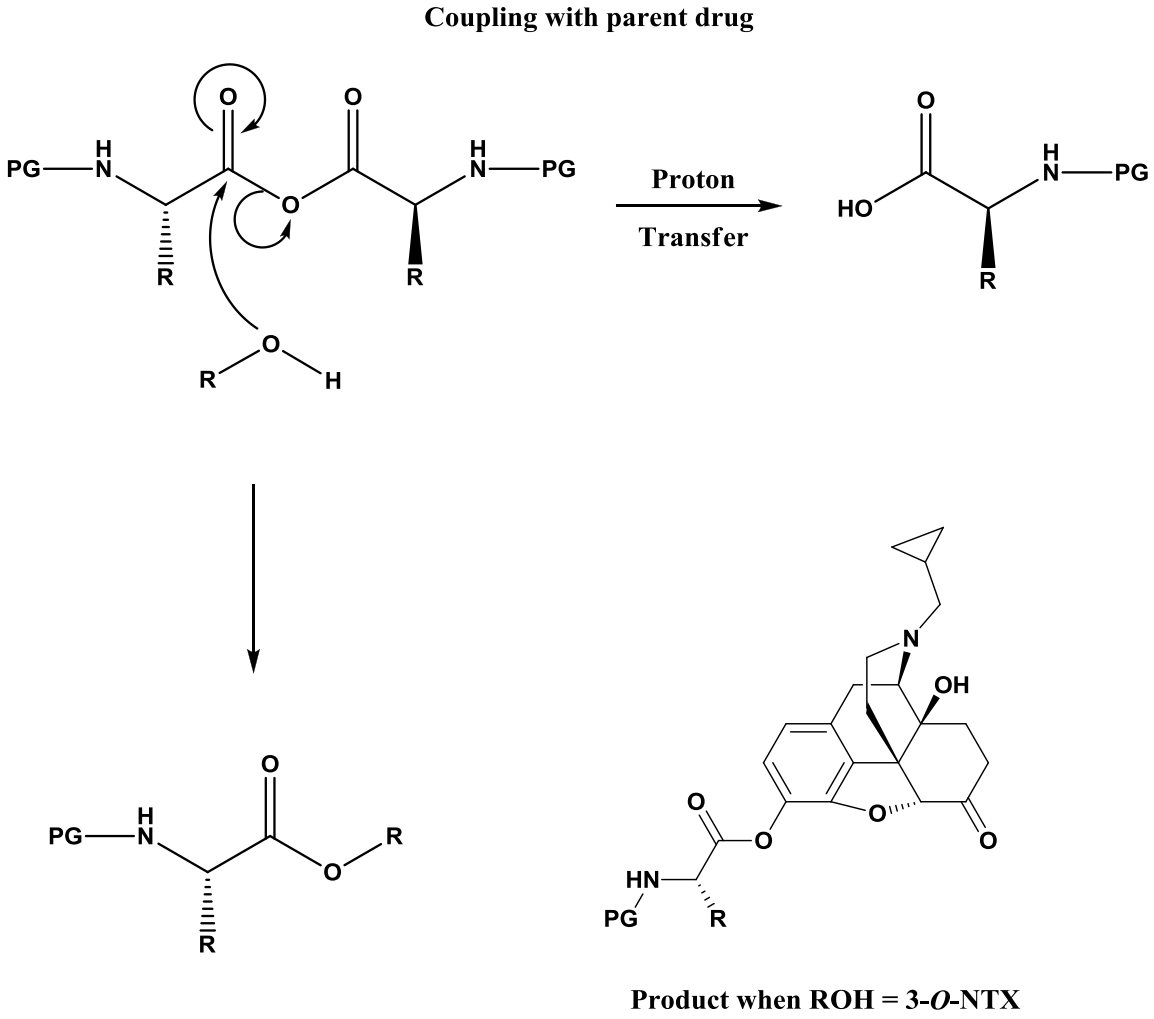

Figure 2.1 Mechanism of carbodiimide coupling (continued).

Direct attack on the O-acylisourea by the parent drug nucelophile

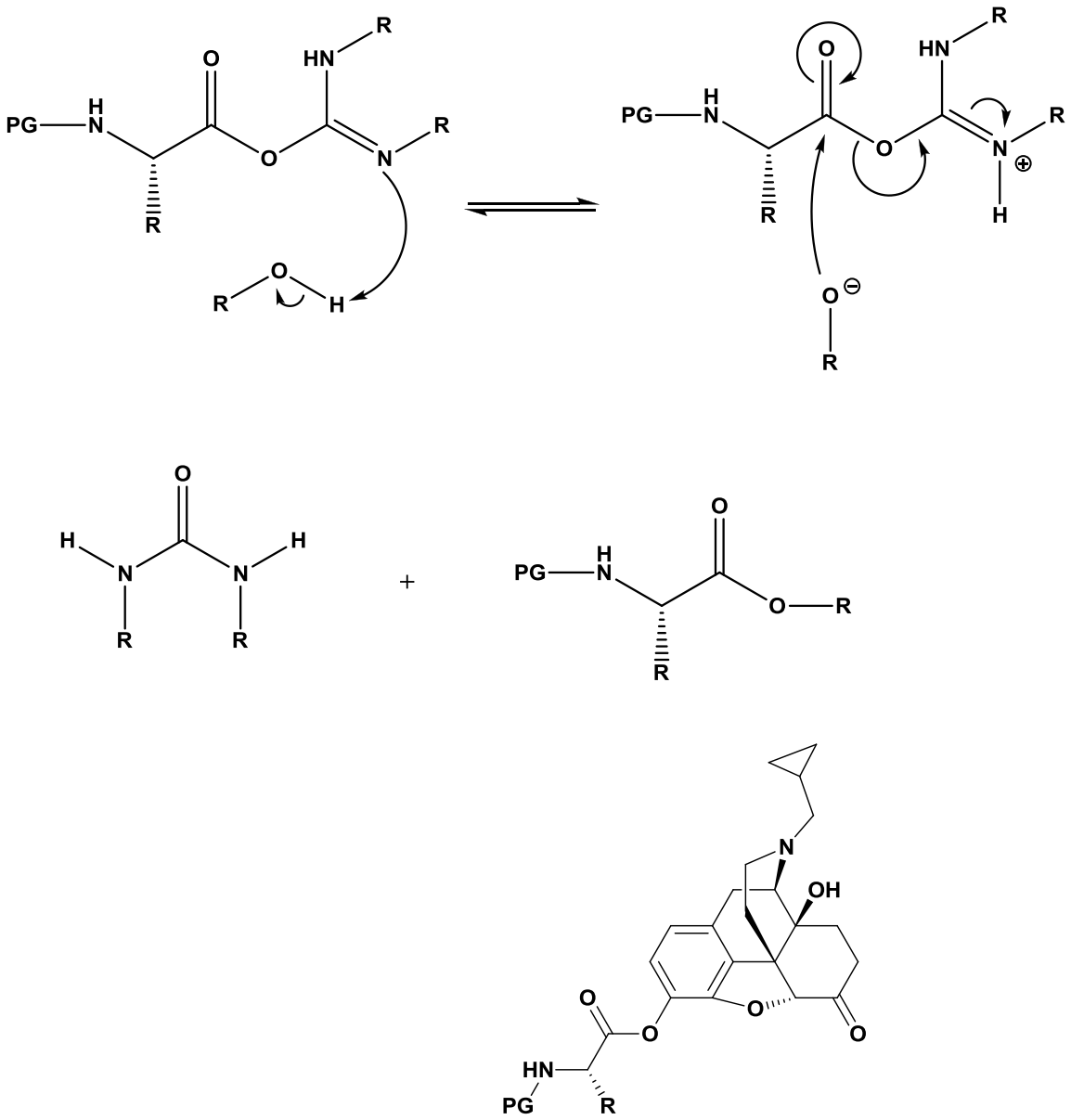

Product when ROH =3-*O*-NTX

Figure 2.1 Mechanism of carbodiimide coupling (continued).

Rearrangement of O-acylisourea to an N-acylurea

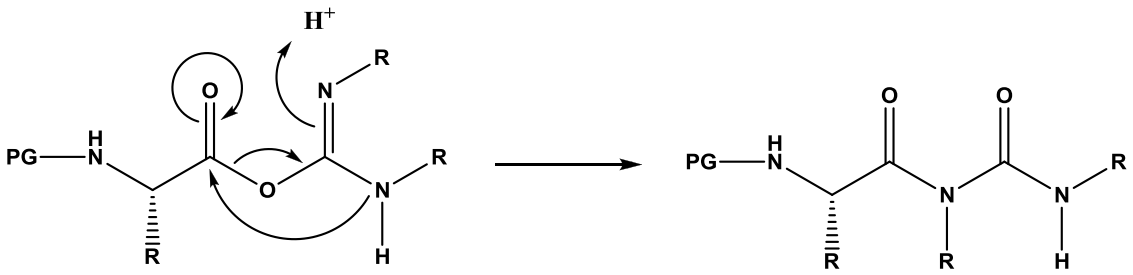

Specific reagents and side product structures:

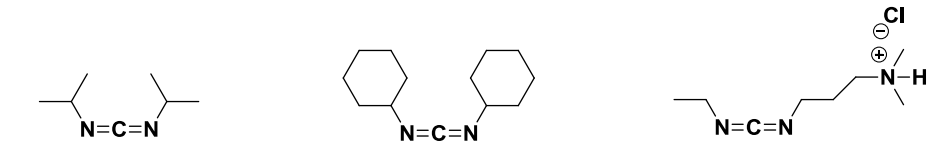

Diisopropylcarbodiimide (DIC)

Dicyclohexylcarbodiimide (DCC)

1-ethyl-3-(3-dimethylaminopropyl) carbodiimide HCl (EDC•HCl)

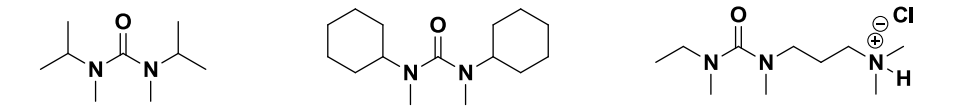

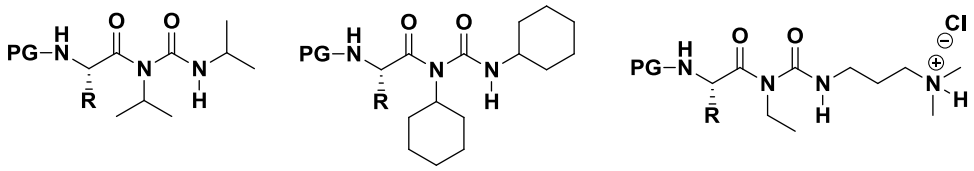

Figure 2.1 Mechanism of carbodiimide coupling (continued).

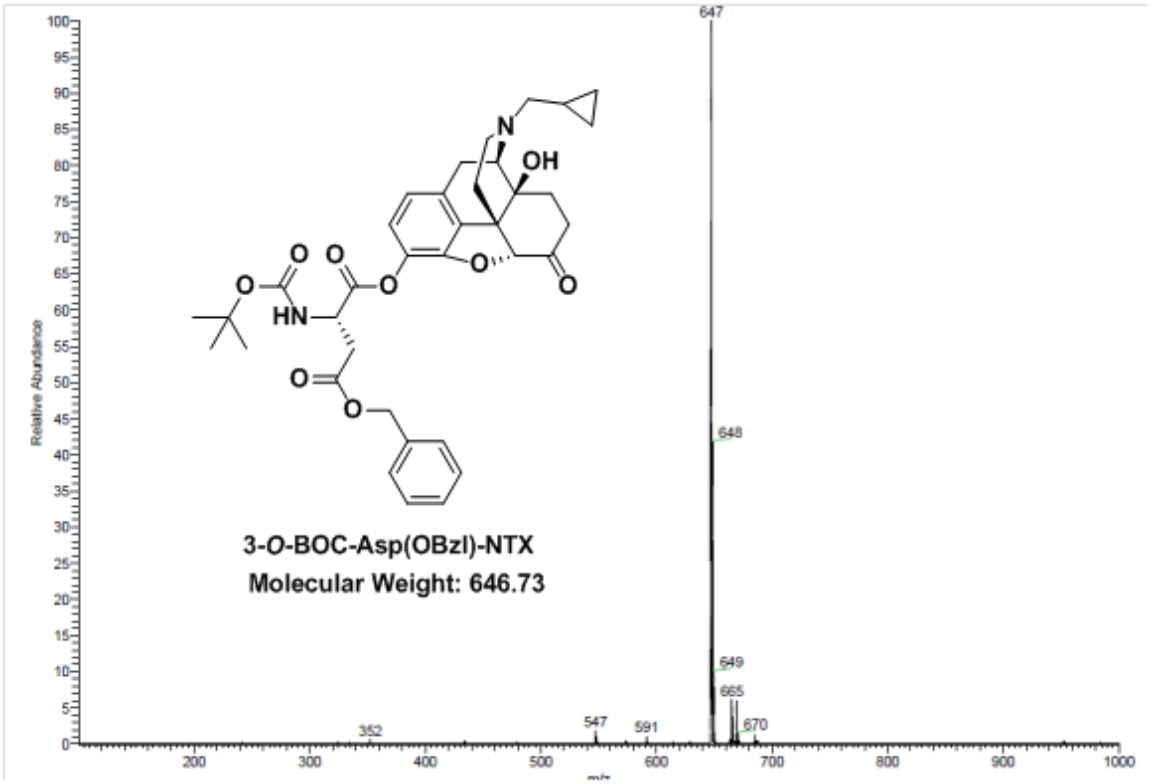

Figure 2.2 ESI-MS of 3-*O*-BOC-Asp(OBzl)-NTX.

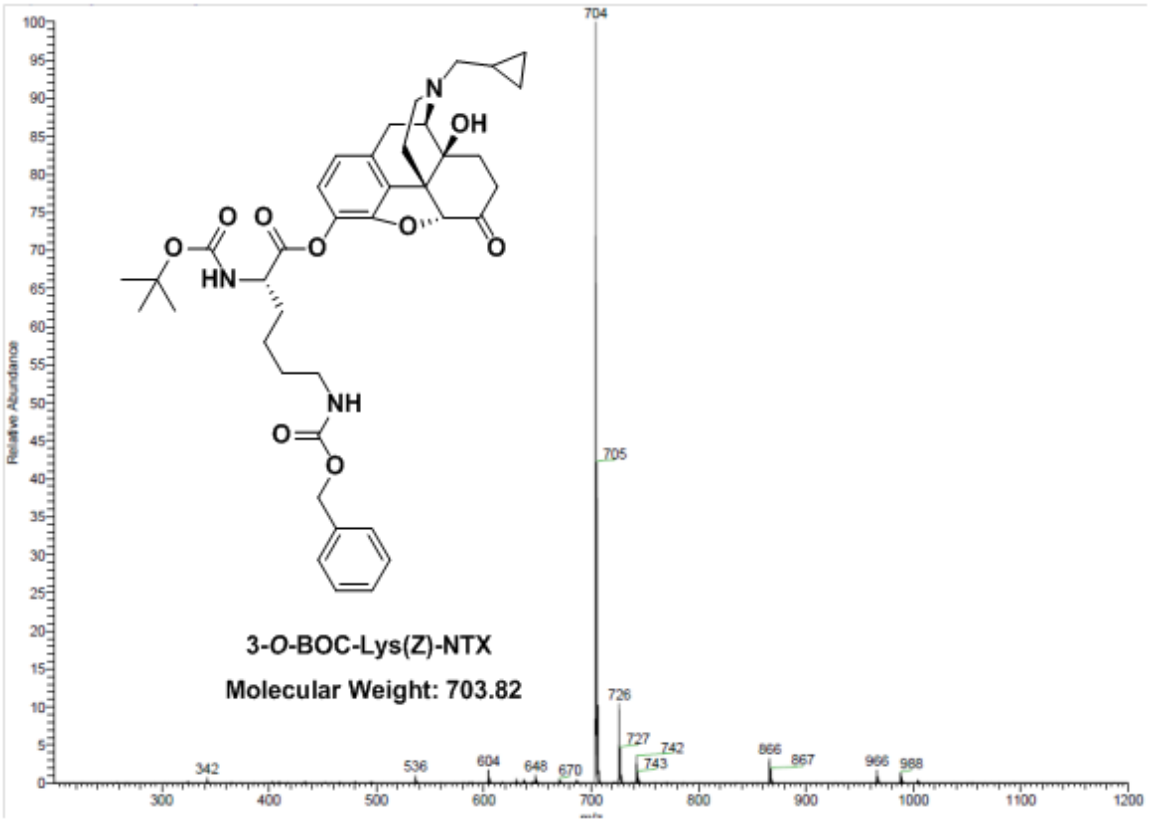

Figure 2.3 ESI-MS of 3-*O*-BOC-Lys(Z)-NTX.

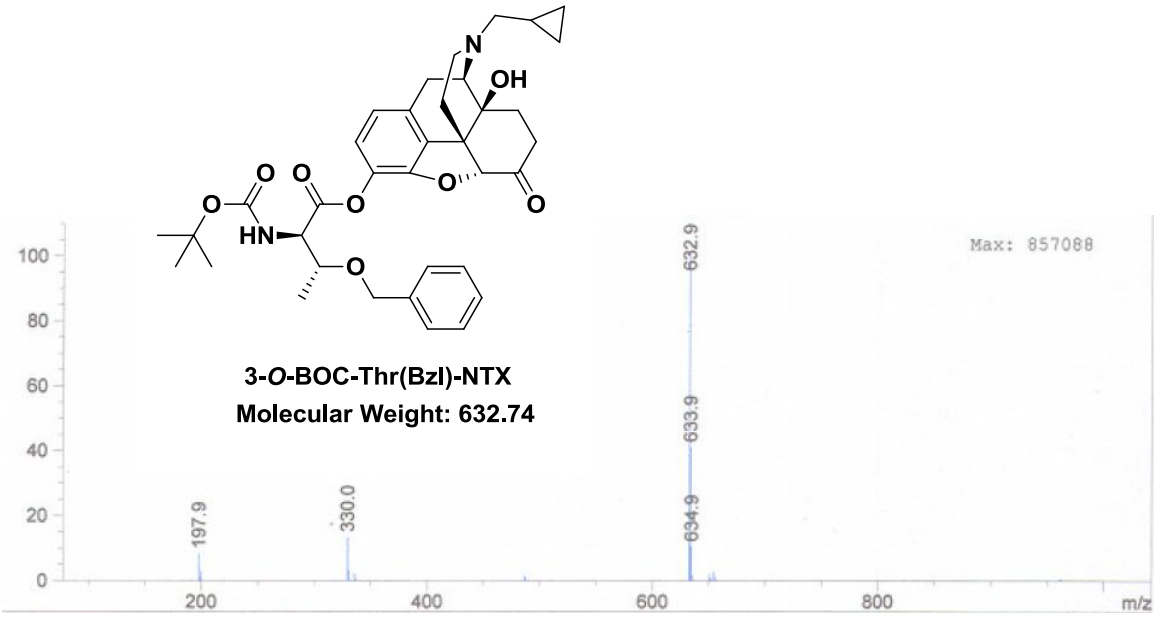

Figure 2.4 ESI-MS of 3-*O*-BOC-Thr(Bzl)-NTX.

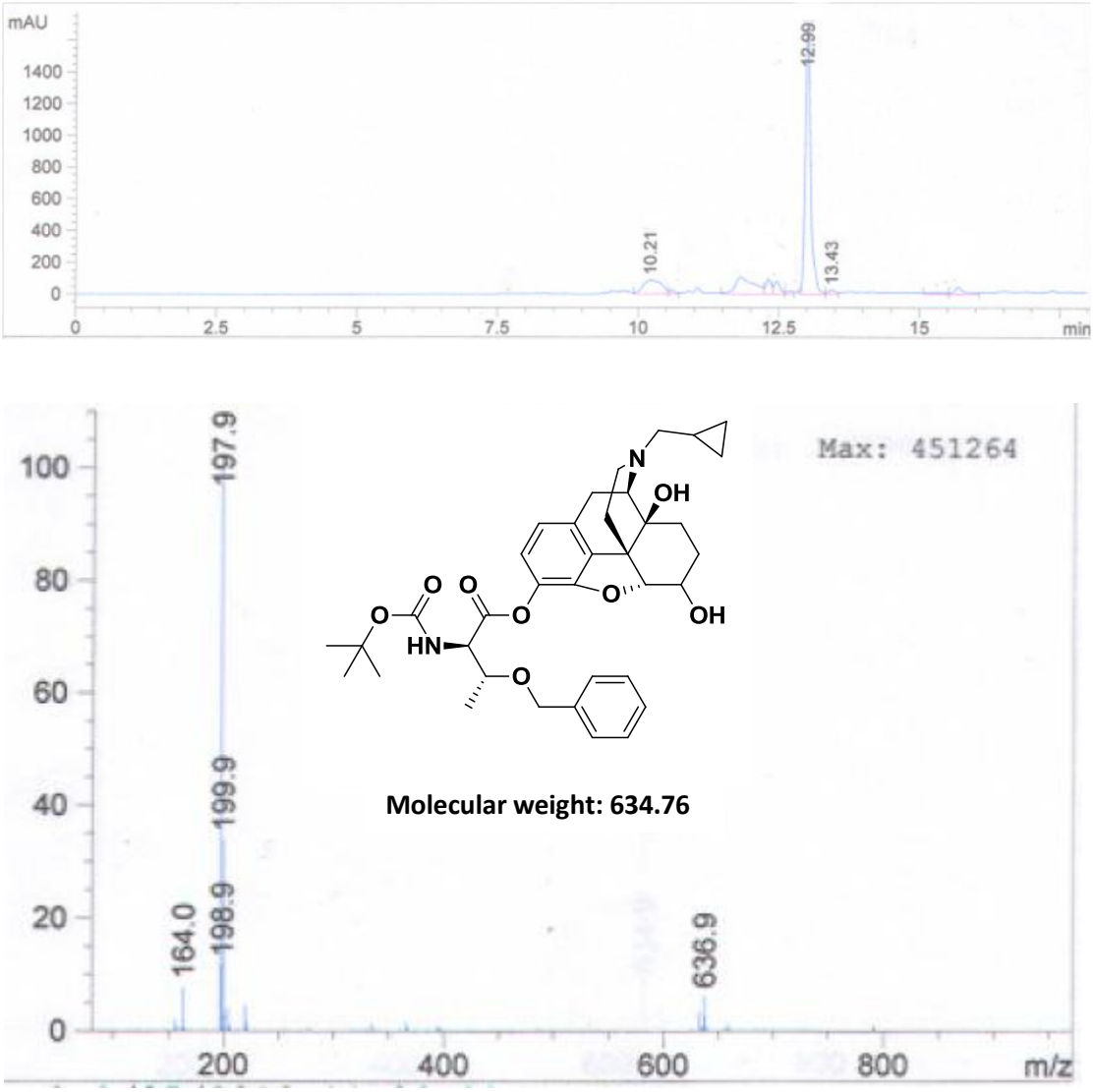

Figure 2.5 LC-UV/ESI-MS of 3-*O*-BOC-Thr(Bzl)-NTX after 48 h hydrogenolysis @ 50 psi H_2 with Pd-C. Mass spectrum extracted from r.t.= 13.43 min.

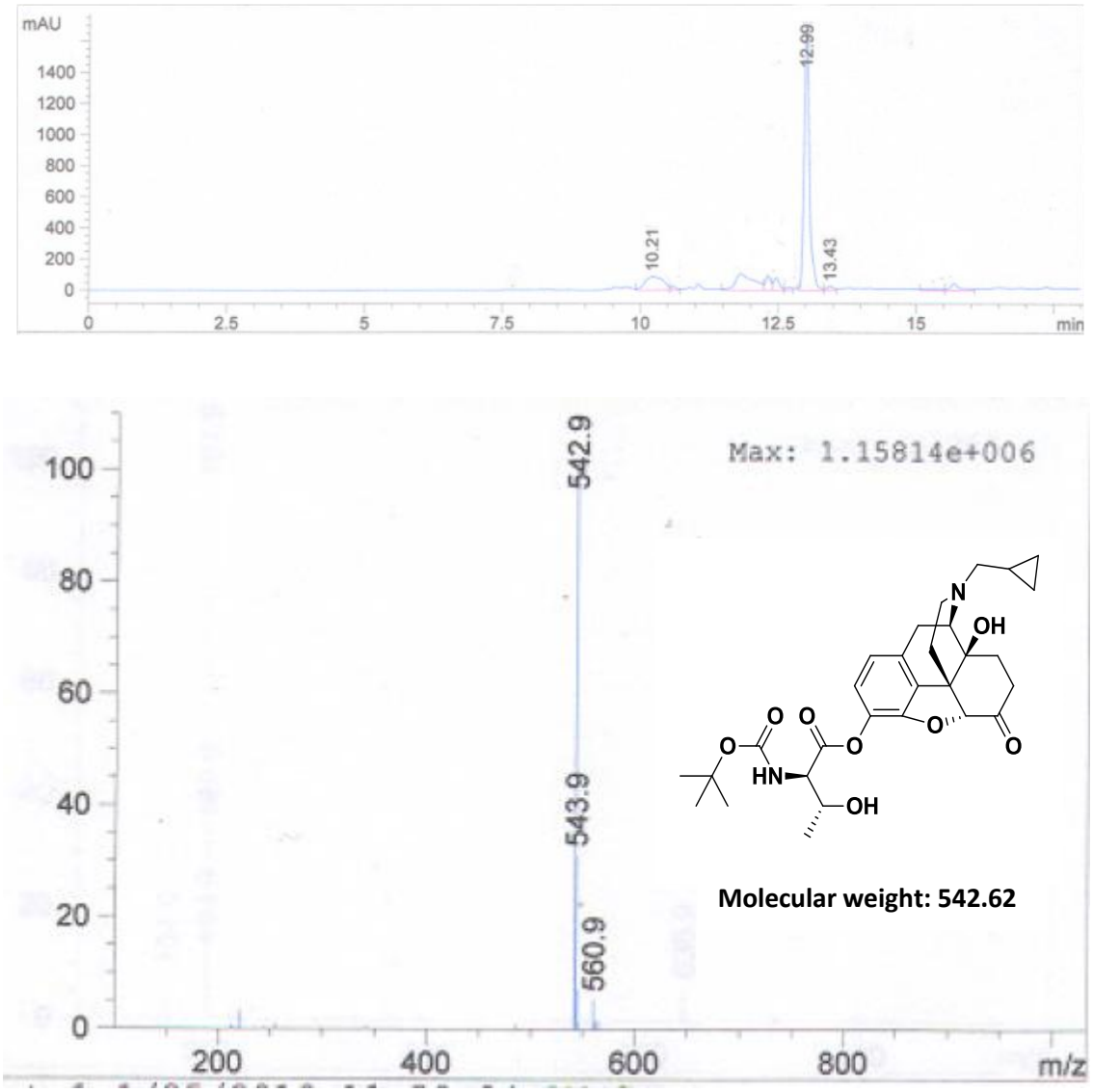

Figure 2.6 LC-UV/ESI-MS of 3-*O*-BOC-Thr(Bzl)-NTX after 48 h hydrogenolysis @ 50 psi H_2 with Pd-C. Mass spectrum extracted from the peak at r.t.= 10.21 min.

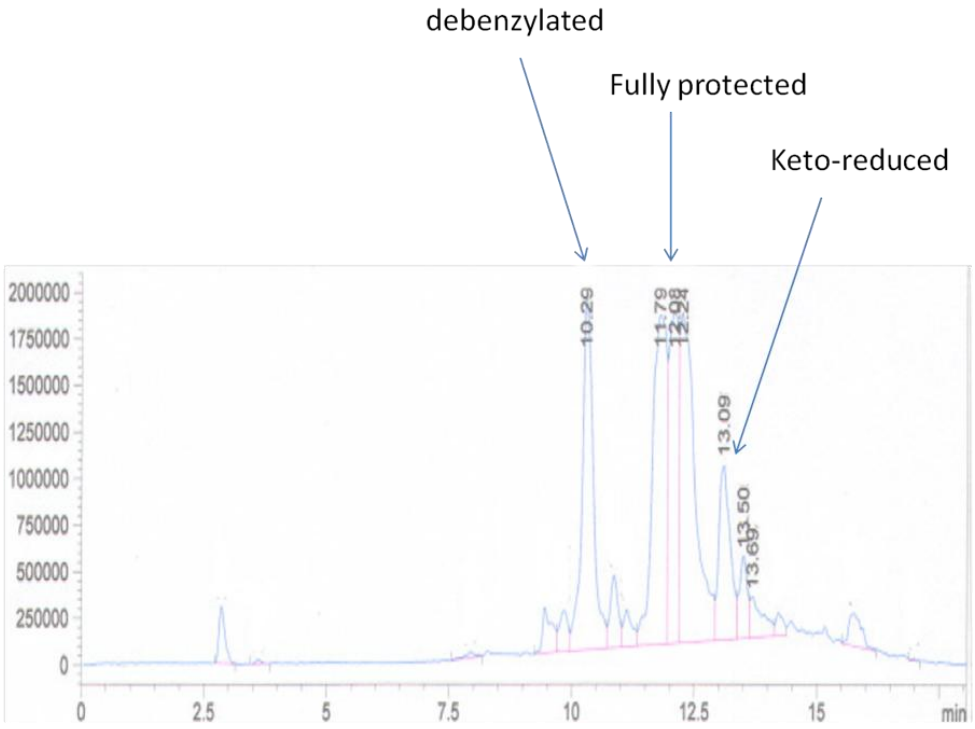

Figure 2.7 Total Ion Count (ESI-MS Positive Scan Mode).

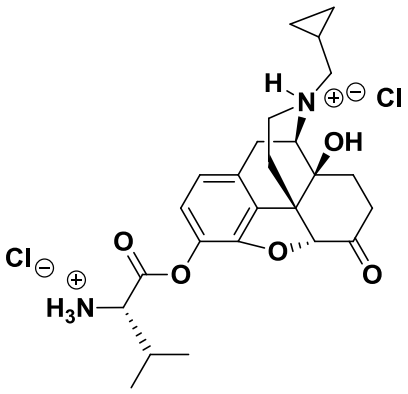

3-*O*-Val-NTX•2HCl
t_{90} = 1.54±0.02 h

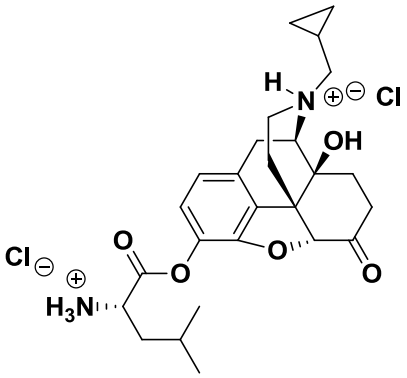

3-*O*-Leu-NTX•2HCl
t_{90} = 2.72±0.03 min

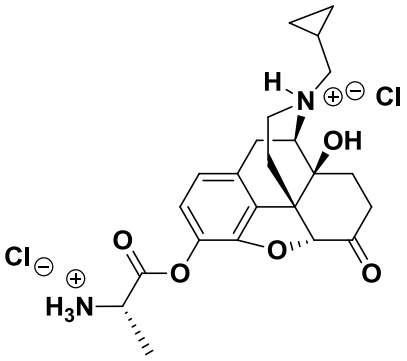

3-*O*-Ala-NTX•2HCl
t_{90} = 1.33±0.05 min

Figure 2.8 Stability of 3-*O*-NTX amino acid dihydrochlorides R=alkyl in pH 5.0 acetate buffer (32 °C).

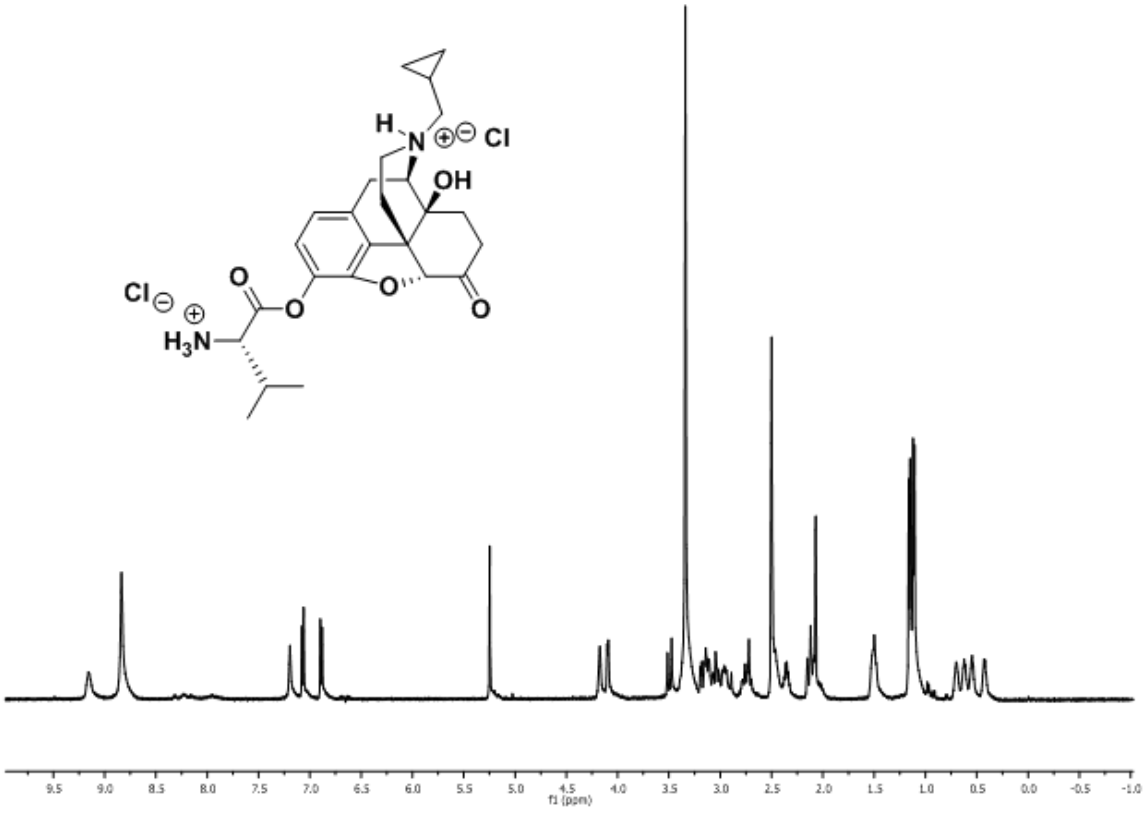

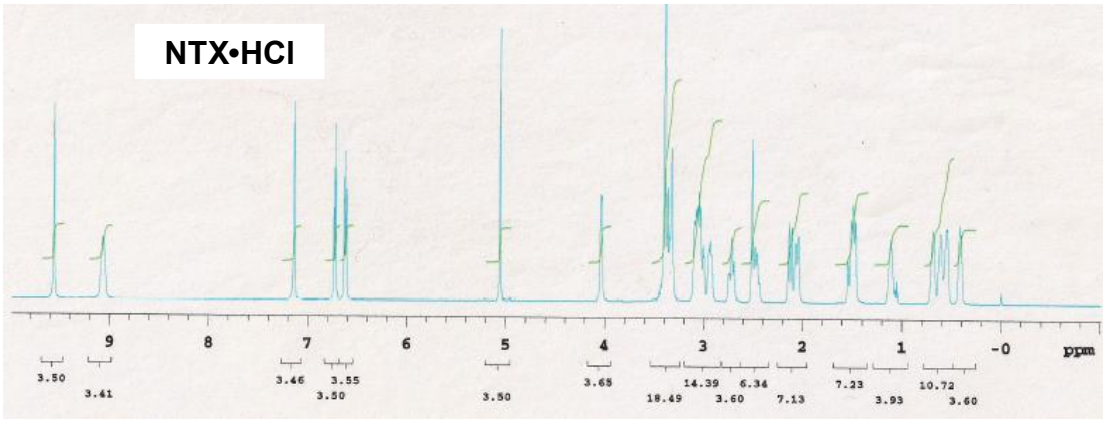

Figure 2.9 ^{1}H NMR spectra of the 3-*O*-Val-NTX dihydrochloride prodrug and NTX•HCl.

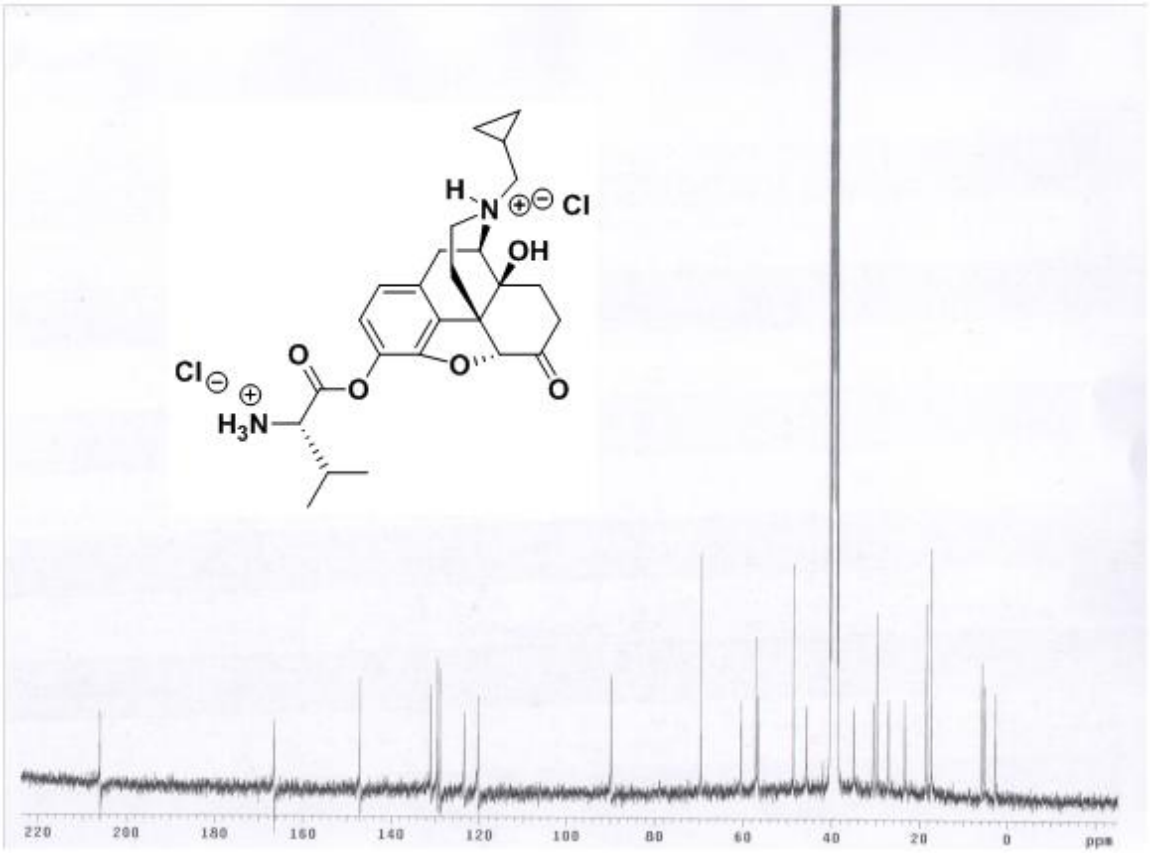

Figure 2.10 ^{13}C NMR spectrum of 3-*O*-Val-NTX dihydrochloride prodrug.

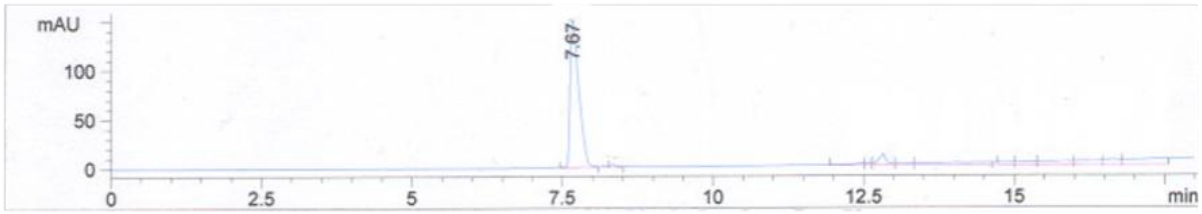

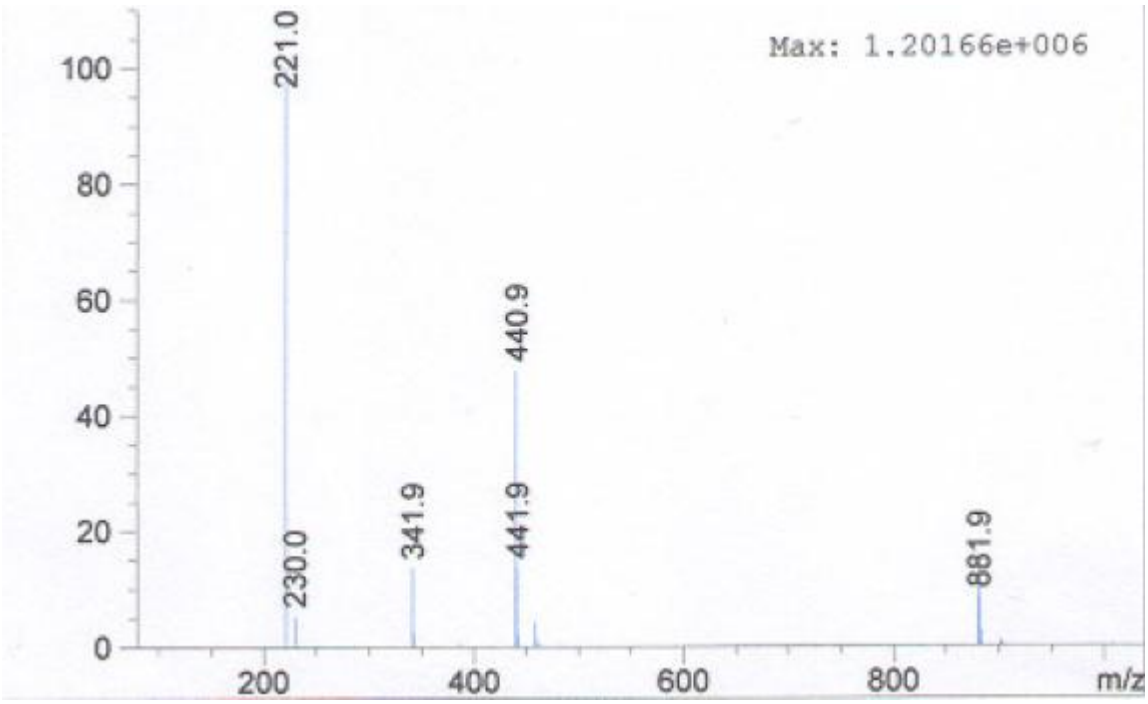

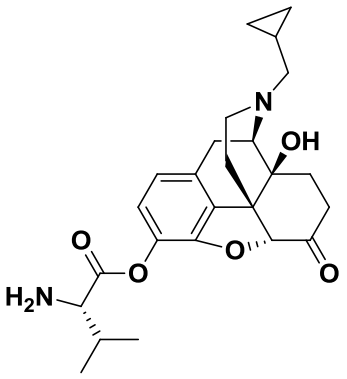

Molecular Weight: 440.53

Figure 2.11 LC-UV/ESI-MS of 3-*O*-Val-NTX prodrug.

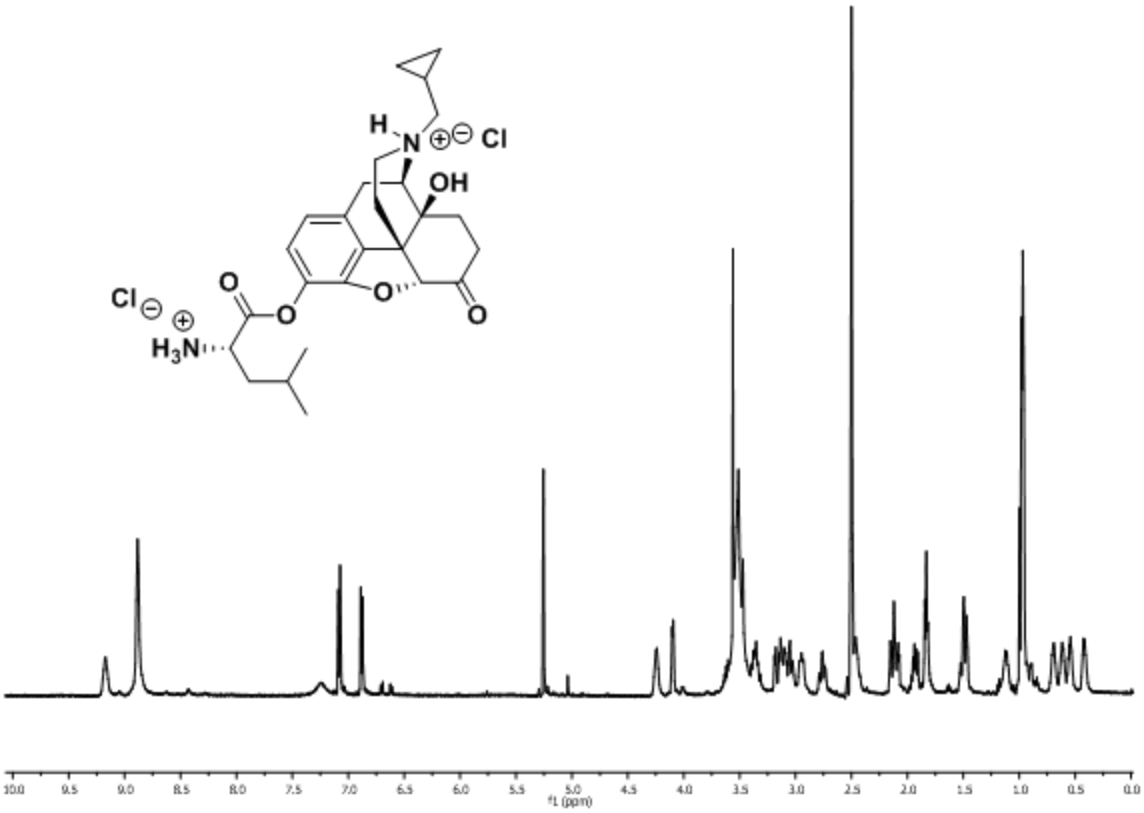

Figure 2.12 ^{1}H NMR spectra of the 3-*O*-Leu-NTX dihydrochloride prodrug and NTX•HCl.

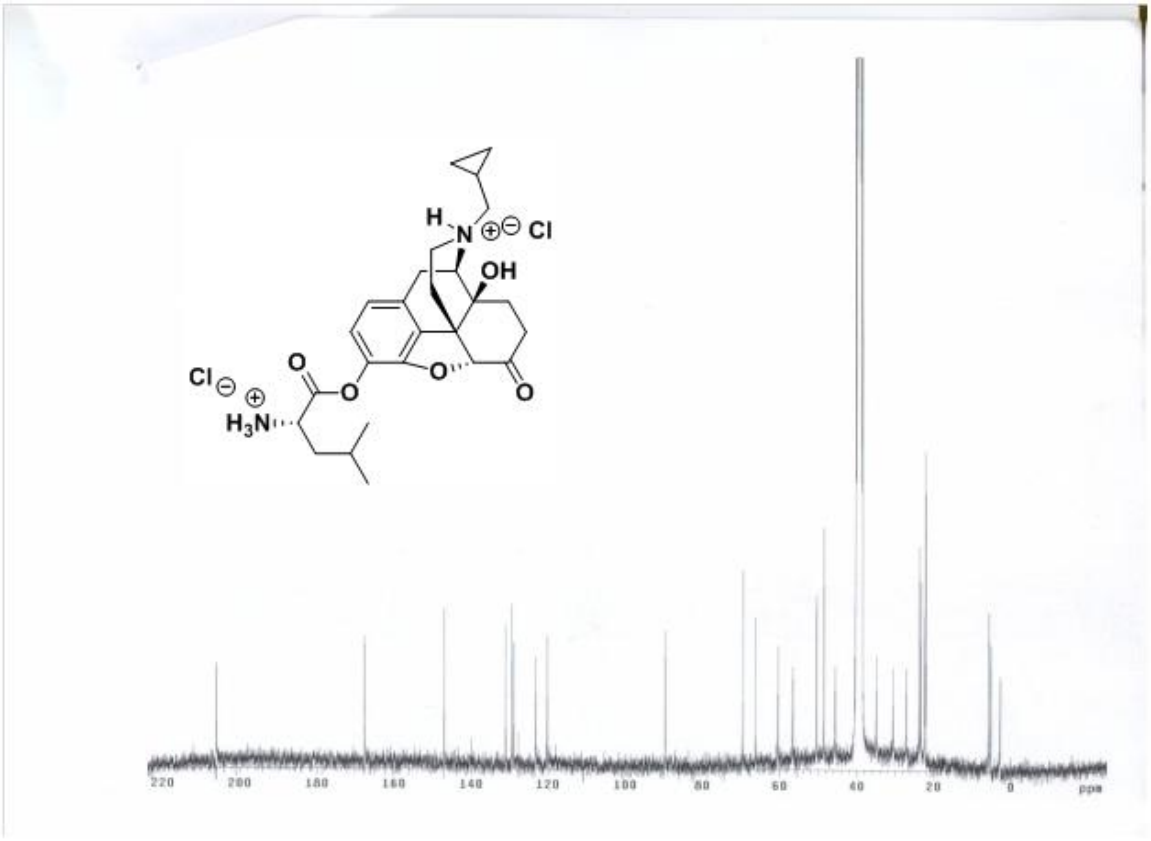

Figure 2.13 ^{13}C NMR spectrum of 3-*O*-Leu-NTX dihydrochloride prodrug.

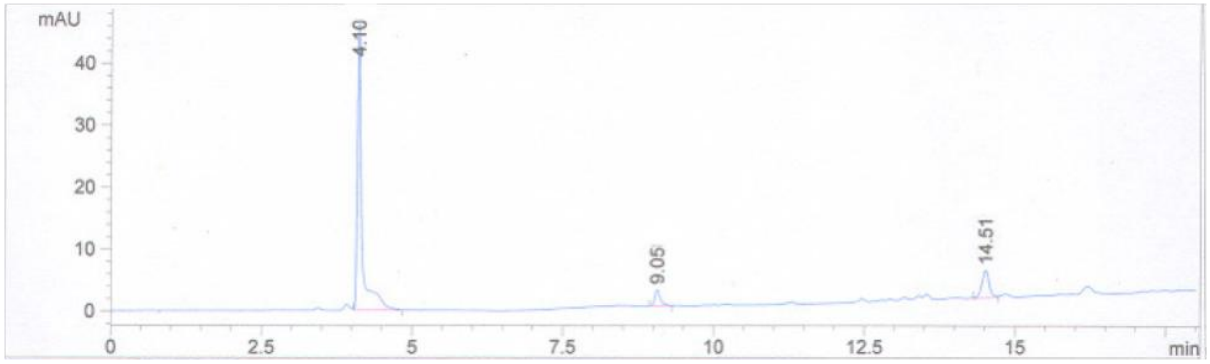

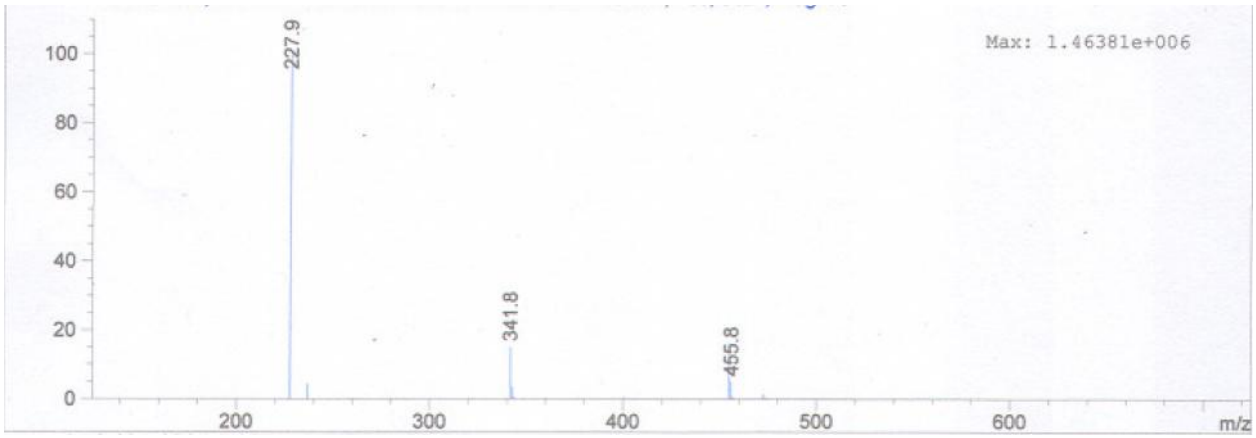

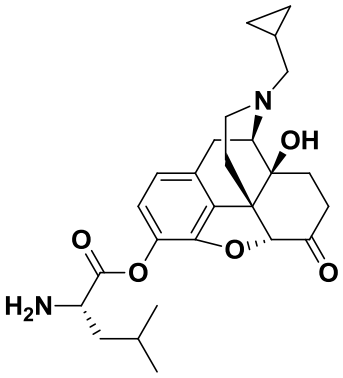

Molecular Weight: 454.56

Figure 2.14 LC-UV/ESI-MS of 3-*O*-Leu-NTX prodrug.

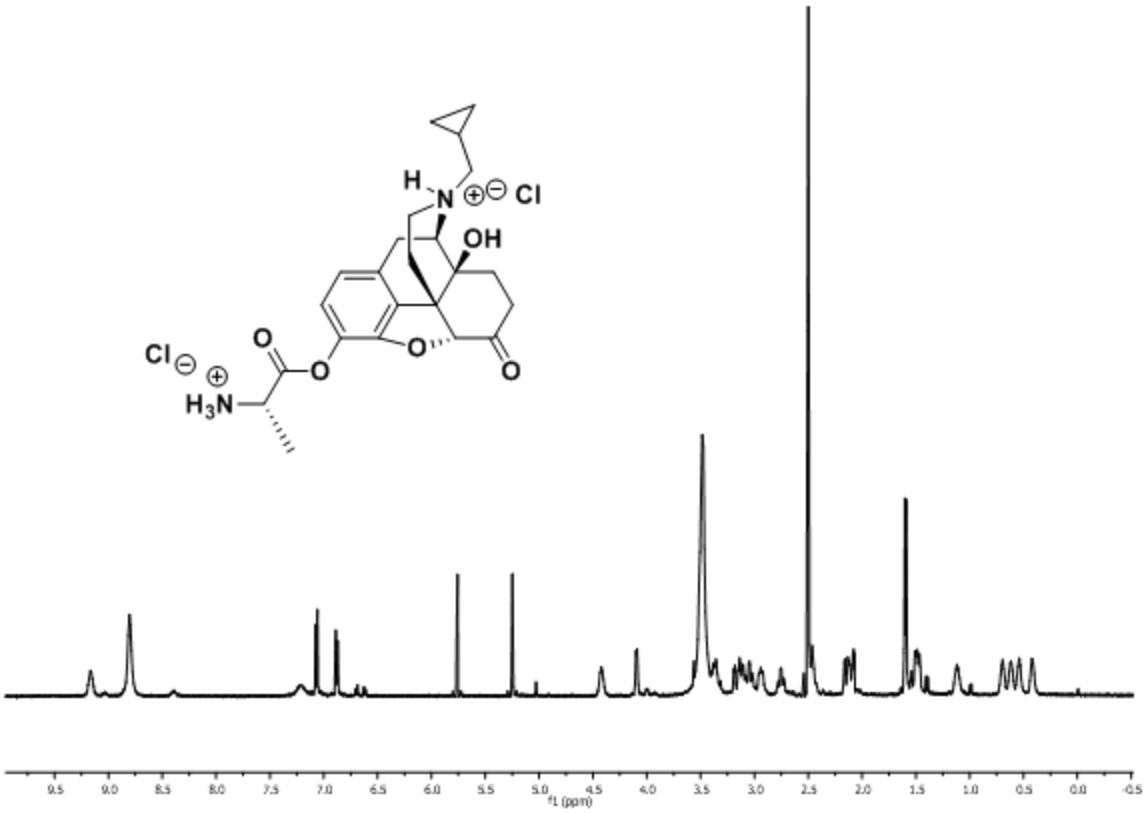

Figure 2.15 ^{1}H NMR spectra of the 3-*O*-Ala-NTX dihydrochloride prodrug and NTX•HCl.

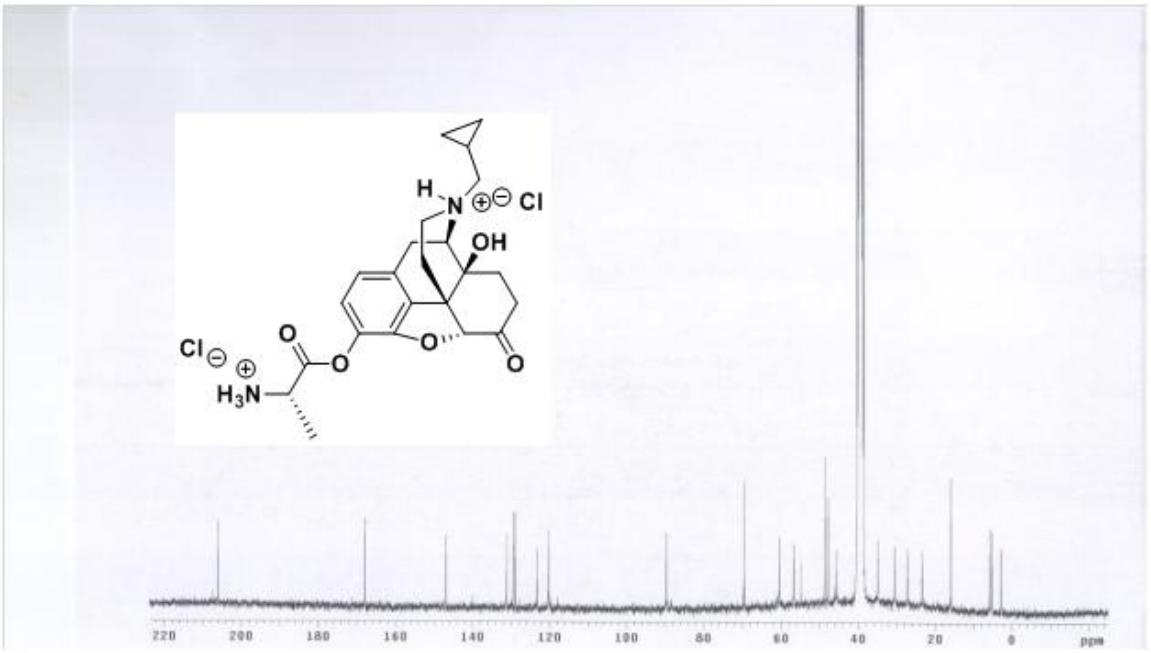

Figure 2.16 ^{13}C NMR spectrum of 3-*O*-Ala-NTX dihydrochloride prodrug.

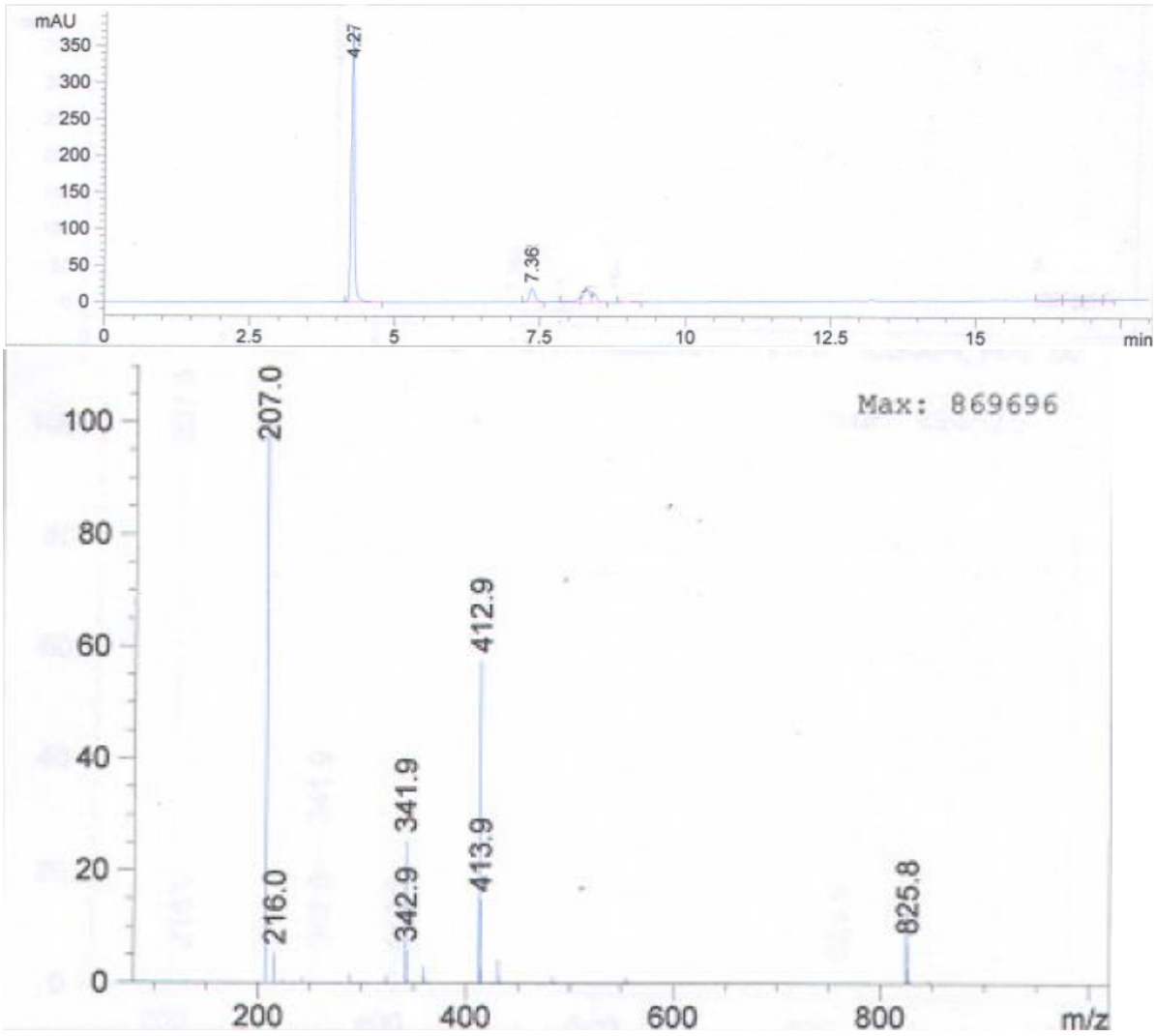

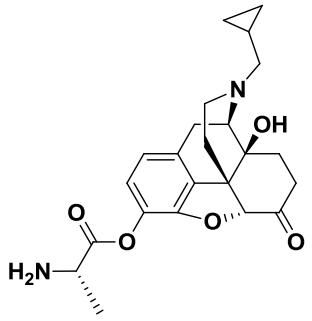

Molecular Weight: 412.48

Figure 2.17 LC-UV/ESI-MS of 3-*O*-Ala-NTX prodrug.

Chapter 3

Synthesis of 6-*O*-NTXOL amino acid esters

3.1 Synthetic Design Considerations

Due to poor stability that was observed in the 3-*O*-amino acid ester series of NTX prodrugs, it was decided that attention should be turned to the development 6-*O*-amino acid ester prodrugs of NTXOL. The only other options for prodrug development on NTX/NTXOL without the addition of linkers would have required one of two approaches. Specifically, the 14-*O* position of NTX or NTXOL could have been accessed, or the 6-*O* ketone of NTX could have possibly been exploited as an enolate acylation position (see evidence for enolate coupling in **Chapter 4**). In any of these cases, the requirement for additional protecting group strategies would have been unavoidable to ensure regioselective synthesis. Therefore, it was considered most attractive to go for the easiest aliphatic nucleophile with which to couple--the 6-*O*-NTXOL hydroxyl position. NTXOL was obtained in 85-92.7% yield, depending on reaction scale, by the method of De Costa *et al*. (De Costa et al. 1992). The reaction was found to be reliable and reproducible throughout this body of work.

Following the preparation of NTXOL, a number of viable strategies were possible to protect the phenolic position of NTXOL in order to proceed with prodrug synthesis. For instance, it was envisaged that Fmoc-protected amino acids could be coupled to a 3-*O*Bn-NTXOL synthon to furnish orthogonally protected 3-*O*Bn-6-*O*-Fmoc-amino acid-NTXOL ester prodrug precursors. Otherwise, it was also

envisioned that a global hydrogenolysis deprotection scheme could be employed to afford amino acid ester prodrugs if 3-*O*Bn-NTXOL and Cbz-protected amino acids could first be coupled and then deblocked simultaneously in the final synthetic step.

3.2 Synthesis of trifunctional amino acid ester prodrugs of NTXOL

The Fmoc/OBn approach was tested first to check for possible problems that can occur in global deblocking protocols. 3-*O*Bn-NTXOL was prepared as the first synthon (**Scheme 3.1, Step 1**). Luckily, a simple method was employed that afforded the desired benzyl protected synthon in 94.5% yield without the need for column chromatography. The first Fmoc-protected pro-moiety that was chosen for conjugation was Fmoc-Asp(OBzl)-OH. The use of this pro-moiety was incorporated into the synthetic design to check the feasibility of using trifunctional amino acids in the 6-*O*-NTXOL prodrug design. Such an approach would give the best range of increased hydrophilicity for MNTD studies. Also, the benzyl ester protecting group on the carboxylate side chain of aspartic acid is susceptible to hydrogenolysis similar to the 3-OBn moiety of NTXOL; however, the final Fmoc removal would still impart an orthogonal final step. Though intramolecular cyclization of the free carboxylate side chain on the aliphatic ester was a possibility, it was still an attractive idea to see if the aspartic acid prodrug could be prepared and assayed for stability. Also, the need for hydrogenolysis was synthetically inconsequential to the structural integrity of NTXOL, due to its lack of a ketone functional group. **Scheme 1, Step 2** shows the approach that was utilized to access the desired prodrug. The EDC carbodiimide coupling strategy

was employed in this case; however, the lower reactivity of the 6-*O* aliphatic hydroxyl functional group compared to the 3-*O* phenolic hydroxyl group forced an increase in the amount of excess carbodiimide that was required to drive the reaction to completion as compared to the EDC protocol that worked for the phenolic NTX esters (2.5 eq vs. 1.7 eq). In this case, the yield went down in recovering the coupled product (~75%), and the purification was more difficult. This reaction also proceeded more smoothly with the addition of a catalytic amount of DMAP base, which is an indicator of the lower reactivity of the aliphatic alcohol.

Regarding the lower yield due to more difficult purification, one is simply forced to drive these coupling reactions to completion when using NTX or NTXOL, because the coupled conjugates, although apparently much more lipophilic than parent drug, adsorb to silica gel quite strongly. NTX and NTXOL are also very difficult to recover from silica gel in high purity. Even with TEA deactivation of silica, recovery of NTX/NTXOL-containing compounds in acceptable purity is a major challenge, and starting material is present in the prodrug precursor samples following chromatography if the reactions are not fully driven to completion.

Scheme 3.1 and **Figures 3.1 – 3.4** adequately summarize the story of the aspartic acid prodrug chemistry. First, 3-*O*Bn-6-*O*-Fmoc-Asp(OBzl)-NTXOL was isolated in 75% yield as depicted in the ^{1}H NMR spectrum shown in **Figure 3.1**. To approach removal of the Fmoc protecting group, a standard protocol was used that is common in solid phase peptide synthesis. 5% piperidine in DMF

was charged to a round bottom flask containing the Fmoc-protected prodrug. Deblocking was very fast (~15 minutes), but it became apparent very quickly that a more volatile base or a base that could be removed more easily would be a better route to success, because it was very difficult to remove all of the piperidine from the reaction mixture. Aqueous work up and two columns were required to get rid of it completely. Eventually, the piperidine was removed, and about 50% of the deblocked material was able to be recovered in satisfactory purity. The proton NMR spectrum for the product, 3-*O*Bn-6-*O*-Asp(OBzl)-NTXOL is shown in **Figure 3.2**. It was during the next step, global deblocking of the benzyl ether and benzyl ester, that major problems began to emerge.

Figures 3.3 and 3.4 show the spectral data that were obtained following 15 minutes of hydrogenolysis of 3-*O*Bn-6-*O*-Asp(OBzl)-NTXOL. Methanol was used as the solvent, because the compound did not dissolve in ethyl acetate or ethanol. Hydrogen was supplied to the reaction mixture containing 10 wt % Pd-C via a balloon and needle. When the TLC showed clear signs of degradation, the reaction was stopped, the catalyst was filtered over celite, and the filtrate was stripped of solvent and analyzed by ESI-MS (**Figure 3.3**) and ^{1}H NMR spectrum (**Figure 3.4**). The masses of the structures provided in Figure 3.3 gave some clarification to the complicated NMR spectrum. There were many undesired side reactions taking place in the hydrogenolysis cocktail. For instance, the major peak at 549 makes sense, because there were two ways that it could have formed. The most likely main contributor is expected to be the free carboxylate compound that forms when the benzyl ester of the aspartic acid pro-moiety is

cleaved (**Figure 3.3, compound II**). The second, and most likely minor contributor, would be expected to be the benzyl ether deblocked prodrug with the benzyl ester still intact (**Figure 3.3, compound III**). The mass at m/z = 459 resulted from the presence of the desired prodrug in the reaction mixture (**Figure 3.3, compound IV**). A small peak of starting material was also noticed at m/z = 639 (**Figure 3.3, compound I**), and NTXOL was also present in the mass spectrum at m/z = 344. Without the ^{1}H NMR spectral data (**Figure 3.4**), it would be difficult to determine that all of these species were actually present in the reaction mixture, because the ESI-MS in this case was also complicated by the presence of M-18 dehydration peaks that typically only arise when high energy ionization is employed (i.e. EI-MS). Under those conditions, a number of ether and ester cleavage reactions could occur in the mass collision chamber. However, **Figure 3.4** clearly shows a great deal of doubling in all regions of the ^{1}H NMR spectrum. In particular, the phenyl protons of NTXOL showed that many NTXOL-containing compounds existed. Close inspection of the pre-hydrogenolysis proton spectra (**Figures 3.1 & 3.2**) illustrate this fact. NTXOL was definitely a product of the reaction, along with the other intermediates that were in various stages of hydrogenolysis. However, the formation of NTXOL was probably a hydrolytic process, and not a hydrogenolytic process, and this was probably the result of cyclization on the ester by the freed carboxylic acid side chain of ASP. At this point, it became important to determine whether or not the ester instability under these conditions was due to cyclization of the free carboxylate on the ester (a five-membered lactone-mediated hydrolysis), or if the

ester was simply unstable to hydrogenolysis in general. This hypothesis could not be tested without the synthesis of another prodrug precursor that did not contain the free carboxylate moiety. It turns out that a simultaneous series of observations were made by another chemist working on Pegylated carboxy-ester prodrugs conjugated at the 6-*O* position of NTXOL (T. Reddy, unpublished). Instability of the ester was again observed under hydrogenolytic conditions using substrates that did not have groups present that could cyclize on the ester linker. However, it will be shown later in this chapter that not all amino acid esters of NTXOL are unstable to hydrogenolysis conditions.

1,4-cyclohexadiene and 10 wt% Pd-C was used as an alternative cocktail on a separate batch of 3-*O*Bn-6-*O*-Asp(OBzl)-NTXOL just to see if catalytic transfer hydrogenolysis could be used instead of H_2 gas. The results were identical, with the exception that the reaction rate was even faster. At this time other protecting strategies were pursued.

3.3 Synthesis of amino acid esters of NTXOL by solid phase strategies

Next, attention was turned to the possibility of docking NTXOL onto solid supports that are commonly used in peptide synthesis. The rationale for this approach was to utilize a solid support as the phenolic protecting group such that excess reagents for the coupling and deblocking procedures could be easily washed away from the resin-bound prodrug at various stages of the synthetic process. Such techniques are gaining more wide-spread popularity due to purification problems of some synthetic procedures, and this type of approach is

now becoming the mainstay of modern peptide synthesis (Misicka 2012). The synthetic approaches that were attempted are detailed in **Schemes 3.2 and 3.3**. Two commercially available solid phase peptide synthesis resins were employed to test the feasibility of the solid phase approach, Hydroxymethyl polystyrene resin (HMPR) and SASRIN®. To begin, the much cheaper HMPR was used. At the time of this work, it had already been established that activated *p*-nitrophenyl carbonates (PNP) were useful NTX/NTXOL coupling synthons. HMPR had also already been utilized by another group as a substrate for PNP activation to dock alcohol-containing drugs and substrates (Dressman, Spangle et al. 1996). Using the exact methods of the latter reference, HMPR-PNP resin was produced on a multi-gram scale to move forward with NTXOL loading tests. **Scheme 3.2** shows the overall plan that was to be employed if loading of the NTXOL drug proved to be successful.

As depicted in the scheme, successful loading of the drug was to be followed up by carbodiimide coupling and Fmoc deblocking on resin. The final step would have been to isolate the TFA salt of the final prodrug. One drawback to this type of strategy is that solid phase resins are known to require swelling and shrinking stages between reagent additions, and there was a fairly large cost to be incurred with the extra amount of drug needed for resin loading (excess could be recovered, but a large amount was needed for multistage loading). Also, additional reagent and solvent loads were needed for the multiple synthetic steps. However, in comparison, previous reactions had also been very difficult to purify, so it was expected that the ease of purification that might be gained from

this type of solid phase approach might overshadow some of the inherent wastefulness of the procedures. HMPR-PNP was first loaded with phenol as a model compound in order to determine the loading economy of a phenolic substituent in general. The activated synthon resin was reacted with phenol under a variety of conditions. **Table 3.1** summarizes the three conditions that were employed in the phenol loading studies. Microwave irradiation (MWI) was used, since it had been discovered in a previous codrug synthesis (CYT-NTX, **Chapter 5**) that nucleophilic attack on *p*-nitrophenyl activated carbonates is faster and more efficient with the use of microwave chemistry. As shown in **Table 3.1**, there were three samples prepared for gravimetric analysis. In all samples 1-3, the amount of resin and phenol (1.1 eq compared to resin) was kept constant. DCM was used as the solvent in samples one and two, but not sample three. THF had to be used with the sodium salt of phenol. Where TEA was used as the base, it was present in 1.5 eq. compared to the loading capacity of HMPR-PNP. The residual amount of material remaining following resin washing, aqueous workup (to remove *p*-nitrophenol) and solvent evaporation (which also removes TEA) was used in the calculations. Any material left on resin was assumed to be covalently bonded as a carbonate when no more washes produced residual material or UV activity on TLC. In **Table 3.1**, the conditions for samples one and two differed only by the temperature at which the microwave reaction was carried out. In sample one, the microwave reaction was conducted at 50°C for ten minutes, while in sample two, the reaction was performed for ten minutes at 100°C. There was essentially no difference in the

amount of material that was loaded on the resin as a function of temperature (sample one = 26.3% and sample two = 27.3%). Phenol was converted to sodium phenolate in sample three. It is interesting to note that the loading was worse in that case (14.1%), which was not expected. The latter result was not too much of an inconvenience though, because it would be very difficult to actually employ sodium hydride to activate the phenol of NTXOL regioselectively. One could expect at least some activation of the 6-OH, and possibly even the 14-OH, under which conditions there would quite likely have been problems with non-specific docking of the NTXOL substrate. A second cycle of the conditions used for sample one revealed that the maximum loading of phenol had essentially been reached in one cycle, which did not bode well for the loading of NTXOL, an even larger molecule. Still, with the loaded resin in hand, it made sense to at least determine how much TFA would be required to dislodge the phenol substrate from the solid support. The results were not too promising, as 90% TFA in DCM was needed to recover all of the phenol, and it had to be done in two consecutive cycles. It was not expected that amino acid ester prodrugs would be able to survive such harshly acidic conditions since TFA had already caused plenty of trouble in the deblocking procedures of the Boc group in the 3-*O*-NTX amino acid ester series.

Despite the drawbacks that emerged in the phenol loading tests, it was decided that the loading of NTXOL to HMPR-PNP should be attempted to see if there were any useful differences between NTXOL and phenol. In keeping with the phenol study, 18.8 mg NTXOL (1.1 eq) was added dry to pre-swelled resin in

DCM containing 1.5 eq. TEA, and the slurry was agitated for several minutes to dissolve the NTXOL base. The mixture was then stirred for ten minutes at 50°C in a Biotage Initiator microwave reactor, and the solid support was removed by filtration and washed with copious amounts of DCM. The filtrate was evaporated in the same manner as phenol to remove solvent and TEA, and it was found that 20% had been loaded on the resin. There was also the need for about 90% TFA in DCM to dislodge the NTX substrate from the resin. Thus, use of the HMPR-PNP resin was abandoned at this stage.

SASRIN, a much more acid sensitive resin, was explored in one loading attempt (**Scheme 3.3**). The same PNP-activation protocol was used. The results indicated approximately 18 % drug loading on SASRIN, so the idea of solid phase chemistry to afford 6-*O*-amino acid ester prodrugs was abandoned altogether at this stage. The reason for abandonment of the solid phase strategy was that 18 - 20% loading of the substrate of interest means that ~80% of the active resin conjugation area is available for side reactions. It is not really advantageous to approach a scheme that is designed to improve purification efficiency with a method that guarantees purification problems (i.e. amino acid coupling to these solid phase conjugation sites is known to be very efficient). The solid phase reactions were also very cumbersome to deal with manually. Clearly, a new strategy was needed.

3.4 Synthesis of bifunctional amino acid esters by multiple protective group strategies

The very popular method of TBDMS (*t*-butyldimethylsilyl) ether protection was investigated next (**Scheme 3.4**). Surprisingly, there was no evidence of 3-*O*-TBDMS-NTXOL formation by TLC or ^{1}H NMR analysis (data not shown) following up to 24 hours of reaction time with NTXOL using a very popular technique for these blocking procedures (Corey and Venkateswarlu 1972). Typically, in the case of phenolic substrates, reactions with *t*-butyldimethylsilyl chloride (TBDMSCl), DMF, and imidazole result in very high yields of the desired phenolic silyl ether synthons. Yet, NTXOL was simply unreactive toward TBDMSCl under these conditions. Alternative blocking cocktails also produced no TBDMS-protected NTXOL, including the conditions that were used to form the 3-*O*Bn-NTXOL compound (**Scheme 3.4**), and alternative strategies had to be pursued.

Allylation of the phenolic 3-*O* position of NTXOL was considered next, and Fmoc or Boc seemed reasonable choices for the amino-terminus protecting groups. Fmoc was pursued first, since there was talk of forming different salts of the final prodrugs at the time of this work. Boc had been restricted to dihydrochlorides in the phenolic NTX prodrug series due to instability of the esters under various deblocking conditions. **Scheme 3.5** summarizes the general prodrug synthesis strategy proceeding from 3-*O*-allyl-NTXOL, and this proved to be the best strategy to employ in order to afford the desired 6-*O*-amino acid esters of NTXOL for stability assays.

It was envisaged that allyl bromide could be directly substituted for benzyl bromide in **Step 1 of Scheme 3.1** in order to afford 3-*O*-allyl-NTXOL. Indeed, the yields were similar in this case (93.2%). With regard to the coupling step, carbodiimide reagents were avoided at first in an attempt to simplify purification procedures, and β-alanine was chosen as the first pro-moiety. Pre-activation of Fmoc-β-Ala-OH to the active ester synthon, Fmoc-β-Ala-Cl, was accomplished with thionyl chloride and sonication in DCM within 1 h, as described by Sureshbabu *et al*. (Sureshbabu and Hemantha 2008). Coupling of 3-*O*-Allyl-NTXOL with the activated acid chloride was then conducted. Purification after coupling was achieved by aqueous work up followed by column chromatography over silica that had been pretreated with 1% TEA in hexanes (76.6% isolation yield). Deallylation was performed utilizing the methods of Chandrasekhar *et al.* (Chandrasekhar, Raji et al. 2001) with significant modifications. It was found that 5 mol% of homogenous tetrakis triphenylphosphine palladium catalyst [$(Ph_3P)_4Pd$], 3.0 equivalents of polymethylhydrosiloxane (PMHS), and excess zinc chloride (2M in diethyl ether) had to be reacted with the protected substrate over the course of 24h to completely remove the allyl protecting group from the phenolic functional group. The biggest challenge that emerged at this point was the purification. Insoluble material was formed (insoluble meaning insoluble in all common laboratory solvents) that was extremely fine in particle size. The solid material was very difficult to filter, often completely clogging filter papers and celite, even under hard vacuum. The reaction mixture at this stage was also quite difficult to work up. Thick emulsions formed that were nearly impossible to

resolve, even with additions of brine and methanol. Ether and hexanes washing was attempted to remove some of the PMHS and zinc materials, since naltrexone containing compounds do not appreciably dissolve in these solvents in most cases. However, these washes had minimal effect on improving the ease of work up and preparation for column chromatography. At the chromatography stage, silica also had the tendency to become clogged with the reaction mixture when it was introduced. For these reasons, preparative TLC was employed on a sample of the deallylated synthon; however, the results of the purification compared to a silica column did not warrant further use of prep-TLC—an expensive and quantitatively restrictive technique. After several attempts to work out the purification problems following the deallylation step, 6-*O*-Fmoc-β-Ala-NTXOL was eventually isolated in 70% yield with sufficient purity to move forward.

Fmoc removal was accomplished by 24h treatment with DBU base (25 mol%) and octanethiol (10 eq.) in dry THF, as described by Sheppeck *et al*. (Sheppeck, Kar et al. 2000). The final free amine was isolated by trituration from diethyl ether (60% yield). An overall yield of 32.2% 6-*O*-β-ala-NTXOL was achieved, and that was good enough to test the material for stability. These tests are summarized in **Chapter 6**.

The same methods were used in an attempt to prepare the 6-*O*-α-amino acid ester prodrugs of NTXOL containing the following promoieties: Val, Pro, Ala, Ile, Leu, and Met. However, the final purification of these prodrugs required a final column chromatography step. Recovery of the prodrugs from TEA-deactivated

silica was difficult in all cases. The less lipophilic the R-group on the amino acid promoiety side chain, the more difficult was the isolation procedure. For instance, 6-*O*-Ile-NTXOL could be washed free from silica with 100% ethyl acetate, while 6-*O*-Ala-NTXOL required acetone and small amounts of TEA and methanol to be liberated from the column. Indeed, in the latter case, this resulted in some degradation of the end product (see NMR data in **Figure 3.22**). 6-*O*-Pro-NTXOL was as difficult as 6-*O*-Ala-NTXOL to purify, and it went through some degradation in the purification process as well (**Figures 3.24 and 3.25**). Evidence of degradation can be seen in the ^{13}C NMR spectra for 6-*O*-Ala-NTXOL and 6-*O*-Pro-NTXOL, because it appears that multiple NTXOL-containing compounds are present. The stability data presented in **Chapter 6** confirm that 6-*O*-Ala-NTXOL and 6-*O*-Pro-NTXOL are not very stable, and TEA in the presence of methanol and acetone appears to degrade these two prodrugs to an appreciable extent. In Milewski's pH 5.0 stability studies, it was noted that these two prodrug samples contained NTXOL at the start of a stability experiment. 6-*O*-Met-NTXOL also could not be isolated cleanly from the column, and it was not pursued further.

The detailed LC-UV/ESI-MS and NMR spectral data relevant to the β-Ala, Val, Ile, and Leu prodrugs are summarized in **Figures 3.9-3.21**, and their stability data are the subject of **Chapter 6**. 6-*O*-Ile-NTXOL was also crystalline in nature, and it's crystal structure is shown in **Figure 3.14**.

As **Table 6.2** of **Chapter 6** indicates, further work to develop the chemistry to afford 6-*O*-Pro-NTXOL or 6-*O*-Ala-NTXOL was not necessary, because neither of

these prodrugs met our minimum criteria for candidacy in MNTD applications. Following stability assays, it was determined that 6-*O*-β-Ala-NTXOL was the lead compound that should be pursued for scale up and MNTD skin diffusion experiments. Unfortunately, attempts to upscale 6-*O*-β-Ala-NTXOL to the ~1.0 g scale failed using the 3-O-allyl/Fmoc strategies summarized in **Scheme 3.5**. The short summary of many efforts is that the practical limit of scale for **Scheme 3.5** was found to be on the order of 200 mg of final prodrug; not enough for drug development studies using MNTD strategies. Therefore, a number of modified deblocking strategies were investigated in an attempt to prepare the β-Ala prodrug, because yield losses were incurred in the deblocking steps following promoiety coupling.

Attention was first turned to the most problematic step of the synthetic sequence; the deallylation step. Indeed the problems with column chromatography at this stage only multiplied when the scale became larger, so there was a need to change the deblocking procedure to a strategy that would avoid the need for the PMHS-$ZnCl_2$ system. Also, the homogenous tetrakistriphenylphosphine palladium catalyst had proven quite difficult to remove completely on a column. Indeed, homogenous palladium catalysts, though excellent in the scope of their synthetic applications, pose purification problems in the pharmaceutical industry in general. With these facts in mind, attempts to deblock the allyl group from the naltrexol scaffold by heterogeneous palladium catalysis were explored. In case a homogenous palladium catalyst proved to be necessary, $PdCl_2$ was also investigated as a substitute homogenous catalyst, and *N,N*-dimethylbarbituric

acid (NMBA) was employed as an allyl scavenger under a variety of conditions as a modification of the deallylation procedure described by Tsukamoto *et al*. (Tsukamoto and Kondo 2003).

As depicted in **Scheme 3.6,** allyloxybenzene was prepared by the same allylation protocol that was used for NTXOL; however, the reaction never reached completion despite the amount of excess allyl bromide employed. Column chromatography was required to isolate the product in pure form in this case, and 83% of the desired allyl-protected phenol was isolated. The first deallylations were designed using the same homogenous palladium catalyst, $(Ph_3P)_4Pd$, in order to establish the optimum amount of NMBA to use in the reaction mixture. It was found that 6.0 equivalents of NMBA were required to fully deblock the allyloxybenzene material to afford native phenol. Utilizing the established optimum of NMBA, the homogenous catalyst $PdCl_2$ was substituted in place of $(PH_3P)_4Pd$ to determine whether or not it might be an optional reagent that could afford easier purification (**Scheme 3.7**). Simultaneously, the same conditions were employed on allyloxybenzene with a change to three other heterogeneous catalysts, palladium black, palladium hydroxide, and palladium on carbon. Unfortunately, the $PdCl_2$ reaction was found to be a viable alternative to the $(Ph_3P)_4Pd$-catlayzed reaction; however, no advantage in purification was observed with this substitution. This could be seen in the proton NMR spectra of the final products, because even tiny amounts of palladium in the end product caused multiple chemical shifts for every proton. The $(Ph_3P)_4Pd$-catalyzed reaction was easier to purify when NMBA was used as an allyl scavenger as

compared to the PMHS-$ZnCl_2$ system, because much of the excess NMBA could be removed by aqueous work up with 1% $NaHCO_3$. Heterogenous catalysts were apparently unable to form the necessary palladium-allyl charged complex that results in allyl deblocking. There was no change in the protected state of allyloxybenzene after many days, as judged by TLC and crude NMR spectral data, when Pd-C, Pd black, or $Pd(OH)_2$ were substituted for the homogenous palladium catalysts, so surface adsorption catalysis could not be used as a method to simplify purification. Therefore, it was decided that the palladium catalyst should remain $(Ph_3P)_4Pd$ and the allyl scavenger should be changed to NMBA for scale up attempts to optimize the problematic deallylation step to afford 6-*O*-β-Ala-NTXOL. Unfortunately, even with excess of greater than 10 equivalents of NMBA, the allyl group could not be removed from 3-*O*-allyl-6-*O*-Fmoc-β-Ala-NTXOL completely, so the model syntheses failed to produce a useful alternative to the original $(Ph_3P)_4Pd$ / PMHS-$ZnCl_2$ system in this case.

Next, an attempt to deblock the allyl and Fmoc protecting groups was attempted in a one-pot fashion. Thiols are good nucleophiles that will add to alkenes. This is the entire basis of using octanethiol to scavenge dibenzofulvene in Fmoc deblocking procedures. The problematic species that complicated purification of the PMHS-$ZnCl_2$ deallyation cocktail was likely to be a polymer of PMHS that formed under the conditions of the reaction (higher polymers tend to be insoluble materials). Naturally, it was envisaged that one could simply use octanethiol (or a similar thiol) from the Fmoc deblocking step, combine the two in one-pot with the fully protected synthon and DBU, and the end result may be a global

deprotection that would need only a solvent wash to afford the final prodrug (**Scheme 3.8**). Although the plan was logical, a mixture of products resulted, and the allyl moiety was not fully removed.

Attention was next turned to improving yields in the final synthetic step. As shown in **Scheme 3.9**, the Boc chemistry that had been developed to afford 3-*O*-amino acid esters of NTX (**Chapter 2**) was investigated as a replacement for Fmoc since there were also some product loss issues associated with Fmoc. This method also had its share of problems, because the allyl protecting group was still present under the original Fmoc/Oallyl conditions, and the final products were not possible to isolate as pure dihydrochloride salts. The compounds were very hygroscopic in nature with the free phenol and two moles of HCl per mole of prodrug. Therefore, the Boc method was also not an alternative to approach for upscale of 6-O-β-Ala-NTXOL.

The decision was made to try to avoid allyl chemistry altogether by exploring the feasibility of 3,6-*O*-bis-coupling on NTXOL with Fmoc-β-Ala-Cl (**Scheme 3.10**). The compound 3,6-*O*-bis-NTXOL was synthesized in a small amount for LC-UV/ESI-MS analysis by doubling the amount of DMAP and Fmoc-β-Ala-Cl prepared as in **Scheme 3.5**. As can be seen in **Figure 3.5**, the fully protected compound (m/z = 930.8) could be 3-*O* deblocked to afford the free phenol (m/z = 636.9) using the same DBU/octanethiol cocktail as before; however, it takes too long for the 3-*O*-ester to degrade, and the Fmoc group also deblocks under these conditions. Precipitation of the final prodrug with concomitant precipitation of free

β-alanine caused separation problems. Therefore, this scheme was also not a route to upscale.

As a final attempt to solve the upscale problem so that the skin diffusion and solubility studies could be performed on 6-*O*-β-Ala-NTXOL, attention was turned once again to deblocking strategies that could use hydrogen gas and Pd-C. Previously, in the attempts to prepare 6-*O*-Asp-NTXOL, it had been observed that the ester bond was rapidly cleaved under the traditional deblocking conditions of H_2/Pd-C in MeOH. However, in that case there was a free carboxylate present that could contribute to cyclization on the ester. To test prodrug ester stability to hydrogenolysis again, palladium black was mixed with a sample of 6-*O*-Leu-NTXOL prodrug in THF, and the material was stirred vigorously overnight under a balloon reservoir of H_2 gas. At the time of the experiment, stability studies of the final prodrugs at pH 5.0 and 7.4 were underway, so it seemed reasonable to inject samples of the filtered reaction mixture on the HPLC to examine the area ratios of peaks for prodrug and NTXOL as compared to a control of the 6-*O*-Leu-NTXOL prodrug that had not been exposed to the hydrogenolysis mixture. The area ratio data were converted to area percents to see if an appreciable amount of NTXOL was being formed by degradation of the ester linker under hydrogenolytic conditions. The reaction was assayed at 24 hours reaction time. To ensure peak identity, the peaks were confirmed as prodrug and NTXOL by spiking one set of reaction samples with NTX and a separate set of reaction samples with prodrug. The data shown in **Table 3.2** represent the average values (n=3) obtained from the analysis, and

representative chromatograms are shown in **Figure 3.6**. The data clearly showed that no appreciable degradation of the prodrug ester bond had occurred at 24 hours reaction time in the presence of palladium black catalyst, H_2 gas (1 atm.), and THF. Therefore, following the hydrogenolysis test, attention was again turned toward benzyl protection of the phenolic hydroxyl group of NTXOL. Also, carboxybenzoyl carbamates (Cbz-protected amino-terminus) of the desired amino acids were sought as promoiety precursors. Both of these protecting groups are removed under hydrogenolysis conditions, and it was expected that the desired 6-*O*-β-Ala ester of NTXOL could be afforded in larger quantities using a global deprotection strategy. Ultimately, such an approach would solve the problems incurred in the allyl chemistry that was used previously, because hydrogenolysis proceeds cleanly with heterogeneous palladium catalysts under most circumstances. Unfortunately, this plan also did not work.

Significant work to optimize the conditions of this chemistry was directed toward 6-*O*-β-Ala-NTXOL, having been established as the most promising prodrug candidate. The various permutations of the synthetic strategy are summarized in **Scheme 3.11**. 3-*O*Bn-NTXOL was obtained in high yield in a single upscaled effort to afford 3.4 g of material for optimization work. Cbz-β-Ala-OH was converted to Cbz-β-Ala-Cl in the exact same manner as the Fmoc material previously, but with excess DMAP present to mop up HCl. Twofold excess of the activated acid chloride was charged to a solution of 3-*O*Bn-NTXOL in DCM containing two equivalents of DMAP. The desired 3-*O*Bn-6-*O*-Cbz-β-Ala-NTXOL prodrug precursor was isolated in good purity at 82.5% yield for hydrogenolysis

optimization, and many different hydrogenolytic cocktails were tested for their ability to afford the desired deprotected prodrug in acceptable final yields. **Figures 3.7and 3.8** show a brief summary of the typical results obtained by LC-UV/ESI-MS. In **Figure 3.7**, the major peak at 11.01 minutes with m/z 548.8 corresponds to a compound with the 3-*O*Bn group deblocked to free phenol. The next major peak at 13.79 minutes with m/z 638.8 corresponds to the fully protected prodrug precursor. There was no evidence of an intermediate with only the Cbz group removed, and it became apparent throughout the course of this work that Cbz could never be removed completely from the protected starting material before the catalyst was poisoned. The only evidence of the fully deprotected prodrug appears to be the peak at 4.20 minutes which does show the m/z 414.9 peak that is akin to the m/z parent molecular ion seen in **Figure 3.11;** the mass spectrum of the original, clean 6-*O*-β-Ala-NTXOL prodrug prepared by the techniques summarized in **Scheme 3.5**. However, it is problematic that the peak at 4.20 minutes in **Figure 3.7** does not give an extracted mass spectrum that matches **Figure 3.11** exactly, so it is not possible to say that the peak does indeed correspond to the desired prodrug. In **Figure 3.8**, the amount of catalyst was increased to attempt to fully deprotect the starting material without poisoning the catalyst, but the washing procedure required to recover any material from the reaction involved the use of THF, and the mass spectrum was too complicated to indicate the prodrug was present. It should be noted that clean ^{1}H NMR spectra were never obtained for the final prodrug under any of the conditions tested. The palladium black catalyst was poisoned in many

of the attempts to afford the final prodrug, and the addition of zinc dust resulted in intractable mixtures. Also, the requisite threefold weight ratio of catalyst compared to the protected prodrug precursor that was needed to avoid poisoning resulted in very tiny amounts of isolated material after solvent washing. Apparently, the 6-*O*-β-Ala-NTXOL prodrug strongly adsorbs to the palladium catalyst surfaces, or it is complexed with palladium somehow. In any event, the conditions of **Scheme 3.5**, although limited in their scalability, represent the only synthetic approach that has proven to work to any acceptable degree at all to afford 6-*O*-amino acid esters of NTXOL. Therefore, the work to prepare these materials was concluded at this stage, and the solubility and skin diffusion studies were never able to be conducted. However, plasma stability studies were conducted to investigate the candidacy of these materials in an MNTD paradigm (**Chapter 6**). Overall, 6-*O*-NTXOL amino acid prodrugs were not simple enough to purify on a large scale to be considered good prodrugs.

3.5 Experimental Section

Materials: All reagents were purchased from, Acros Organics, Sigma-Aldrich, and Advanced Chemtech, and were used without further purification. Naltrexone was obtained from Mallinckrodt-Covidien. All solvents were dried and stored over molecular sieves prior to use.

LC-ESI-MS characterization: Mass spectral data were obtained from the Mass Spectral facility at UK, or by using an Agilent 1200 series HPLC system coupled to an Agilent 6120 LC-ESI-MS electrospray ionization detector. A Zorbax

Eclipse XDB-C18 column was employed, and the mobile phase was 0.1% formic acid:acetonitrile set on a gradient elution program 95:5 to 5:95 over the course of 12 min. Spectra are scanned copies of the original printed data.

NMR: All NMR spectra were obtained on a Varian 300 MHz or a Varian 500 mHz instrument. Line data and integral values for ^{1}H NMR were acquired with Mestrenova Lite (Mesterlab Research Chemistry Software Solutions, Escondido, CA) using 500 MHz spectra. ^{13}C NMR frequencies were obtained from Varian Mercury 300 MHz NMR software. TMS was used as an internal standard.

Synthesis of 6-β-NTXOL

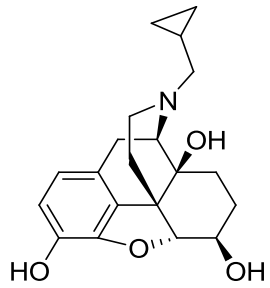

The synthesis of NTXOL utilized the exact method of De Costa *et al*. (De Costa et al. 1992), and afforded white crystals in multi-gram scale at 84 – 85% yield consistently at the 500 mg scale. The synthesis performed better in upscale in this case (2.7981 grams from 3.0000 g NTX, 92.7%) so one is advised to prepare large quantities of NTXOL in a single synthetic event rather than to prepare smaller batches.

^{1}H NMR ($CDCl_3$) 500 MHz: δ 6.71 (d, *J*=10 Hz, 1H), 6.56 (d, *J*=10 Hz, 1H), 4.53 (d, *J*=10 Hz, 1H), 3.63-3.55 (m, 1H), 3.50 (d, *J*=5 Hz, 1H), 3.10 (d, *J*=5 Hz, 1H),

3.03 (d, *J*=15 Hz, 1H), 2.68-2.52 (m, 2H), 2.36 (d, *J*=5 Hz, 2H), 2.29-2.22 (m, 1H),), 2.18-2.11 (m, 2H), 2.04-1.94 (m, 1H), 1.68-1.59 (m, 1H), 1.52-1.47 (m, 1H), 1.41-1.34 (m, 2H), 0.88 -0.80 (m, 1H), 0.56-0.51 (m, 2H), 0.15-0.11 (m, 2H) ppm.

LC-MS: 344.9 (MH^+); r.t. = 8.74 min (ESI-MS positive mode).

Synthesis of 3-*O*Bn-NTXOL

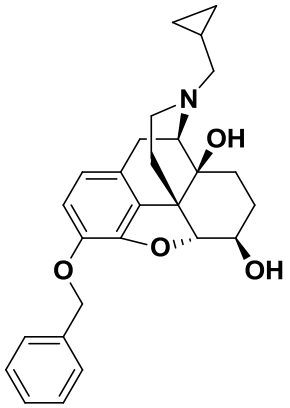

2.798 grams of NTXOL was dissolved in about 50 mL of acetone containing 4.505 g K_2CO_3 (4.0 eq) held at reflux. The solution was charged immediately with 1.533 g benzyl bromide (1.1 eq), and the reaction was conducted for 5.5 hours at reflux. The mixture was allowed to cool to room temperature, and the acetone was stripped in vacuo. Copious amounts of DCM were used to wash the desired synthon away from the solid materials in the reaction flask, and the DMC volume was then reduced under vacuum, and the crude organic mixture was washed 3 times with DI water and twice with brine (100 mL each). The organic layer was

dried over sodium sulfate, collected, and evaporated to a constant weight, and multiple washes with hexanes were carried out to remove the residual benzyl bromide. Following these washes, the product was dried under hard vacuum overnight to afford 3.336 g (94.5%) of a waxy white solid. The final material was characterized by ^{1}H NMR analysis and found to be the desired 3-*O*Bn-NTXOL sython.

^{1}H NMR ($CDCl_3$) 300 MHz:

δ 7.22-7.45 (m, 5H), 6.71 (d, *J*=10 Hz, 1H), 6.56 (d, *J*=10 Hz, 1H), 5.20 (s, 2H), 4.45 (d, *J*=10 Hz, 1H), 3.46-3.42 (m, 1H), 3.50 (d, *J*=5 Hz, 1H), 3.10 (d, *J*=5 Hz, 1H), 3.03 (d, *J*=15 Hz, 1H), 2.68-2.52 (m, 2H), 2.36 (d, *J*=5 Hz, 2H), 2.29-2.22 (m, 1H),), 2.18-2.11 (m, 2H), 2.04-1.94 (m, 1H), 1.68-1.59 (m, 1H), 1.52-1.47 (m, 1H), 1.41-1.34 (m, 2H), 0.88 -0.80 (m, 1H), 0.56-0.51 (m, 2H), 0.15-0.11 (m, 2H) ppm.

Synthesis of 3-*O*-allyl-NTXOL

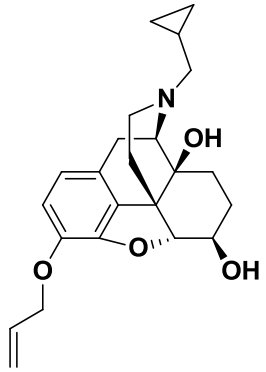

5.000 grams of NTXOL was dissolved in about 50 mL of acetone containing 8.049 g K_2CO_3 (4.0 eq) held at reflux. The solution was charged immediately with 1.938 g allyl bromide (1.1 eq), and the reaction was conducted for 5.5 hours at reflux. The mixture was allowed to cool to room temperature, and the acetone was stripped in vacuo. Copious amounts of DCM were used to wash the desired synthon away from the solid materials in the reaction flask, and the DMC volume was then reduced under vacuum, and the crude organic mixture was washed 3 times with DI water and twice with brine (100 mL each). The organic layer was dried over sodium sulfate, collected, and evaporated to a constant weight, and multiple washes with hexanes were carried out to remove the residual allyl bromide. Following these washes, the product was dried under hard vacuum overnight to afford 5.204 g (93.2%) of translucent oil. The final material was characterized by ^{1}H NMR spectrometry and found to be the desired 3-*O*-allyl-NTXOL sython.

^{1}H NMR ($CDCl_3$) 300 MHz:

δ 6.71 (d, *J*=10 Hz, 1H), 6.56 (d, *J*=10 Hz, 1H), 6.11-6.02 (m, 1H), 5.39 (d, *J*=10 Hz, 1H), 5.26 (d, *J*=10 Hz, 1H), 4.70-4.60 (m, 2H), 4.50 (d, *J*=10 Hz, 1H), 3.65-3.55 (m, 1H), 3.52 (d, *J*=5 Hz, 1H), 3.10 (d, *J*=5 Hz, 1H), 3.03 (d, *J*=15 Hz, 1H), 2.68-2.52 (m, 2H), 2.36 (d, *J*=5 Hz, 2H), 2.29-2.22 (m, 1H),), 2.18-2.11 (m, 2H), 2.04-1.94 (m, 1H), 1.68-1.59 (m, 1H), 1.52-1.47 (m, 1H), 1.41-1.34 (m, 2H), 0.88 -0.80 (m, 1H), 0.56-0.51 (m, 2H), 0.15-0.11 (m, 2H) ppm.

General Synthesis of the 3-*O*-allyl-6-*O*-Fmoc-amino acid NTXOL ester conjugates

For each coupling reaction 300 mg of 3-*O*-allyl-NTXOL and two equivalents of DMAP were dissolved at room temperature in DCM. The Fmoc-protected amino acid promoiety was converted to the activated acid chloride in a separate flask by sonicating it in DCM with thionyl chloride under an argon stream. Relative to 3-*O*-allyl-NTXOL, 2.00 equivalents of the amino acid precursor and 1.99 equivalents of thionyl chloride were used. The preactivation reactions were complete within one hour in each case, as described by Sureshbabu *et al*. (Sureshbabu and Hemantha 2008), and the residual HCl that had not been blown off in the argon stream was quenched with 2.00 equivalents of DMAP base (DMAP served the purpose of activating the 6-OH group to coupling as well as a quenching agent). The cocktail containing 3-*O*-allyl-NTXOL and DMAP was then added dropwise to the acid chloride solution over the course of two minutes at 0°C, and the reaction mixture was warmed to room temperature and left to react for four hours. In every case, the reactions were worked up with DI water and brine, and the organic fraction was dried over anhydrous sodium sulfate. Final purification was achieved by chromatography over silica that had been pretreated with 1% TEA in hexanes. It was very difficult to remove all of the Fmoc-protected pro-moiety starting materials in these reactions, so they were present in the final NMR spectra in a small percentage. The acid chlorides were quenched in the workup and chromatography steps, and the presence of free carboxylic acid of the pro-moiety was inconsequential for the deallylation chemistry. Two columns

were required to completely remove the promoiety precursors, so it was decided that these unwanted materials could best be removed in the purification procedures of the deallylation step. Therefore, the crude mixtures were used without further purification in every case. Estimated isolation yields were on the order of 75 - 90%.

General Synthesis of the 6-*O*-Fmoc-amino acid NTXOL ester conjugates by 3-*O* deallylation

Deallylation was performed utilizing the methods of Chandrasekhar *et al.* (Chandrasekhar, Raji et al. 2001) with significant modifications. The fully protected 3-*O*-allyl-6-*O*-Fmoc-amino acid ester conjugate was dissolved in about 9.0 mL of dry THF and treated with 5 mol% of $(PPh_3)_4Pd$ and 3.0 eq. of polymethylhydrosiloxane (PMHS). 52 drops of diethyl ether 2M in zinc chloride was added with rapid stirring, and the reaction was run for 24 h. The THF was evaporated under an argon stream, and the gummy residue was reconstituted in DCM for workup. The crude material was then worked up with DI water and brine and dried over sodium sulfate. The combined organic fractions were concentrated and chromatographed as before to afford the deallylated prodrug product in estimated yields ranging from 50 to 85%. As mentioned earlier in the chapter, the purification of these materials was very difficult such that the cleanest fractions obtained from chromatography were advanced to the next step

without further purification. The Fmoc-protected promoiety contaminants from the previous step were removed completely at this stage.

General Synthesis of the 6-*O*-amino acid NTXOL ester conjugates by Fmoc removal

Fmoc removal was accomplished by 24h treatment with DBU base (25 mol%) and octanethiol (10 eq.) in dry THF, as described by Sheppeck *et al*. (Sheppeck, Kar et al. 2000). In the case of 6-*O*-β-Ala-NTXOL, the final prodrug was isolated by precipitation and trituration from diethyl ether (60% yield). The α-amino acid ester prodrugs were recovered via aqueous workup (exactly as described above) and column chromatography. Again, silica was deactivated with 1% TEA in hexanes, and the final prodrugs were eluted with copious column washes using ethyl acetate. 6-*O*-Ala-NTXOL and 6-*O*-Pro-NTXOL required acetone and TEA to be eluted from the columns, and hydrolytic degradation of these prodrugs resulted. The range of yields at this stage was 20% (6-*O*-Ala-NTXOL) to 80% (6-*O*-Ile-NTXOL). The final overall yields of the prodrugs are summarized in **Table 3.3.**

6-*O*-β-Ala-NTXOL

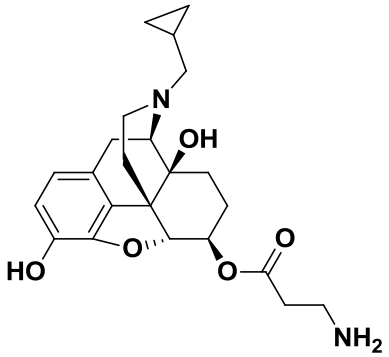

^{1}H NMR 500 MHz (d_6-DMSO): δ 6.59 (d, *J*=10 Hz, 1H), 6.53 (d, *J*=10 Hz, 1H), 4.87 (s, broad), 4.45 (m, 2H), 3.64-3.57 (m, 1H), 3.03 (d, *J*=5 Hz, 1H), 2.96 (d, *J*=20 Hz 1H), 2.76 (t, *J*=15 Hz, 2H), 2.62-2.53 (td, 2H), 2.40 (t, *J*=15 Hz, 2H), 2.36-2.27 (m, 2H), 2.23-2.12 (m, 1H), 1.85-1.72 (m, 2H), 1.70-1.57 (m, 2H), 1.48 (d, *J*=10 Hz, 1H), 1.33-1.19 (m, 3H), 0.87-0.79 (m, 1H), 0.42-0.51 (m, 2H), 0.16-0.06 (m, 2H) ppm.

^{13}C NMR (d_6-DMSO) 300 MHz: δ 171.49, 165.90, 141.62, 140.31, 131.11, 123.21, 118.63, 117.05, 90.43, 75.09, 69.33, 61.45, 58.33, 53.9, 47.30, 43.44, 37.93, 30.23, 29.28, 23.26, 22.15, 9.31, 3.78 ppm.

LC-UV/ESI-MS: r.t = 3.50 min; (MH^+) m/z 415.9

6-*O*-Ile-NTXOL

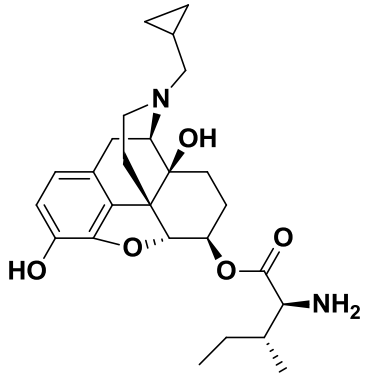

^{1}H NMR 500 MHz $CDCl_3$: δ 7.70-7.65 (m, <1H), 7.58-7.53 (m, <1H), 7.50-7.44 (m, <1H), 6.70 (d, J=10Hz, 1H), 6.58 (d, J=10Hz, 1H), 4.85-4.94 (m, 1H), 4.52 (d, J=5Hz, 1H), 3.67 (d, J=5Hz, 1H), 3.10 (d, J=5Hz, 1H), 3.02 (d, J=15 Hz, 1H), 2.69-2.55 (m, 2H), 2.39 (d, J=5Hz, 2H), 2.31-2.21 (m, 1H), 2.2-2.12 (m, 1H), 2.12-2.02 (m, 1H), 1.96-1.85 (m, 1H), 1.70-1.57 (m, 2H), 1.53-1.44 (m, 2H), 1.44-1.36 (m, 1H), 1.30-1.19 (m, 2H), 0.95-0.89 (m, 7H), 0.89-0.79 (m, 2H), 0.58-0.50 (m, 2H), 0.19-0.09 (m, 2H) ppm.

^{13}C NMR ($CDCl_3$) 300 MHz: δ 175.58, 142.01, 140.98, 132.29, 130.83, 128.54, 123.11, 119.58, 118.66, 92.29, 70.12, 62.46, 59.43, 57.60, 48.33, 44.16, 39.24, 30.99, 29.67, 25.86, 24.34, 22.88, 15.56, 12.33, 9.81, 4.28 ppm.

LC-UV/ESI-MS: r.t = 2.99 min; (MH^+) m/z 457.9

6-*O*-Leu-NTXOL

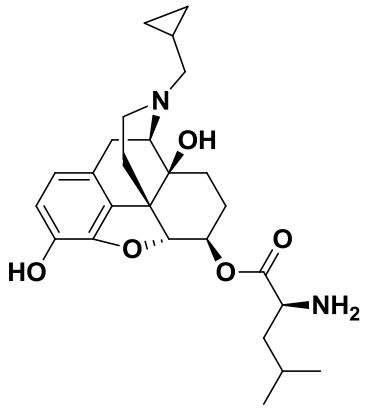

^{1}H NMR 500 MHz ($CDCl_3$): δ 7.70-7.65 (d, J=10Hz, 1H), 6.59 (d, J=10Hz, 1H), 4.91-4.83 (m, 1H), 4.54 (d, J=5Hz, 1H), 3.68 (t, J=15 Hz, 1H), 3.11 (d, J=5Hz, 1H), 3.03 (d, J=20Hz, 1H), 2.70-2.56 (m, 2H), 2.39 (d, J=5Hz, 2H), 2.30-2.22 (m, 1H), 2.21-2.12 (m, 1H), 2.12-2.02 (m, 1H), 1.87-1.75 (m, 1H), 1.71-1.62 (m, 2H), 1.62-1.58 (m, 1H), 1.58-1.52 (m, 1H), 1.52-1.44 (m, 3H), 0.92 (t, 7H, overlap with cyclopropyl methine), 0.59-0.50 (m, 2H), 0.19-0.12 (m, 2H) ppm.

^{13}C NMR ($CDCl_3$) 300 MHz: δ 176.91, 142.00, 141.15, 130.87, 119.66, 118.75, 92.37, 76.52, 70.19, 62.55, 59.50, 52.31, 48.40, 44.22, 43.92, 31.08, 29.66, 25.04, 24.21, 23.01, 22.93, 22.63, 9.84, 4.34 ppm.

LC-UV/ESI-MS: r.t = 2.89 min; (MH^+) m/z 457.8

6-*O*-Val-NTXOL

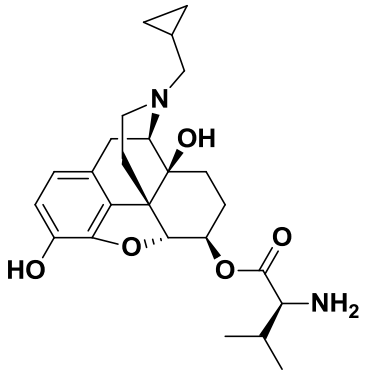

^{1}H NMR 500 MHz ($CDCl_3$): 7.72-7.63 (m, <1H), 7.60-7.53 (m, <1H), 7.50-7.44 (m, <1H), 6.71 (d, J=10Hz, 1H), 6.59 (d, J=10Hz, 1H), 4.95-4.82 (m, 1H), 4.53 (d, J=10Hz, 1H), 3.56 (d, J=5Hz, 1H), 3.11 (d, J=5Hz, 1H), 3.03 (d, J=15Hz, 1H), 2.69-2.55 (m, 2H), 2.39 (d, J=5Hz, 2H), 2.31-2.21 (m, 1H), 2.20-2.10 (m, 2H), 2.10-2.01 (m, 1H), 1.76-1.65 (m, 1H), 1.64-1.57 (m, 1H), 1.53-1.42 (m, 2H), 1.33-1.19 (m, 2H), 1.04 (d, J=5Hz, ½ H), 1.00 (d, J=5Hz, 3H), 0.97 (d, J=5Hz, ½ H) 0.93 (d, J=5Hz, 3 H), 0.89-0.79 (m, 3H), 0.58-0.48 (m, 2H), 0.19-0.09 (m, 2H) ppm.

^{13}C NMR ($CDCl_3$) 300 MHz: δ 175.48, 141.98, 141.01, 132.14, 130.82, 128.69, 123.01, 119.58, 118.70, 92.34, 70.09, 62.41, 59.42, 58.77, 48.30, 44.16, 31.98, 31.01, 29.59, 24.31, 22.85, 19.00, 17.96, 9.77, 4.30 ppm.

LC-UV/ESI-MS: r.t = 3.50 min; (MH^+) m/z 443.9

Table 3.1 Phenol loading on HMPR-PNP solid phase synthesis resin.

Sample	Amount of Resin (mg)	Amount of PhOH (mg)	Amount of TEA (mg)	MWI temp/time (°C/min)	% loaded to resin
1	50.0	51.8	75.9	50/10	26.3
2	50.0	51.8	75.9	100/10	27.3
3	50.0	51.8	None*	50/10	14.1

* PhOH was preactivated as the sodium salt with 0.99 eq. NaH

Table 3.2 6-*O*-Leu-NTXOL ester hydrogenolysis test.

Sample	RT (min)	Avg. Area% (215 nm)
NTXOL control	1.87	0.63
Prodrug control	2.52	99.37
Hydrogenolysis (24 h)	1.88	0.93
Hydrogenolysis (24h)	2.56	99.07
Hydrogenolysis (24 h + NTXOL spike)	1.89	83.34
Hydrogenolysis (24 h + NTXOL spike)	2.55	16.66
Hydrogenolysis (24 h + prodrug spike)	1.88	0.83
Hydrogenolysis (24 h + prodrug spike)	2.51	99.17

Table 3.3 6-*O*-NTXOL amino acid esters final material recovery.

Compound	MW (g/mol)	mg isolated	Theoretical yield (mg) (overall)	% Yield (overall)
6-*O*-Ile-NTXOL	456.57	142.9	357.2	40.0
6-*O*-β-Ala-NTXOL	414.49	97.3	324.3	32.2
6-*O*-Val-NTXOL	442.55	125.3	346.2	36.2
6-*O*-Leu-NTXOL	456.57	137.2	357.2	38.4
6-*O*-Ala-NTXOL	414.49	27.2	324.3	~8.4
6-*O*-Pro-NTXOL	440.53	21.0	344.6	~6.1

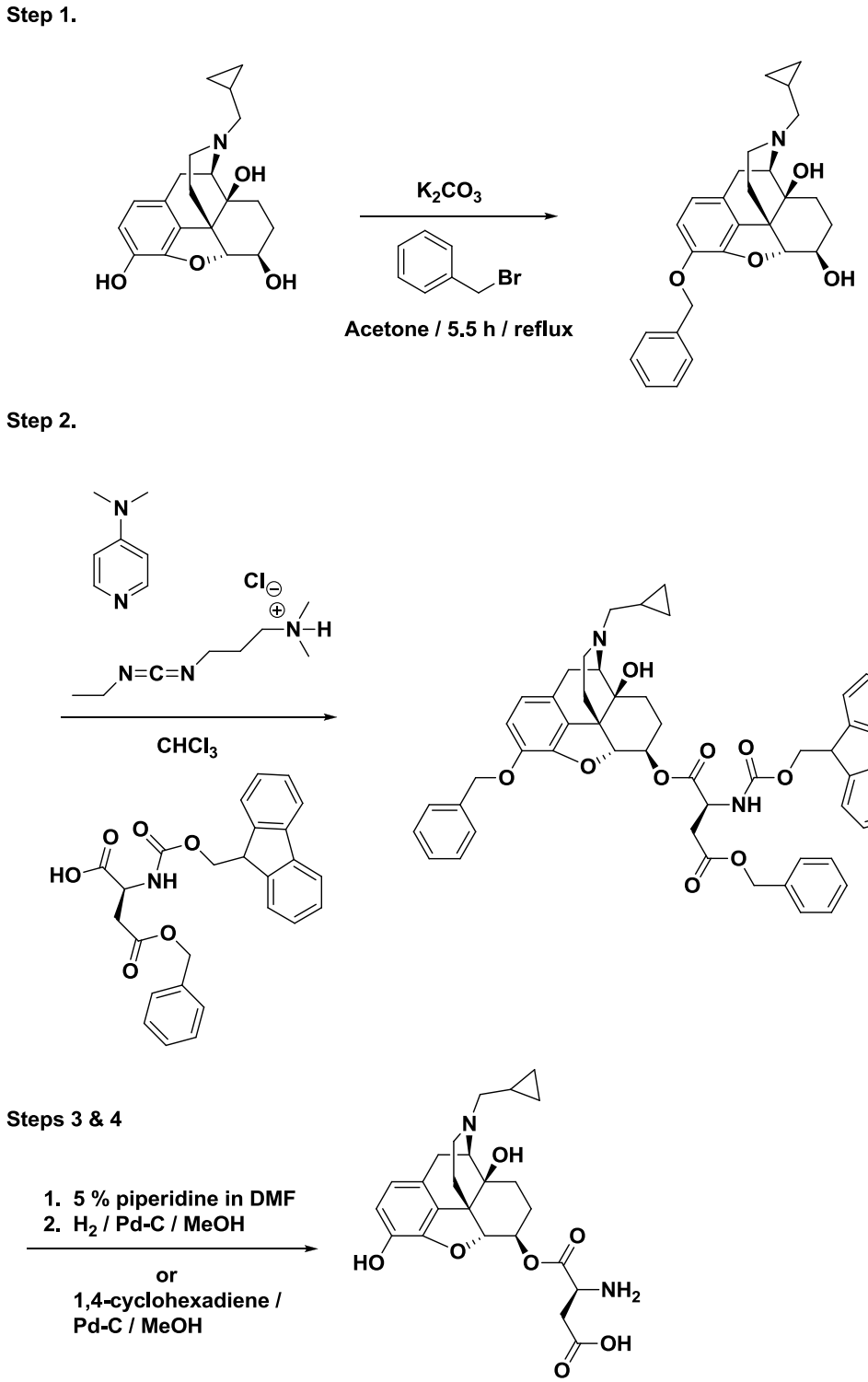

Scheme 3.1 Synthesis of 6-*O*-Asp-NTXOL by the Fmoc/OBn route.

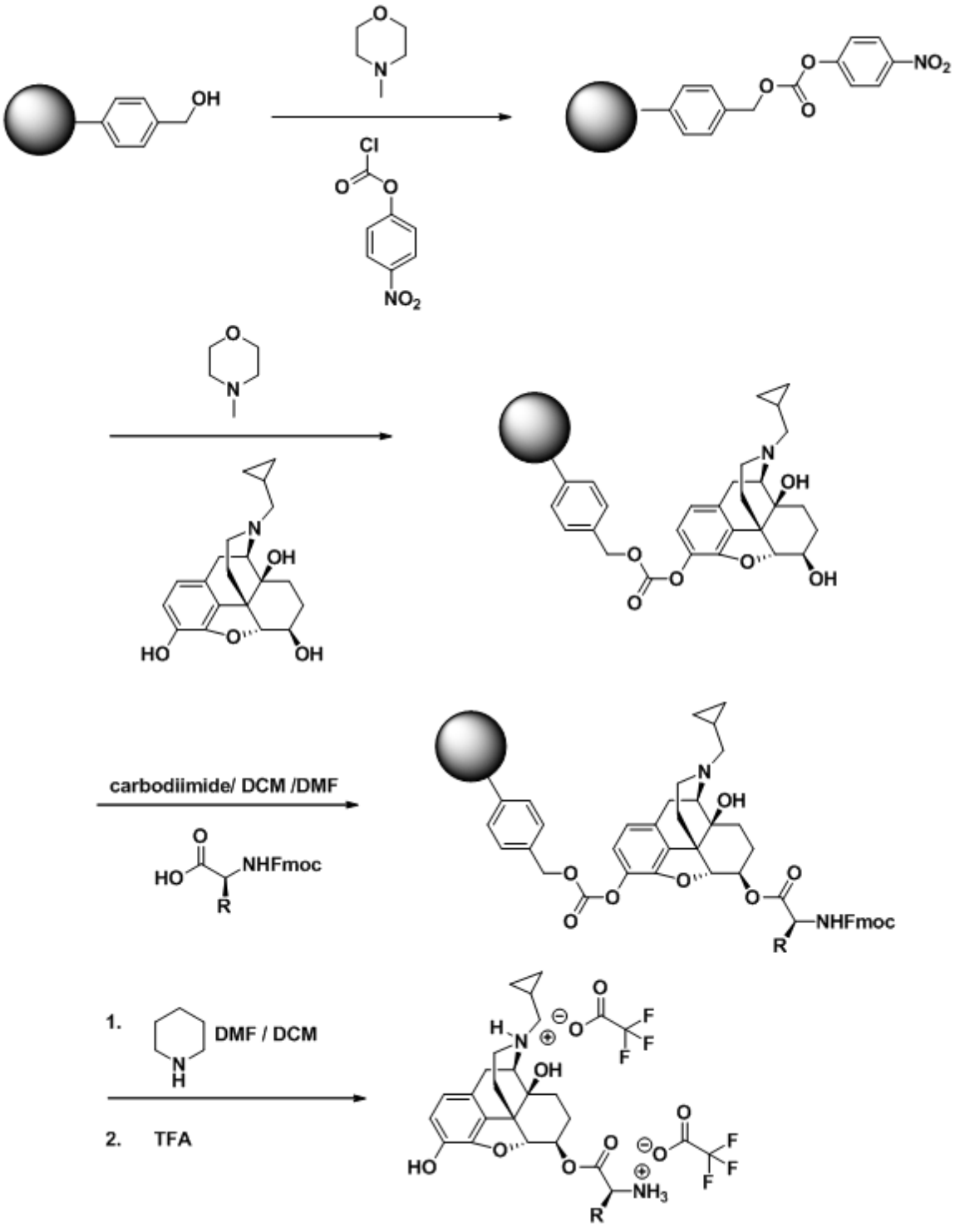

Scheme 3.2 Hydroxymethyl polystyrene resin solid phase synthesis approach to 6-*O*-amino acid esters of NTXOL.

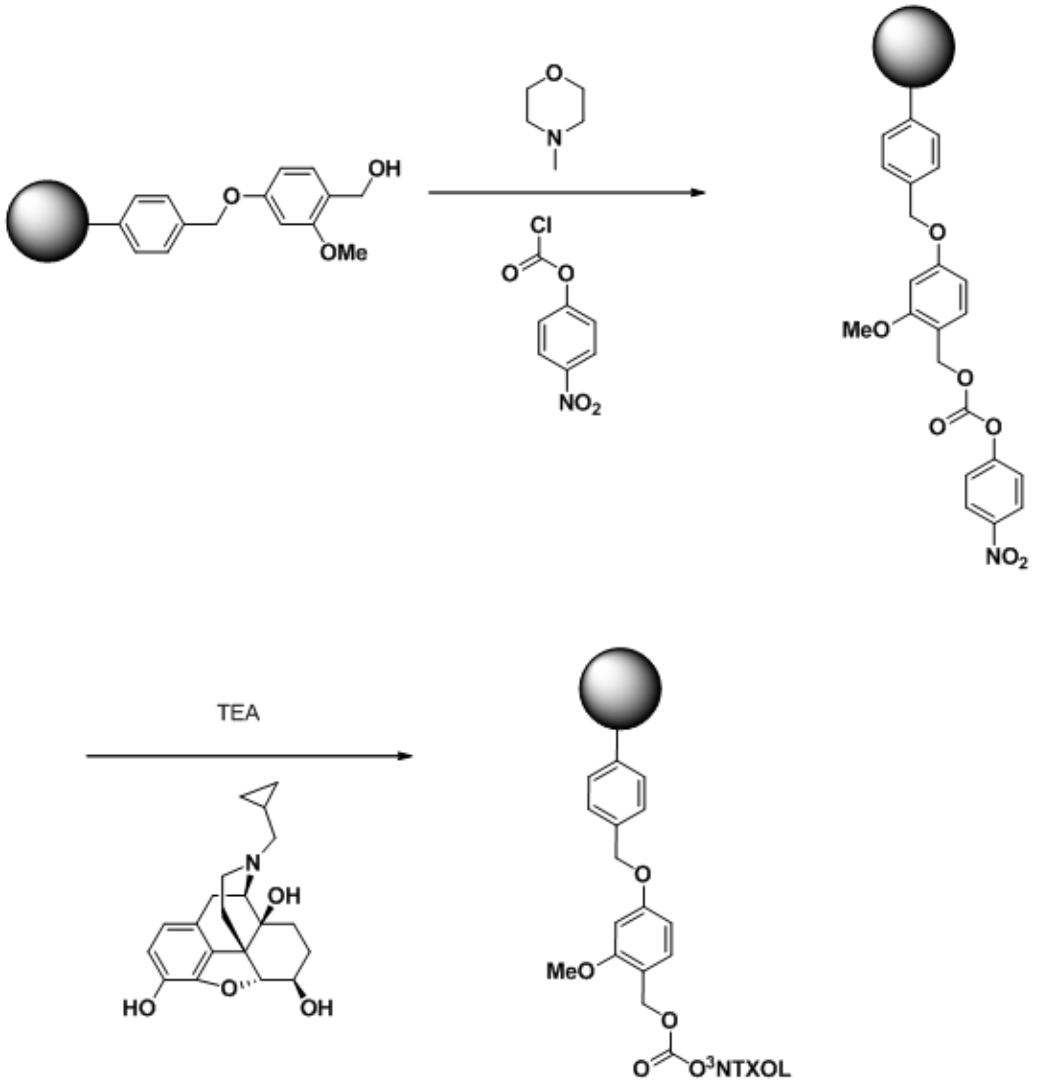

Scheme 3.3 SASRIN resin solid phase synthesis approach to 6-*O*-amino acid esters of NTXOL.

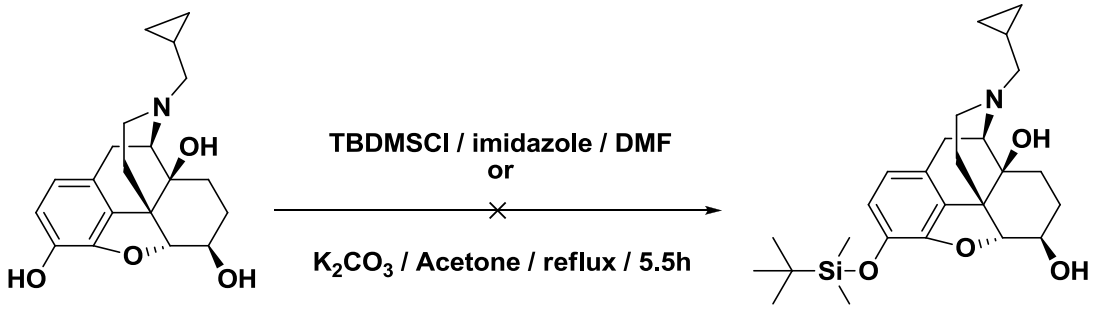

Scheme 3.4 Synthesis of 3-*O*-TBDMS-NTXOL ether synthon.

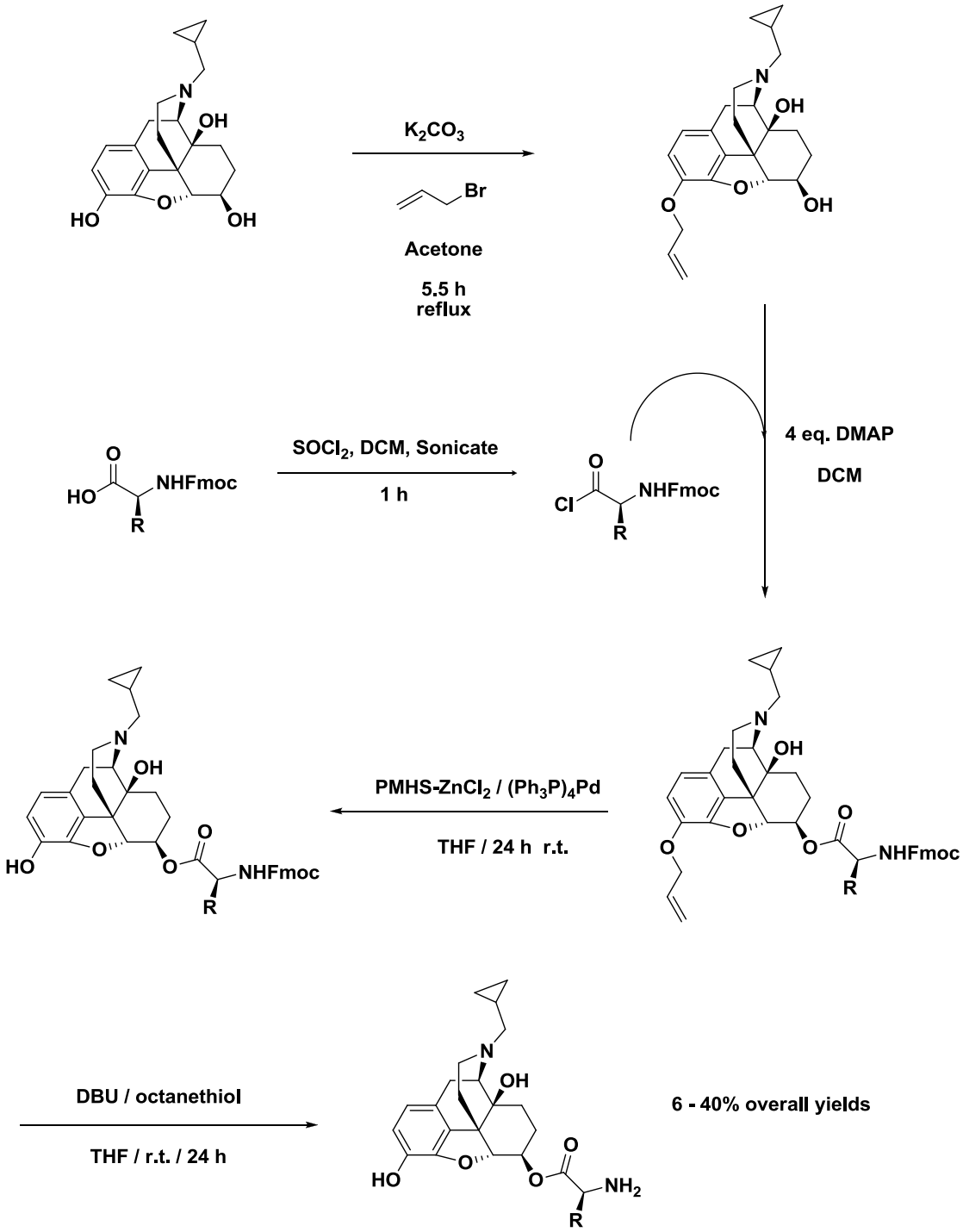

Scheme 3.5 Synthesis of 6-*O*-amino acid esters of NTXOL by the Fmoc/OAllyl route.

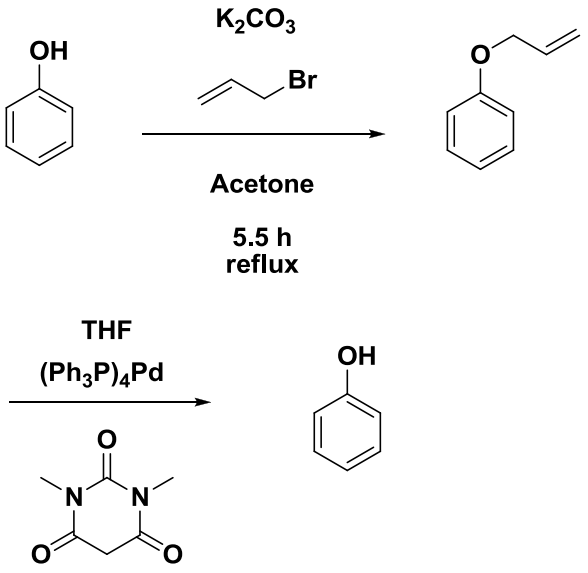

Scheme 3.6 Allyloxybenzene model deallylation with homogenous palladium catalyst and NMBA allyl scavenger.

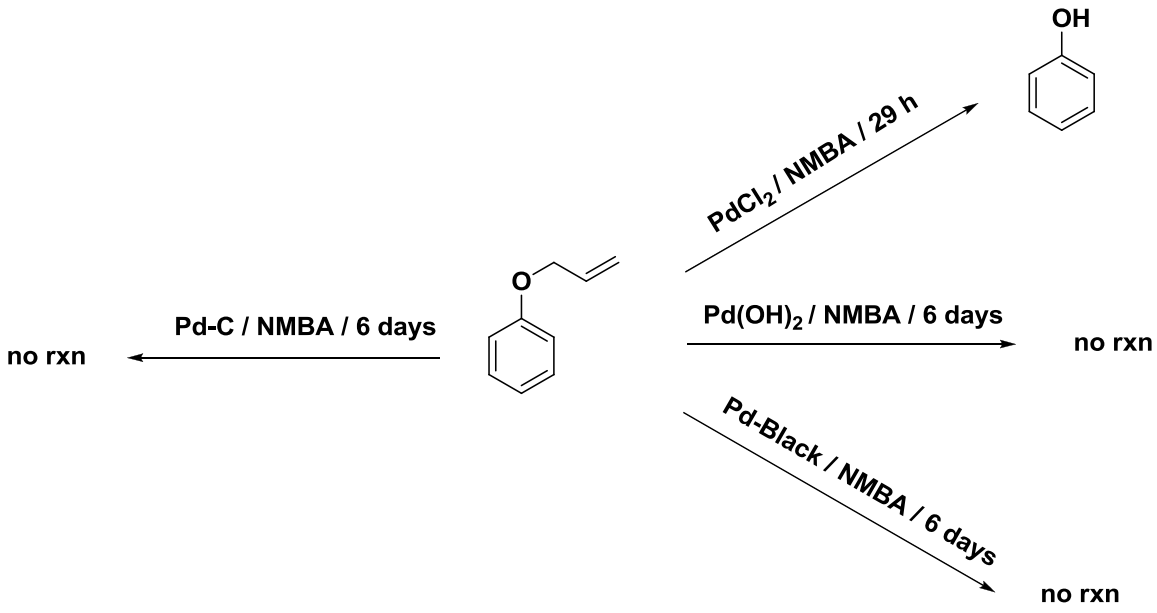

Scheme 3.7 Allyloxybenzene model deallylation with $PdCl_2$ and alternative heterogenous palladium catalysts using NMBA allyl scavenger.

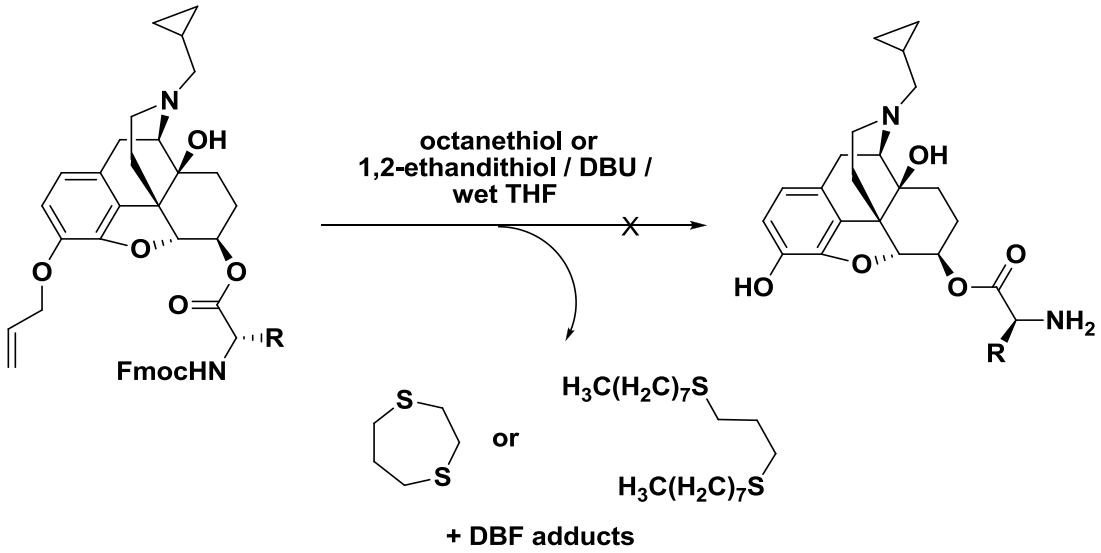

Scheme 3.8 Synthesis of 6-*O*-amino acid esters of NTXOL by the Fmoc/OAllyl global deblocking route.

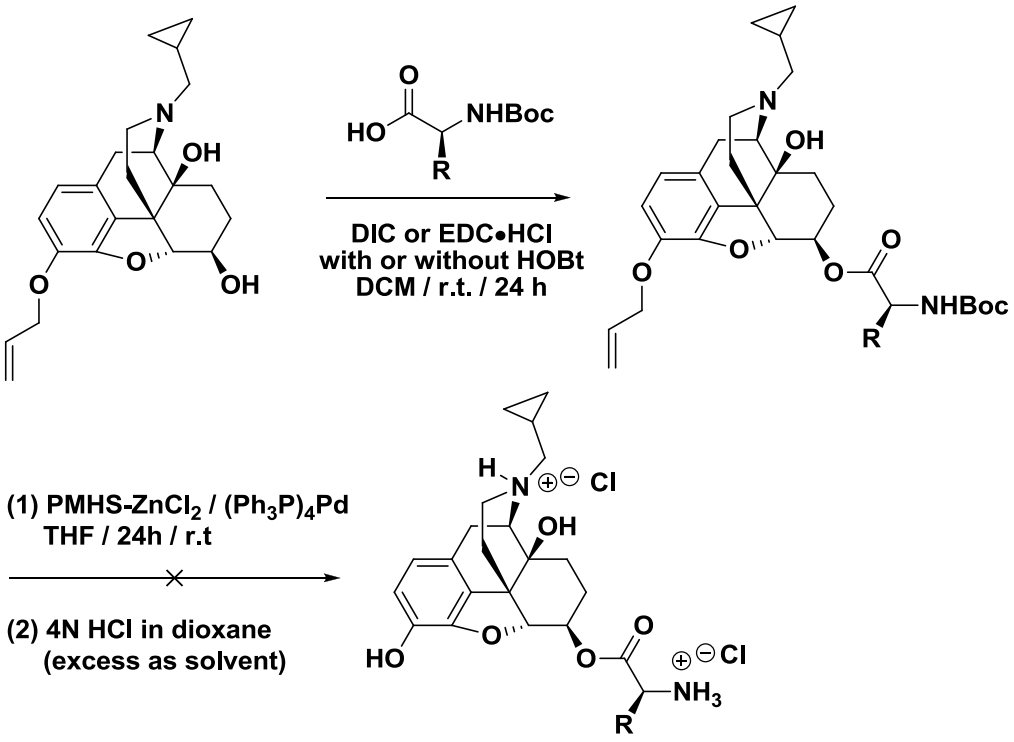

Scheme 3.9 Synthesis of 6-*O*-amino acid esters of NTXOL by the Boc/OAllyl route.

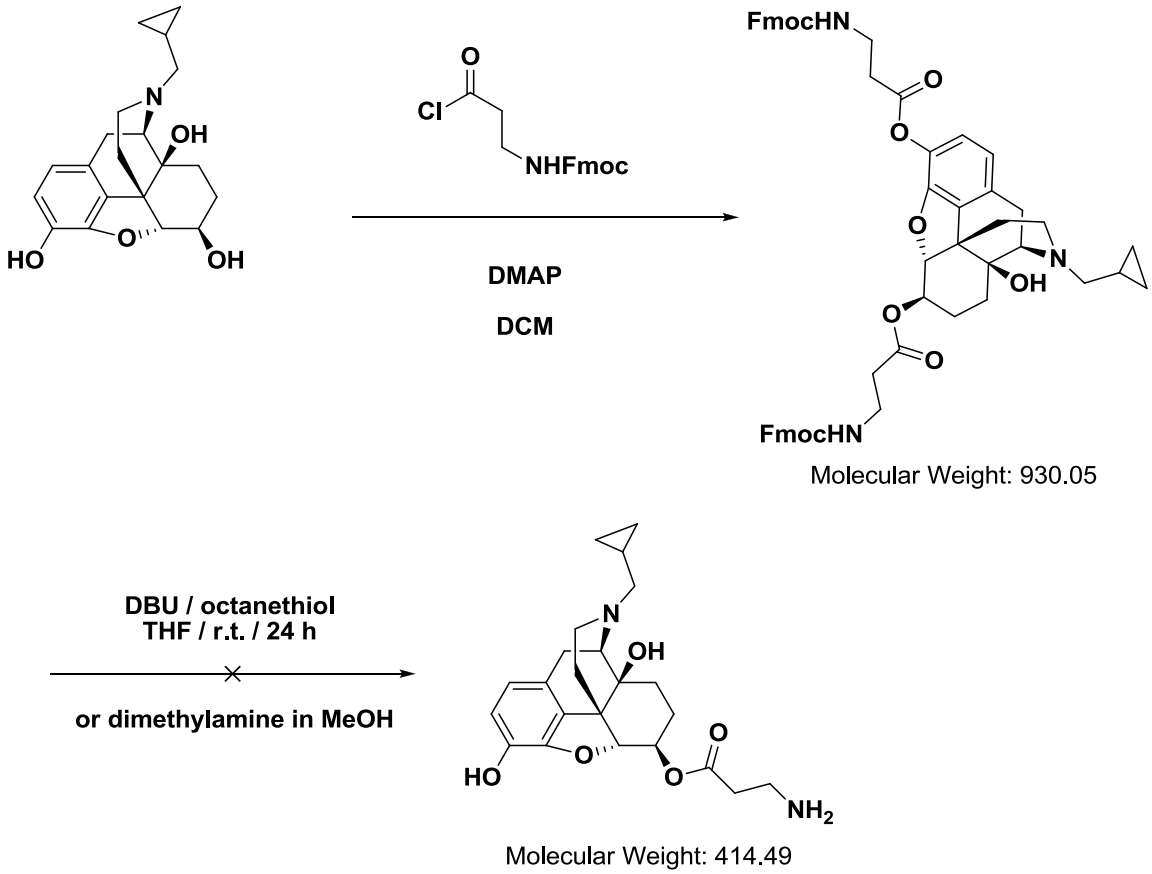

Scheme 3.10 Synthesis of 6-*O*-amino acid esters of NTXOL by the Bis-coupling route.

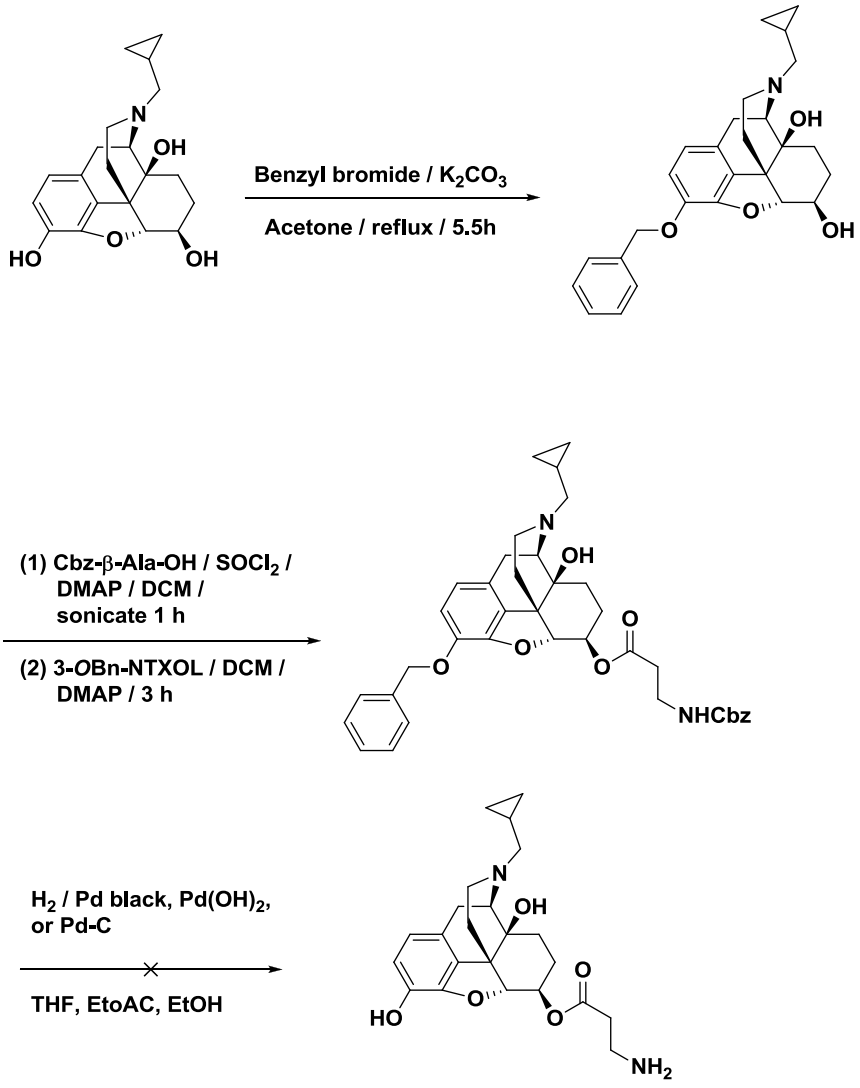

Scheme 3.11 Synthesis of 6-*O*-β-Ala-NTXOL by the Cbz/OBn route.

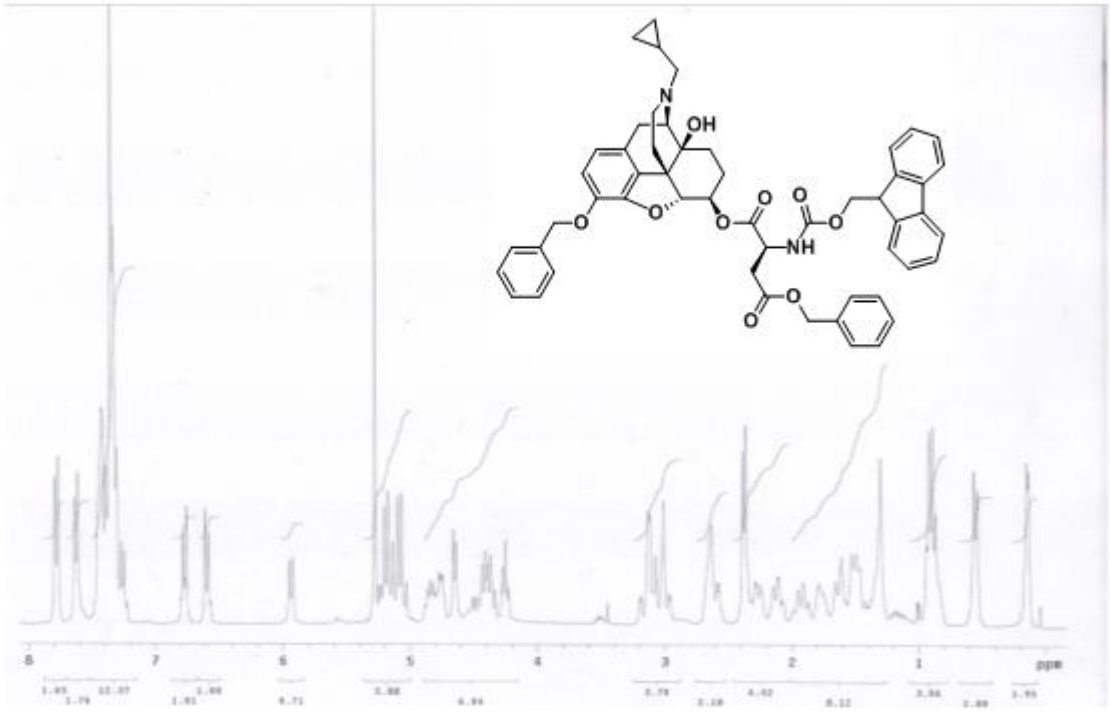

Figure 3.1 ^{1}H NMR spectrum of 3-*O*Bn-6-*O*-Fmoc-Asp(OBzl)-NTXOL.

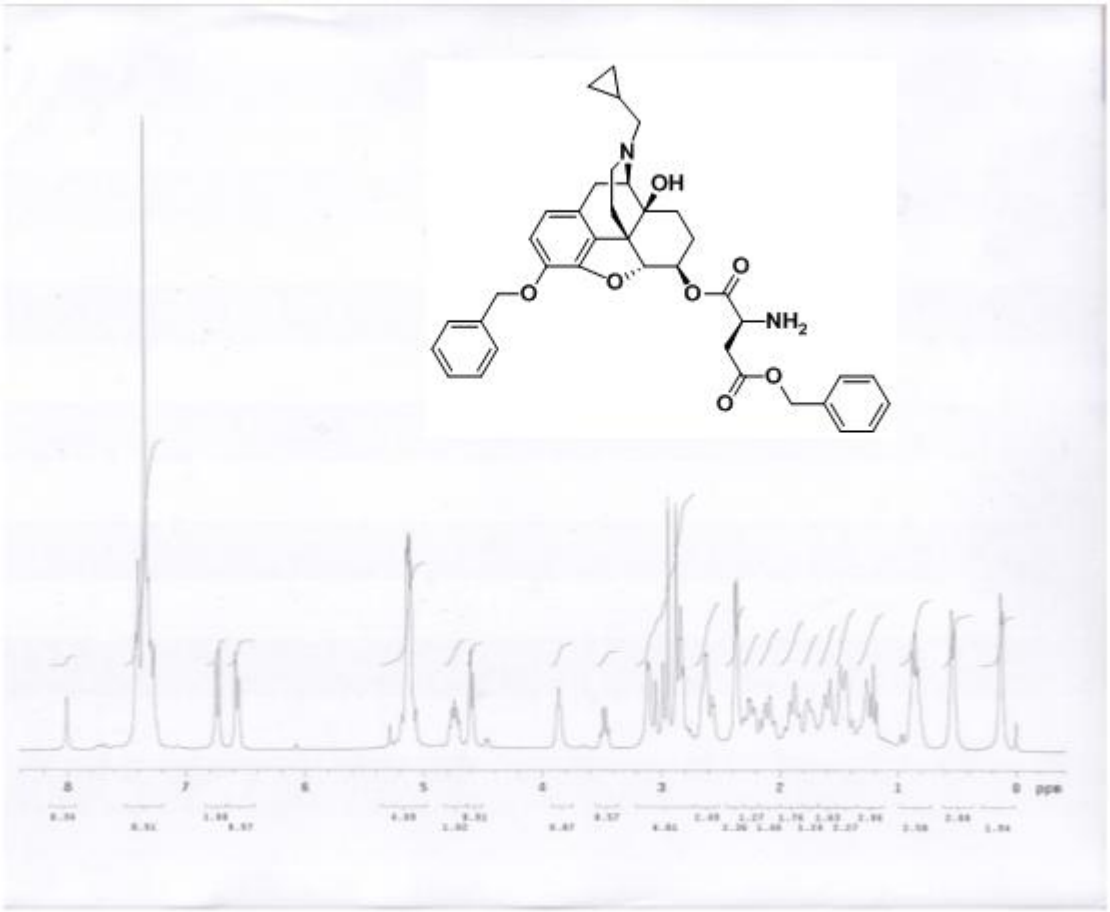

Figure 3.2 ^{1}H NMR spectrum of 3-*O*Bn-6-*O*-Asp(OBzl)-NTXOL.

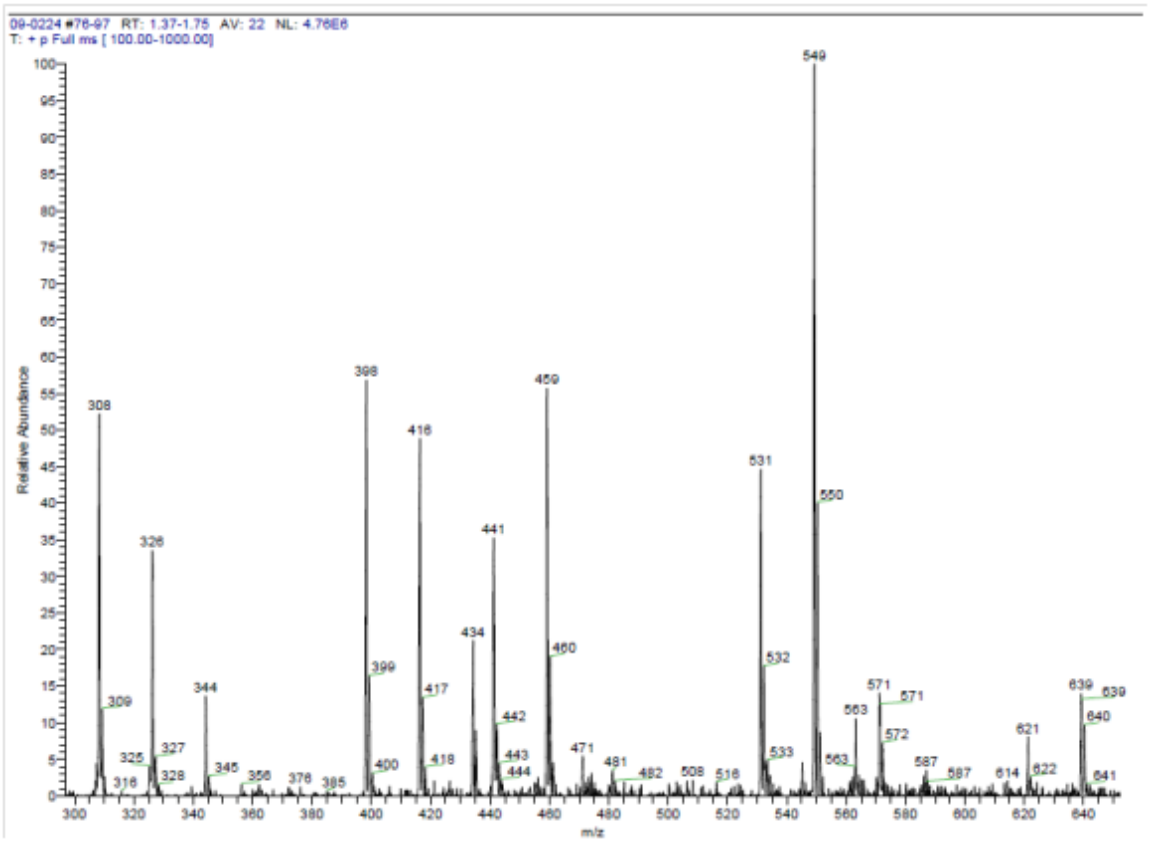

Figure 3.3 ESI-MS of 3-*O*Bn-6-*O*-Asp(OBzl)-NTXOL hydrogenolysis products.

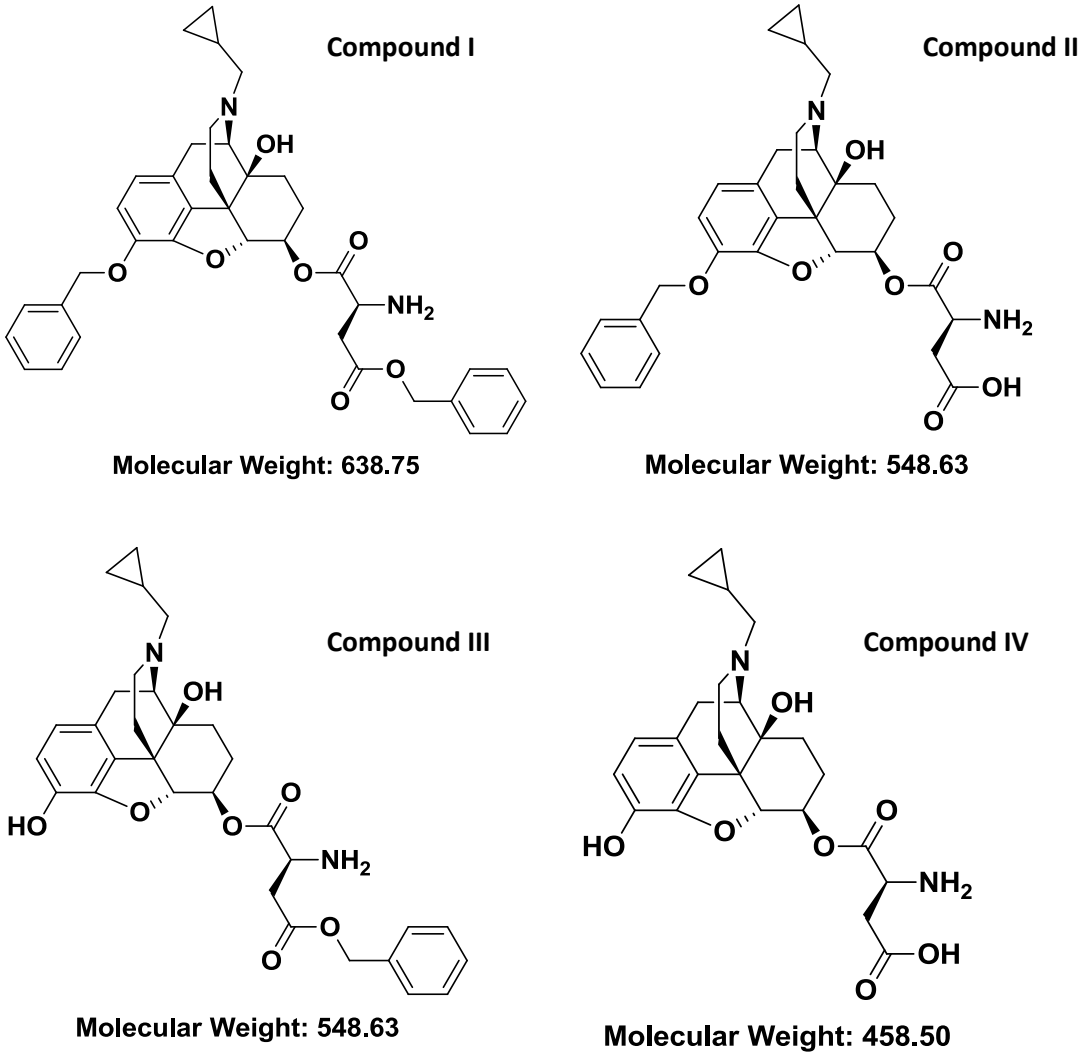

Figure 3.3 (cont.) ESI-MS of 3-*O*Bn-6-*O*-Asp(OBzl)-NTXOL hydrogenolysis products.

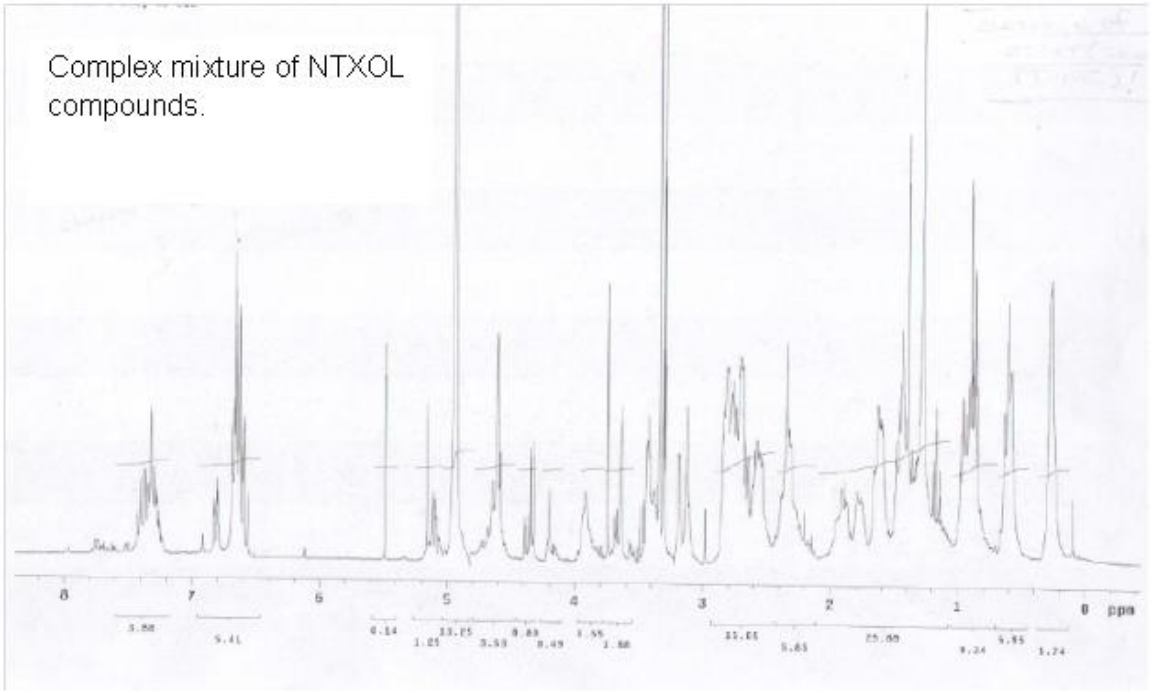

Figure 3.4 ^{1}H NMR spectrum of 3-*O*Bn-6-*O*-Asp(OBzl)-NTXOL hydrogenolysis products.

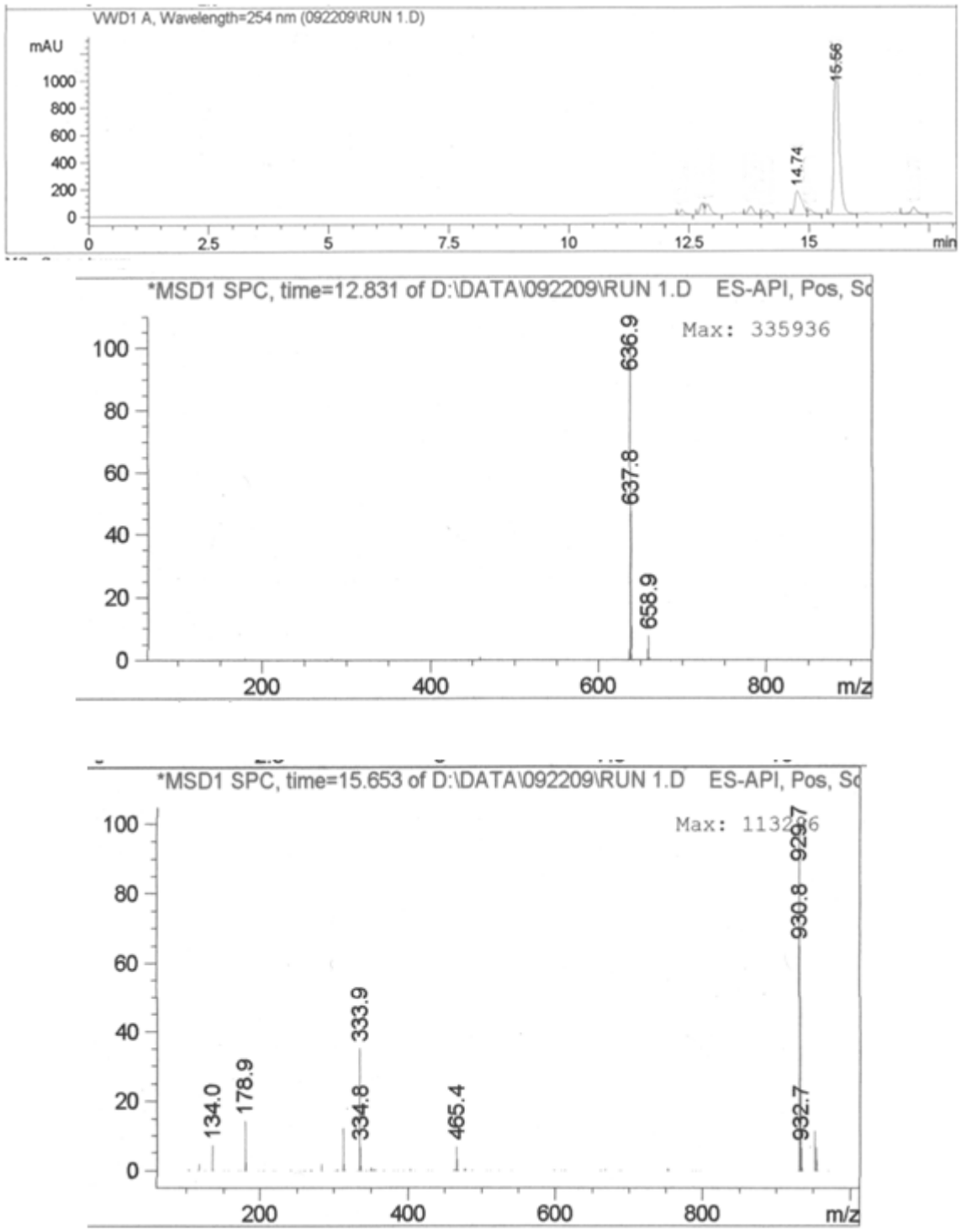

Figure 3.5 LC-UV/ESI-MS of 3,6-*O*-Bis-Fmoc-β-Ala-NTXOL deblocking test.

6-*O*-Leu-NTXOL (control)

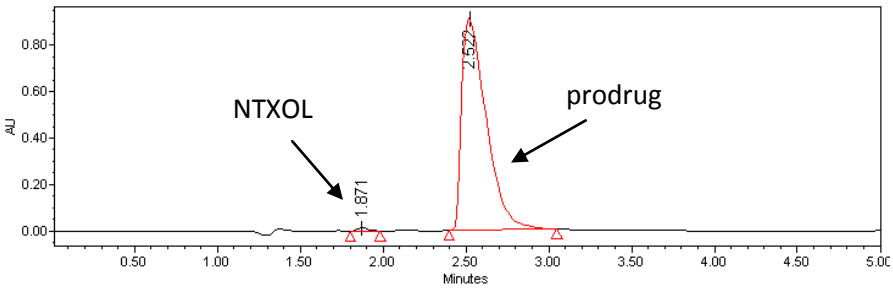

6-*O*-Leu-NTXOL (Hydrogenolysis 24 h)

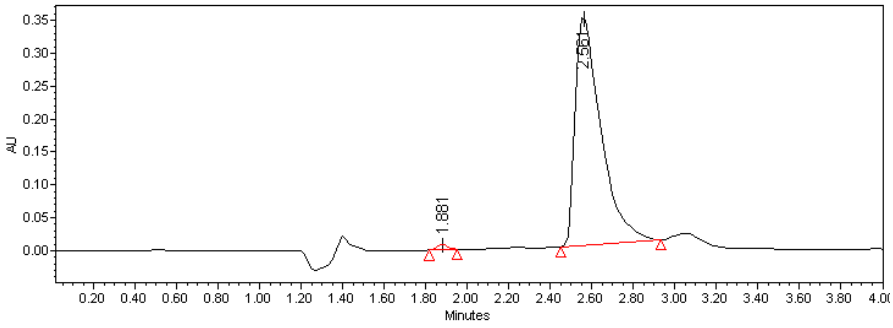

Figure 3.6 6-*O*-Leu-NTXOL ester hydrogenolysis test.

6-*O*-Leu-NTXOL (Hydrogenolysis 24 h + NTXOL spike)

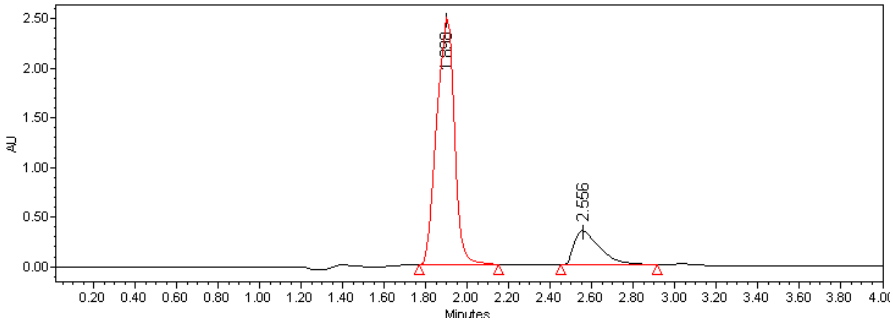

6-*O*-Leu-NTXOL (Hydrogenolysis 24 h + prodrug spike)

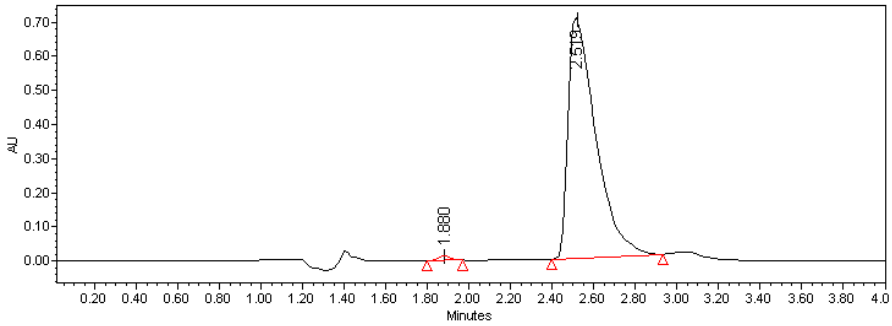

Figure 3.6 (cont.) 6-*O*-Leu-NTXOL ester hydrogenolysis test.

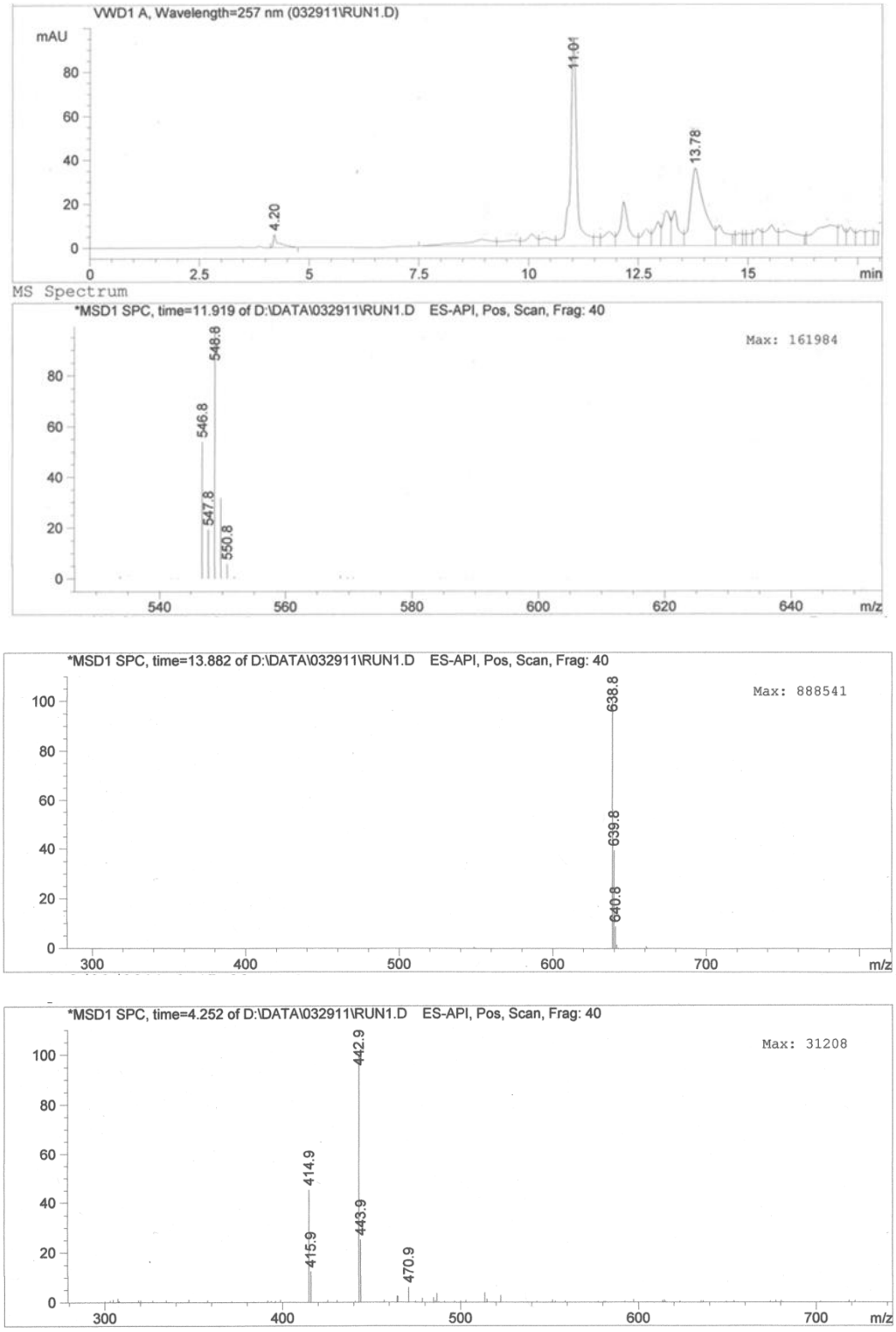

Figure 3.7 LC-UV/ESI-MS of 3-*O*Bn-6-*O*-Cbz-β-Ala-NTXOL hydrogenolysis products. Conditions: 10 mol% Pd Black / EtOAc / H_2 @ 50 psi / 4 days.

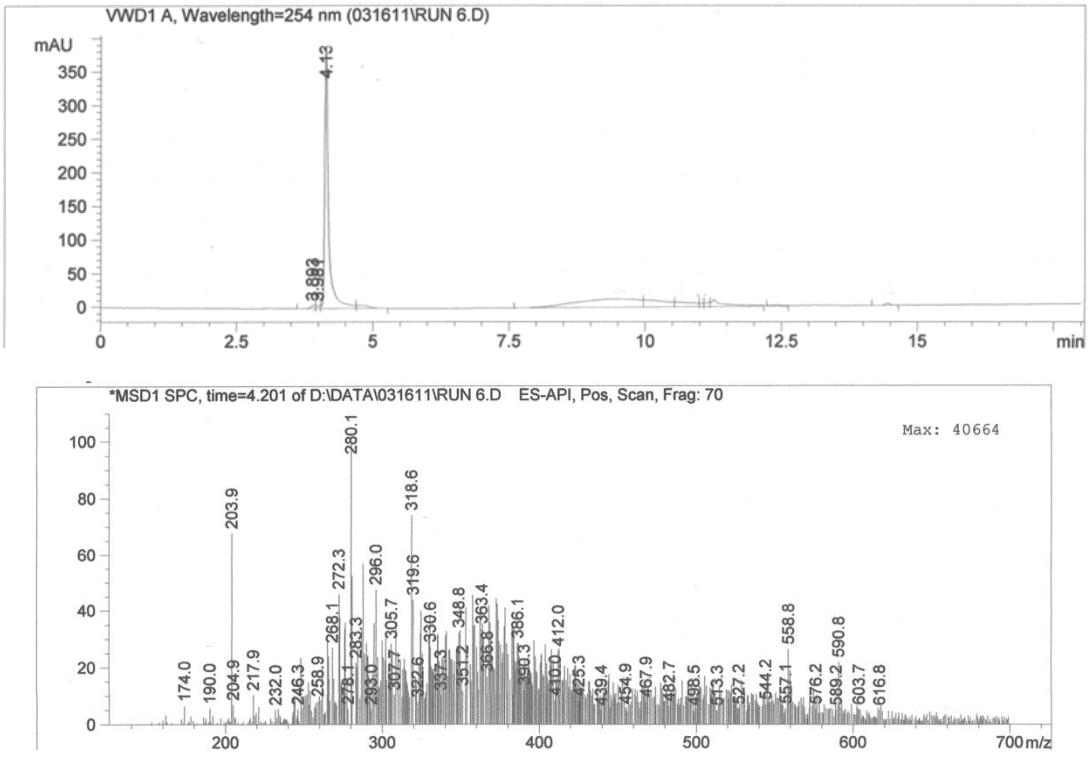

Figure 3.8 LC-UV/ESI-MS of 3-*O*Bn-6*O*-Cbz-β-Ala-NTXOL hydrogenolysis products. Conditions: Pd Black 3 x wt% / EtOAC/ THF wash / 24 h / H_2 @ 50 psi.

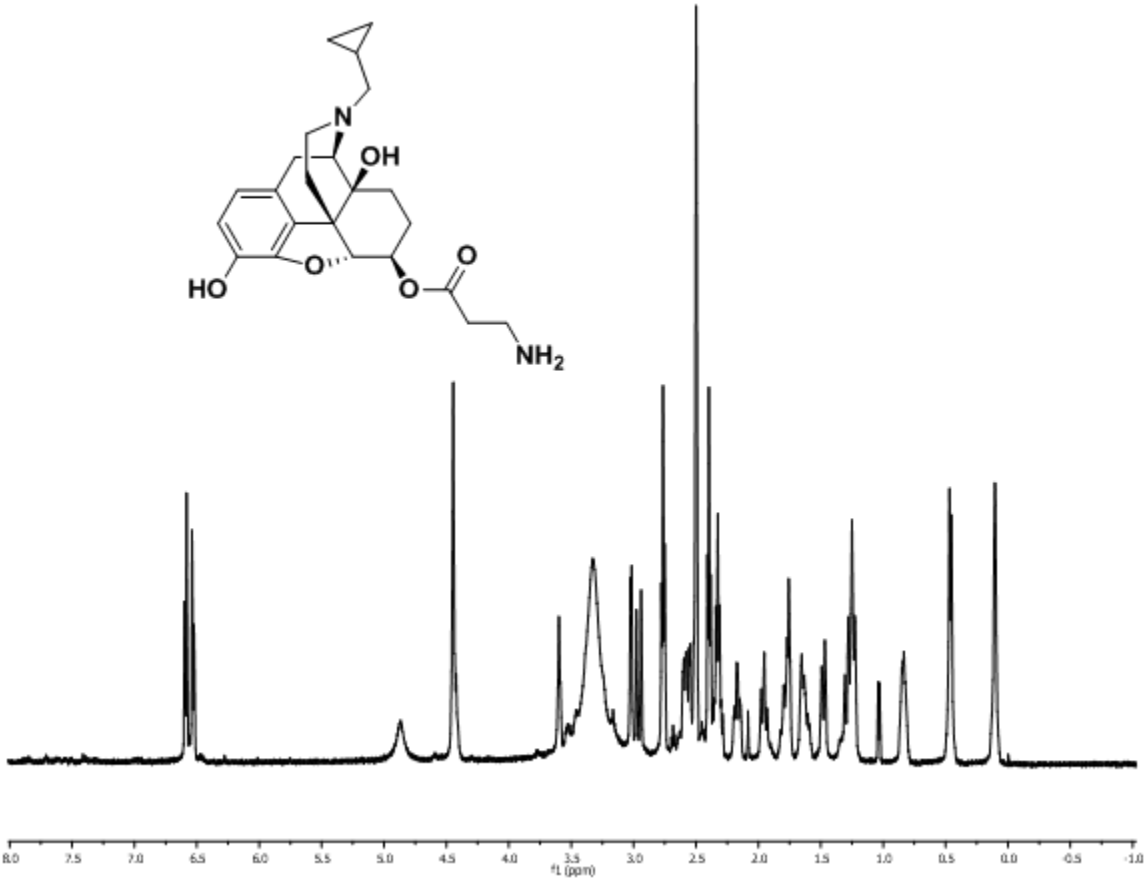

Figure 3.9 ^{1}H NMR spectrum of 6-*O*-β-Ala-NTXOL.

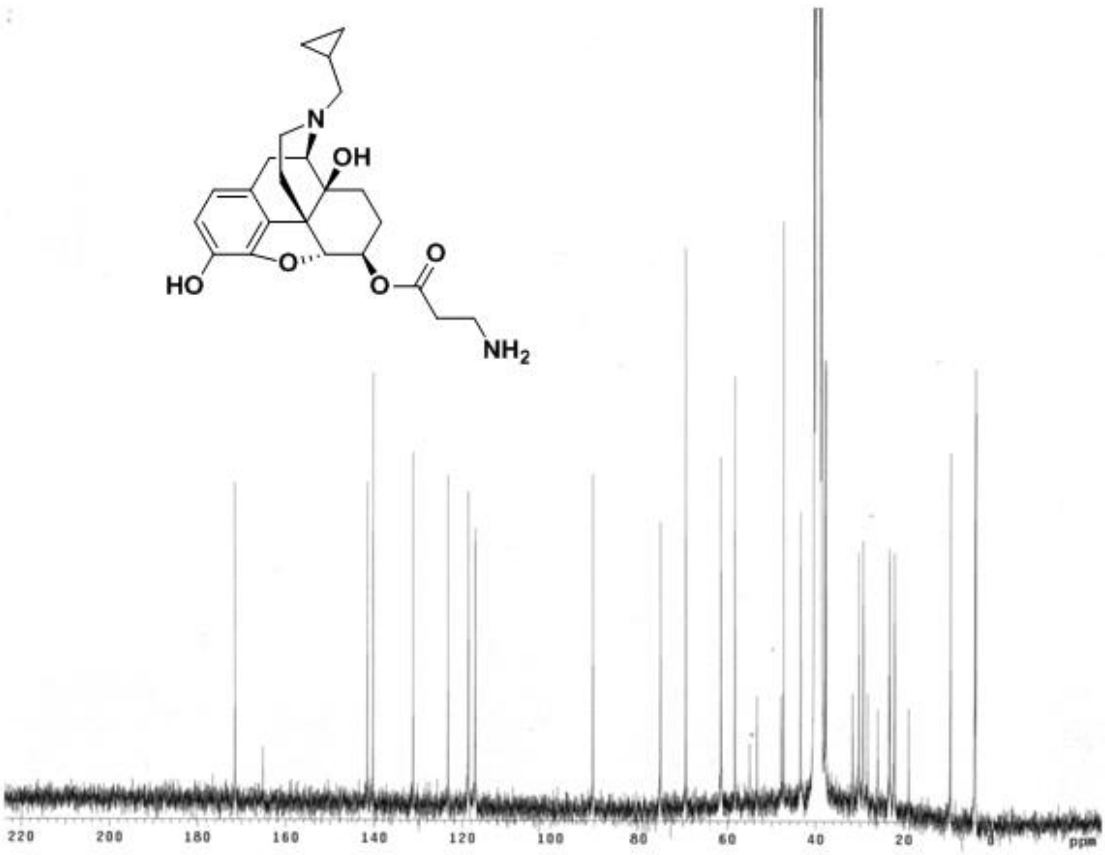

Figure 3.10 ^{13}C NMR spectrum of 6-*O*-β-Ala-NTXOL.

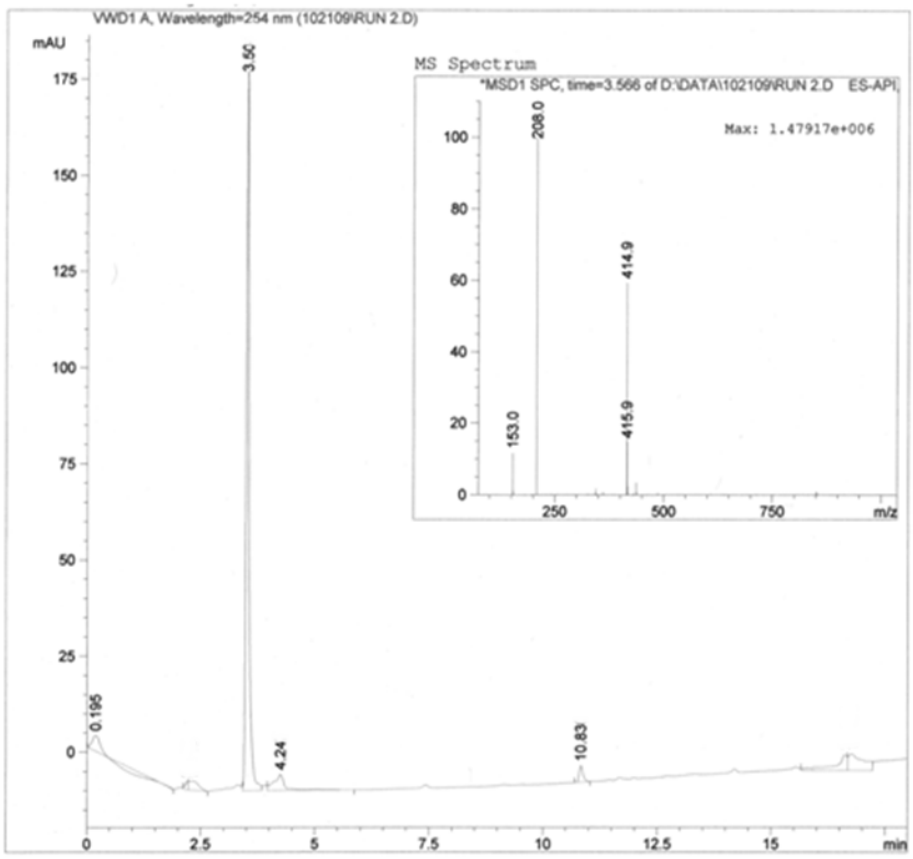

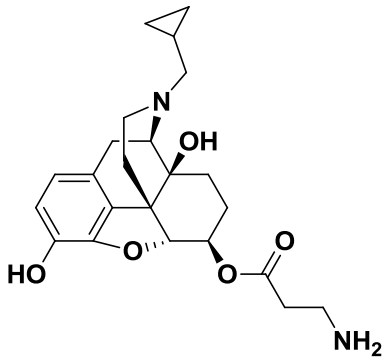

Molecular Weight: 414.49

Figure 3.11 LC-UV/ESI-MS of 6-*O*-β-Ala-NTXOL.

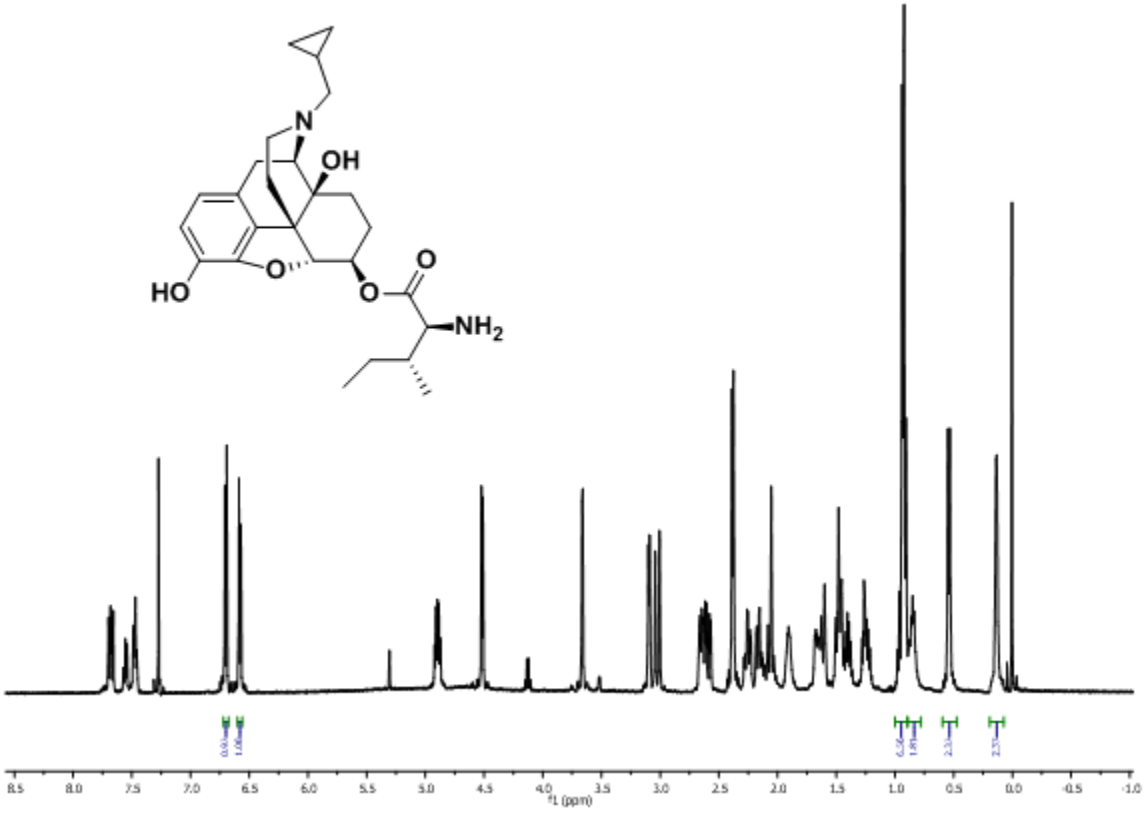

Figure 3.12 ^{1}H NMR spectrum of 6-*O*-Ile-NTXOL.

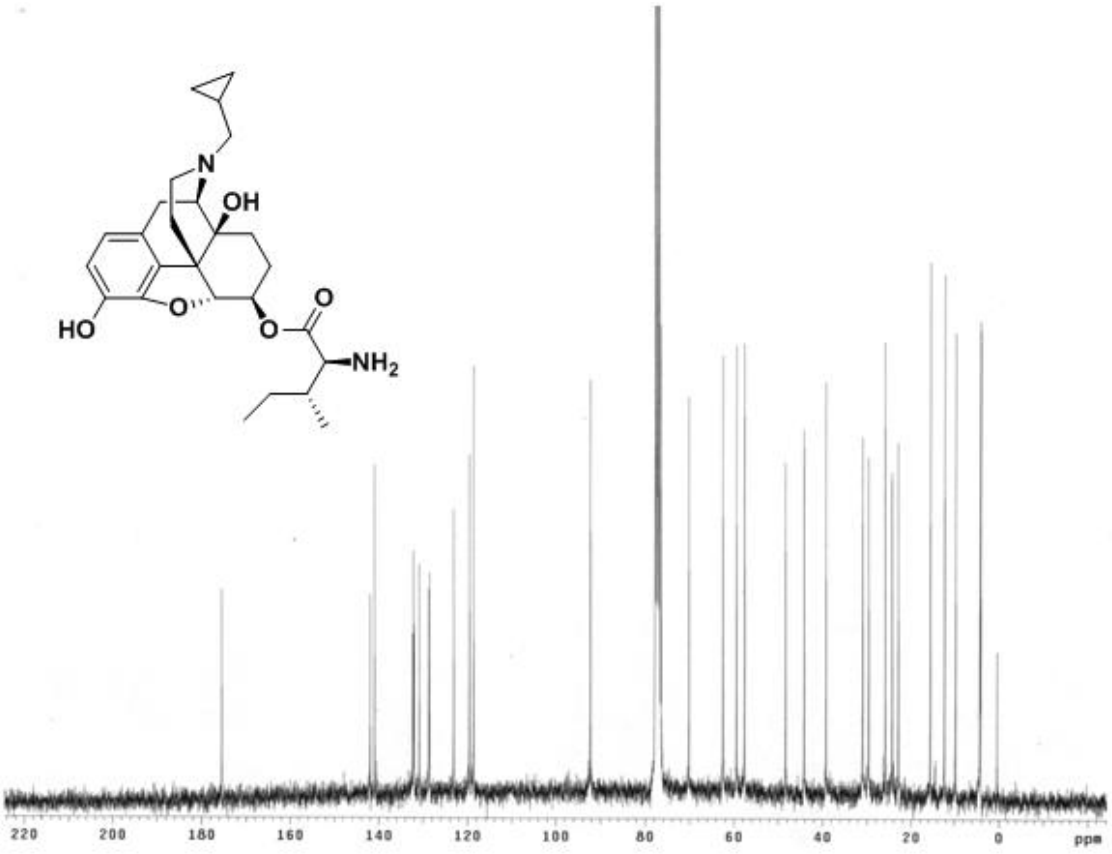

Figure 3.13 ^{13}C NMR spectrum of 6-*O*-Ile-NTXOL.

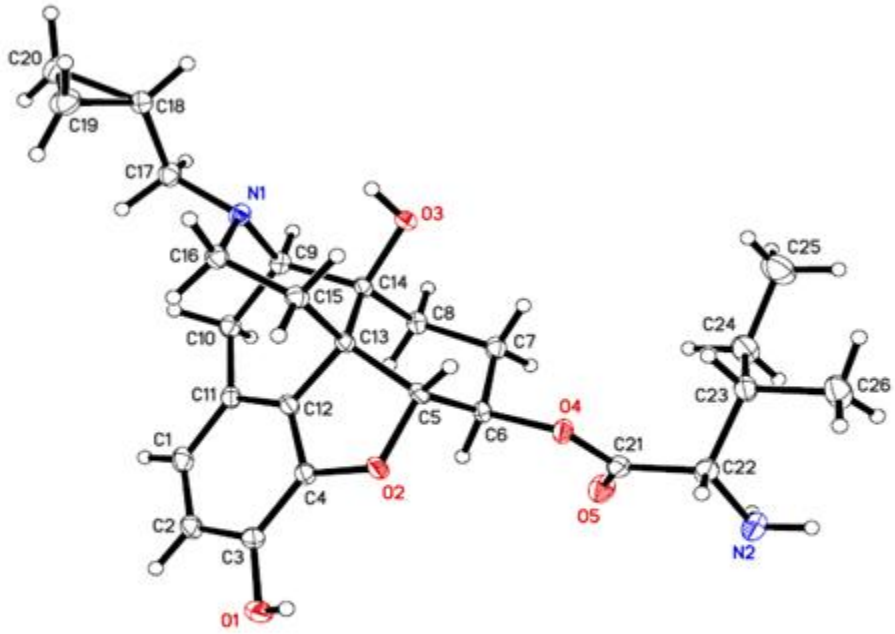

Figure 3.14 X-ray crystal structure of 6-*O*-Ile-NTXOL.

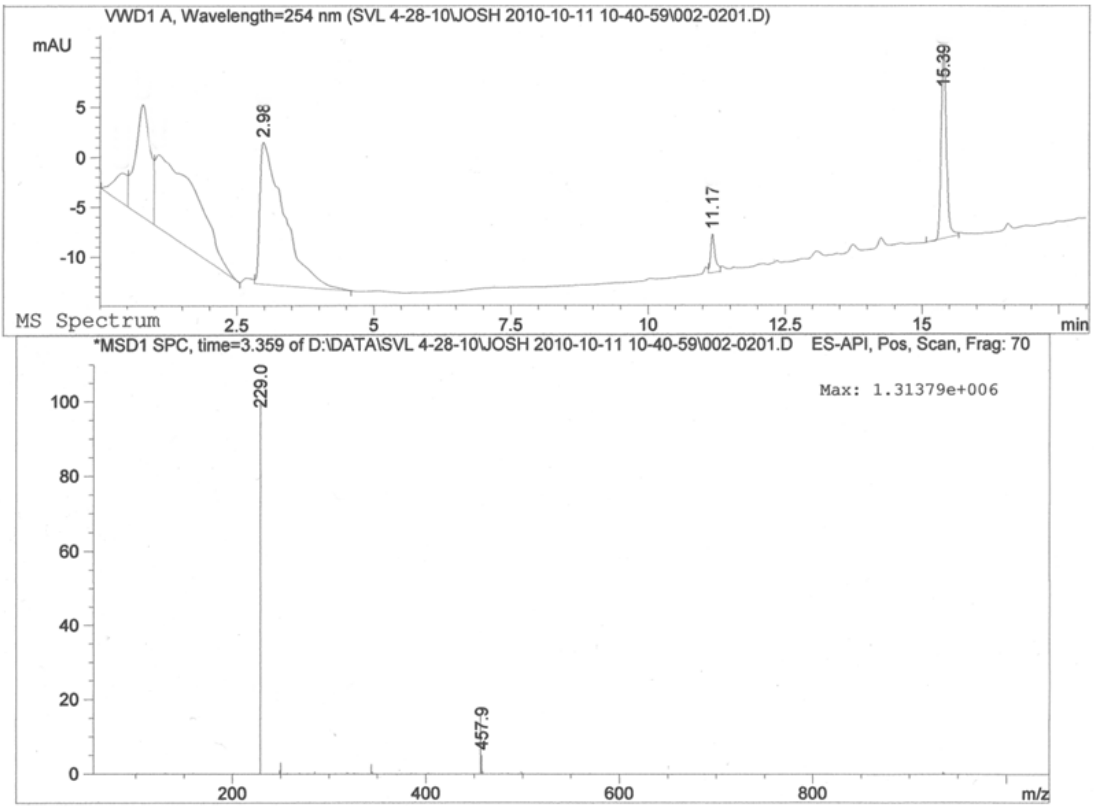

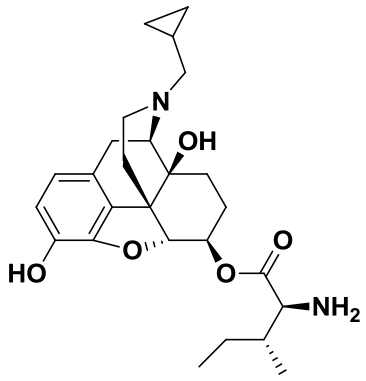

Molecular Weight: 456.57

Figure 3.15 LC-UV/ESI-MS of 6-*O*-Ile-NTXOL.

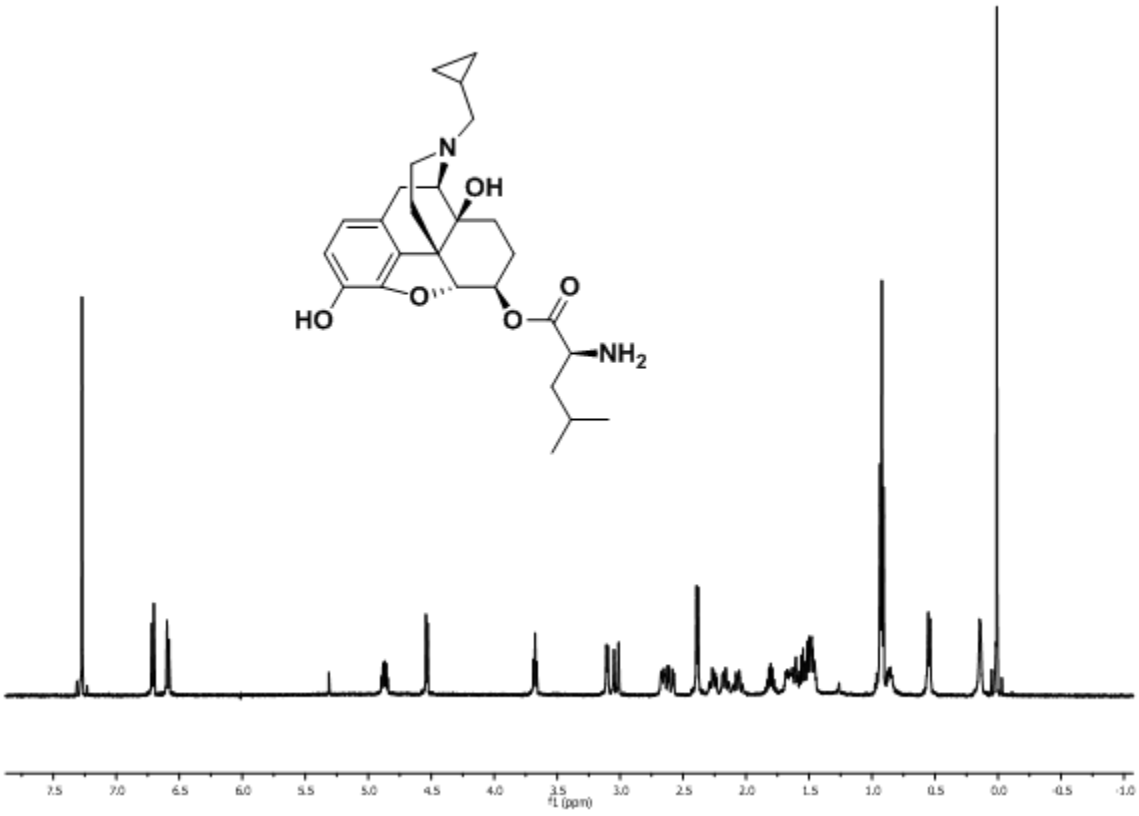

Figure 3.16 ^{1}H NMR spectrum of 6-*O*-Leu-NTXOL.

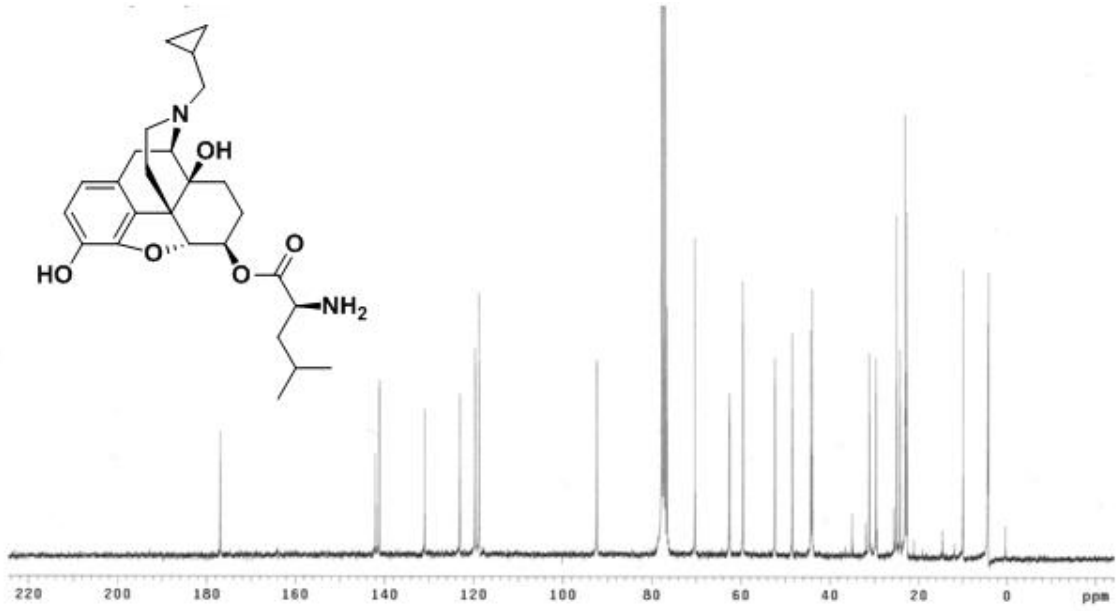

Figure 3.17 ^{13}C NMR spectrum of 6-*O*-Leu-NTXOL.

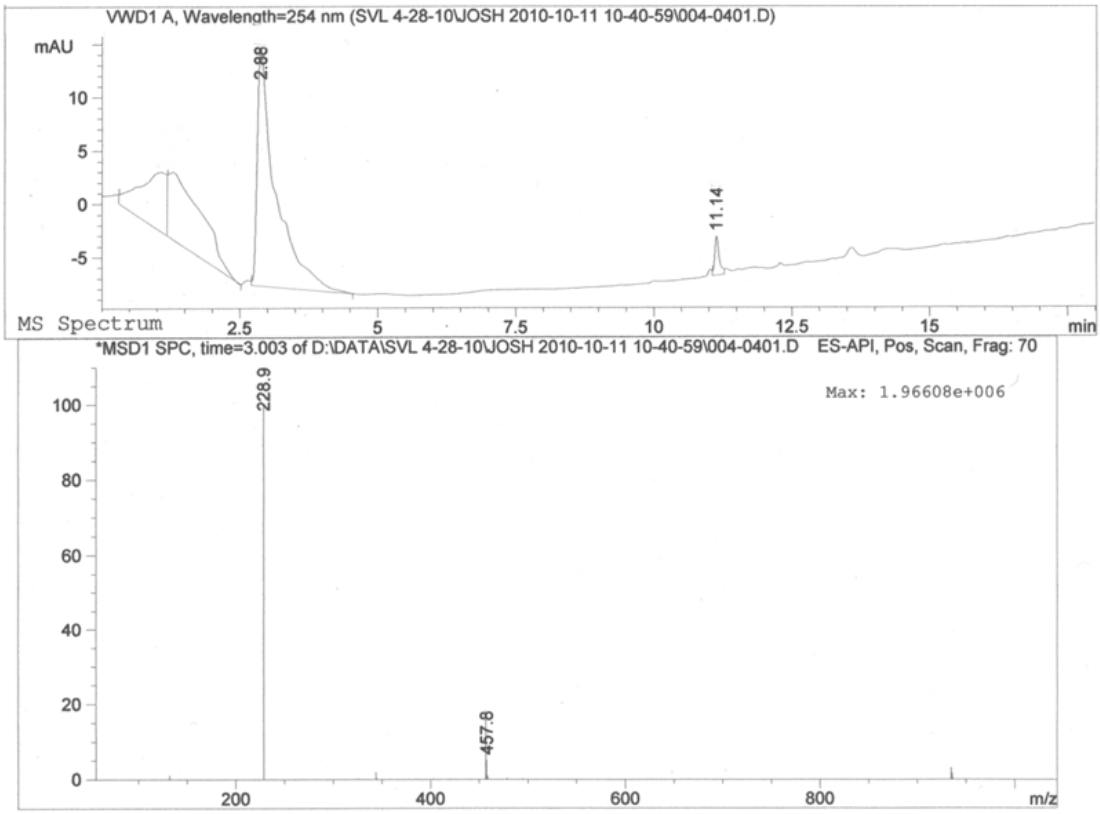

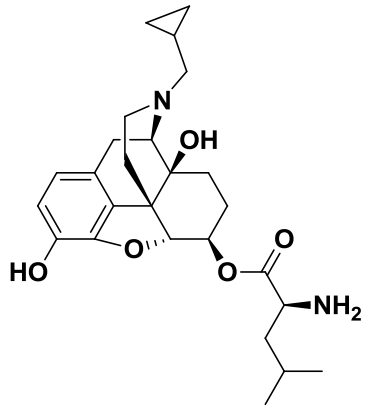

Molecular Weight: 456.57

Figure 3.18 LC-UV/ESI-MS of 6-*O*-Leu-NTXOL.

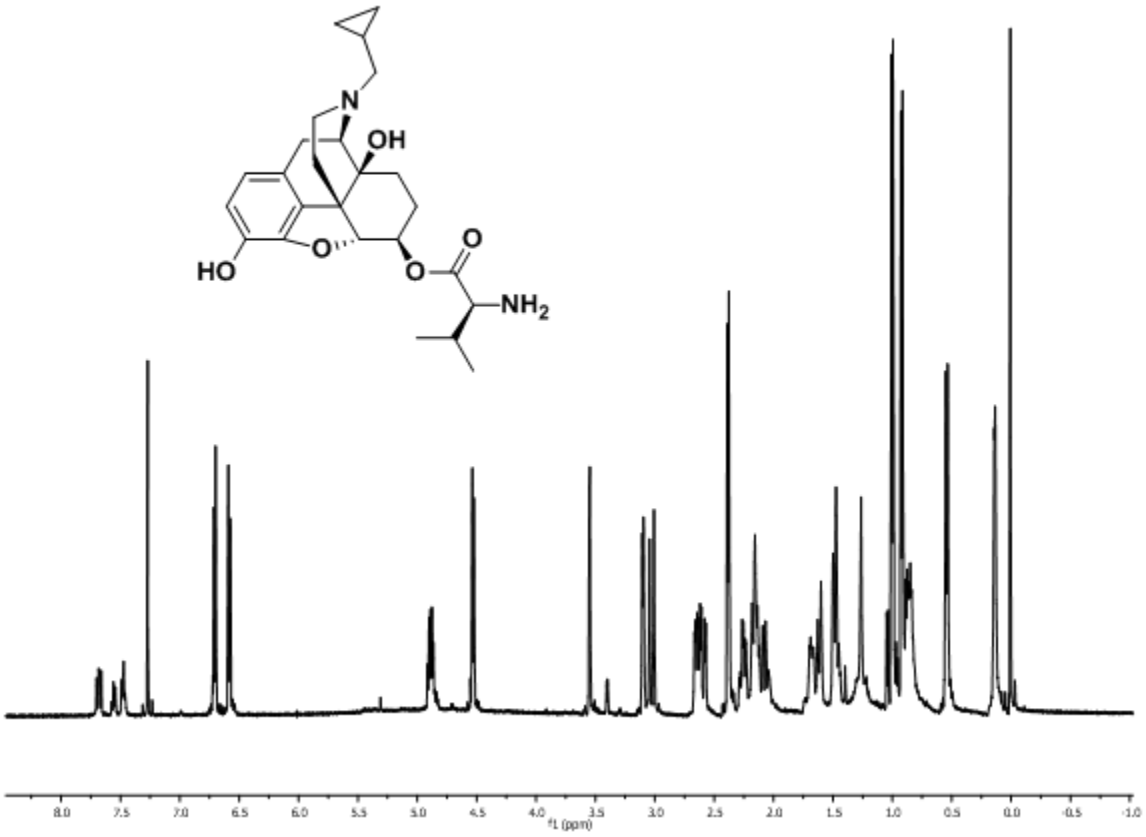

Figure 3.19 ^{1}H NMR spectrum of 6-*O*-Val-NTXOL.

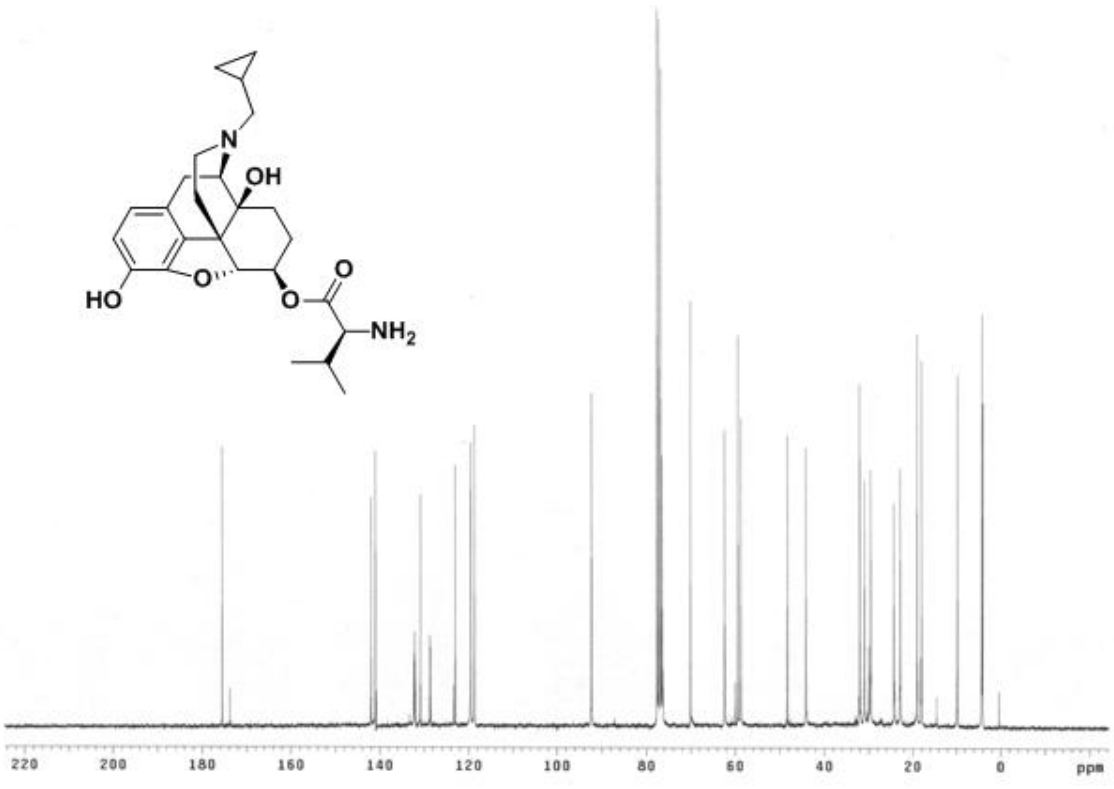

Figure 3.20 ^{13}C NMR spectrum of 6-*O*-Val-NTXOL.

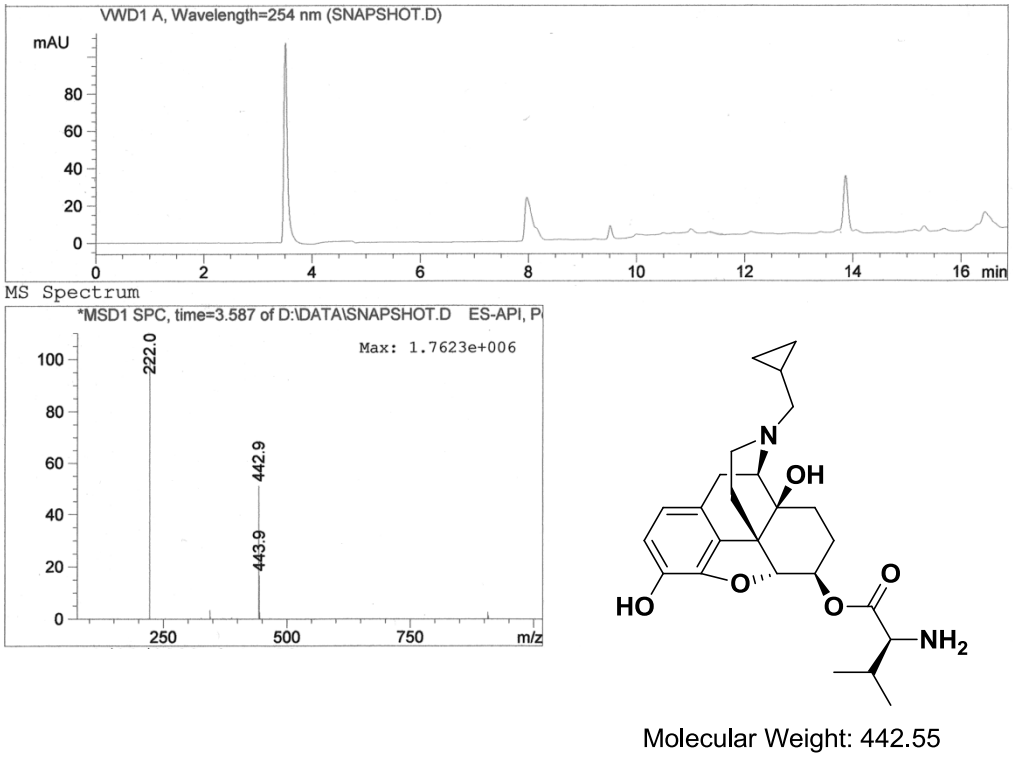

Figure 3.21 LC-UV/ESI-MS of 6-*O*-Val-NTXOL.

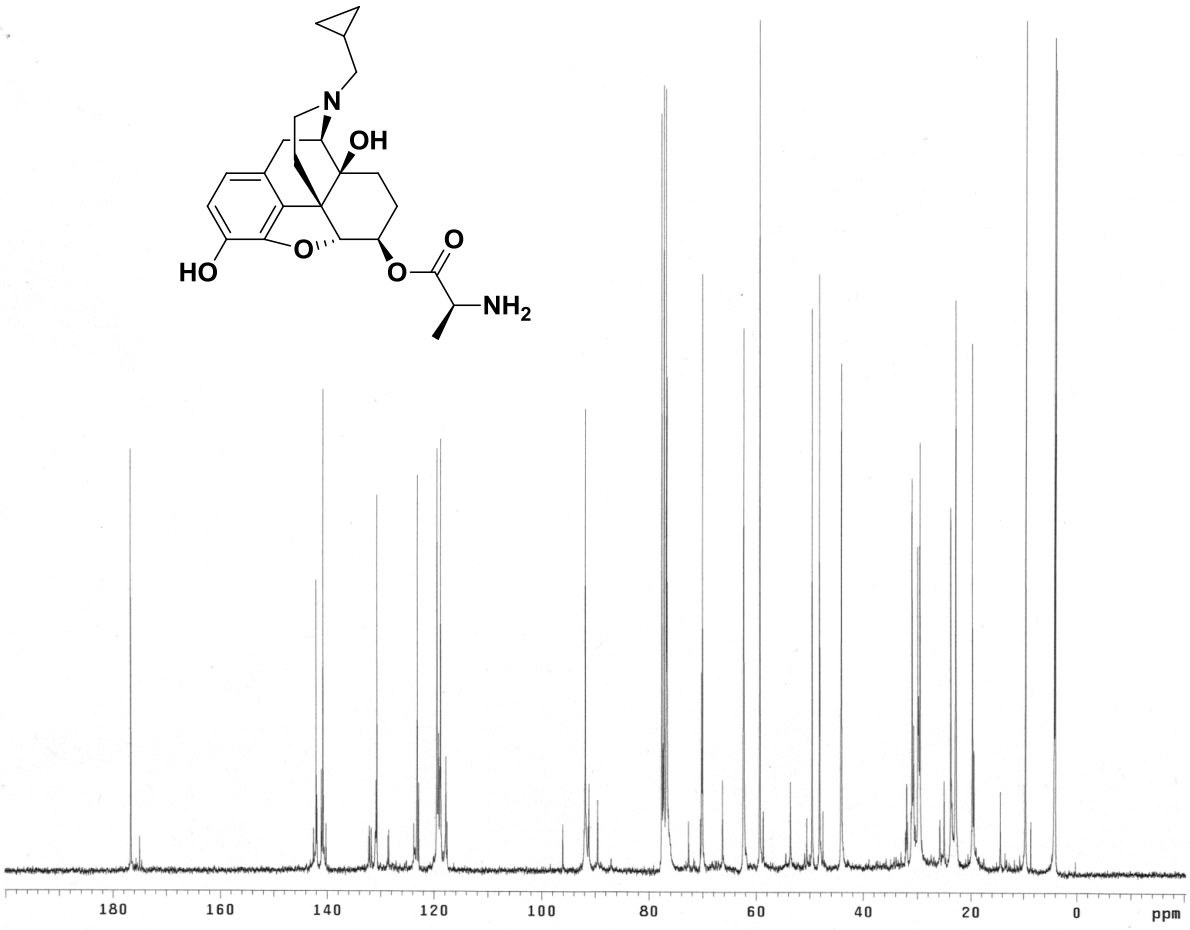

Figure 3.22 ^{13}C NMR spectrum of 6-*O*-Ala-NTXOL.

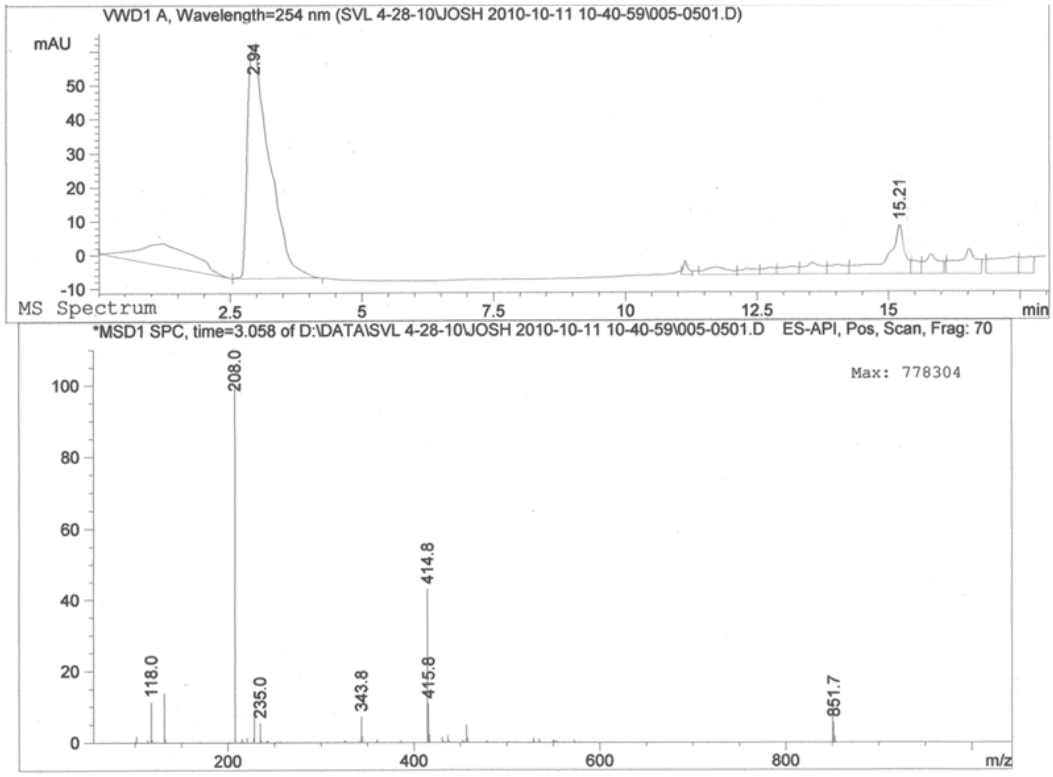

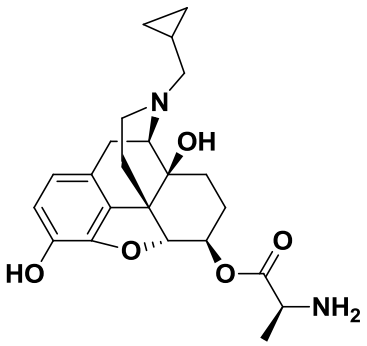

Molecular Weight: 414.49

Figure 3.23 LC-UV/ESI-MS of 6-*O*-Ala-NTXOL.

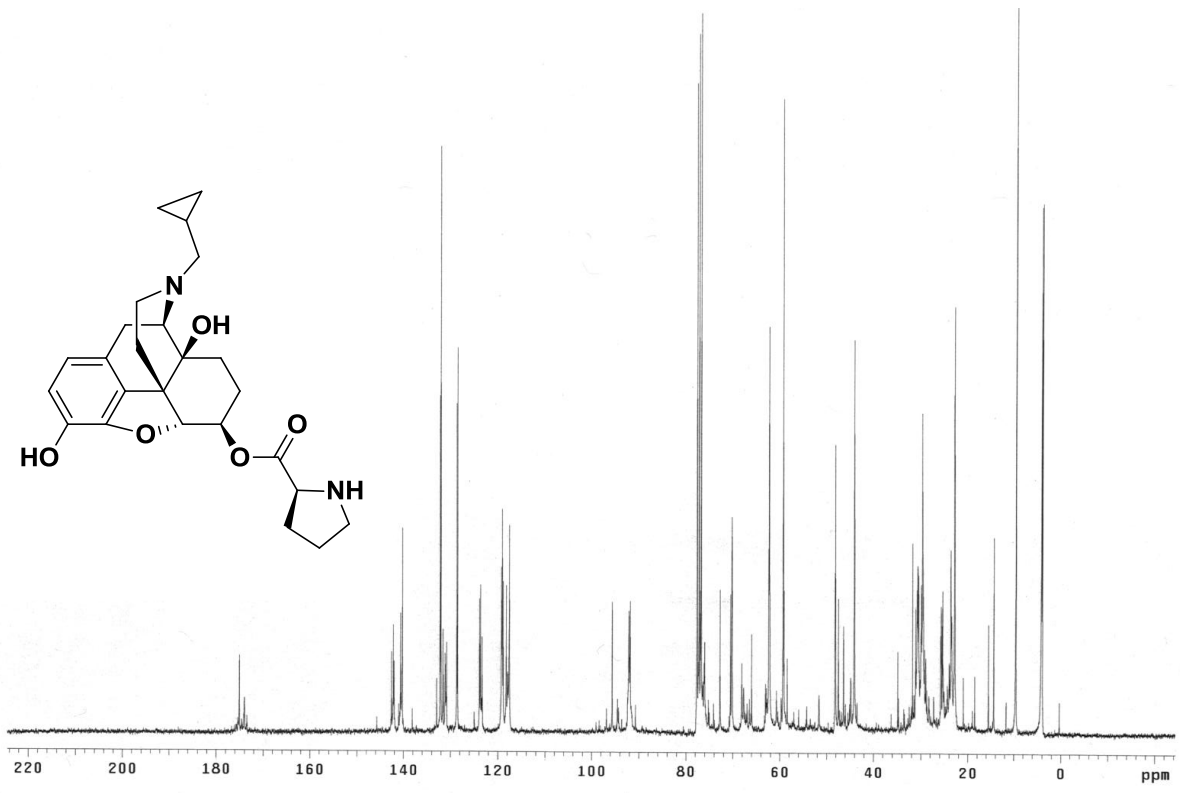

Figure 3.24 ^{13}C NMR spectrum of 6-*O*-Pro-NTXOL.

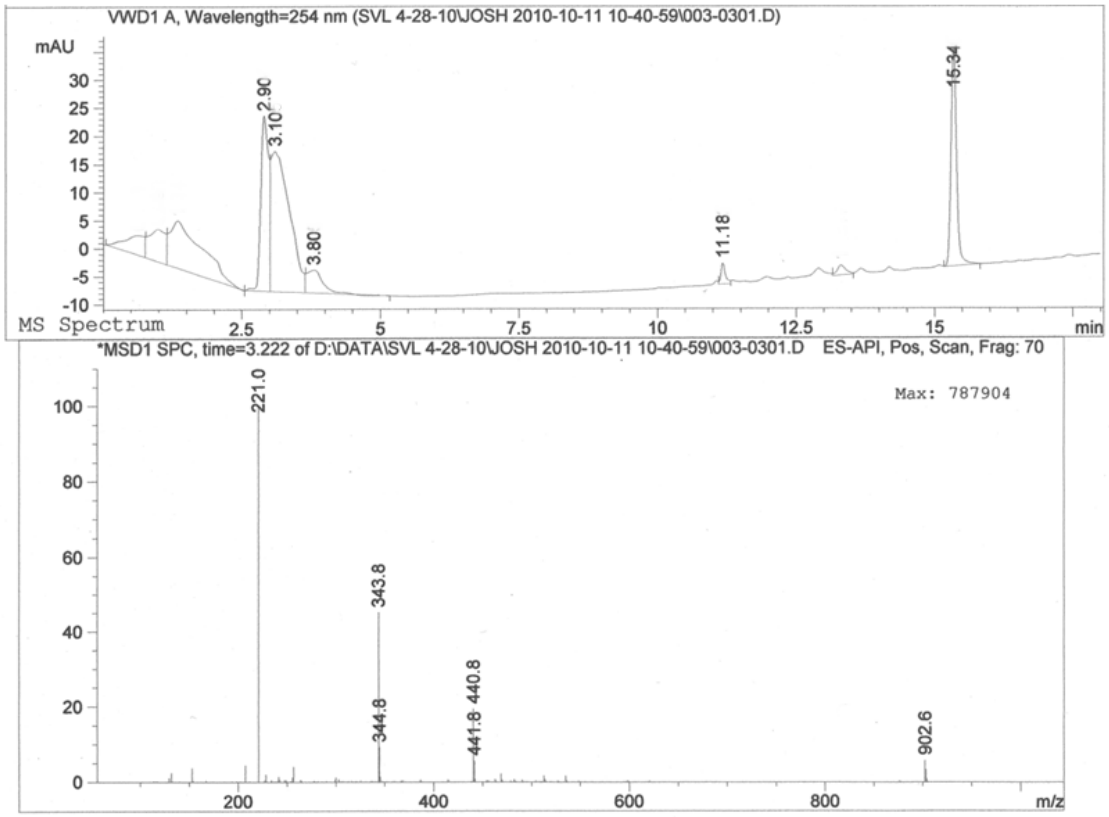

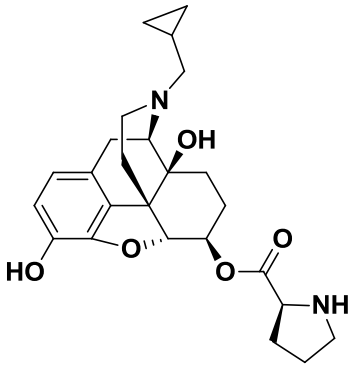

Molecular Weight: 440.53

Figure 3.25 LC-UV/ESI-MS of 6-*O*-Pro-NTXOL.

Chapter 4

Synthesis of 14-*O*-amino acid esters and miscellaneous prodrugs of NTX

In order to exploit all the possible acylation positions on NTX and NTXOL, the poorly reactive 14-*O* position of the morphinan ring system was also considered in synthetic designs. It was envisioned that esters formed at the tertiary aliphatic hydroxyl position of NTX would have interesting stability characteristics compared to their 3-*O*-phenolic and 6-*O*-aliphatic counterparts, in particular with respect to enzyme kinetics of hydrolysis at the more sterically-hindered 14-*O* position. Synthesis of the desired esters was not simple to achieve however, because the 14-*O* positions of NTX and NTXOL have proven to be highly unreactive under a variety of conditions, as is indicated by the lack of need for a protecting group on the 14-*O* position in other hydroxyl coupling reactions. Ultimately, the recurrent evidence in our laboratories has shown that the 14-*O* position requires the assistance of microwave irradiation to become reactive toward electrophilic coupling reagents. In the case of 14-*O*-amino acid esters of NTX, microwave irradiation was found to be required for 14-*O* coupling as well. Sonication and simple heating were also explored as alternatives to microwave irradiation, but there was no evidence of coupling in the crude ^{1}H NMR spectra of reaction products from those conditions. Overall, the coupling step was found to require the Fmoc-β-Ala-Cl synthon that had originally been employed in the 6-*O*-NTXOL amino acid ester prodrug series (**Chapter 3**). Carbodiimide strategies failed under all conditions, as determined by ^{1}H NMR spectrometric analysis of crude reaction products. The best coupling results that were obtained from many

attempts under various reaction conditions are summarized in **Scheme 4.1**. Aside from generally poor coupling at the 14-*O* position under all conditions, even with up to 6 equivalents of the amino acid activated acid chloride, a problematic side reaction involving the enolate of the 6-keto group of the morphinan scaffold furnished a *bis*-coupled prodrug precursor as a significant side product. Nonetheless, the major product could be separated by column chromatography and analyzed gravimetrically to indicate a 15% yield. The 7% undesired *bis*-coupled side product also appeared as one spot on TLC under a variety of conditions. In general, the major product, and the minor product had complicated NMR spectra (**Figures 4.1, 4.2, 4.4, and 4.5**) and fairly clean MALDI-TOFMS spectra (**Figures 4.3 and 4.6**). The proton NMR spectra in the case of both the major product, 3-*O*-allyl-14-*O*-Fmoc-β-Ala-NTX (**Fig. 4.1**), and the minor product, 3-*O*-allyl-6-O,14-*O*-bis-Fmoc-β-Ala-NTX (**Fig. 4.4**), show an interesting shift of the cyclopropyl methylene peaks upfield of TMS. This is unexpected since the crystal structure of 6-*O*-Ile-NTXOL in **Fig. 3.14** does not suggest that a 14-*O*-amino acid conjugate of β-alanine should have steric characteristics that add significantly to the ring strain on the relatively distant cyclopropylmethyl amine substituent. Nonetheless, it seems that 14-*O*-coupling shows this characteristic, and the minor product is expected to be a 14-*O*-conjugate as well. With so many other overlapped peaks and doubling in many of the regions of the proton NMR spectrum of the major product, multiple conformers seem to be showing in the NMR spectrum. The MALDI-TOFMS spectra provide additional evidence that the two products are as suggested in

Scheme 4.1 (m/z = 675 & 968 compared to MW = 674.78 & 968.10). ^{13}C NMR spectra are also shown in **Figures 4.2 and 4.5**; however these spectra do not seem to indicate that the single spots on TLC for the major and minor products are indicative of totally clean prodrug precursors. For instance, the major product $C_{41}H_{42}N_2O_7$ has more than 41 carbon peaks, and the minor product $C_{59}H_{57}N_3O_{10}$ has more than 63 unique carbons in the NMR. It is likely that stable conformations and/or hydrogen bonding phenomena could play a role in the number of peaks observed in these spectra.

In terms of competing reactions, it was also evident that a large amount of the coupling synthon was quenched to the parent carboxylic acid, regardless of the use of dried solvents, under the harsh conditions of 80°C microwave irradiation for thirty minutes. Also, a twofold excess of DMAP base was required to quench HCl formed in the preactivation and coupling reactions, but those conditions also favored premature removal of Fmoc under the microwave coupling reaction conditions. The obvious problems associated with the Fmoc removal at the coupling stage were peptide polymerization of the β-Ala pro-moiety, and free amine-dibenzofulvene adduct formation with the deblocked prodrug precursor and dibenzofulvene (DBF). In order to suppress these side reactions, alternative secondary amine bases were explored to replace DMAP, a tertiary base that cannot participate in scavenging of the DBF Michael acceptor that forms in Fmoc removal. When other bases were used as scavengers, the 14-*O* coupling yield suffered even more. Therefore, the optimized conditions for coupling using Fmoc and allyl protecting group strategies were achieved with disappointing results. In

order to attempt suppression of the 6-*O*-enolate ester that formed in the reaction, 6-keto blocking was explored using the typical 1,4-dioxane and 1,4-dithiane approaches that employ ethylene glycol and 1,2-ethanedithiol, respectively (**Scheme 4.2**).

Referring to **Scheme 4.2**, the 6-(1,4-dioxaspiro-ethylene)-NTX synthon did form with conditions "i" and "ii," while the 6-(1,4-dithiaspiro-ethylene)-NTX synthon could not be obtained at all using conditions "iv" and "v." 6-(1,4-Dioxaspiro-ethylene)-NTX was also inaccessible by conditions "iii." The evidence supporting the 6-(1,4-dioxaspiro-ethylene)-NTX observations was obtained via ^{13}C NMR analysis, as there was no apparent new spot on TLC under any conditions, and one can most easily surmise reaction progress in this case by looking for the characteristic chemical shift of the ketone carbonyl carbon in the NMR spectrum. **Figure 4.8** shows the reference ^{13}C NMR spectrum for NTX **[Fig. 4.8(a)]**, the crude ^{13}C NMR spectrum of "Scheme 4.2 Conditions iii [**Fig. 4.8(b)**]," and the ^{13}C NMR spectrum of the crude product of "Scheme 4.2 Conditions i and ii [**Fig. 4.8(c)**]." **Figure 4.8(c)** represents a snapshot of the reaction progress at 8 hours reflux in toluene (following 4 hours without trimethyl orthoformate and 4 hours with trimethyl orthoformate). There is clear evidence that NTX is still present in the ^{13}C NMR spectrum, as the line data imply; however, there is also evidence of a new material with the expected peaks present in the 120-118 ppm range (hemiketal carbon) and at around 65 ppm (methylene carbons of the dioxane ring). In the case of the materials reacted with BF_3 etherate (conditions iii and iv), there was no sign of a new naltrexone-containing compound following workup

with 5% sodium bicarbonate. For instance, **Figure 4.8(b)** is identical to NTX, **Figure 4.8(a)**. When the cupric Lewis acid catalyst was used (conditions v), as per a recent literature method (Oksdath-Mansilla and Penenory 2007), only a multi-solvent insoluble material was formed. Therefore, attention was turned predominantly to the optimization of conditions ii, the tosylic acid-catalyzed reaction under dehydrating conditions (ethylene glycol is extremely hygroscopic, and the reaction favored water loss to drive the equilibrium). However, even with 24h of reflux in a Dean Stark apparatus and the addition of trimethyl orthoformate for added dehydrating power, the desired 6-(1,4-dioxaspiro-ethylene)-NTX synthon could not be formed quantitatively. The problem then arose that purification of the desired keto-protected material from the mixture with NTX was simply not possible. NTX and the 6-(1,4-dioxaspiro-ethylene)-NTX synthon had identical migration on silica gel plates under all solvent conditions, even with TEA treatment to destroy the acidity of the silica. Since no suitable method for keto protection could be found, the 14-*O*-amino acid ester prodrugs of NTX were abandoned at this stage. The final steps to afford the end products from the protected intermediates would have had all the same problems that the 6-*O*-amino acid esters of NTXOL had exhibited, and with vast diminishing returns to scale following a disappointing coupling yield, pursuit of this chemistry was not time and cost effective. For instance, removal of the allyl protecting group on phenol would have required palladium-catalyzed tributyl tin hydride chemistry that had previously proved unsuccessful in the 6-*O*-NTXOL amino acid esters work. Ketones are easily reduced non-stereospecifically to secondary alcohols

using the PMHS-$ZnCl_2$ and homogenous palladium catalyst system (Chandrasekhar, Reddy et al. 1997). The latter would have resulted in a mixture of 6-α/β-NTXOL diastereomers that would have complicated purification procedures to an unacceptable degree. Benzylation of the phenol group was out of the question due to the susceptibility of the 6-keto substituent to yet another non-stereospecific reduction under the conditions of hydrogenolysis, and TBDMS ether formation on the 3-*O* phenol had also previously failed. Still, it would be extremely interesting to know the differences in hydrolytic behavior between the 6-*O*-NTXOL amino acid prodrugs and their 14-*O*-NTX counterparts, with regard to enzyme-catalyzed hydrolysis in particular.

Aside from 14-*O* amino acid esters, which conclude the development of amino acid esters in this body of work, it was also envisioned that the 6-keto position of NTX might serve as a site of nucleophilic substitution by the free amine of amino acids, which could then possibly be further converted by microwave chemistry into novel, ring-closed 1-oxa-4-azaspiro prodrugs via an imine intermediate (**Scheme 4.3**). The idea is perhaps a mechanistic long-shot; however, brief attempts were made to investigate the feasibility of preparing these materials for assay as potential prodrug candidates. There is no particular hydrophilicity increase to be gained by this approach. Yet, classical transdermal delivery is enhanced by increased lipophilicity on the parent NTX scaffold (see **Chapter 1**), and it was expected that successful chemistry to afford these interesting spiro prodrug species might lend some utility to the classical transdermal podrugs literature. Because the stereochemistry of such a reaction would be the object of

intense study, it was decided to simplify the R-group influence of the substituted α-amino acids and check the reaction with glycine (R=H). β-Alanine would have also been a good choice for the initial investigations; however, it would have formed a 6-membered ring compared to the expected 5-membered ring with the glycine reaction. Since 5-membered ring closures represent the most rapid ring-closing reactions in organic chemistry, the 5-membered ring that could be obtained from glycine was expected to be better able to out-compete the water nucleophile that would form if the reaction proceeded. With these thoughts in mind, the reaction was pursued with various iterations using microwave chemistry. Unfortunately, employing the various conditions depicted in **Scheme 4.3**, there was no evidence of any reaction at all in dry DMF. Methanol could not be used for obvious reasons. Other solvents simply do not dissolve glycine to any useful extent, so the desired spiro prodrug product could not be obtained by this approach.

Next, a model reaction was conducted to confirm reactivity of the 6-ketone functionality of NTX toward the free amine group of α-amino acids (**Scheme 4.4**). This was done simply to rule out the possibility that these amines do not form imine intermediates on NTX. The best way to trap the imine in an irreversible reaction is to employ the standard procedure of reductive amination. Within the laboratory, NH_2-Val-O-*t*-Bu was available for the model reaction. This particular *t*-Bu ester-protected amino acid was a perfect species for the model synthesis, because the carboxylic acid was blocked from nucleophilic attack on the imine. The reductive amination could then be performed using sodium

cyanoborohydride, the results of which provided ESI-MS evidence for the formation of the desired 6-NH-Val-O-*t*-Bu analogue(s) (**Figure 4.7**). Although the model compound is certainly an interesting precursor whose chemistry could be refined, optimized, and taken all the way to the fully deblocked 6-NH-Val-O-*t*-Bu opioid analogue with relative ease (no hydrolysis would occur on this compound under acidic deblocking conditions), the goal of this body of work was to develop prodrugs of NTX, and not analogues. Overall, the results of this model reaction indicate that the necessary imine intermediate does form, and one might be able to make the desired spiro compounds for assay using other techniques.

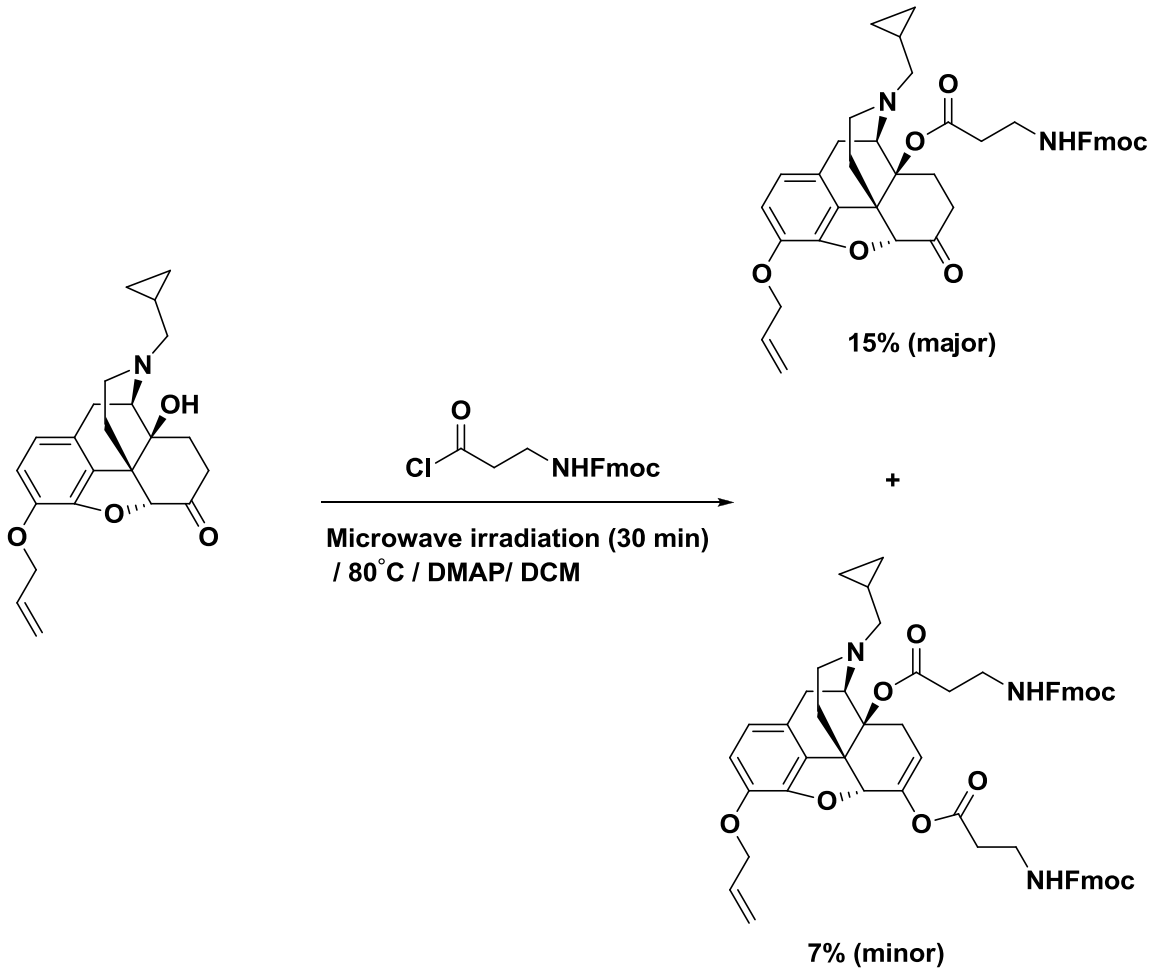

Scheme 4.1 Synthesis of 3-*O*-allyl-14-*O*-Fmoc-β-Ala-NTX.

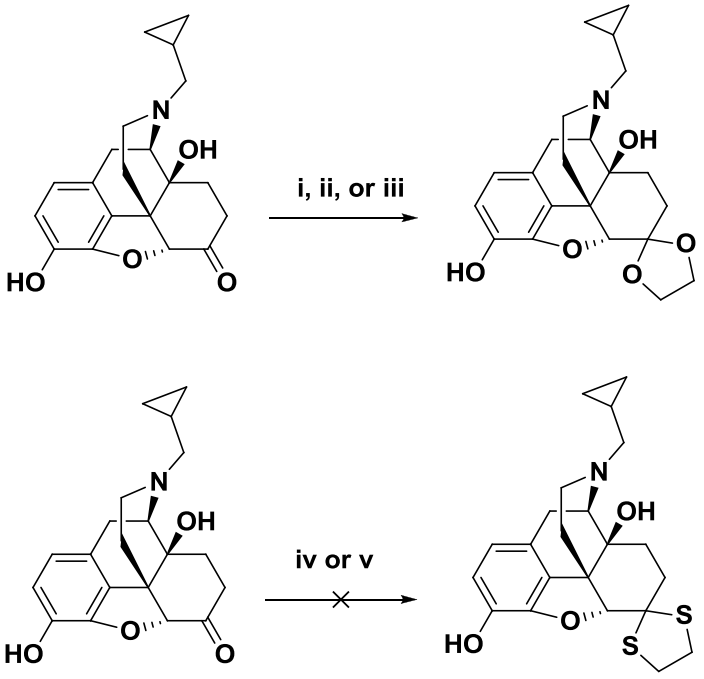

i. ethylene glycol / TsOH / Dean Stark apparatus / Toluene reflux
ii. ethylene glycol / TsOH / Dean Stark apparatus / Toluene reflux / trimethyl orthoformate
iii. BF_3 etherate / Dry THF / ethylene glycol
iv. BF_3 etherate / Dry THF / 1,2-ethanedithiol
v. $Cu(BF_4)_2 \bullet xH_2O$, 1,2-ethanedithiol, solvent free

Scheme 4.2 Synthesis of keto-protected NTX synthons.

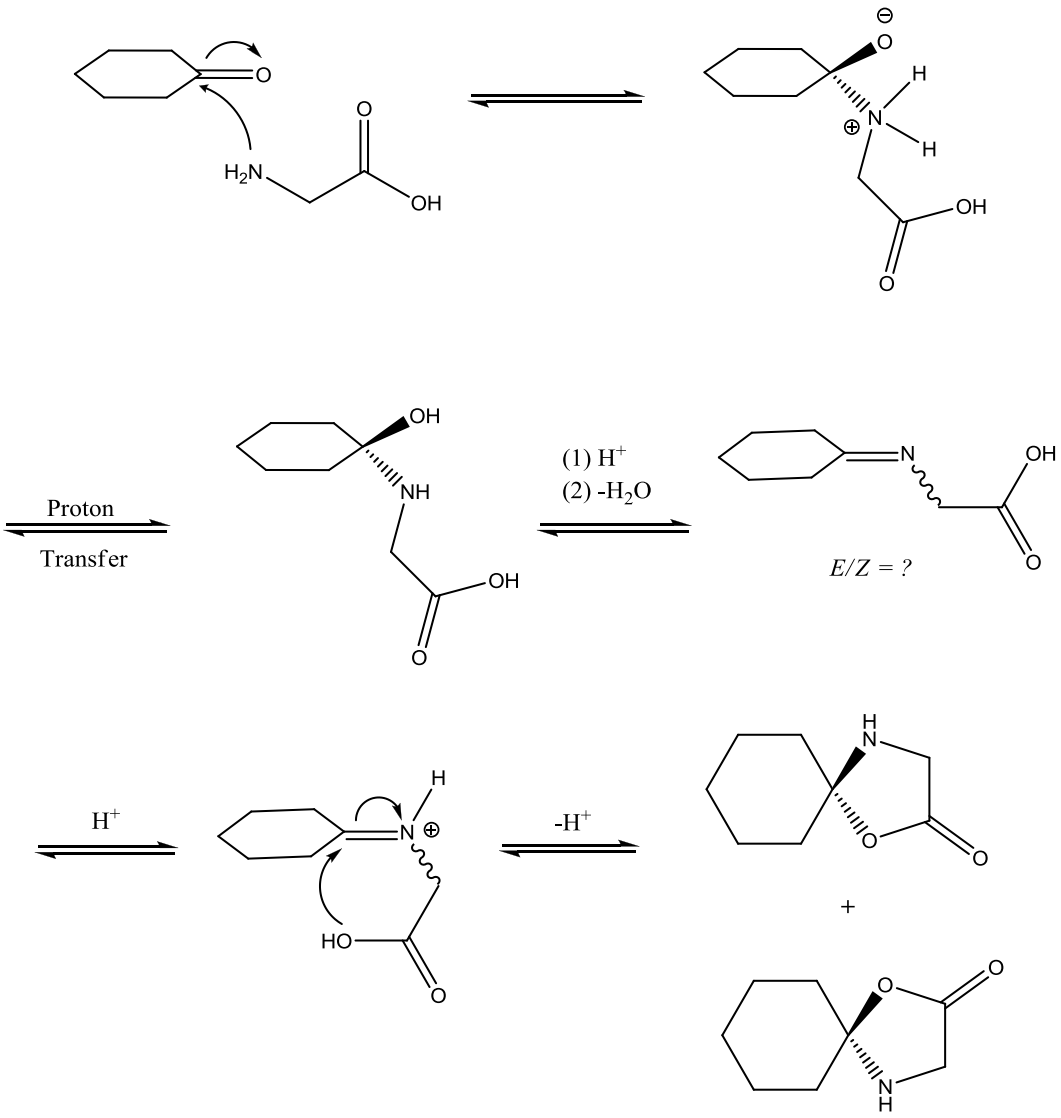

Scheme 4.3 Synthesis of 6-(1-oxa-4-azaspiro-glycinyl)-NTX.

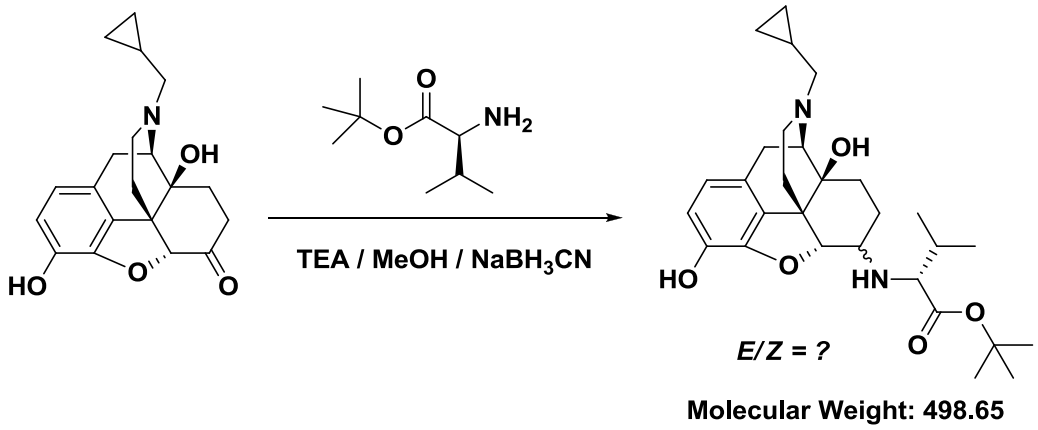

Scheme 4.4 Synthesis of 6-NH-Val-tBu-NTX.

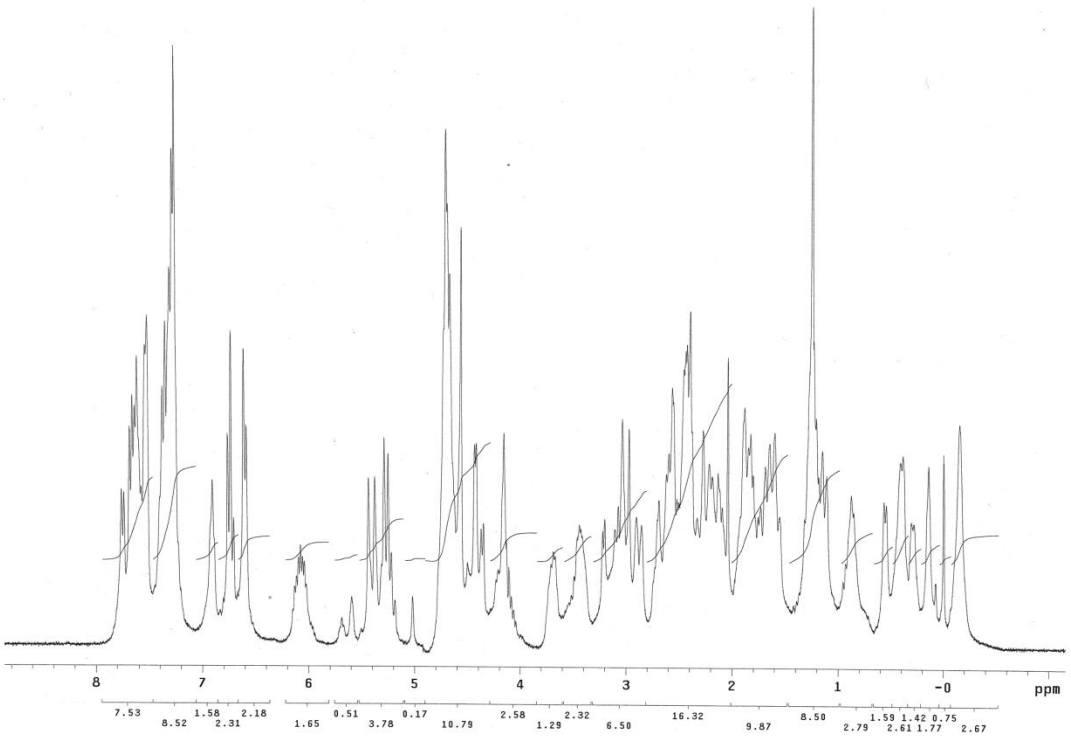

Figure 4.1 ^{1}H NMR spectrum of 3-*O*-allyl-14-*O*-Fmoc-β-Ala-NTX.

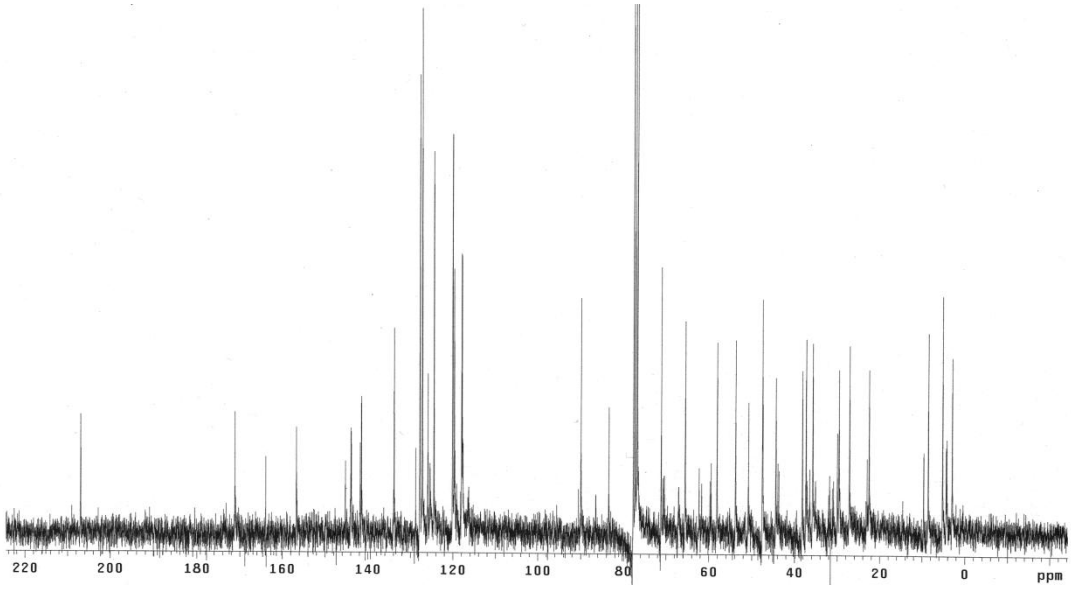

>41 unique carbons above the noise level

$C_{41}H_{42}N_2O_7$

Figure 4.2 ^{13}C NMR spectrum of 3-*O*-allyl-14-*O*-Fmoc-β-Ala-NTX.

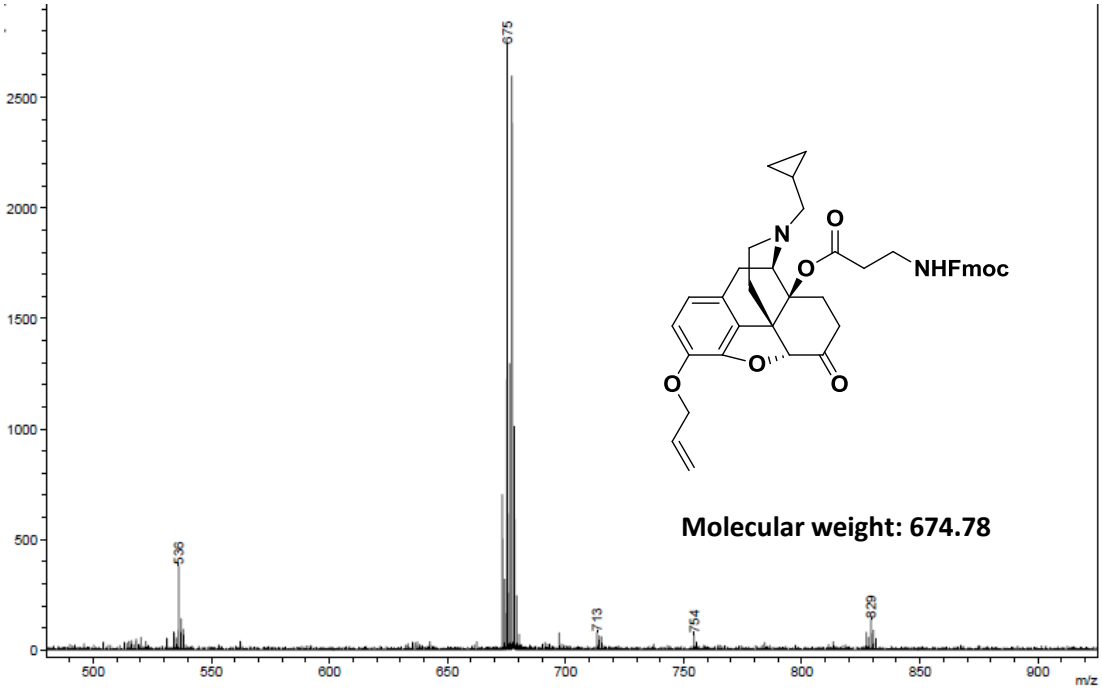

Figure 4.3 MALDI-TOFMS of 3-*O*-allyl-14-*O*-Fmoc-β-Ala-NTX.

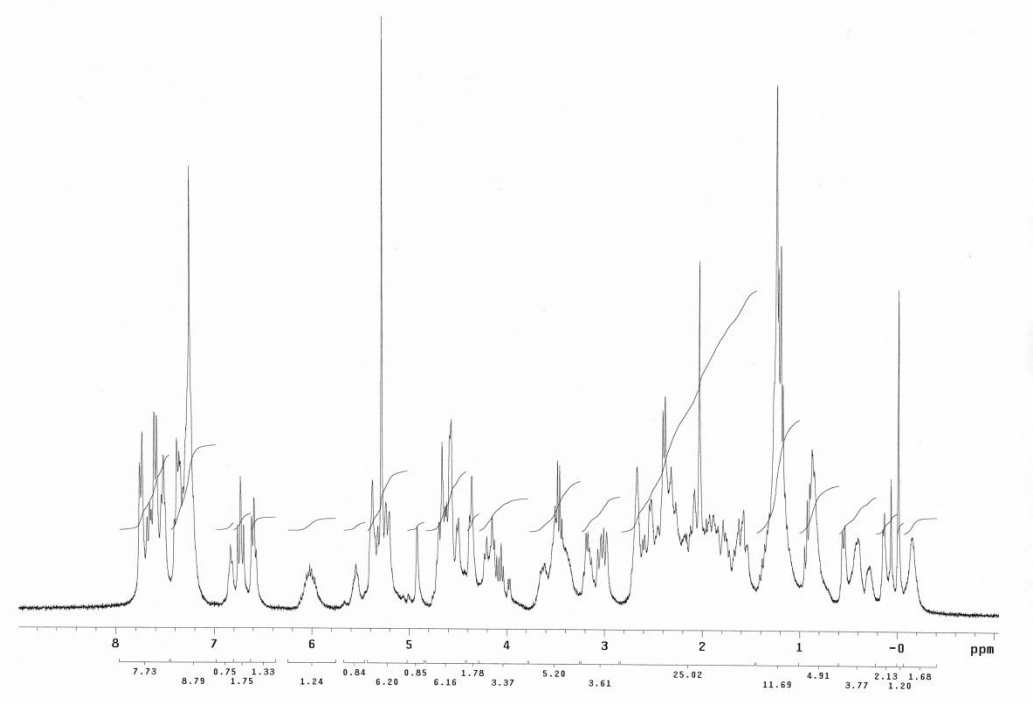

Figure 4.4 ^{1}H NMR spectrum of 3-*O*-allyl-6-O,14-*O*-bis-Fmoc-β-Ala-NTX.

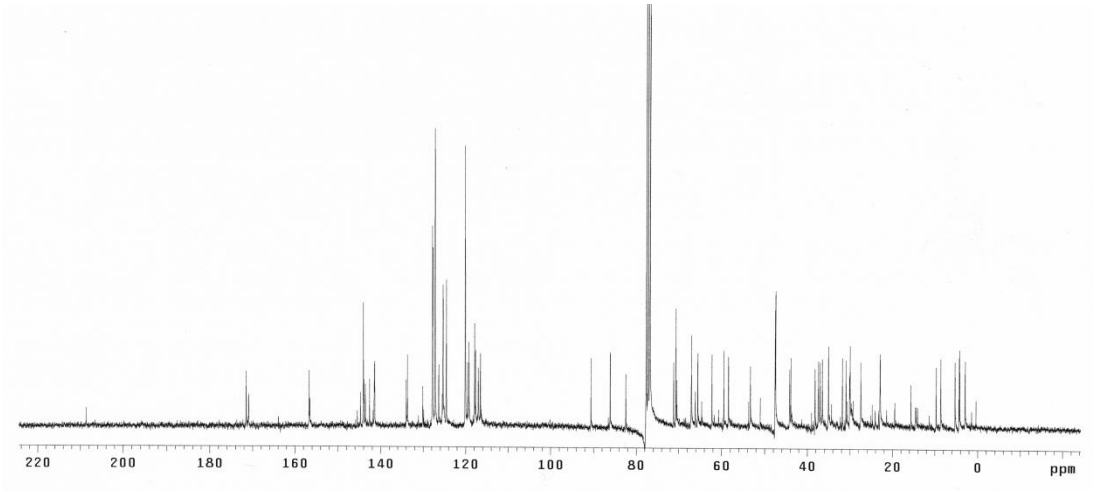

> 63 unique carbons above the noise level

$C_{59}H_{57}N_3O_{10}$

Figure 4.5 ^{13}C NMR spectrum of 3-*O*-allyl-6-O,14-*O*-bis-Fmoc-β-Ala-NTX.

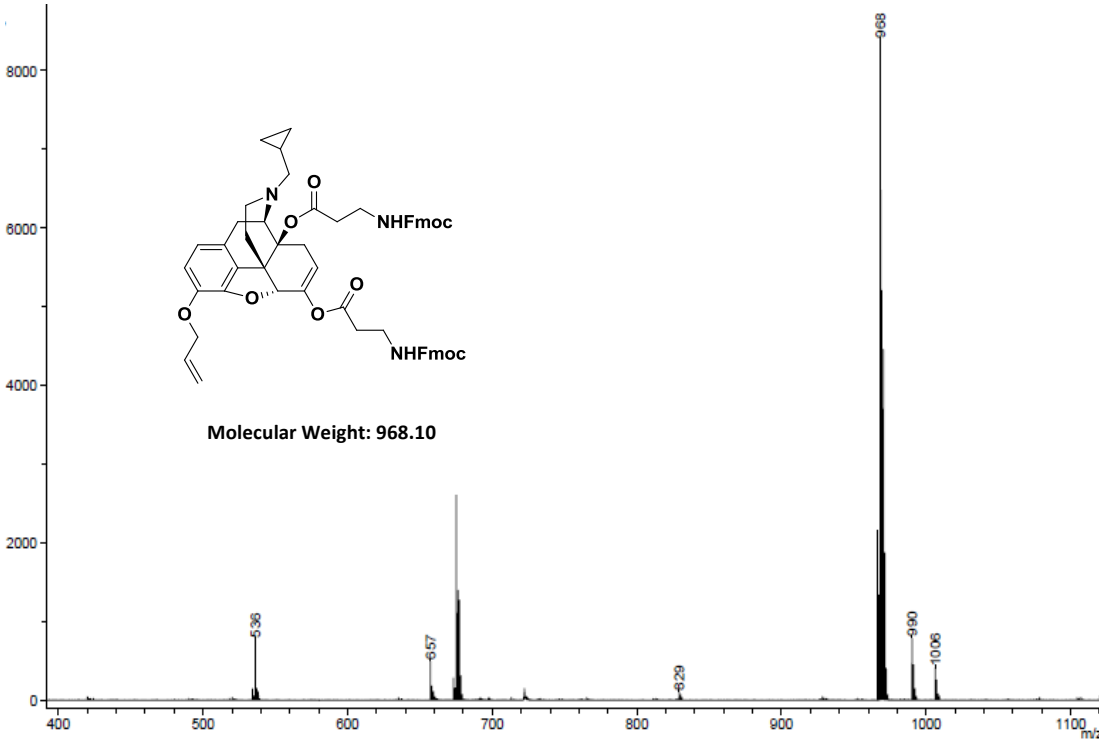

Figure 4.6 MALDI-TOFMS of 3-*O*-allyl-6-O,14-*O*-bis-Fmoc-β-Ala-NTX.

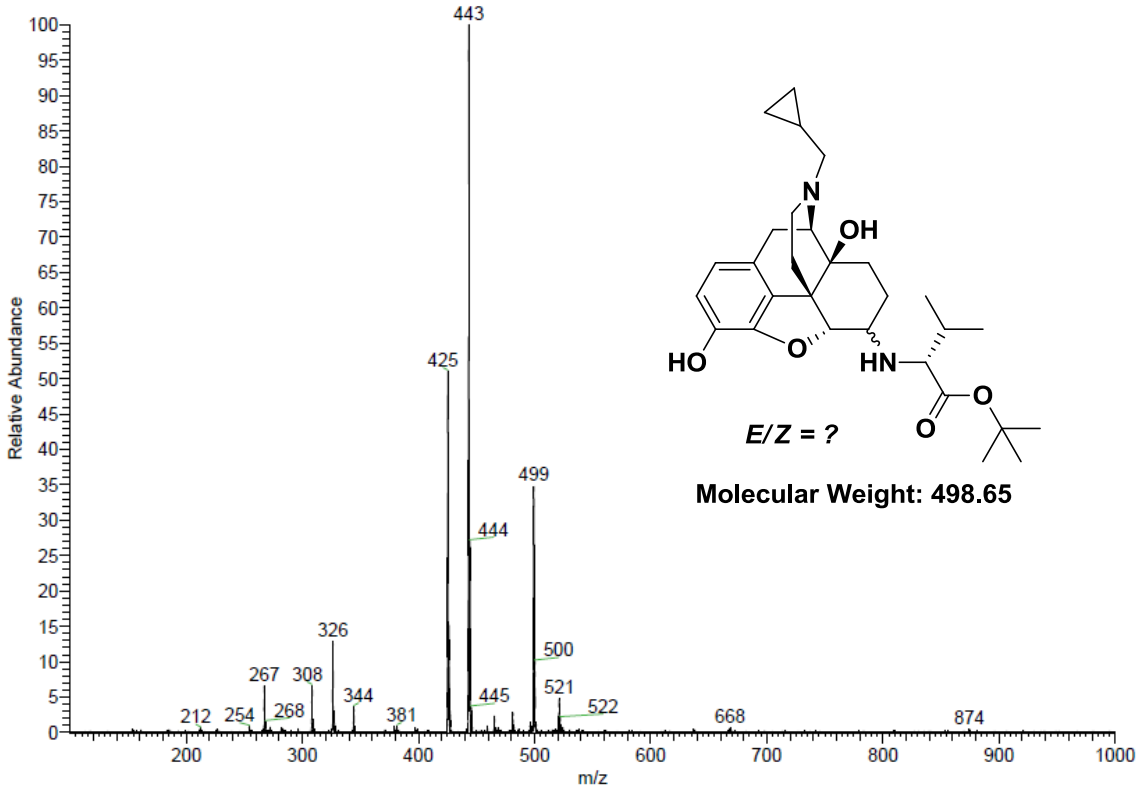

Figure 4.7 ESI-MS of 6-NH-Val-tBu-NTX.

Fig. 4.8 (a) ^{13}C NMR spectrum of Naltrexone ($CDCl_3$)

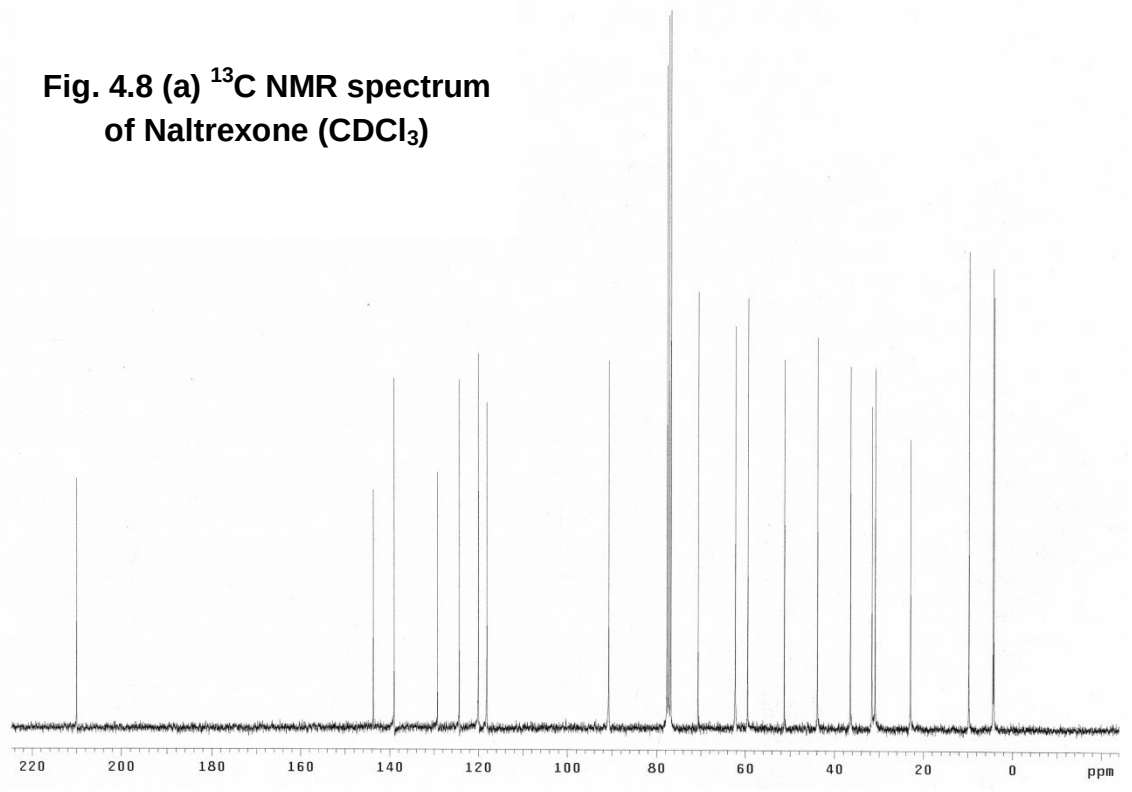

^{13}C NMR ($CDCl_3$) 300 MHz: δ 209.97 (C=O, 6-*O* ketone), 143.70, 139.00, 129.23, 124.31, 120.01, 118.09, 90.78, 70.68, 62.25, 59.49, 51.33, 43.94, 36.53, 31.67, 30.95, 22.97, 9.77, 4.43, 4.18 ppm.

Figure 4.8 Comparison of ^{13}C NMR spectral data obtained from Scheme 4.2.

Fig. 4.8 (b) ^{13}C NMR spectrum of Scheme 4.2 Conditions iii ($CDCl_3$)

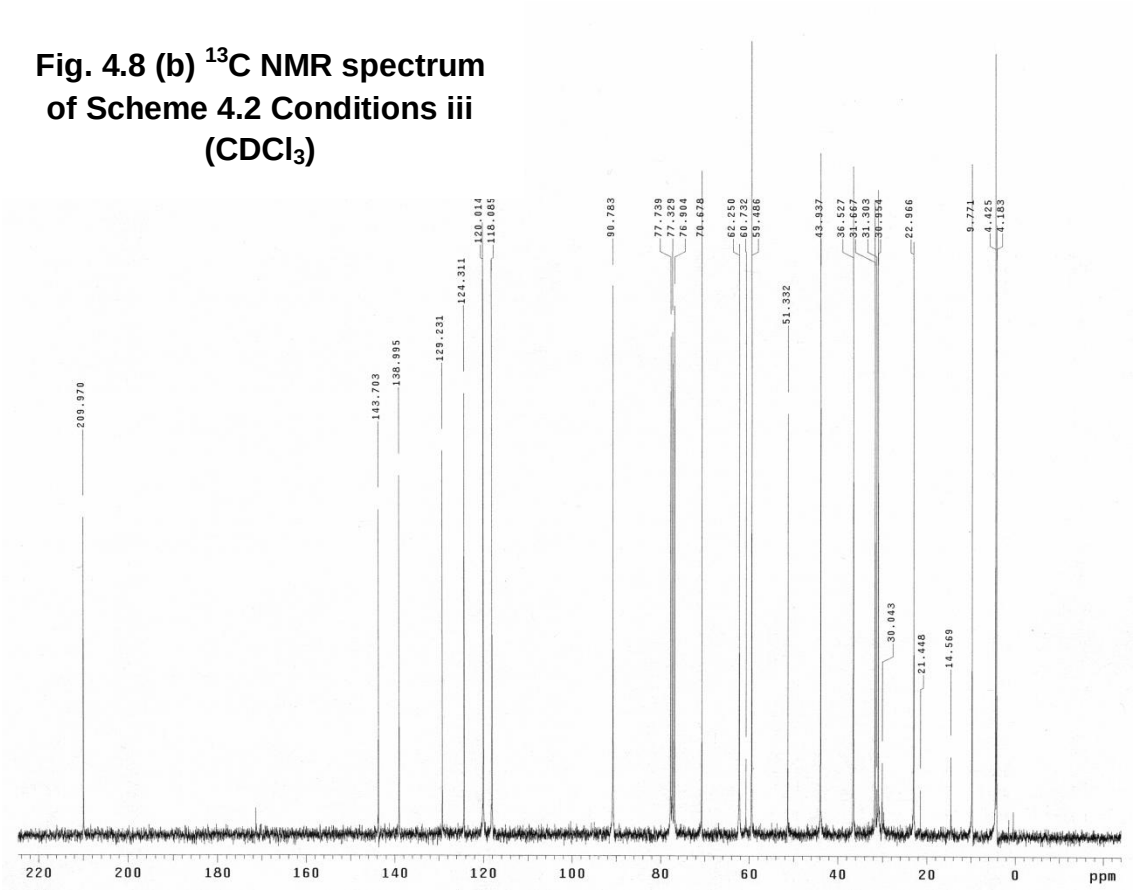

^{13}C NMR ($CDCl_3$) 300 MHz: δ 209.97 (C=O, 6-*O* ketone), 143.70, 139.00, 129.23, 124.31, 120.01, 118.09, 90.78, 70.68, 62.25, 59.49, 51.33, 43.94, 36.53, 31.67, 30.95, 22.97, 9.77, 4.43, 4.18 ppm. (Identical to NTX with some impurity peaks not associated with the expected hemiketal carbon @ ~ 120)

Figure 4.8 Comparison of ^{13}C NMR spectral data obtained from Scheme 4.2 (continued).

Fig. 4.8 (c) ^{13}C NMR of Scheme 4.2 Conditions i and ii ($CDCl_3$)

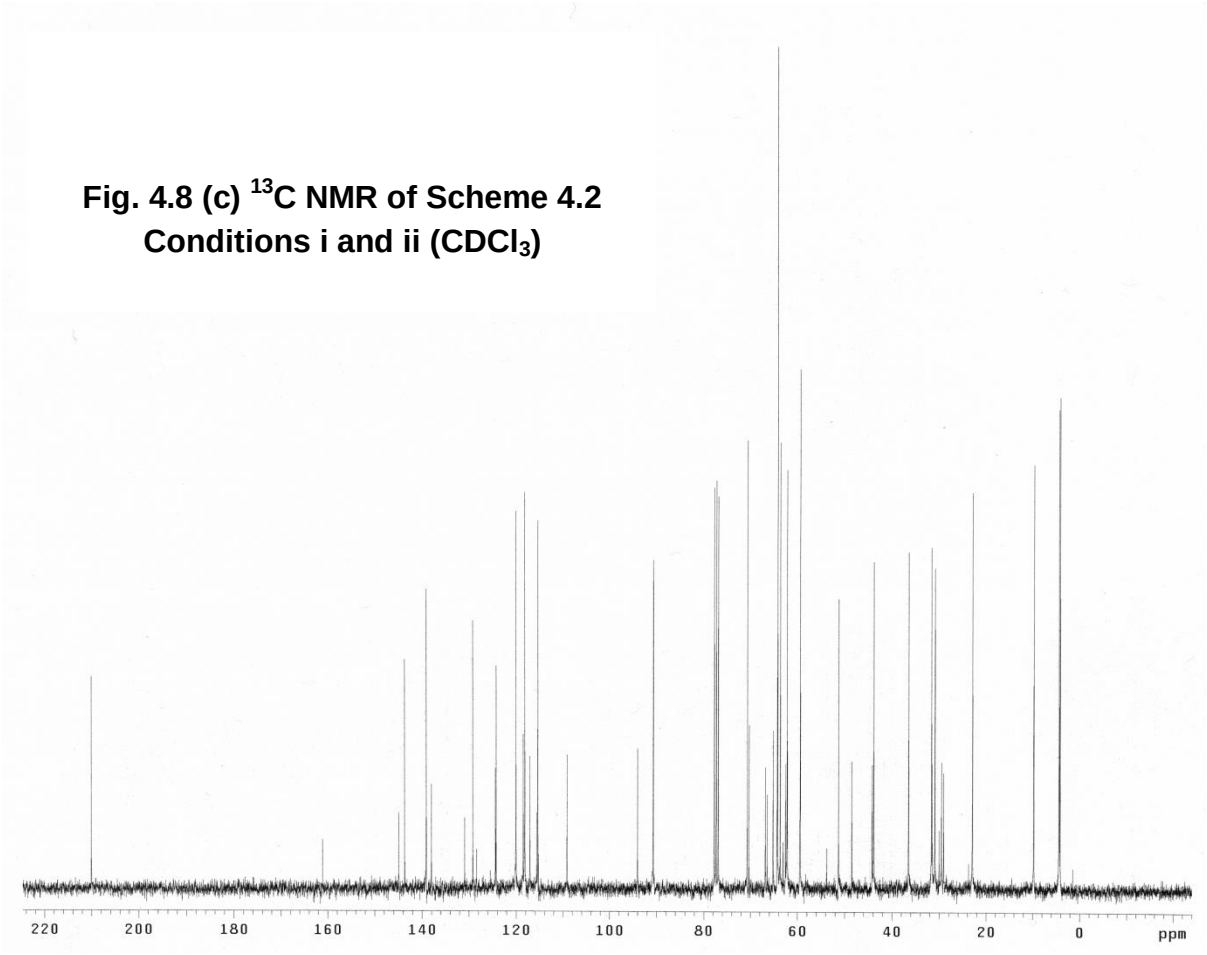

^{13}C NMR ($CDCl_3$) 300 MHz: δ 209.97 (C=O, 6-*O* ketone), 143.70, 139.00, 129.23, 124.31, 120.01, 118.09, 90.78, 70.68, 62.25, 59.49, 51.33, 43.94, 36.53, 31.67, 30.95, 22.97, 9.77, 4.43, 4.18 ppm. (NTX set) New Peaks: δ 209.97 (C=O, 6-*O* ketone) still present, several new peaks as expected in the range of 120-118 ppm (hemiketal carbon) and 65 ppm (methylenes of the dioxane ring).

Figure 4.8 Comparison of ^{13}C NMR spectral data obtained from Scheme 4.2 (continued).

Chapter 5

Synthesis of Codrugs of Naltrexone with Bupropion and (-)-Cytisine

Within the present study, a revisit was paid to the synthesis of a codrug of NTX and bupropion (BUP) (**Figure 5.1**). However, like the efforts before it (Hamad, Kiptoo et al. 2006), the synthesis of BUP-NTX was not successful under any conditions. Several attempts to form that compound will be discussed. The codrug that did come to fruition in this body of work is 3-*O*-(-)-cytisine-naltrexone (CYT-NTX), which is a secondary carbamate conjugate of (-)-cytisine (CYT) and NTX (**Figure 5.1**). Its preparation is discussed first.

5.1 (-)-Cytisine-NTX (CYT-NTX) carbamate as a codrug for oral delivery

Throughout the duration of this dissertation, microneedle-enhanced transdermal delivery has been the intended drug delivery system for all of the prodrugs that have been designed. CYT-NTX is a unique compound in the present body of work, because it is a codrug, and we evaluated it in an oral drug delivery paradigm. The stability studies of CYT-NTX are the subject of **Chapters 6 and 7**. The following discussion summarizes the synthesis of CYT-NTX.

5.2 Synthesis of CYT-NTX carbamate

Scheme 5.1 shows the synthesis of CYT- NTX (MW=557.64 g•mol^{-1}) that worked the best. The 3-*O*-PNP carbonate synthon of NTX was first prepared by Y.T. Reddy and given as a gift to attempt the synthesis, and TEA and DMAP bases were employed as proton mops. However, the 3-*O*-PNP-NTX synthon is very

difficult to purify completely due to its instability in solution, and its isolation later proved to be unnecessary. Despite the fact that CYT should be a really good nucleophile, the reaction did not really progress much over a temperature range from 0°C up to room temperature in dry DCM when CYT was reacted with 3-*O*-PNP-NTX in the presence of DMAP or TEA bases. Therefore, it was decided to use microwave chemistry with dry THF as a solvent.

The reaction was run in dry THF at 50 °C in a Biotage Initiator microwave reactor for ten minutes. 3-*O*-PNP-NTX was formed from NTX and 4-nitrophenylchloroformate *in situ* at 0 °C with DMAP and NTX in excess, and CYT was subsequently reacted directly in a one-pot procedure in the Biotage microwave reactor. The codrug product conveniently crashed out of solution under these conditions, and was isolated in 80% yield. All of the excess reagents could be washed away with cold THF and cold methanol washes. Unreacted NTX and CYT were recovered by washing with ether, and then they were isolated from each other by column chromatography. Regarding recovery of the desired product, the procedure thus described had the following advantages: (1) one-pot synthesis; (2) no chromatography, and (3) substantial yield. However, the caveat was that CYT-NTX formed under these conditions was actually not one compound. Rather, it appears as though a mixture of two geometric isomers was isolated (see spectral data discussion below). This was an expected result since CYT is an asymmetric secondary amine, and carbamate rotation about the amido bond is restricted, as is observed in amides. Some attempts were made to separate the compounds as individual isomers; however,

these attempts failed under a variety of conditions. Therefore, it is important that the reader understand that "CYT-NTX" refers to a mixture of geometric isomers, and not to one individual codrug molecule. It is noteworthy to mention that the small amount of CYT-NTX formed under non-microwave conditions was spectroscopically identical to CYT-NTX prepared by microwave assisted synthesis. Only the yields were different. Therefore, microwave synthesis did not affect the end products; rather, it greatly enhanced the amount of conversion of starting materials to CYT-NTX.

ESI-MS, HPLC, ^{1}H NMR, and ^{13}C NMR spectra of the final material are shown in **Figures 5.2 - 5.4**. A discussion about the data appears in the experimental section.

5.3 Attempted syntheses of BUP-NTX carbonate

From a drug design point of view, BUP-NTX (**Fig 5.1**) could be a desirable codrug molecule with the following properties: (1) equimolar delivery of two FDA-approved medications that can simultaneously treat alcohol and tobacco co-abuse following bioconversion; (2) physiochemical properties that allow transdermal delivery; and (3) a secondary carbamate linker that is likely to be formulation stable and cleavable *in vivo*. With regard to premise (3), these linkers often require hepatic metabolism to be cleaved *in vivo* (see **Chapter 7** on in vivo pharmacokinetics of CYT-NTX), so BUP-NTX may well be a potential oral delivery candidate as well.

Many attempts were made to prepare the BUP-NTX codrug that had originally been pursued in the PTD codrugs project (Hamad, Kiptoo et al. 2006). From the previous work, it had become obvious that phosgenation of the bupropion molecule, whether by enol trapping or *N*-conjugation, resulted in rapid 5-membered ring cyclization to form a cyclic enol carbamate intermediate (See **Figures 5.5 and 5.8**). In the series of reactions that were conducted by Hamad, it was also noted that attempts to phosgenate NTX to prepare a chloroformate synthon also failed and resulted in the formation of the "Gemini" NTX-NTX duplex codrug (Hammell, Hamad et al. 2004, Hamad, Kiptoo et al. 2006). In a new chapter of synthetic methodology, the 3-*O*-PNP-NTX carbonate synthon was developed in our labs, and it had proven to be useful in the synthesis of a variety of NTX prodrugs (Yerramreddy, Milewski et al. 2010). Before the microwave chemistry to afford CYT-NTX had been established, work had already been initiated to attempt to prepare an activated PNP carbamate synthon of BUP, or to simply react BUP with the already developed 3-*O*-PNP-NTX carbonate. Later, the same conditions that afforded CYT-NTX were attempted. With great misfortune, none of these methods eventually afforded the desired BUP-NTX carbamate prodrug. Nontheless, insights can be gained from the failed attempts to prepare this material, and they are included here as a significant portion of the work that was executed in our attempts to make codrugs of smoking cessation agents and NTX.

5.3.1 Attempt to prepare *N*-PNP-BUP carbamate.

Scheme 5.2 shows the conditions that were utilized to attempt the preparation of *N*-PNP-BUP carbamate. BUP•HCl salt was converted to its free base using the technique of Hamad et al (Hamad, Kiptoo et al. 2006). In working with BUP, one must always prepare the free base from the hydrochloride salt, because the free base is extremely labile to oxidation in air in just a very short while. The free base in solution has a considerably longer lifetime, especially when DCM is used as the solvent. Following recovery of the freebase, the material was immediately dissolved in dry DCM containing 1.5 eq. DMAP base, and the reaction flask was purged under argon to prevent degradation. The flask was also jacketed with aluminum foil since BUP is photosensitive as well. 1.1 equivalent of 4-nitrophenyl- chloroformate was added dropwise in DCM at 0 °C over the course of 10 minutes, and the reaction was allowed to stir for 15 minutes before checking the evolution of products by TLC. The TLC showed BUP as a prominent spot, and only a slight bit of any new products, so the reaction was continued and monitored over the course of several hours. The temperature was allowed to warm to room temperature, and the reaction was continued overnight. When the BUP had not been consumed by morning, an additional 0.5 eq. of the chloroformate was added, and the reaction mixture was brought to reflux under argon. BUP was never consumed under any of these conditions, so the reaction was stopped, and a sample was injected onto GC-MS for analysis of the product distribution. **Figures 5.5 – 5.9** show the GC chromatogram and the EI mass spectrum. It is very clear from the chromatogram and the identified peaks that

this approach has all the same problems as the previous phosgenation chemistry. BUP is very sluggish to react in the first place, and when it does, it forms the unwanted cyclized 2,4-oxazolidine material very rapidly. A second attempt at this reaction was done only at 0 °C to see if temperature would help solve the unwanted cyclization issue, since BUP is significantly sterically hindered. The results were identical. Another iteration of this reaction with no DMAP base was also conducted to see if enolate formation could be suppressed, but this afforded the exact same results as well. BUP activation was simply a failed route to the codrug. These results are not really surprising since five-membered intramolecular cyclizations of this type are kinetically favored.

5.3.2 Attempts to prepare BUP-NTX via 3-*O*-PNP-NTX carbonate

With evidence of prodrug formation via 3-*O*-PNP-NTX already well established at the time of these experiments, the next most logical route to pursue in an attempt to afford BUP-NTX was obvious. **Scheme 5.3** shows the next methods that were employed to prepare BUP-NTX. Reactions A and B used the same molar equivalents of reactants, but different reaction conditions. Reaction A was run at room temperature in THF for 24 hours and then refluxed for 5 hours when no spots on TLC indicated a new material other than NTX or 4-*p*-nitrophenol. Reaction B utilized microwave chemistry in THF since those conditions were known to afford CYT-NTX in good yield. However, BUP-NTX could not be formed under any of these conditions. Aliquots were submitted for ESI-MS, and the mass spectra are shown in **Figure 5.10** and **5.11**. In the case of reaction A, it appears that reflux in THF resulted in degradation of 3-*O*-PNP-NTX to NTX. No

mass for the desired product was observed (MW=607.14). Interestingly, Reaction B also resulted in degradation of 3-*O*-PNP-NTX, but the m/z = 709.5 major product happens to coincide with the mass of the NTX-NTX Gemini prodrug (MW=708.80) that was formed as an accidental side product in the original syntheses conducted by Hamad *et al* (Hamad, Kiptoo et al. 2006). This result is particularly interesting, because the CYT-NTX microwave chemistry did not result in the formation of the Gemini prodrug, which means that the secondary amine nucleophile CYT reacted with 3-*O*-PNP-NTX at a fast enough rate to suppress its degradation and subsequent reaction with released NTX. Bupropion is much more sterically hindered than CYT, and that was the reason why CYT was used to replace it in the first place. These data indicate that synthesis of the BUP-NTX codrug would require a very different strategy, such as building up the linker between NTX and *t*-butylamine before reacting with *m*-chloropropiophenone. Nonetheless, for the purposes of this body of work, BUP-NTX was not isolated under any conditions, and CYT-NTX proved to be a very interesting material to work with in *in vitro* and *in vivo* stability studies (**Chapters 6 and 7**).

5.4 Experimental Section

Materials: All reagents were purchased from Acros Organics or Sigma-Aldrich and were used without further purification. Naltrexone was obtained from Mallinckrodt-Covidien. (-)-Cytisine was purchased from Fisher via special order from Astatech. All solvents were dried and stored over molecular sieves prior to use.

NMR: All NMR spectra were obtained on a Varian 300 MHz or a Varian 500 mHz instrument. Line data and integral values for ^{1}H NMR were acquired with Mestrenova Lite (Mesterlab Research Chemistry Software Solutions, Escondido, CA) using 500 MHz spectra. ^{13}C NMR frequencies were obtained from Varian Mercury 300 MHz NMR software. TMS was used as an internal standard.

MS data: ESI-MS data were acquired by Dr. Jack Goodman at the University of Kentucky Mass Spectral Facility. EI-MS data were acquired on an Agilent 1100 series GC-MS instrument.

Synthesis of CYT-NTX codrug (geometric isomers)

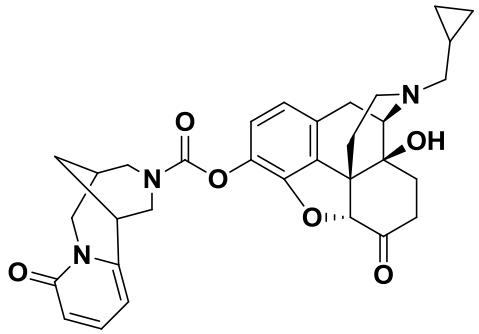

Chemical Formula: $C_{32}H_{35}N_3O_6$
Molecular Weight: 557.64

3-*O*-(4-nitrophenyl) NTX carbonate (3-*O*-PNP-NTX) was formed *in situ* for direct reaction with CYT. The solvent was dry THF. The reaction was designed to proceed in two separate stages with an overall one-pot goal. 50.0 mg of CYT would yield 146.56 mg of CYT-NTX codrug for testing, assuming 100% yield, and the equivalents of other reagents were designed around that amount of CYT. 3-*O*-PNP-NTX was formed at 0 °C by dissolving NTX (107.7 mg, 1.2 Eq.) and DMAP (38.5 mg, 1.2 Eq.) in a 5.0 mL microwave reactor vial containing dry THF.

In a separate dry vial, 4-nitrophenlychloroformate (52.9 mg, 1.0 Eq.) was dissolved in dry THF under argon, and this solution was added to the microwave vial containing NTX and DMAP with dropwise addition and heavy stirring over the course of 5 minutes under argon. After the spot for 4-nitrophenylchloroformate appeared to be consumed on TLC (10 minutes), the vial septum was removed, and 50.0 mg CYT (1.0 Eq.) was charged to the reaction vial. The vial was then sealed with a microwave reaction cap to hold pressure, and the reaction solution was irradiated for 10 minutes at 50 °C with a Biotage Initiator EXP-US microwave reactor. The solvent volume was approximately 4.0 mL.

Reaction progress was visibly detectable by the brilliant yellow color of the liberated 4-nitrophenol in solution and the codrug product precipitated as a fine white amorphous solid. The precipitate was washed with 3 x10 mL cold THF followed by 3 x10 mL cold methanol and analyzed by TLC as only one spot. The material yield after drying was (117.2 mg, 80%). The material was analyzed by Electrospray Ionization Mass Spectroscopy, ^{1}H NMR and ^{13}C NMR spectrometry, and HPLC. NMR spectral data suggested the presence of two unique isomers of CYT-NTX.

^{1}H NMR ($CDCl_3$) 500 MHz:

δ 7.30 – 7.37 (m, ~2H [overlap with CDCl3 in peak portion from 7.2 -7.3]), 6.75 (d, *J*=5 Hz, 1H), 6.41 – 6.64 (m, 4H) 6.32 (d, *J*=5 Hz, 1H), 6.04-6.15 (m, 2H), 4.65 – 4.72 (m, 2H) 4.28 – 4.58 (m, 4H), 4.20 (d, *J*=10 Hz, 1H), 3.85 – 3.98 (m, 2H), 3.23 – 3.43 (m, 2H), 2.94 – 3.24 (m, 11H), 2.63 – 2.71 (dd, 2H), 2.50 – 2.60

(m, 4H, looks like dd with overlap), 2.34 – 2.54 (m, 6H), 2.24 – 2.32 (m, 2H), 1.98 – 2.17 (m, 7H), 1.80 – 1.91 (m, 2H), 1.43 – 1.65 (m, 5H), 0.80 – 0.92 (m, 2H), 0.51 – 0.61 (m, 4H), 0.11 – 0.18 (m, 4H) ppm.

^{13}C NMR ($CDCl_3$) 300 MHz:

δ 208.24, 163.49, 152.95, 148.99, 148.62, 148.02, 139.15, 139.04, 138.86, 133.05, 129.90, 129.67, 123,26, 119.52, 117.62, 105.67, 90.77, 70.30, 68.23, 68.10, 59.38, 53.76, 52.48, 51.74, 51.30, 50.89, 50.74, 49.61, 49.25, 43.99, 36.44, 35.00, 31.63, 30.69, 30.02, 27.83, 27.39, 26.27, 26.02, 25.95, 23.38, 9.45, 4.548, 4.17 ppm.

ESI-MS: m/z 558

Discussion of spectral data

An HPLC analytical method was developed to separate the codrug product from NTX and CYT. Using the method described in **Chapter 6,** it can be seen in **Figure 5.3 (A) & (B)** that the product gave a clean peak for codrug, and no CYT or NTX was detected. NTXOL was not an issue in this synthesis, and it only appears in **Figure 5.3 (A)** because the method was designed to also separate NTXOL in case we pursued a CYT-NTXOL codrug in the future. The ESI-MS spectrum shown in **Figure 5.2** also suggests that the product gave a clean mass profile with the expected m/z for CYT-NTX. However, NMR spectral data are much more information rich than either the HPLC or the MS data, and it is clear from the ^{1}H NMR spectrum of the isolated codrug material that a single CYT-NTX codrug was not obtained by this synthesis. This is particularly obvious in the

phenyl region of the spectrum, where complex multiplets emerge due to the different magnetic environments of the phenyl protons on the NTX and the CYT moieties. Indeed, the proton spectrum is very complex, and multiple multiplets are seen throughout the entire field. This type of complexity suggests an isomeric mixture of products in the CYT-NTX sample, in particular since the CYT moiety is an asymmetric secondary amine, and amide-like linkers (such as the secondary carbamate in CYT-NTX) have restricted rotation about the carbonyl C-N bond. Since there is an opportunity for CYT to attack 3-*O*-PNP-NTX by a variety of vectors, it may be expected that geometric isomerism is possible in the product.

^{13}C NMR spectral analysis also confirms that the material isolated in this synthesis cannot be a single isomer of CYT-NTX. There are 44 individual peaks that can be discerned from background noise when the spectrum is expanded and the frequencies are assigned (see **Figure 5.4 A** for a peak-expanded view of the spectrum after 30 minute acquisition time and **Figure 5.4 B** for the unexpanded spectrum from overnight acquisition). The molecular formula for CYT-NTX is $C_{32}H_{35}N_3O_6$, and each of the 32 carbons should be magnetically unique. If one CYT-NTX isomer is described by $C_{32}H_{35}N_3O_6$, and another CYT-NTX isomer is identical except for rotation of the CYT moiety with 11 carbons, it is reasonable to assume that $C_{32} + C_{11} = C_{43}$ unique carbons may appear in the ^{13}C NMR spectrum. Here we see C_{44}, which may mean the carbonyl carbon is also showing magnetic inequivalence.

Returning to proton spectra, if one assumes two compounds are present and assigns one methylene set of the cyclopropyl peaks the normalized integral value of 4.00 for 4 protons (would be 2H for a single isomer) and then analyzes the proton data with 500 MHz NMR and Mestrenova software, 70 protons are accounted for. Two isomers of CYT-NTX would have 70 protons. Therefore, ^{1}H NMR data are also consistent with the assumption that there appear to be two unique compounds present in the CYT-NTX sample. Furthermore, the ratio of isomers appears to be 1:1. Solvent peaks were not included in these analyses.

HPLC analysis showed one peak for the codrug under a variety of conditions using the following stationary phases: Zorbax C18, Apollo C18, Kinetex PFP, and phenyl. TLC analyses also indicated a single spot under various conditions. All of the reagents employed in the synthesis also contained chromophores that could be detected by the HPLC analytical method that was employed. Geometric isomers can generally be separated by chromatography, although this may not be an easy task, since the two structures are very similar. Attempts to observe two peaks for the product utilizing a more selective Cyclobond 2000 chiral column also failed. Since we could not successfully separate CYT-NTX isomers for individual study, we decided to pursue the isomeric mixture in our stability and PK studies that are detailed in **Chapters 6 and 7**. For simplicity, “CYT-NTX” is referred to in this dissertation, but the reader should note that CYT-NTX is really a mixture of two unique geometric isomers, as evidenced by NMR spectrometry.

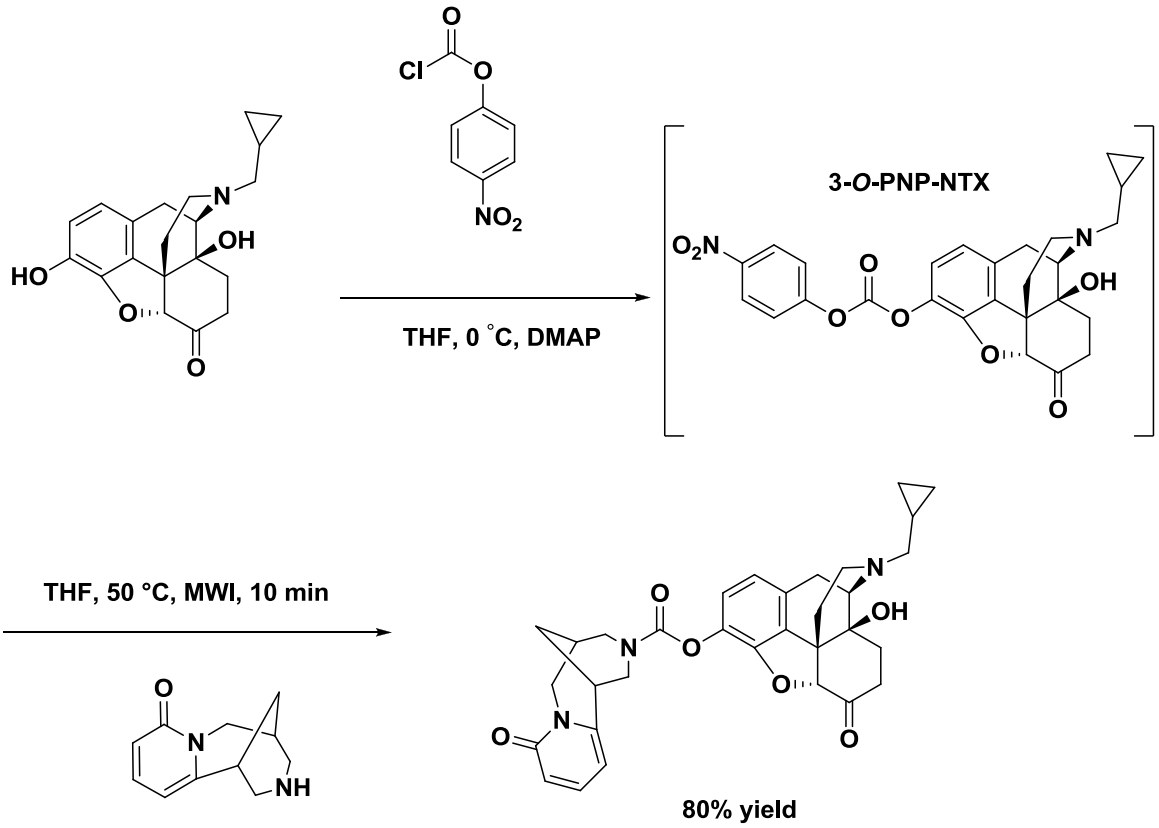

Scheme 5.1 One-pot synthesis of CYT-NTX via microwave chemistry.

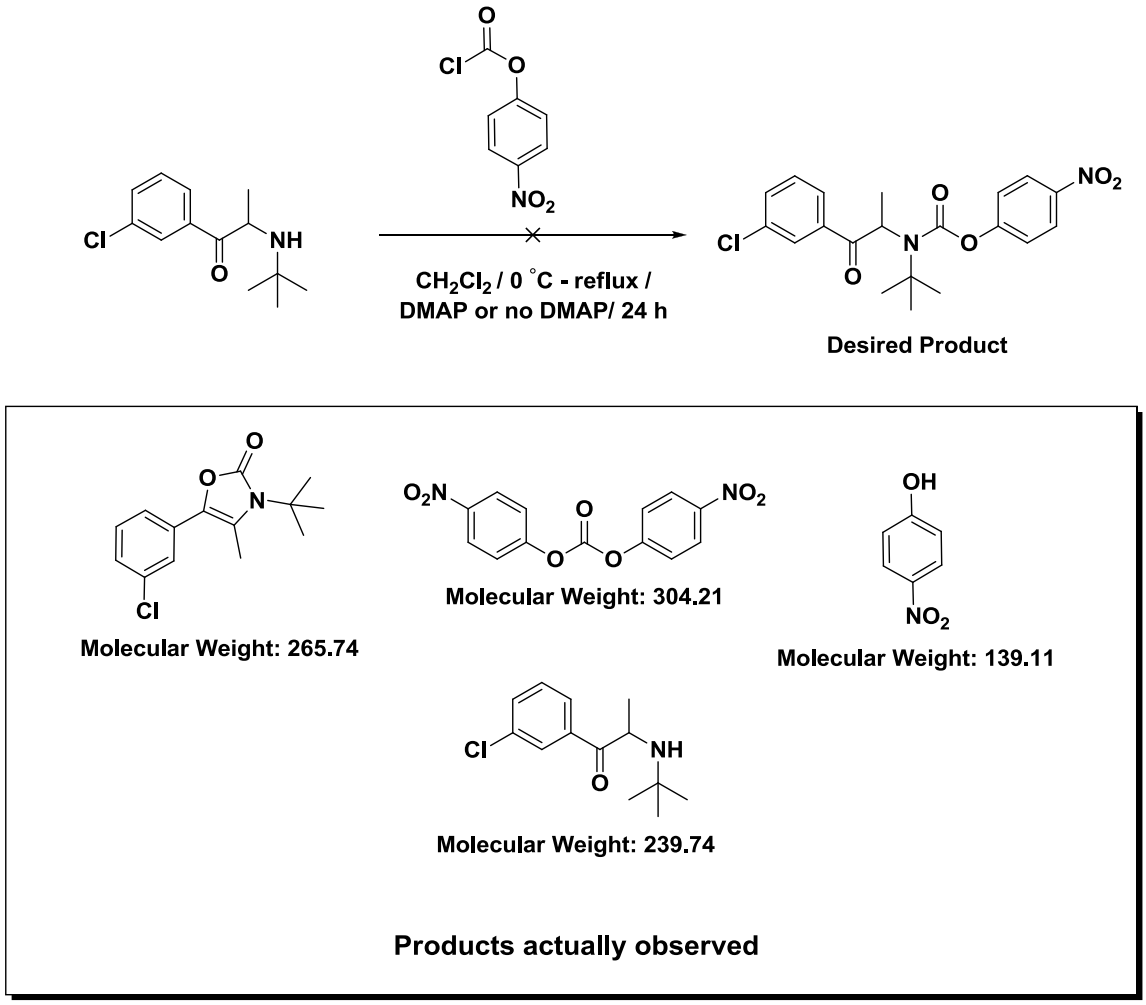

Scheme 5.2 Attempted synthesis of *N*-PNP-BUP carbamate synthon.

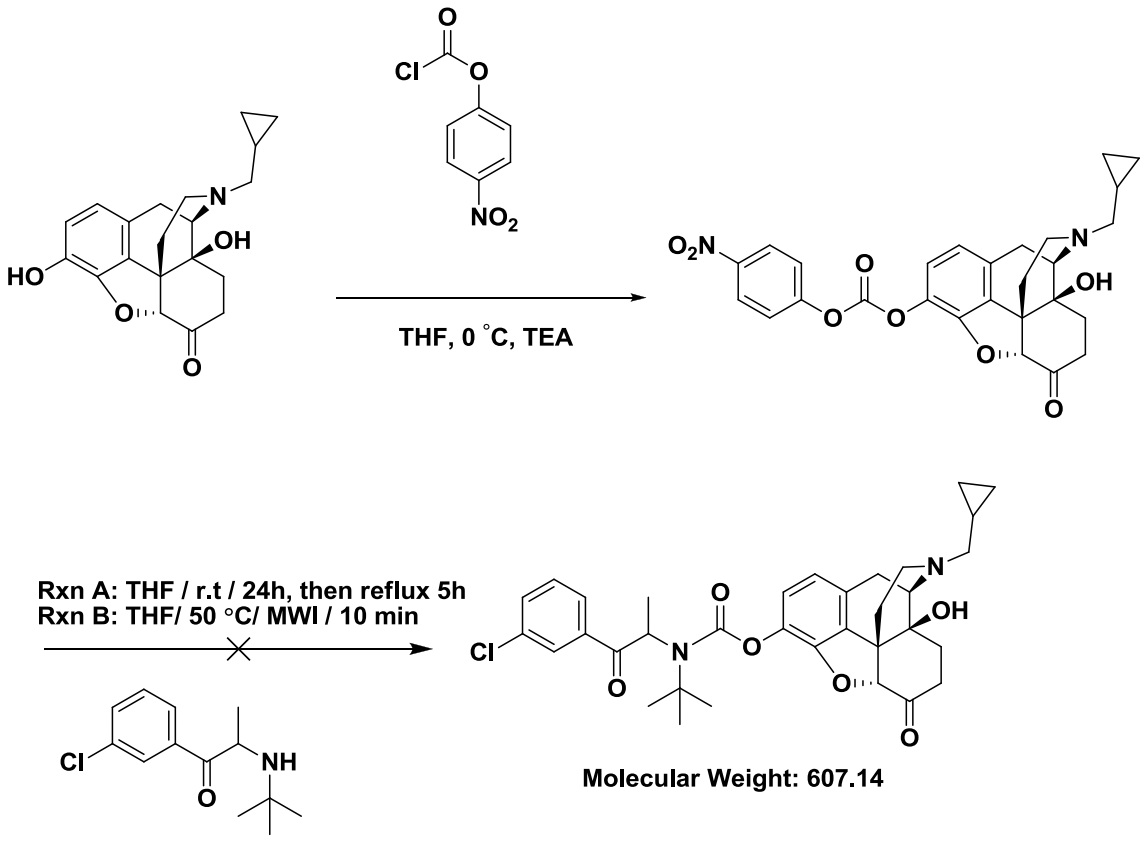

Scheme 5.3 Attempted synthesis of BUP-NTX via 3-*O*-PNP-NTX carbonate.

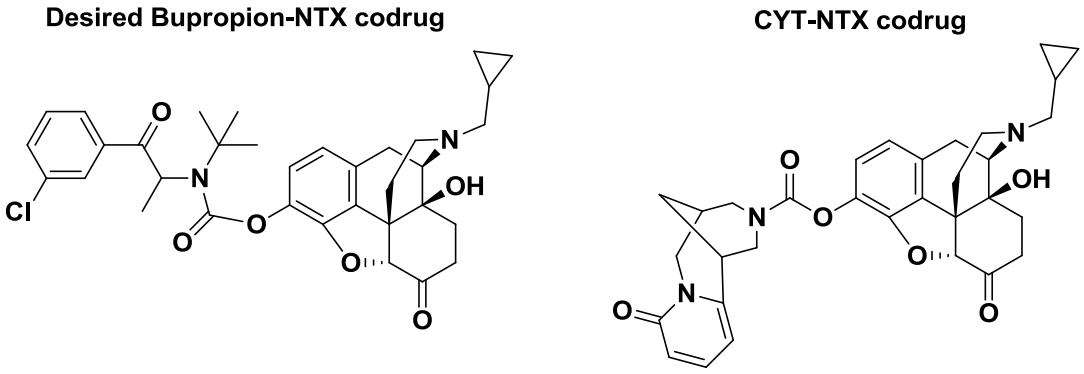

Figure 5.1 Codrug structures.

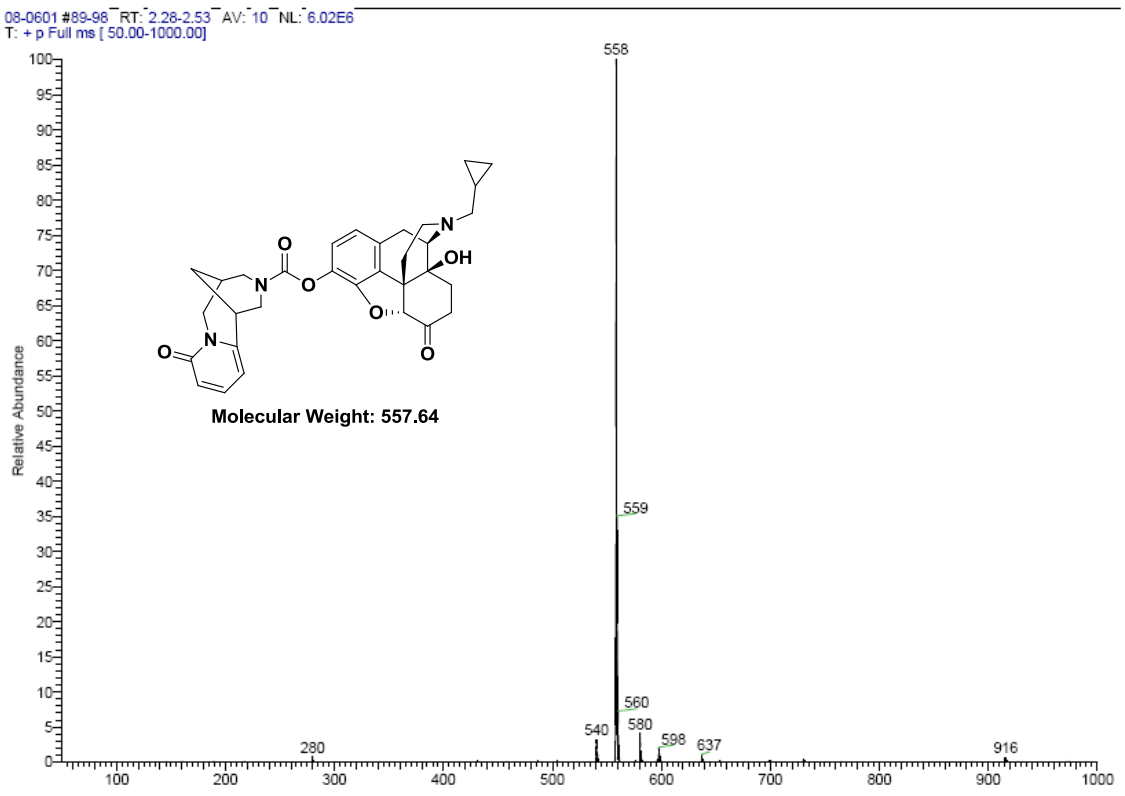

Figure 5.2 ESI-MS of 3-*O*-(-)-cytisine naltrexone (CYT-NTX) carbamate.

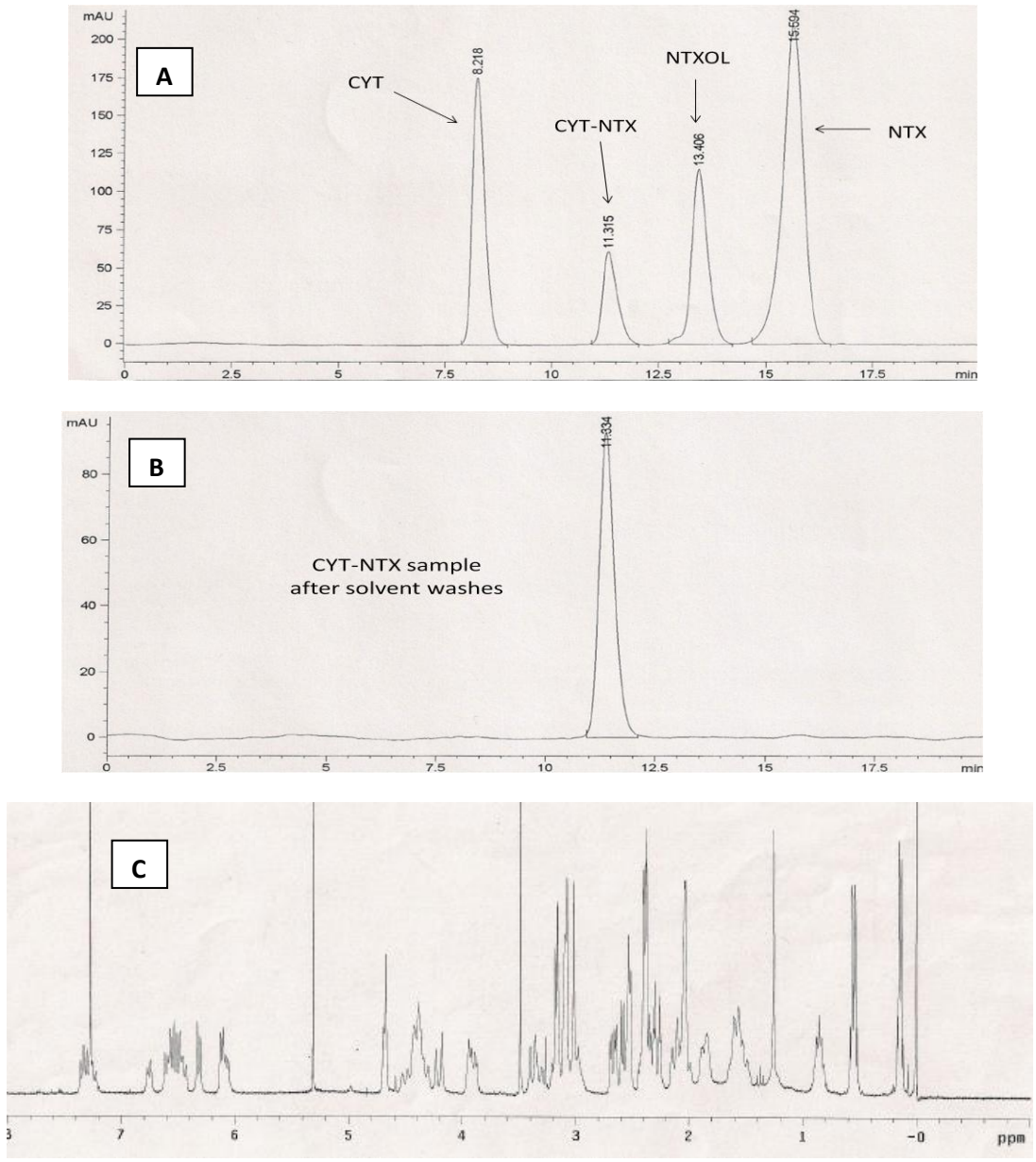

Figure 5.3 (A) HPLC chromatogram of CYT, CYT-NTX, NTXOL and NTX. (B) Clean chromatogram of CYT-NTX after solvent washes with THF and MeOH. (C) ^{1}H NMR spectrum of CYT-NTX after solvent washes with THF and MeOH *(solvent peaks: MeOH δ 1.22, 3.5 ppm; DCM δ 5.3 ppm; $CDCl_3$ δ 7.26 ppm)*.

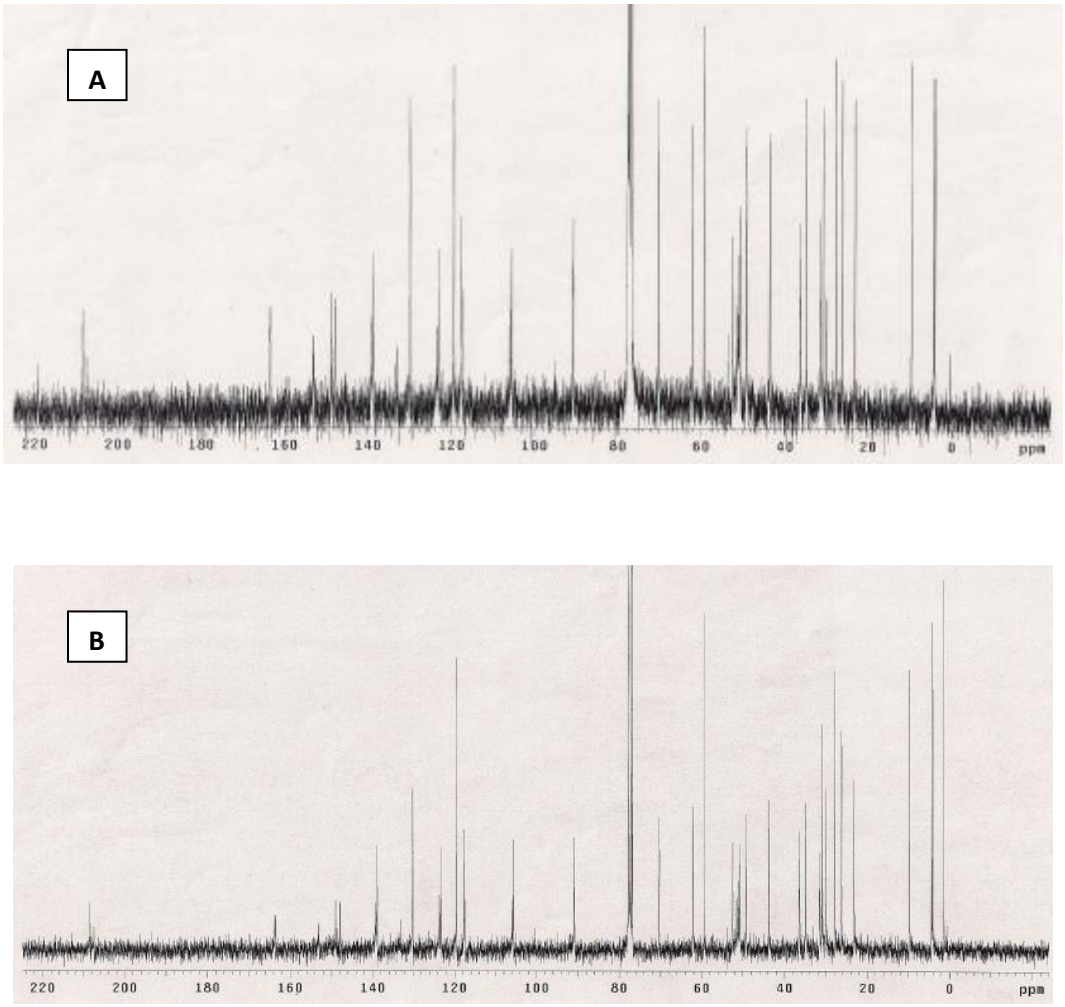

Figure 5.4 (A) ^{13}C NMR spectrum of CYT-NTX (expanded view). (B) ^{13}C NMR spectrum of CYT-NTX with overnight acquisition time and no peak expansion *(CDCl$_3$ triplet δ 77.2 ppm is cut off to emphasize product peaks)*.

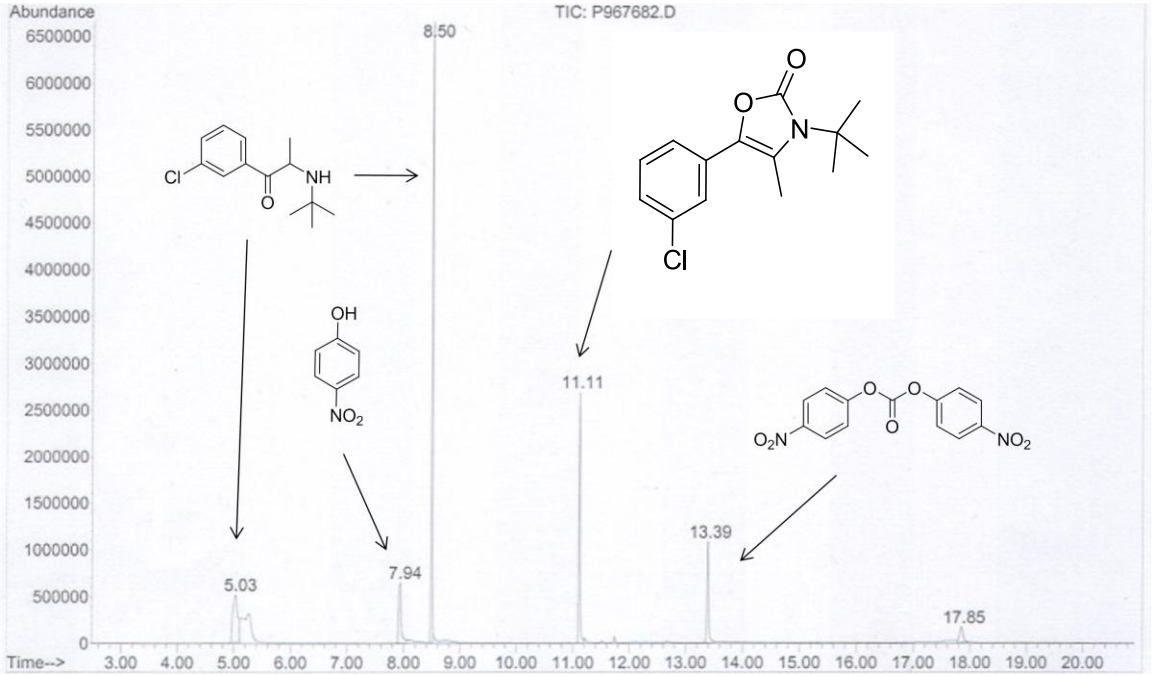

Figure 5.5 GC-MS of the *N*-PNP-BUP-carbamate synthesis.

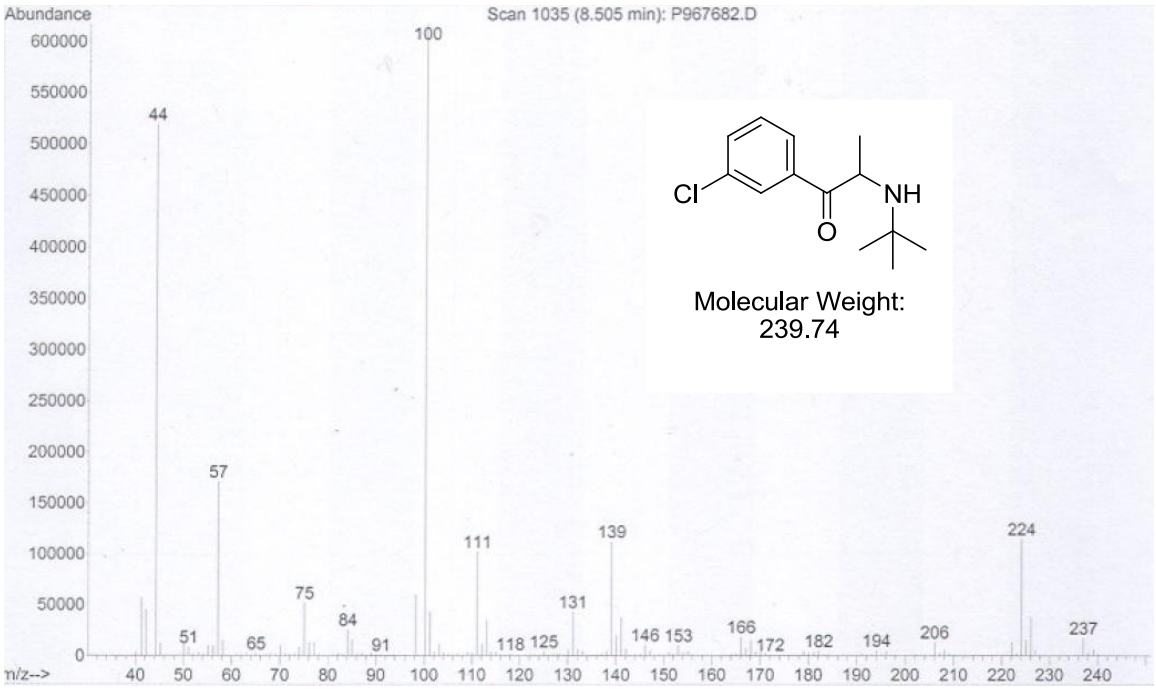

Figure 5.6 EI-MS of bupropion.

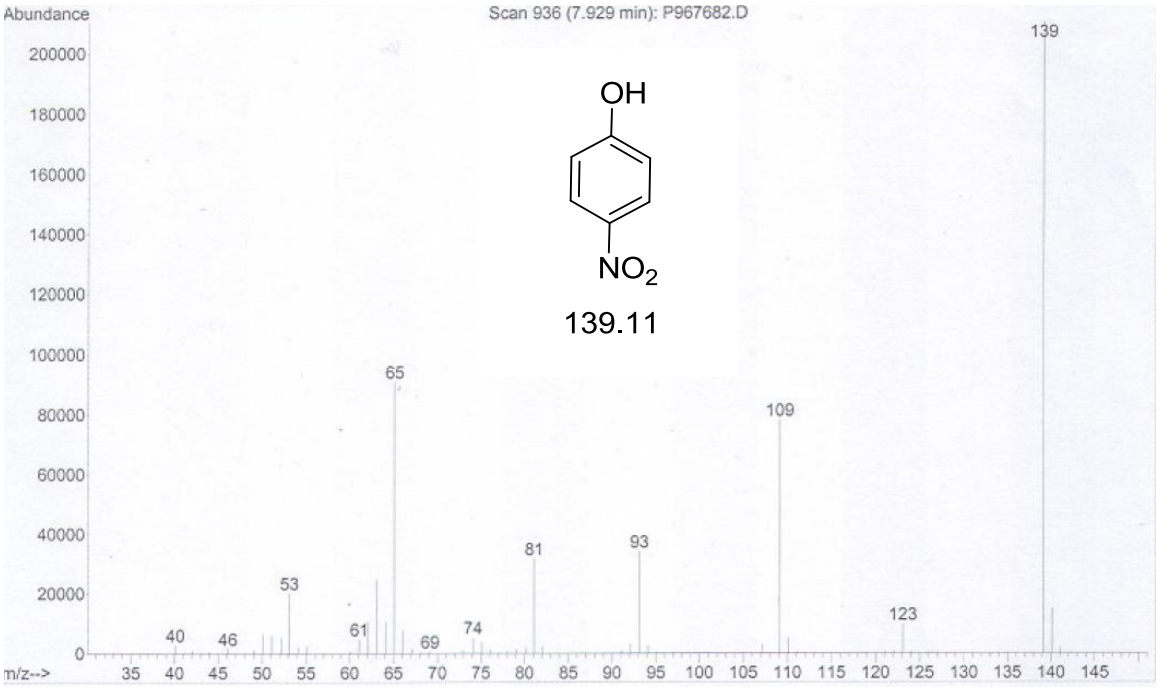

Figure 5.7 EI-MS of *p*-nitrophenol.

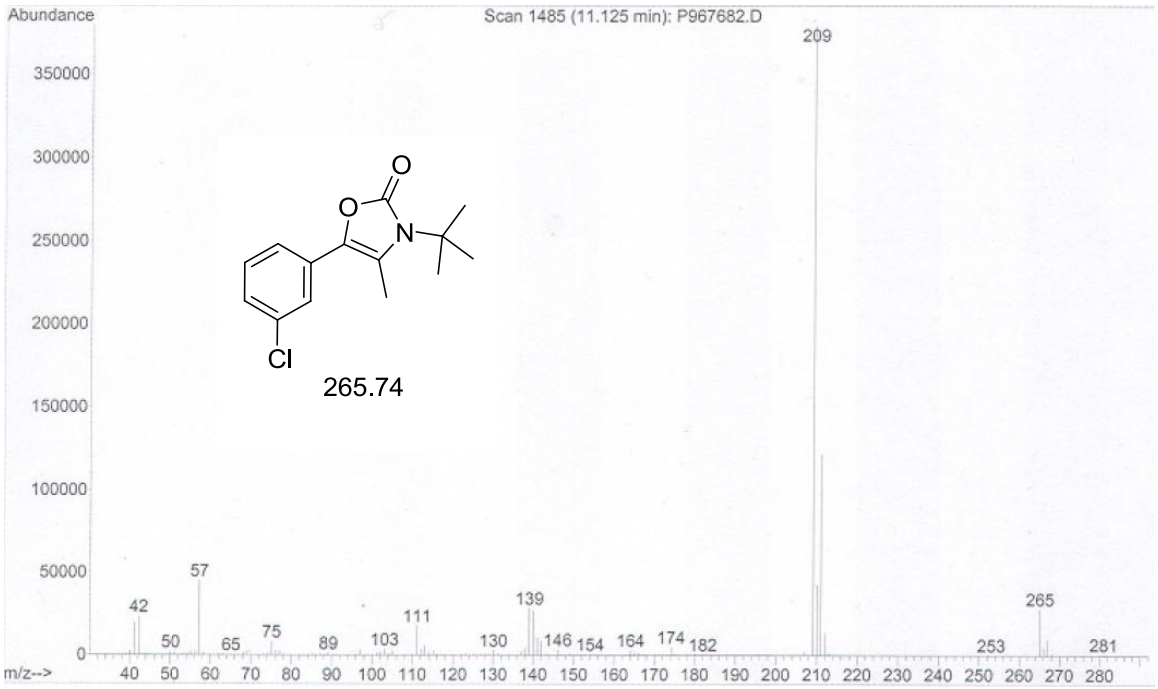

Figure 5.8 EI-MS of 3-*tert*-butyl-5-(3-chlorophenyl)-4-methyl-oxazolidin-2-one.

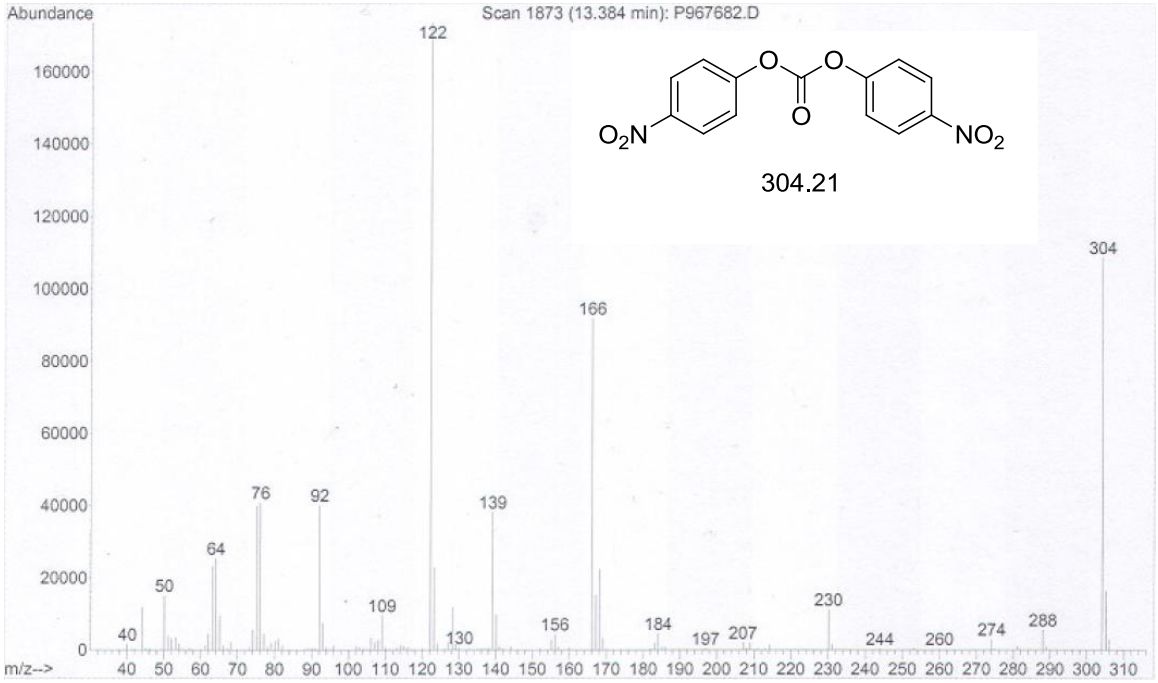

Figure 5.9 EI-MS of *p*-nitrophenol gemini carbonate.

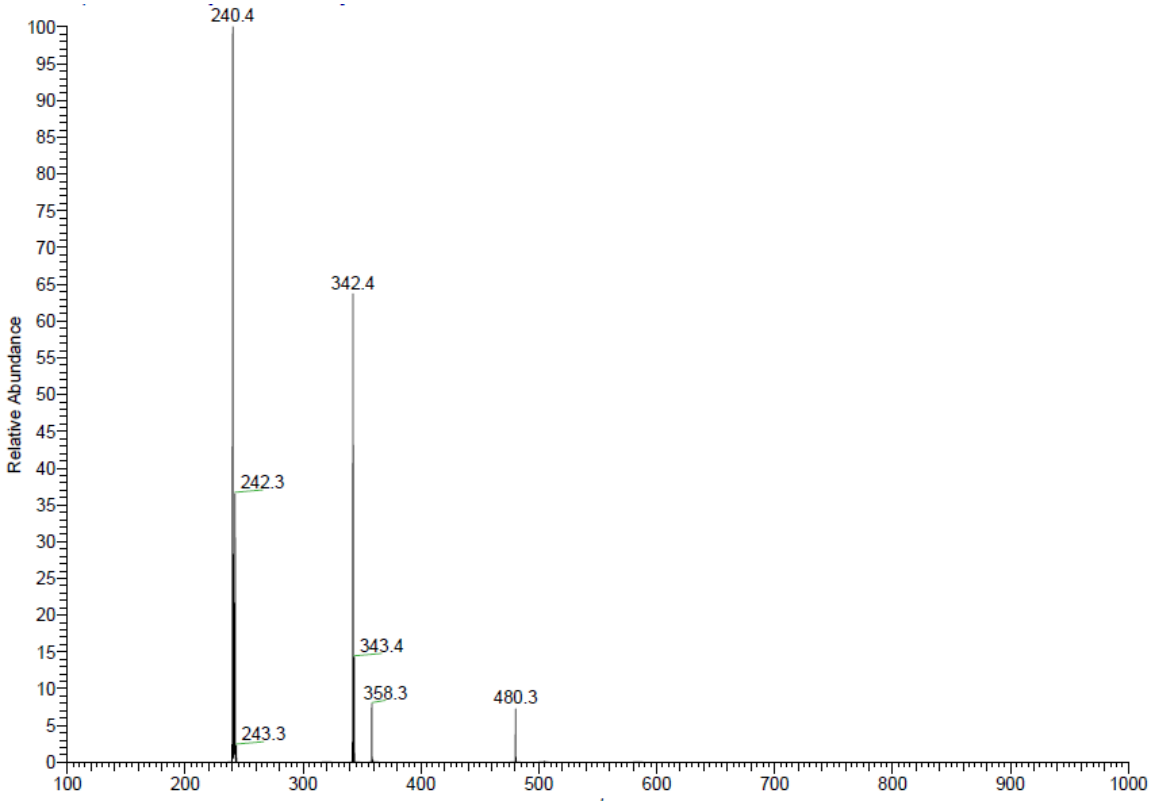

Figure 5.10 ESI-MS of BUP and NTX (failed reflux in THF).

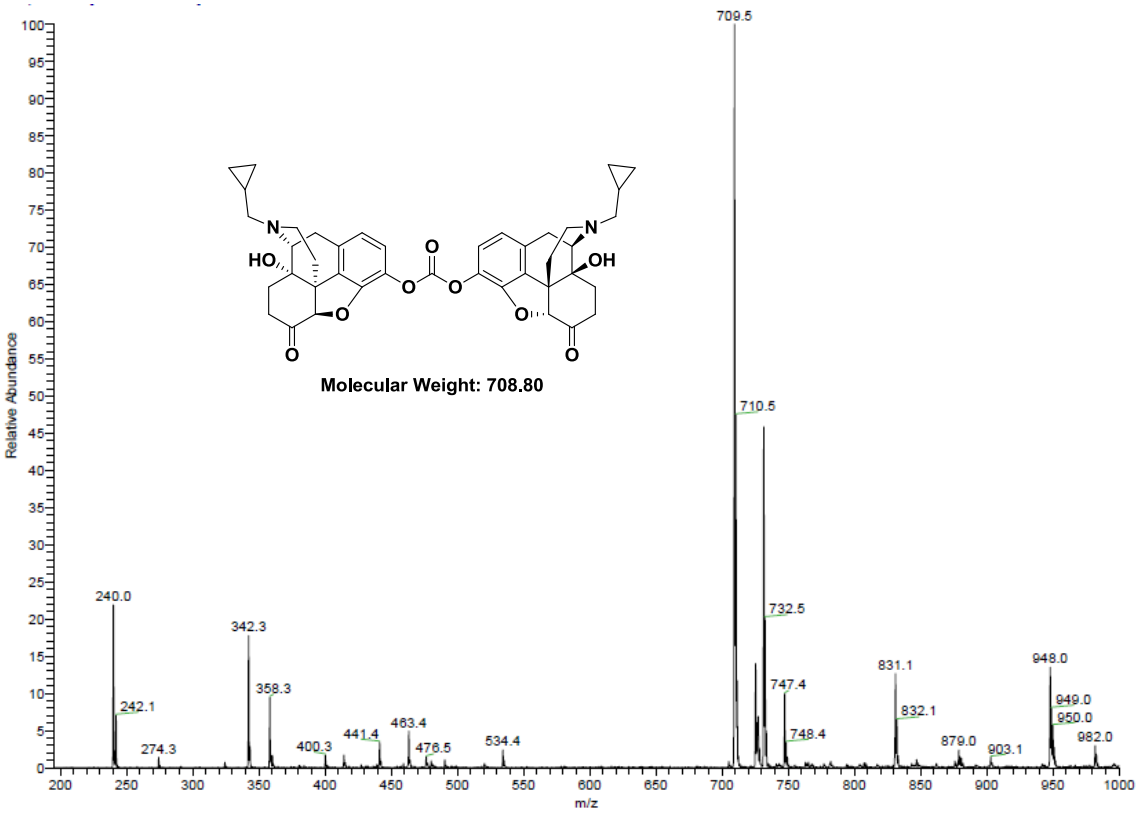

Figure 5.11 ESI-MS of NTX-NTX Gemini prodrug, the major product from microwave chemistry.

Chapter 6

In vitro stability studies of the prodrugs

6.1 Introduction

In order to assess the candidacy of our amino acid ester prodrugs for MNTD, several stability criteria needed to be met. For instance, a prodrug intended for percutaneous delivery through aqueous microchannels should be able to demonstrate adequate stability at skin-relevant pH and temperature over the time course of a skin diffusion experiment (t_{90} ≥ 48 hours @ pH 5.0 and 32°C). Also, prodrugs intended for this purpose should be readily hydrolyzed at physiological pH and temperature, or in the presence of human plasma at appropriate body temperature (pH 7.4 and 37°C). Rapid hydrolysis at pH 7.4 with or without enzymatic assistance is desired for two reasons. First, rapid hydrolysis ensures that parent drug is systemically available following skin transport. Second, it has been shown that extensive prodrug bioconversion in viable skin facilitates NTX and NTXOL transdermal flux enhancements (see **Chapter 1** for references). Therefore, all of the prodrugs that were synthesized in **Chapters 2 & 3** were assayed for MNTD candidacy by answering the following stability questions with HPLC-UV analyses:

- Is the prodrug stable enough for skin diffusion studies in 0.3 M acetate buffer (pH 5.0 & 32°C) with t_{90} ≥ 48 hours?

- Using 25mM HEPES-buffered Hanks' balanced salt solution or 50% Dulbecco's phosphate–buffered saline (PBS), is prodrug stability at pH 7.4 and 37°C less than that observed at pH 5.0 and 32°C?
- Does prodrug stability in 50% human plasma suggest that the prodrug will rapidly hydrolyze to parent drug and promoiety in the biophase?

The stability story for CYT-NTX turned out to lead us in a different drug delivery direction than MNTD after certain critical data were obtained. Initial assessment of codrug stability at pH 5.0 and 7.4 demonstrated that the codrug was not labile to hydrolysis. Initial qualitative assays of codrug in the presence of 100% human plasma also showed no peaks for parent drugs, and no apparent reduction in the area of the codrug peak (37 °C x 4 days, data not shown). Therefore, it was determined that CYT-NTX may need first-pass metabolism to hydrolyze the secondary carbamate linker in its structure. Evidence to support that hypothesis is presented in **Chapter 7.** With these data in hand, we decided to undertake a full stability analysis of CYT-NTX in an oral drug delivery paradigm. Therefore CYT-NTX required different analyses than the MNTD prodrug series.

A codrug or prodrug intended for oral delivery must demonstrate stability under a broader scope of conditions. For instance, a compound ingested orally must first encounter the environment of the stomach, which can vary in pH from about pH 1 to 2 in a fasted state. Additionally, the stomach contains a milieu of enzymes that can hydrolyze labile linker moieties. Following exposure to these conditions,

an orally ingested compound encounters pH 4 to 5 in the beginning of the small intestine and pH 7 to 9 in the small intestine and colon. There are also different enzymes present throughout the small intestine and colon. Expounding even further, a compound that is absorbed into the systemic circulation encounters a new environment of about pH 7.4 with a new host of widely variegated enzymes that can bind a molecule and increase its rate of hydrolysis dramatically. So it is clear that a broad range of stability analyses are necessary to assess the candidacy of a compound for oral delivery. In that regard, we tested CYT-NTX in the following *in vitro* hydrolysis media to determine if this codrug should be advanced to *in vivo* studies in the live Sprague-Dawley (S-D) rat:

- Chemical buffer systems of pH 1.5, 5.0, 7.4 & 9.0 (37 °C)
- Simulated Gastric Fluid (SGF, USP, 37 °C)
- Simulated Intestinal Fluid (SIF, USP, 37 °C)
- 80% rat plasma (37 °C)
- 80% human plasma (37 °C)

SGF contains pepsin and SIF contains pancreatin. These features set the simulated fluids apart from the chemical buffers that have no enzymatic activity. 80% human plasma (HP) was used in comparison to 80% rat plasma (RP) to investigate any interspecies differences between humans, for which the codrug would be intended clinically, and S-D rats, for which *in vivo* studies would be conducted to see if the codrug hydrolyzed in a living animal model.

6.2 Kinetics of hydrolysis in aqueous solutions (non-enzymatic)

Amino acid prodrugs

Buffer stability studies of the amino acid prodrugs at pH 5.0 and pH 7.4 were conducted by Mikolaj Milewski in Audra Stinchcomb's lab, with the exception of 6-*O*-Ile-NTXOL whose stability at pH 7.4 was done by the author in Dr. Crooks' lab. Therefore, 6-*O*-Ile-NTXOL stability at pH 7.4 is summarized separately.

Prodrug stability studies in donor (0.3M acetate buffer, pH 5.0) and receiver solution (25mM HEPES-buffered Hanks' balanced salt solution, pH 7.4) were initiated by charging a 10ml volume of hydrolysis media thermostated at 32 °C (pH 5.0 samples) and 37 °C (pH 7.4 samples) with ≈ 1.0 mg of prodrug. The suspension was then filtered through a 0.45µm nylon syringe filter (Acrodisc® Premium 25mm Syringe Filter). Aliquots were withdrawn, and the filtrates were collected over a period of approximately 3 half lives. Samples were then diluted with ACN-water 70:30 (v/v) for HPLC analysis. All amino acid ester prodrug hydrolysis studies showed pseudo-first-order kinetic behavior. Apparent pseudo-first-order hydrolysis rate constants (K_{app}) were estimated from the slope of the log-transformed amount of prodrug remaining in the medium. All stability studies were carried out in duplicate (n=2). **Table 6.2** summarizes the stability data as acquired by Milewski (unpublished).

6-*O*-Ile-NTXOL

A stock solution of 0.75 mg/mL (1.6 mM) prodrug was prepared in DMSO. A stock internal standard (IS) solution of salicylamide (0.076 mg/mL, 0.55 mM) in methanol containing 0.04% heptafluorobuyric acid ion pairing agent (HFBA) was also prepared. Reactions were initiated by adding 40.0 µL of the prodrug stock solution to 760.0 µL of a pre-warmed (37±0.5 °C) solution of 50% PBS (initial reaction concentration of 0.038 mg/mL, 82 µM). The initial reaction concentration was within the linear range of the standard curve, and more concentrated reactions were impossible due to extensive prodrug precipitation at higher levels. Sampling over the course of time was done by the following method. 50.0 µL aliquots of the reaction mixture were removed at pre-determined time points. 50.0 µL of internal standard solution and 50.0 µL of blank 0.04% HFBA in methanol were added to the reaction mixture aliquots in low volume inserts, and the solutions were vortexed. Samples were immediately injected on the HPLC column and analyzed. The data are summarized in **Table 6.2**.

CYT-NTX

All stability studies of the CYT-NTX codrug were conducted by the author in Dr. Crooks' lab. The codrug was challenged at 37±0.5 °C in four different pH environments (pH 1.5, 5.0, 7.4, & 9.0). Stability studies were conducted using a 0.2 M hydrochloric acid buffer (pH 1.5); a 0.2 M phosphate buffer (pH 7.4); a 0.2 M phosphate buffer (pH 5.0); and a 0.2 M boric acid and potassium chloride buffer (pH 9.0). Reactions were initiated by adding 5.0 mL of a 1.00 mM stock

codrug solution in THF to 5.0 mL of the appropriate thermostated (37±0.5 ^{o}C) aqueous buffer solution. Aliquots (455.0 µL) were taken at various time intervals, mixed with 45.0 µL of 10.0 mM internal standard solution (*N*-1-naphthylacetamide in THF) and analyzed by HPLC. The data are summarized in **Table 6.3**.

6.3 Kinetics of hydrolysis in human plasma and/or rat plasma

Amino acid prodrugs

All stability studies of the amino acid prodrugs in enzymatic media were conducted by the author in Dr. Crooks' lab. Stock solutions of prodrugs were prepared in DMSO. The stock concentrations were 0.75 mg/mL (1.6 mM) 6-*O*-Ile-NTXOL, 1.0 mg/mL (2.3 mM) 6-*O*-Val-NTXOL, and 3.0 mg/mL (7.2 mM) 6-*O*-β-Ala-NTXOL in DMSO (*see the discussion section for an explanation why the same reaction concentrations could not be used*). A stock internal standard (IS) solution of salicylamide (0.076 mg/mL, 0.55 mM) in methanol containing 0.04% HFBA was also prepared. Reactions were initiated by adding 40.0 µL of the prodrug stock solution to 760.0 µL of a pre-warmed (37±0.5 °C) solution of 50% HP in 50% PBS buffer (pH 7.4). This equates to the following initial reaction concentrations: 6-*O*-Ile-NTXOL = 0.038 mg/mL, 8.2 x 10^{-5} M; 6-O-Val-NTXOL = 0.050 mg/mL, 1.1 x 10^{-4} M; and 6-*O*-β-ala-NTXOL = 0.15 mg/mL, 3.6 x 10^{-4} M. 80% HP was not used, because HP supplies were limited. Also, it has been shown that there is not a significant difference between hydrolysis rate data obtained with 50% HP and 80% HP stock solutions when hydrolysis reactions

are initiated with drug dissolved in DMSO (Di, Kerns et al. 2005). This is true for final reaction concentrations of DMSO up to 5%, and the reactions in this study were 5% DMSO. The buffer concentration of 50% PBS was used, because clouding of the plasma solutions was observed over the course of a stability experiment if 80% PBS was used. Sampling over the course of time was done by the following method. 50.0 µL aliquots of a reaction mixture were removed at various time points and placed into 1000 µL eppendorf tubes. 50.0 µL of internal standard solution was added to the samples, and 300.0 µL of ice cold methanol containing 0.04% HFBA was charged to the tubes to precipitate proteins. The mixtures were vortexed for exactly 30 seconds and subsequently centrifuged for exactly 10 minutes at 12,000 rpm. Supernatants were removed into individual culture tubes and dried under N_2 gas in a bath maintained at 37±0.5 °C. Residues were reconstituted in 150.0 µL methanol containing 0.04% HFBA with vortexing for exactly 30s and then visually inspected for solid material. All of the samples were clear, and they were immediately transferred to low-volume inserts and injected onto the HPLC column for analysis. The data are summarized in **Table 6.2**.

CYT-NTX

All stability studies of the CYT-NTX codrug in enzymatic media were conducted by the author in Dr. Crooks' lab. The procedure for CYT-NTX used identical sampling and reaction volumes as the prodrugs above. However, several modifications were required. First, a 2.5 mg/mL (4.5 mM) stock solution of

codrug in DMSO was employed. Second, the extraction solvent was 5% formic acid in acetonitrile, because the codrug was insoluble in methanol containing HFBA. Third, protein precipitation was achieved with 600.0 µL of chilled extraction solvent rather than 300.0 µL. Finally, the HP and RP reactions were run with 80% plasma in 50% PBS buffer (pH 7.4). The data are summarized in **Table 6.3**.

6.4 Kinetics of hydrolysis in SGF and SIF

SGF and SIF were prepared by the methods of the USP. A 2.5 mg/mL (4.5 mM) CYT-NTX codrug stock solution was prepared in DMSO. Reactions were initiated by adding 40.0 µL of the prodrug stock solution to 760.0 µL of pre-warmed (37±0.5 °C) SGF or SIF (reaction concentrations of 2.2×10^{-4} M). 50.0 µL aliquots of the reaction mixture were removed. 50.0 µL of internal standard solution and 50.0 µL of blank 0.04% HFBA in methanol were added to the reaction mixture aliquots in low volume inserts, and the solutions were homogenized with vortexing. Samples were immediately injected on the HPLC column and analyzed. The data are summarized in **Table 6.3**.

6.5 Standard Curves and Data Analysis

<u>Amino acid prodrugs in 50% HP (and 6-*O*-Ile-NTXOL in 50% PBS control)</u>

In the stability studies of amino acid ester prodrugs, salicylamide was used as an internal standard (IS). Stock solutions of prodrugs and a stock solution of IS was prepared in methanol containing 0.04% HFBA. Standard curves with eight

different concentration points were generated and analyzed in the stability studies. In the case of HP studies, standards were prepared by spiking 300.0 µL of prodrug diluted stock solutions to eppendorf tubes containing 50.0 µL of blank 50% HP and 50.0 µL of IS solution. Then the samples were worked up and reconstituted as described in **Section 6.3**. In the case of the 6-*O*-Ile-NTXOL control study (50%PBS), standards were prepared by dissolving the prodrug in methanol containing 0.04% HFBA and making a series of dilutions. 50.0 µL of the appropriate diluted stock solution was spiked to 50.0 µL of blank buffer and 50.0 µL of IS solution. The calibration curves obtained from standards were prepared using quadratic least-squares regression of area-under-the-curve (AUC) ratios ($AUC_{prodrug}/AUC_{IS}$) versus prodrug concentration. The amount of remaining prodrug over the course of time was then determined using the standard curves. The linear ranges and R^2 data for the standard curves are reported in **Table 6.1**.

CYT-NTX chemical stability assays

In the stability studies of CYT-NTX, two different methods were employed. *N*-1-naphthylacetamide was used as an IS in the CYT-NTX chemical stability studies that were initially conducted (Buffers pH 1.5 – 9.0). Standards for NTX, CYT, and CYT-NTX were prepared in solutions with the exact composition of the mobile phase since the study involved four different buffers and isocratic HPLC mobile phase conditions (details in the next section). It was also expected that the codrug would not degrade. It turned out that the standard curves were

unnecessary since the average AUC_{codrug}/AUC_{IS} value was robust in all buffers tested for 24 hours (One-way ANOVA, $p > 0.05$). This is an indicator of codrug stability, because the concentration of analyte remaining over the course of time is determined by inserting the value $Y = AUC_{analyte}/AUC_{IS}$ into the equation of the standard curve least squares regression line. Since no peaks were observed for CYT or NTX in any of these studies, and since average AUC_{codrug}/AUC_{IS} values did not significantly change during stability experiments, it can be concluded that the codrug was stable in these media. The linear ranges and R^2 data for the standard curves that were generated in the buffer assays are reported in **Table 6.1**.

CYT-NTX enzymatic stability assays (Plasma, SGF and SIF)

The CYT-NTX stability studies that were performed in enzymatic media used salicylamide as an IS and a different HPLC-UV method. Standard curves were not generated in the first run of these studies, because it was possible to check stability of the codrug by examining the ratio AUC_{codrug}/AUC_{IS} over time and checking for statistically different ratios during the stability experiment. If changes were observed, standard curves could be generated after the studies. Following satisfactory evidence that the codrug did not degrade (n = 1), the experiments were repeated for a total of n=3, and the average AUC_{codrug}/AUC_{IS} was examined for statistically significant change ($p \leq 0.05$). In all cases, $p > 0.05$ was observed (One-way ANOVA).

Determination of half-lives

All of the amino acid ester prodrugs showed pseudo-first-order kinetic behavior. Apparent pseudo-first-order hydrolysis rate constants (K_{app}) were calculated from the slope of log transformed $AUC_{prodrug}/AUC_{IS}$ as a function of time. K_{app} data were converted to half-life values using the equation $t_{1/2} = \ln(2)/ K_{app}$ and the average half-lives and their standard deviations were determined using Microsoft Excel. All stability studies were carried out in triplicate (n=3) by the author, except for those which were conducted in duplicate by Milewski (n=2) as described in **Section 6.2**. The stability studies conducted by the author employed standard curves with salicylamide as internal standard. **Table 6.2** summarizes the stability data which are reported as $t_{1/2(avg)} \pm$ SD.

6.6 HPLC Analysis

There were multiple HPLC methods utilized to determine the stability of our amino acid ester prodrugs and the CYT-NTX codrug. In particular, developing methods that worked for the CYT-NTX codrug and its key analytes proved to be challenging. Milewski utilized a modification of the HPLC method employed by Hussain et al., and the details are reported elsewhere (Milewski 2011). This section focuses only on the methods that were developed by the author.

All of the studies employed an Agilent 1100 series HPLC instrument equipped with a G1322A Degasser, a G1311A Quat Pump, a G1313A autosampler, and a

photodiode array detector. Agilent software was used to drive the instrument and to collect area data for half-life calculations.

CYT-NTX buffer stability assays

The first method was developed for stability analysis of the CYT-NTX codrug. The mobile phase was A:B = 23:77 (isocratic) where A = THF and B = 0.067% HFBA and 0.067% octane sulfonate sodium (base adjusted to pH 4.0 with triethylamine). The flow rate was 0.55 mL/min, and 280 nm UV detection was used. **Fig. 6.4(A)** shows a representative chromatogram of the method with the four analytes clearly marked. **Figure 6.4(B)** is an overlaid snapshot of the codrug and *N*-1-naphthylacetamide internal standard at t =24 hours in the four different buffers. No degradation of CYT-NTX was observed in any of the buffers tested.

Amino acid prodrug stability studies and CYT-NTX enzymatic stability studies

These studies utilized the same column and guard column and the same mobile phase solutions; however, different gradients had to be employed to separate the compounds properly, and to ensure no overlap with matrix peaks. In every case, the stationary phase consisted of a 4 µm Waters Phenyl Column (3.9 x 150 mm) attached to a 4 µm Nova-pak® C_{18} 3.9 x 20 mm guard column. The mobile phase in each assay was as follows: solvent A = aqueous solution of 0.04% heptafluorbutryic acid (HFBA); and solvent B = 0.04% HFBA in methanol. The flow rates varied between 0.3 mL/min and 0.5 mL/min for the different prodrugs

and the codrug. The specific details regarding analytes, flow rates and gradient programs are shown along with representative chromatograms for each set of compounds in **Figures 6.1, 6.2, 6.3 and 6.5**.

6.7 Discussion

CYT-NTX demonstrated stability in all of the media tested (**Table 6.3**). The peak at r.t. = 16.0 - 16.7 min in **Figure 6.4 B** appeared to represent hydrolysis of the codrug at pH 1.5; however, that same peak also appeared in buffer blanks, and it was not due to NTX or CYT. Therefore, CYT-NTX was advanced to *in vivo* studies in the S-D rat to determine if it could be hydrolyzed in a living animal model (**Chapter 7**). In contrast, each of the amino acid esters tested demonstrated pseudo first-order hydrolysis kinetics. From the data observed, we were able to determine which of the compounds was best suited for an MNTD paradigm.

<u>pH 5.0 stability to assess MNTD candidacy</u>

It can be seen in **Table 6.2** that the majority of the amino acid ester prodrugs were not suitable for MNTD based on our minimum stability criterion that t_{90} must be greater than or equal to the intended time course of a skin diffusion experiment (48 hours) at pH 5.0 and 32 °C. The latter cutoff was established for our studies, because it becomes difficult to estimate the extent of bioconversion in the viable skin following a diffusion experiment if the prodrug extensively degrades by simple chemical means during the experiment. Also, high levels of

hydrolysis before skin transport do not allow a true estimation of drug flux. In total, the results are not too surprising. The phenolic esters were extremely labile as expected, and aliphatic esters outperformed their phenolic counterparts by at least an order of magnitude (with the exception of Pro and Ala prodrugs). Bulky side chains on aliphatic ester promoieties (Ile and Val) provided the best recipe for success in this series of prodrugs, with β-Ala also showing similar stability enhancing results. These observations are well within the expectations one can glean from the review of amino acid prodrugs in **Chapter 1**. Overall, the MNTD candidates were determined to be 6-*O*-Ile-NTXOL, 6-*O*-Val-NTXOL and 6-*O*-β-Ala-NTXOL. Prodrugs that did not meet the minimum criteria were not pursued in further stability tests.

pH 7.4 Stability (chemical and enzymatic) to assess prodrug behavior

Adequate stability at pH 5.0 was not enough to establish our prodrugs as appropriate MNTD candidates. In a prodrug design, rapid degradation under physiological conditions is desired, because the prodrug itself is just a delivery system for the parent drug. As such, an ideal prodrug for the MNTD paradigm should have pH 5.0 stability as stated in the last section with nearly instantaneous hydrolysis at pH 7.4 (enzyme assisted in plasma or in a simple chemical buffer). This is true because rapid skin bioconversion at pH 7.4 is expected to greatly enhance flux of the parent drug, and that is the paramount objective of an MNTD prodrug design. Unfortunately, it is very difficult to design a prodrug with these ideal characteristics. Greater rates of hydrolysis can be

expected at pH 7.4 compared to pH 5.0, simply because the concentration of hydroxide ion in an aqueous system is higher at pH 7.4. In **Table 6.2**, it is obvious that significant hydrolysis rate enhancements of approximately one order of magnitude were observed at pH 7.4 as compared to pH 5.0; however, these rates were not rapid enough to ensure enhanced skin transport of NTXOL. Therefore, we examined the hydrolysis behaviors of the Ile, Val and β-Ala prodrugs in 50% HP to see if further rate enhancements could be expected *in vivo*.

The stability data for our prodrugs that advanced to 50% HP turned out to be very interesting. From the data summarized in **Table 6.2**, it appears as though a critical design feature that increases pH 5.0 stability of α-amino acid ester prodrugs of NTXOL (bulky side chains) also renders them susceptible to extensive protein binding which slows hydrolysis. This is evident due to the increased plasma stabilities of the Ile and Val prodrugs compared to their stabilities in 50% PBS or HEPES buffers (pH 7.4). On the other hand, the β-Ala prodrug did not demonstrate evidence of protein binding, because its rate of hydrolysis was significantly increased in plasma to yield a half-life of 2.2 ± 0.1 hours. Therefore, 6-*O*-β-Ala-NTXOL is the lead compound of this series of prodrugs.

Although, 6-*O*-β-Ala-NTXOL is the established lead compound, its half-life is still fairly long for an MNTD candidate, and it would be necessary to perform skin

diffusion and disposition studies to see if faster rates of bioconversion could be achieved in viable skin tissue. Unfortunately, these studies require fairly large amounts of prodrug, and it was not possible to scale-up the procedures described in **Chapter 3** to afford enough material for the studies. Further optimization of the synthetic strategy for scale-up would be needed.

One inconsistency in the amino acid ester prodrug stability studies should be explained. The hydrolysis reactions were not all run at the same concentration, because the 6-*O*-Ile-NTXOL and 6-*O*-Val-NTXOL prodrugs demonstrated precipitation problems when reactions were run at concentrations equivalent to the 6-*O*-β-Ala-NTXOL prodrug reactions (0.15 mg/mL, 3.6×10^{-4} M). 6-*O*-Ile-NTXOL is crystalline in nature, and it precipitates very easily at pH 7.4. Therefore, reactions involving 6-*O*-Ile-NTXOL had to be run at the lowest concentration of all the prodrugs (0.038 mg/mL, 8.2×10^{-5} M) to avoid this precipitation. 6-O-Val-NTXOL also showed precipitation problems, but it could be run at higher reaction concentrations (0.050 mg/mL, 1.1×10^{-4} M). 6-*O*-β-ala-NTXOL did not precipitate from plasma media at the concentrations tested, but it exhibited less extraction efficiency than the other two prodrugs. Therefore, it had to be run at higher reaction concentrations than either of the other two prodrugs (0.15 mg/mL, 3.6×10^{-4} M) in order to obtain a good peak for quantitation over the time course of the study. In the ideal case, comparative stability studies in enzymatic media should be carried out at equivalent concentrations to control for an unknown enzyme saturation level; however, it was not possible to do this

utilizing HPLC-UV under the analysis conditions of this study. More sensitive LC-MS or LC-MS/MS procedures would have been required, and the instrument time necessary to employ these resources was not available. Nonetheless, the stability data indicate that 6-*O*-β-Ala-NTXOL had a much faster rate of conversion to parent drug than either the Val or the Ile prodrugs, even at greater hydrolysis reaction concentrations. Moreover, the propensity of the Val and Ile prodrugs to precipitate at pH 7.4 is not a desirable characteristic for an MNTD prodrug. Thus, it should be noted that at the concentrations used in these studies, the prodrugs remained in solution, so the reported rates of hydrolysis were not artificially accelerated by precipitation.

Table 6.1 Standard curve data for the analytes. *(No standard curves generated for plasma, SGF and SIF studies of CYT-NTX since AUC_{codrug}/AUC_{IS} was robust throughout a stability experiment ($p > 0.05$)).*

Analyte	Linear Range	R^2
6-O-β-Ala-NTXOL	19 µM – 1.2 mM	0.9999
6-O-Val-NTXOL	18 µM – 1.1 mM	0.9998
6-O-Ile-NTXOL *(plasma study)*	26 µM – 1.7 mM	0.9999
6-O-Ile-NTXOL *(control study)*	20 µM – 5.0 mM	0.9999
CYT-NTX *(buffer stability studies)*	56 µM – 0.90 mM	0.9982
CYT *(buffer stability studies)*	0.16 mM – 2.6 mM	0.9965
NTX *(buffer stability studies)*	92 µM – 1.5 mM	0.9952

Table 6.2 Stability of amino acid ester prodrugs of NTX and NTXOL. Data are reported as $t_{1/2(avg)}$ ± SD as determined from two (n=2) or three (n=3) independent experiments.

Prodrug	t_{90} (pH 5.0) (n=2)	$t_{1/2}$ (pH 7.4) (n=2)	$t_{1/2}$ (50% HP) (n=3)
6-O-β-Ala-NTXOL	5.6 ± 0.5 d	0.47 ± 0.24 d	2.2 ± 0.1 h
6-O-Val-NTXOL	5.2 ± 0.2 d	0.48 ± 0.03 d	0.76 ± 0.03 d
6-O-Ile-NTXOL	14.3 ± 0.3 d	0.88 ± 0.02 d*	1.3 ± 0.1 d
6-O-Ala-NTXOL	9.9 ± 0.5 h	no data	no data
6-O-Pro-NTXOL	5.2 ± 0.7 h	no data	no data
6-O-Leu-NTXOL	0.93 ± 0.0 d	no data	no data
3-O-Val-NTX	1.5 ± 0.0 h	instantaneous	no data
3-O-Ala-NTX	1.3 ± 0.1 min	instantaneous	no data
3-O-Leu-NTX	2.7 ± 0.0 min	instantaneous	no data

* *6-O-Ile-NTXOL was assayed (n =3)*

Table 6.3 Stability of CYT-NTX.

pH 1.5	stable
pH 5.0	stable
pH 7.4	stable
pH 9.0	stable
SGF	stable
SIF	stable
50% HP	stable
80% RP	stable

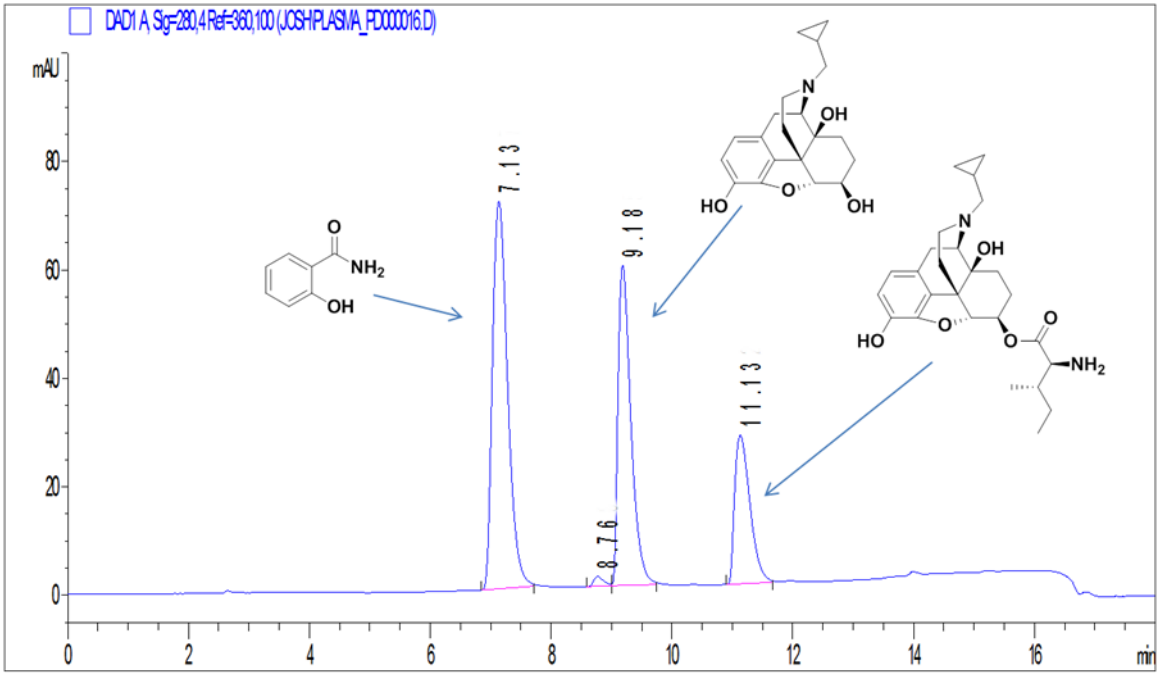

4 µm Waters Phenyl Column (3.9 x 150 mm) + 4 µm Nova-pak® C_{18} 3.9 x 20 mm guard column. Solvent A: Aqueous solution of 0.04% (HFBA); Solvent B: 0.04% HFBA in methanol.

Gradient Elution at 0.5 mL/min:

Time (min)	%A	%B
0	65	35
0.3	65	35
10	10	90
12	10	90
12.1	65	35
21	65	35

Figure 6.1 HPLC chromatogram of salicylamide, NTXOL and 6-*O*-Ile-NTXOL (gradient elution).

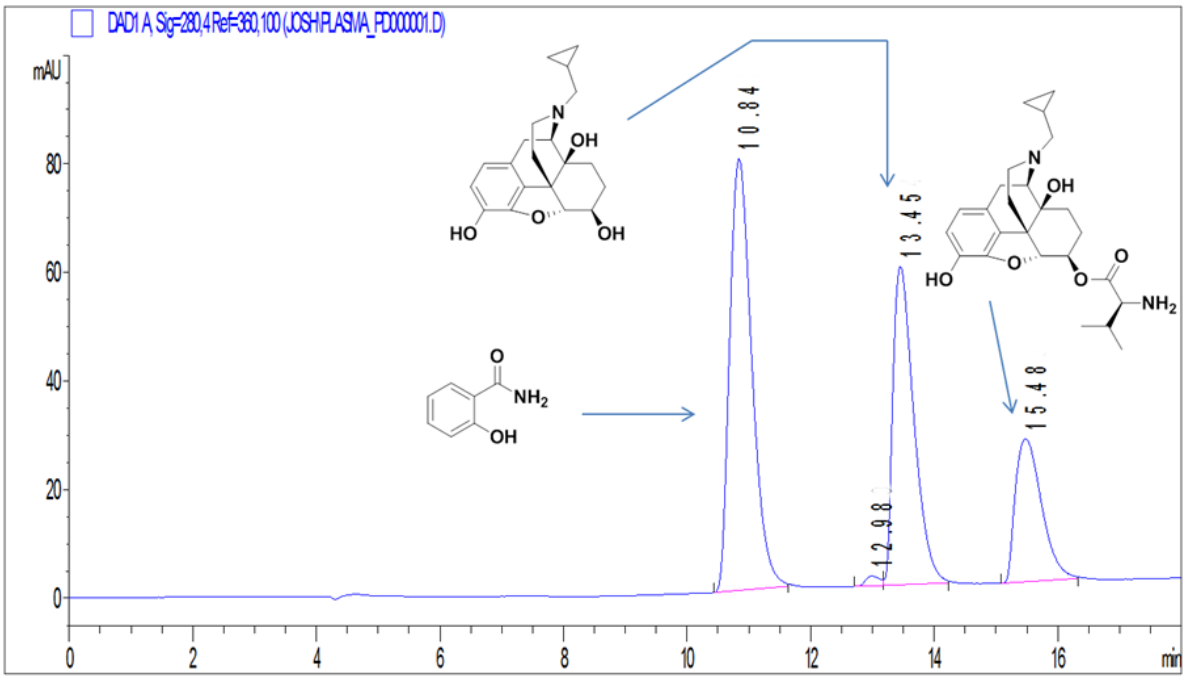

4 µm Waters Phenyl Column (3.9 x 150 mm) + 4 µm Nova-pak® C_{18} 3.9 x 20 mm guard column. Solvent A: Aqueous solution of 0.04% HFBA; Solvent B: 0.04% HFBA in methanol.

Gradient Elution 0.3 mL/min:

Time (min)	%A	%B
0	65	35
0.3	65	35
10	10	90
12	10	90
12.1	65	35
21	65	35

Figure 6.2 HPLC chromatogram of salicylamide, NTXOL and 6-*O*-Val-NTXOL (gradient elution).

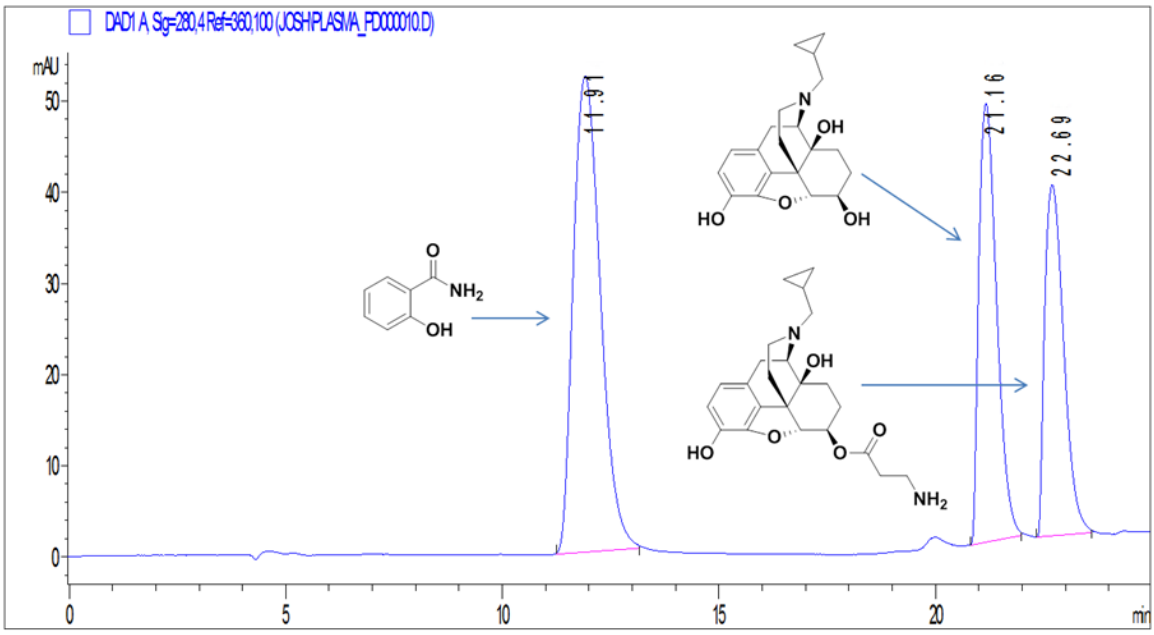

4 µm Waters Phenyl Column (3.9 x 150 mm) + 4 µm Nova-pak® C_{18} 3.9 x 20 mm guard column. Solvent A: Aqueous solution of 0.04% HFBA; Solvent B: 0.04% HFBA in methanol.

Gradient Elution at 0.3 mL/min:

Time (min)	%A	%B
0	65	35
10	65	35
20	10	90
21	65	35
30	65	35

Figure 6.3 HPLC chromatogram of salicylamide, NTXOL and 6-*O*-β-Ala-NTXOL (gradient elution).

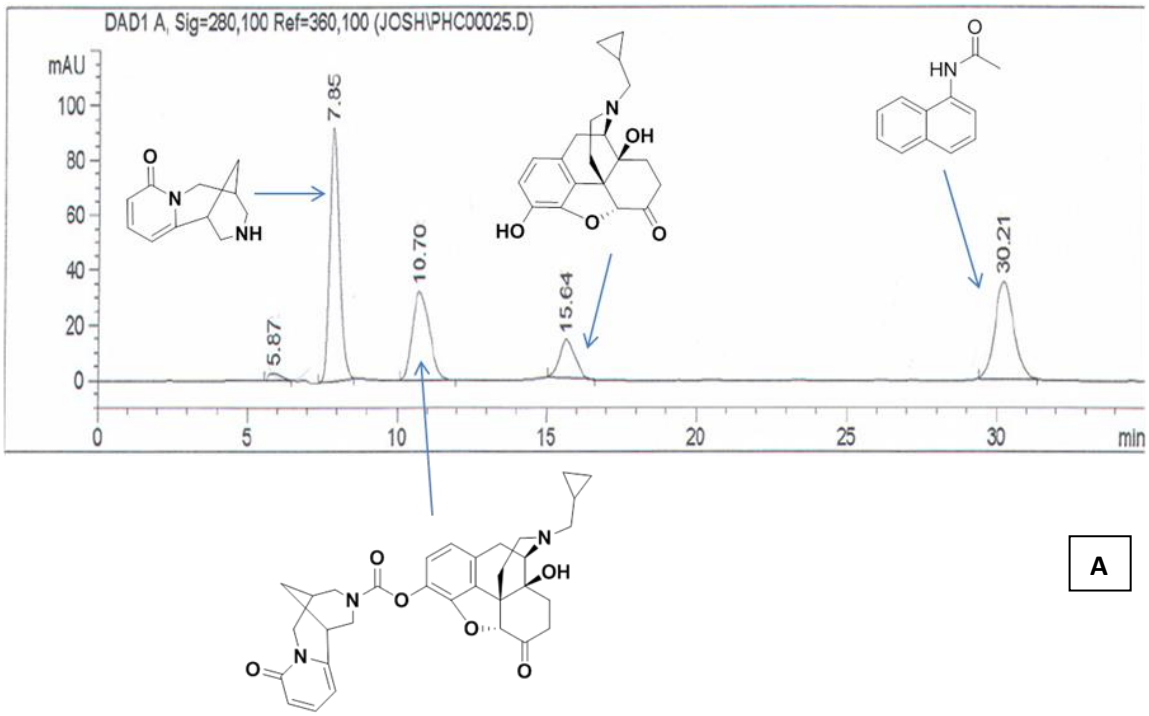

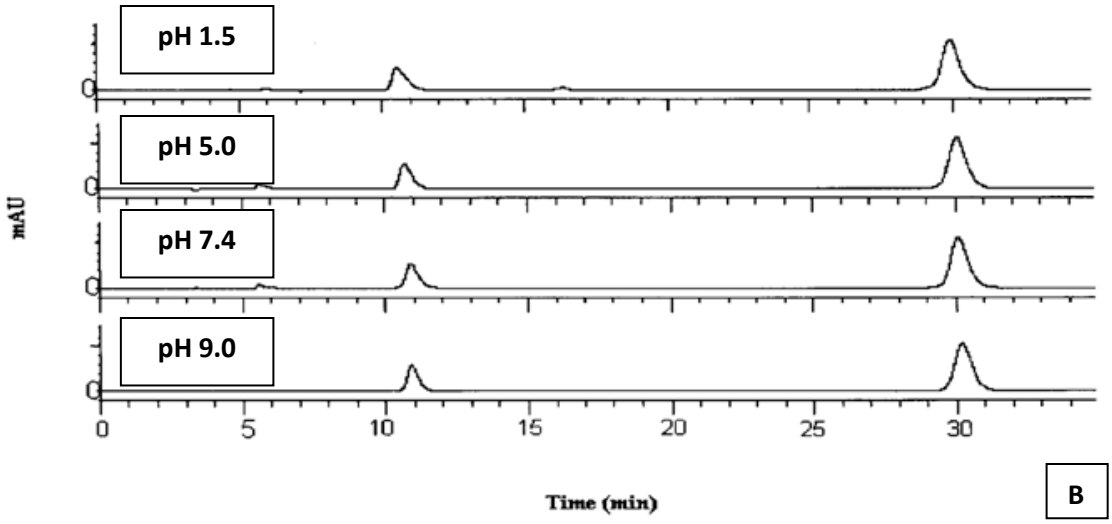

Figure 6.4 (A) HPLC chromatogram of (-)-cytisine, CYT-NTX, NTX and N-1-naphthylacetamide (isocratic elution). (B) Representative HPLC Chromatograms of CYT-NTX in buffers at t = 24 hours. ***Broad peak at r.t. = 16.0 - 16.7 min (pH 1.5) is present in blank buffer.***

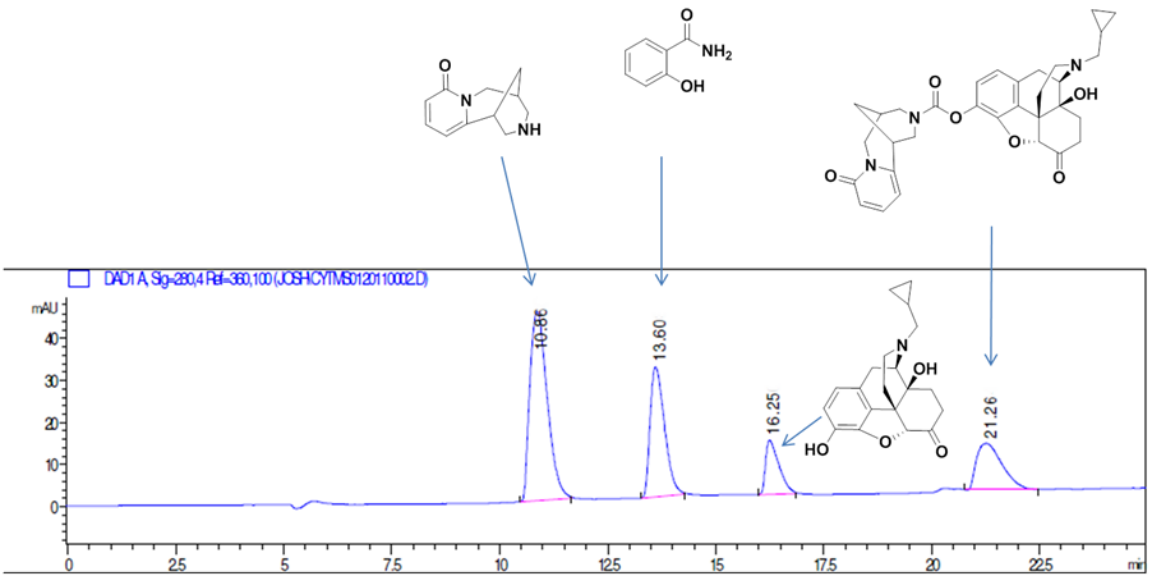

4 µm Waters Phenyl Column (3.9 x 150 mm) + 4 µm Nova-pak® C_{18} 3.9 x 20 mm guard column. Solvent A: Aqueous solution of 0.04% heptafluorbutryic acid (HFBA). Solvent B: 0.04% heptafluorbutryic acid (HFBA) in methanol.

Gradient Elution at 0.3 mL/min:

Time (min)	%A	%B
0	75	25
0.3	75	25
17	10	90
26	10	90
27	75	25
36	75	25

Figure 6.5 HPLC chromatogram of (-)-cytisine, salicylamide, NTX and CYT-NTX (gradient elution).

Chapter 7

Pharmacokinetic Analysis of CYT-NTX in male Sprague-Dawley Rats

The ultimate test of performance for a given codrug candidate resides in its ability to behave as an *in vivo* delivery form of its two constituent drugs. Therefore, in order to investigate the codrug-like behavior of CYT-NTX, male Sprague-Dawley (S-D) rats were chosen as an *in vivo* model. The data described in this chapter were obtained through a collaborative effort. The author was responsible for the synthesis and characterization of CYT-NTX; for participation in the dosing of animals and removal/preservation of plasma from blood samples; and for the extraction and preparation of plasma samples for PK analysis. Dr. Zaineb Albayati (UK) was responsible for the appropriate treatment of animals; for animal surgeries; for the dosing of animals and the removal of blood samples; and for the PK analysis of chromatographic data using WinNonlin software. Dr. Manjula Sunkara (UK) is to be credited with the LC-MS/MS method development and the collection of analytical data from rat plasma samples. Special thanks are due to Dr. Andrew J. Morris (UK) for allowing the use of his LC-MS/MS resources and for allowing Dr. Sunkara's participation in the study, and to Dr. Philip Breen (UAMS) for his review and suggestions regarding the PK study.

7.1 Animals

All procedures that involved the use of S-D rats were conducted in accordance with the guidelines set forth by the University of Kentucky Institutional Animal Care and Use Committee established by the National Institutes of Health's *Guide*

for the Care and Use of Laboratory Animals (1996). Male S-D rats weighing 250 – 300 grams were housed two per cage with *ad libitum* access to food and water in the Division of Laboratory Animal Resources within the College of Pharmacy at the University of Kentucky. Rats were anesthetized with 40 mg/kg pentobarbital i.p. and surgically implanted with cannulae in the femoral (blood sampling) and jugular (i.v. dosing) veins. Three to four days post-surgery, rats were observed for signs of local infection at surgical sites, for hair yellowing, for the presence of blood around the nose or eyes, for indications of lessened appetite, and for signs of lessened or absent fecal activity. Following appropriate evidence of successful recovery from surgery, i.v. or p.o dosing was performed and blood samples (0.15 mL) were withdrawn over the course of 7 hours at 5, 15, 30 and 45 min, and 1, 2, 3, 5 and 7 h. The withdrawn blood was replaced with heparinized saline (0.15 mL). Rats were euthanatized after collecting the last plasma sample by administration of an overdose of pentobarbital (150 mg/kg, i.v.) via the femoral cannula followed by thoracotomy.

7.2 Objectives

In an effort to deliver NTX and CYT as an equimolar mixture *per os*, the CYT-NTX codrug was prepared by the methods described in **Chapter 5**. This work was designed to investigate the oral bioavailability and plasma pharmacokinetics (PKs) of the new CYT-NTX codrug in S-D male rats after a single 1.0 mg/kg (1.79×10^3 nmol/kg) i.v. bolus dose or an oral dose of 10.0 mg/kg (1.79×10^4 nmol/kg). Blood samples were taken up to 7 h as described in **Section 7.4**.

7.3 Methods

Six (3 rats/group) S-D male rats were dosed 1.0 mg/kg (1.79 x 10^3 nmol/kg) with CYT-NTX codrug, i.v. or 10.0 mg/kg (1.79 x 10^4 nmol/kg), p.o. Plasma CYT-NTX codrug, NTX, and CYT concentrations were quantitated utilizing an LC-MS/MS assay method described below. Plasma PK parameters were calculated using a two-compartment open model for both CYT-NTX codrug and NTX. CYT was not detected in plasma in this study (see **Section 7.10**).

7.4 CYT-NTX dose preparations

CYT-NTX codrug was dissolved in a saline solution containing 15% w/v concentration of PEG-400 and filtered through a 0.2-µm filter. The animals were administered a 10.0 mg/kg oral dose or a 1.0 mg/kg i.v. dose of CYT-NTX codrug. Blood samples (0.15 mL) were obtained at 5, 15, 30 and 45 min, and 1, 2, 3, 5 and 7 h after oral dosing and i.v. injection. The withdrawn blood was replaced with heparinized saline (0.15 mL) after each blood-draw. Blood samples were centrifuged at 8,000 rpm for 15 min, and plasma was separated, frozen immediately on dry ice, and stored at -20 °C prior to analysis.

7.5 Analyte Sample Preparation

50.0 µL of plasma was transferred to polypropylene tubes to which 50.0 µl of working internal standard (salicylamide dissolved in acetonitrile) was added followed by treatment with 600.0 µL of a solution of acetonitrile containing 5% formic acid. Vortex mixing was carried out for one minute. The samples were

then centrifuged for 15 min at 8,000 rpm. The supernatant was transferred into glass tubes and evaporated to dryness under nitrogen gas at 37 °C. Following drying, the residue was dissolved in 150.0 µl of HPLC mobile phase by vortexing for 1 min. Ten (10.0 µl) of the sample was then injected onto the HPLC column, and analytes were quantified by an LC-MS/MS spectrometric analysis.

7.6 LC-MS/MS Analysis

Standard curves for CYT-NTX, CYT, NTX, and salicylamide were generated by preparing stock solutions of these analytes in acetonitrile containing 5% formic acid. Ten standards were prepared by spiking diluted stock solutions to 50.0 µL of blank S-D rat plasma and then proceeding with the treatment procedure described above. Standard curves showed good linearity (R^2=0.9800 - 0.9988).

An LC-MS/MS method was successfully developed to determine the PK profiles of the CYT-NTX codrug, and NTX in rat plasma after a single oral dose of 10.0 mg/kg (1.79 x 10^4 nmol/kg) or an i.v. dose of 1.0 mg/kg (1.79 x 10^3 nmol/kg) of the codrug. CYT was not detected in rat plasma for reasons that are unclear. Each of the analytes (including CYT) demonstrated a quantifiable detector response at the plasma concentrations that were relevant to this study. See **Section 7.10** for a discussion on possible reasons why CYT was not observed in rat plasma samples.

Analysis of the analytes was carried out using a Shimadzu UFLC system coupled to an AB Sciex 4000-Qtrap hybrid linear ion trap triple quadrupole mass

spectrometer in multiple reaction monitoring (MRM) mode, operating in the positive electrospray ionization mode with optimal ion source settings determined by standards of CYT-NTX codrug, CYT and NTX. Salicylamide was used as an internal standard. A curtain gas of 20 psi, an ion spray voltage of 5500 V, an ion source gas1/gas2 of 40 psi and a temperature of 550 °C were employed. MRM transitions monitored were as follows: CYT-NTX codrug- m/z 558.2/540.2, m/z 558.2/217.3; CYT- m/z 191.1/148.2, m/z 191.2/133.1; NTX-m/z 342.1/324.1, m/z 342.1/270.1; and for salicylamide, m/z 138.0/121.1, m/z 138.0/65.1. CYT-NTX codrug, CYT, NTX and salicylamide were separated using a Kinetex PFP, 2.6 um, 100 X 4.60 mm column (from Phenomenex). The mobile phase consisted of water with 0.04% heptafluorobutyric acid as solvent A and methanol with 0.04% heptaflorobutyric acid as solvent B. Separation of CYT-NTX codrug, CYT, NTX and salicylamide was achieved using a gradient of 20 % solvent B in the first minute, followed by an increase to 100% solvent B in the next 5 minutes. 100% solvent B was maintained for the last four minutes and equilibrated back to initial conditions over 3 minutes. The flow rate was 0.5 mL/min with a column temperature of 30 ^{0}C. The sample injection volume was 10.0 µL. The optimal ion source settings for each MRM transition are summarized in **Table 7.1**. **Figs. 7.4A** and **7.4B** show the LC-MS/MS chromatograms and the extracted ion chromatograms for the 4 analytes using the analytical methodology described above.

7.7 Plasma Pharmacokinetics

Individual CYT-NTX codrug and NTX plasma concentration-time profiles after i.v. bolus administration were best fitted by a two-compartment open model and first order elimination (Phoenix WinNonlin, Professional, version 6.2, Pharsight, Mountain View, CA) with inverse-variance weighing, and the goodness of fit was determined by the AIC (Akaike criteria), SC (Schwartz criteria), and WSSR (weighted sum of square of residuals). The lower the AIC, SC, and WSSR the more appropriate is the selected model. PK parameters were calculated with the Gauss–Newton minimization method (Yamaoka, Nakagawa et al. 1978, Ludden, Beal et al. 1994) and a weighting factor as $1/Y^2$. The following exponential expression was used;

Equation 7.1. $C_p = Ae^{-\alpha t} + Be^{-\beta t}$

where C_p is the plasma concentration of CYT-NTX codrug or NTX; A and B are pre-exponential constants, α and β are the distribution rate constant and the elimination rate constant, respectively, and t is time. The PK parameters including elimination half-life $t_{1/2}$, volume of distribution $V_{d,}$ area under the curve from 0 to infinity ($AUC_{0\text{-}inf}$), and total body clearance (CL_{tot}), were estimated using the computer program described above.

Following oral administration, data were analyzed by the two-compartment open model and first order absorption to determine peak concentration (C_{max}), the time to reach maximum plasma concentration (t_{max}), and area under the curve from 0 to infinity ($AUC_{0\text{-}inf}$). Plasma concentration (C_p) is described by an equation with three exponential terms:

Equation 7.2. $\mathbf{C_p = Ae^{-\alpha t} + Be^{-\beta t} + Ce^{-k_a t}}$**, where C = - (A+B)**

C_p is the plasma concentration of CYT-NTX codrug or NTX; A, B and C are pre-exponential constants; k_a, α and β are the absorption rate constant, the distribution rate constant and the elimination rate constant, respectively; and t is time. PK parameters including absorption half-life $t_{1/2}(a)$, elimination half-life $t_{1/2}$, and $AUC_{0\text{-}inf}$ were estimated using the computer program described above.

Absolute bioavailability of the codrug was determined using **Equation 7.3**:

Equation 7.3. $\mathbf{F\% = [(AUC_{p.o.} \times Dose_{i.v.}) / (AUC_{i.v.} \times Dose_{p.o})] \times 100\%}$

where $AUC_{p.o.}$, $AUC_{i.v.}$, $Dose_{p.o.}$, and $Dose_{i.v.}$ represent the $AUC_{0\text{-}inf}$ and corresponding doses of the codrug, respectively.

The fraction of orally administered co-drug appearing as NTX in the portal circulation (f_a) was determined by **Equation 7.4**.

Equation 7.4. $$f_a = \frac{AUC_{p.o.} \quad Dose_{i.v.}}{AUC_{i.v.} \quad Dose_{p.o.}}$$

In the above expression, the different values of $AUC_{(0\text{-inf})}$ for NTX obtained by the two different dosing routes of codrug are a measure of NTX release and absorption across the gastrointestinal barrier from orally administered codrug. However, the parameter f_a does not include any decrease in NTX appearing in the systemic circulation due to first pass elimination. This equation is a rearrangement of Equation 89 reported by Houston *et al* (Houston 1981).

7.8 Results

An LC-MS/MS method has been successfully applied to the PK study of the CYT-NTX codrug. The codrug hydrolyzed to release NTX in the live S-D rat after administration of a single oral dose of 10.0 mg/kg (1.79×10^4 nmol/kg) or a 1.0 mg/kg (1.79×10^3 nmol/kg) i.v dose. **Figure 7.1** is a plot of the mean plasma concentration versus time profile of the codrug, and NTX released from the codrug, by the p.o. route of administration, while **Figure 7. 2** is a plot of the mean plasma concentration versus time profile of the codrug, and NTX released from the codrug, by the i.v. route. **Figure 7.3** shows an overlay of the mean plasma levels of NTX as a function of time which were observed following p.o. and i.v. dosing of the codrug. The carbamate linker of the CYT-NTX codrug apparently cleaves *in vivo* to produce NTX; however, the presence of constituent CYT was not observed at any time point. Thus, only NTX was observed as a hydrolysis product of the CYT-NTX codrug. Determination of the fate of released CYT in

the rat would require further study; however, some possible explanations for why we did not detect CYT are offered in **Section 7.10.**

7.9 Pharmacokinetic Properties

Oral administration of the codrug in S-D rats resulted in NTX delivery with a peak plasma concentration of 6.8 ± 0.9 nmol/L which was reached within 1.08 ± 0.36 hours. The value of $f_{a(NTX)}$ calculated using **Equation 7.4** was 0.13 (13%). The areas under the plasma concentration-time curves ($AUC_{0\text{-}inf}$) for codrug and released NTX after oral and i.v. dosing were as follows: 26.9 ± 2.8, 34.8 ± 15.9 hr•nmol/L (p.o.); and 237 ± 103, 27.0 ± 0.6 hr•nmol/L (i.v.), respectively. The codrug is very lipophilic in nature, and this is reflected in its large volume of distribution of 17.7 ± 9.2 L/kg and its rapid clearance of 0.126 ± 0.1 L/min/kg which were observed following bolus administration. The solubility properties of the codrug also support these data (soluble in benzene and DCM, but very poorly soluble in THF, alcohols or neutral water). The PK parameters are summarized in **Table7. 2**.

7.10 Discussion

The cytisine-naltrexone (CYT-NTX) codrug was designed as a drug delivery system in which the end goal was to achieve equimolar release of the two separate therapeutic agents, CYT and NTX, in the biophase. The CYT-NTX codrug exhibited desirable *in vitro* stability characteristics for an oral drug delivery candidate (**Chapter 6**). Indeed, there was no evidence of degradation of the

compound to its constituent drugs over the course of 24 hours in chemical buffers adjusted to pH 1.0, 5.0, 7.4, and 9.0 (n=3). Likewise, the codrug was stable over a 24 hour time course in 80% rat plasma, 80% human plasma, and in simulated gastric fluid and simulated intestinal fluid that had been prepared by the methods of the USP (n=3). Having established the codrug as a stable entity for oral delivery, our next goals were as follows: (1) to determine if the codrug would hydrolyze *in vivo* in the S-D rat; and (2) to investigate the PK profile of the codrug and/or its released constituent drugs (CYT and NTX).

The CYT-NTX codrug was shown to hydrolyze in the rat to release NTX, but CYT was not detected. The hydrolysis is not complete, as intact codrug can be seen along with NTX at all time points regardless of the route of administration (**Figs. 7.1 & 7.2**). Therefore, these data show a prolonged release of NTX from the codrug over time. The release of NTX and CYT from the codrug should occur in an equimolar ratio according to the codrug structure; however, CYT was not observed in the plasma at any time point. We suspect that CYT may not have been observed for one of the following reasons: (1) a pre-hydrolysis metabolic event may have chemically modified the CYT moiety before carbamate cleavage occurred; (2) CYT may have been metabolized or eliminated immediately after hydrolysis; (3) the CYT plasma level may have dropped below the limit of quantitation of our LC-MS/MS assay due to substantial loss of CYT by biotransformation and/or sequestration into an unknown tissue compartment; or (4) it is possible that the ester side of the carbamate linker of CYT-NTX cleaves

readily *in vivo* to release NTX while the amide side remains intact as a carbamic acid intermediate following release of NTX. Also, it is noteworthy that in New Zealand rabbits, CYT has a short *in vivo* half-life of 0.86 ± 0.17 hours and an oral bioavailability of 32.18% (Astroug, H., et al. 2010). Nonetheless, the CYT-NTX codrug hydrolyzes *in vivo*, because measurable levels of NTX were observed in all of the rats, regardless of the route of administration.

A two-compartment model adequately describes the PK of oral CYT-NTX codrug and its released NTX. It can be shown that at any time point after the C_{max} of 9.7 ± 1.4 nmol/L at t_{max} of 0.74 ± 0.04 hr, the codrug is present at a lower concentration than NTX, **Fig. 7.1**. Absorption of the codrug appears to be very rapid ($t_{1/2(a)}$ = 0.30 ± 0.04 hr). Also, fast linker cleavage to release NTX occurs, because NTX was detected in plasma within 5 min after oral dosing, and it reached a C_{max} of 6.8± 0.9 nmol/L with a t_{max} of 1.08 ± 0.36 hr.

A two-compartment model also describes i.v. dosing of the codrug and its release of NTX (**Fig. 7.2**). Peak plasma levels of released NTX (C_{max} = 9.6 ± 2.8 nmol/L) were detected within 5 min, indicating rapid cleavage of the codrug. In contrast to oral dosing, plasma codrug concentrations were significantly higher than NTX levels at all time points resulting in $AUC_{(0\text{-}inf)}$ values of 237 ± 103 hr•nmol/L (codrug) and 27.0 ± 0.6 hr•nmol/L (NTX) (**Fig. 7.2 and Table 7.2**). Therefore, it appears as though first-pass metabolism contributes significantly to the hydrolysis of the codrug *in vivo*.

7.11 Bioavailability of CYT-NTX and fraction of NTX absorbed

Use of **Equation 7.3** with the data obtained from the individual oral delivery experiments resulted in an average Apparent F value of 1.02 ± 0.1%. This small value is partly due to fast first pass metabolism of orally administered codrug. Also, some of the very early codrug concentration points occurred before blood was sampled for codrug levels, and these concentrations were not able to be included in the calculation of AUC. Moreover, it is important to note that calculation of the bioavailability of the codrug is not straight forward due to rapid hydrolysis *in vivo*. Since the intravenously administered codrug also undergoes hydrolysis, a true bioavailability estimate cannot be made by comparison of AUC data of the codrug alone. AUC data for the codrug and NTX can be summed and entered into **Equation 7.3** in the form

$$F\% = [\Sigma(AUC_{codrug,NTX(p.o.)}) \times dose_{(i.v.)}] / [\Sigma(AUC_{codrug,NTX(i.v.)}) \times dose_{(p.o.)}] \times 100\%$$

In this way, an oral bioavailability estimate of the codrug that includes the released NTX can be obtained. However, in the case of this study, any contributions that are made by CYT cannot be added into the summed AUC expression for total bioavailability. Nonetheless, the average estimated total bioavailability of codrug based on summed AUC data of CYT-NTX and NTX from the individual rats is 2.53 ± 0.82%.

Another feature of codrug bioavailability must be mentioned. In the design of a codrug, it is desirable for plasma levels of constituent drugs to far exceed the plasma levels of the codrug. In the perfect case, codrug bioavailability of zero with therapeutic delivery of the constituent drugs would be observed. This is because the codrug would be functioning as a "chemical" delivery system, and only the constituent drugs would be delivered to the systemic circulation. Oral administration of CYT-NTX in S-D rats showed that the codrug did achieve higher plasma levels of NTX compared to CYT-NTX at every time point after t_{max}, while intravenous administration resulted in higher plasma levels of codrug over a seven hour time course.

As determined by **Equation 7.4,** oral administration of the codrug resulted in $f_{a(NTX)}$ = 0.13 (13%) compared to iv administration**.** This f_a value is indicative of the conversion of codrug to NTX. In comparison, the fraction of administered codrug that was converted to NTX after intravenous administration was approximately 0.11 (11%) ($AUC_{NTX(i.v.)}/AUC_{codrug(i.v.)}$ = 27/237 hr•nmol/L) . These are reasonable available fractions of NTX by either route. However, oral delivery has the advantage that at every time point after t_{max}, the codrug is present in lower concentration than NTX (**Fig. 7.1**). The opposite is true after i.v. administration (**Fig. 7.2**). As previously mentioned, it is not desirable for codrug levels to exceed constituent drug levels *in vivo*. The ratio of AUC_{codrug} to AUC_{NTX} following oral codrug administration is 0.77 (77%), and the reciprocal ratio is 1.29 (129%). This value that is greater than unity simply indicates that the process is

NTX elimination rate limited and has no ramifications for comparative bioavailability between NTX and codrug.

It was observed in **Chapter 6** that plasma hydrolysis of the codrug does not occur in 80% phosphate-buffered S-D rat plasma within 24 hours. Therefore, these observations suggest that hydrolysis of the codrug is taking place in tissue compartments other than plasma, and that first-pass bioconversion likely plays a role in the hydrolysis of the codrug. Disposition and tissue homogenate studies would be required to determine which tissues host the enzymes that participate in the bioconversion. Nonetheless, the current body of work demonstrates that the CYT-NTX codrug is stable for oral formulation purposes, and that it is hydrolyzed to yield quantifiable NTX levels in the S-D rat.

7.12 Conclusions

In this study, oral administration of the CYT-NTX codrug resulted in NTX delivery with prolonged exposure (AUC) and an f_a value of approximately 0.13 (13%) compared to i.v. The mean plasma concentration versus time profiles for NTX indicate that the codrug performs best by the oral route, because intravenous administration results in higher levels of codrug compared to NTX at all time points, while oral delivery achieves significantly higher levels of NTX compared to codrug after about 45 minutes. The fate of CYT was not determined in this study, since it could not be detected/quantitated in rat plasma after i.v. or oral

administration of the codrug; however, CYT-NTX may hold promise as a potential lead compound for further design optimization and development.

7.13 Future Directions

The CYT-NTX and NTX plasma levels measured in this study were low due to the large volume of distribution and rapid clearance of CYT-NTX. Inasmuch, optimization of the codrug structure will likely be necessary to observe better oral absorption and higher free drug levels in rat plasma following oral and intravenous administration, respectively. Regarding CYT-NTX itself, drug disposition studies should be conducted in order to investigate the areas where the drug distributes, and to determine whether or not deposition occurs in tissues such as fat. The latter is highly likely with a volume of distribution of 17.7 L/kg. Brain exposure studies could also reveal more information about the degree of exposure of CYT-NTX in the CNS. Most importantly, it needs to be known what is happening to the CYT moiety in the rodent model, since no claim can be made that CYT-NTX is an effective codrug without such knowledge. Some attractive ideas to pursue in the future would include linkers between CYT and NTX to change the physiochemical properties toward greater hydrophilicity. For instance, short polyethylene glycol linkers may lower the volume of distribution of the codrug and increase its solubility and oral absorption; however, they would also change the stability properties of the codrug in the GI tract.

With regard to bioavailability measurements of constituent CYT and NTX, bolus doses of CYT and NTX alone should be administered to the S-D rat to make

more appropriate bioavailability estimates of the constituent drugs released from the codrug *in vivo (*after the fate of CYT is sorted out). Also, these data could be greatly enhanced by a greater power of n = 8 – 10 animals per group, because it is obvious that there was substantial variability in our plasma concentration data. This is to be expected with an n = 3 animal study. However, we were interested in obtaining preliminary evidence that CYT-NTX can be hydrolyzed in the S-D rat, and our data clearly show this to be the case. CYT-NTX can therefore be considered a lead compound for further study and development, but not as an effective delivery system of CYT and NTX under the present observations.

Table 7.1 Optimal ion source settings for each MRM transition

	Q1	Q3	Time (msec)	DP (volts)	CE (volts)	CXP (volts)
CYT	191.126	148.2	200	36	33	8
	191.126	133.1	200	36	41	6
CYT-NTX codrug	558.213	540.2	200	121	43	14
	558.213	217.3	200	121	61	12
	558.213	350.2	200	121	51	8
	558.213	235.2	200	121	55	14
	558.213	431.2	200	121	47	10
	558.213	486.3	200	121	49	12
NTX	342.123	324.1	200	96	31	16
	342.123	270.1	200	96	37	16
salicylamide	137.997	121.1	200	101	23	6
	137.997	65.1	200	101	37	10

Table 7.2 Two-compartmental pharmacokinetic parameters of NTX after administration to male rats of 1.0 mg/kg (1.79 x 10^3 nmol/kg) CYT-NTX codrug i.v. or 10.0 mg/kg (1.79 x 10^4 nmol/kg) p.o. *Data are represented as mean ± SEM, n =3 of CYT-NTX codrug for each route (p.o. and i.v.).*

PK Parameter	Codrug (i.v.)	Codrug (p.o.)	NTX (i.v.)	NTX (p.o.)
Dose (nmol/kg)	1.79 x 10^3	1.79 x 10^4	1.79 x 10^3	1.79 x 10^4
C_{max} (nmol/L)	–	9.7±1.4	9.6±2.8	6.8±0.9
t_{max} (hr)	–	0.74±0.04	–	1.08±0.36
$t_{1/2}$ (hr)	1.32±0.63	2.60±1.05	2.50±0.05	2.72±2.43
$t_{1/2(a)}$ (hr)	–	0.30 ± 0.04	–	–
$AUC_{(0\text{-inf})}$ (hr•nmol/L)	237±103	26.9±2.8	27.0±0.6	34.8±15.9
V_d (L/kg)	17.7±9.2	–	–	–
CL_{tot} (L/min/kg)	0.126±0.1	–	–	–
Apparent F%	100	1.02 ± 0.1	–	–

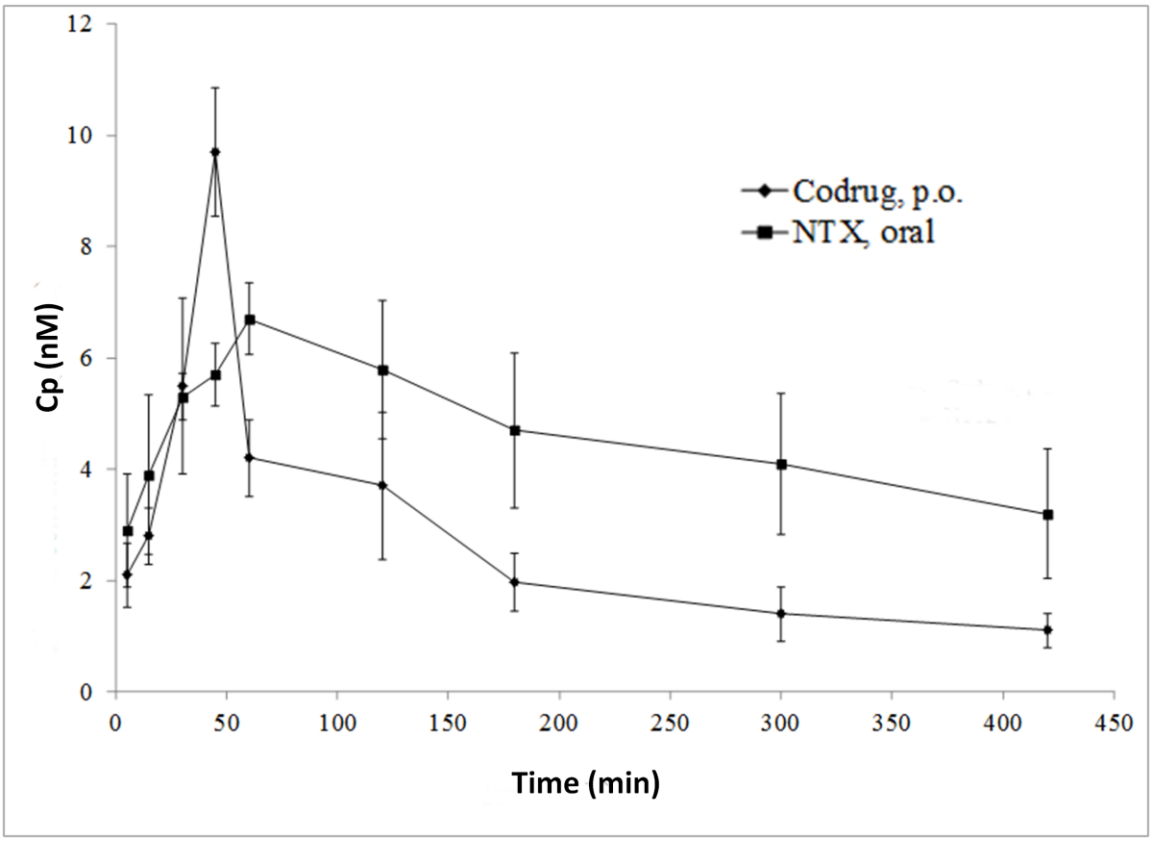

Figure 7.1 Plot of mean plasma concentration vs. time of the CYT-NTX codrug and NTX released from the codrug after a single oral dose of 1.79 x 10^4 nmol/kg. *Results are the mean of 3 rats ± SEM.*

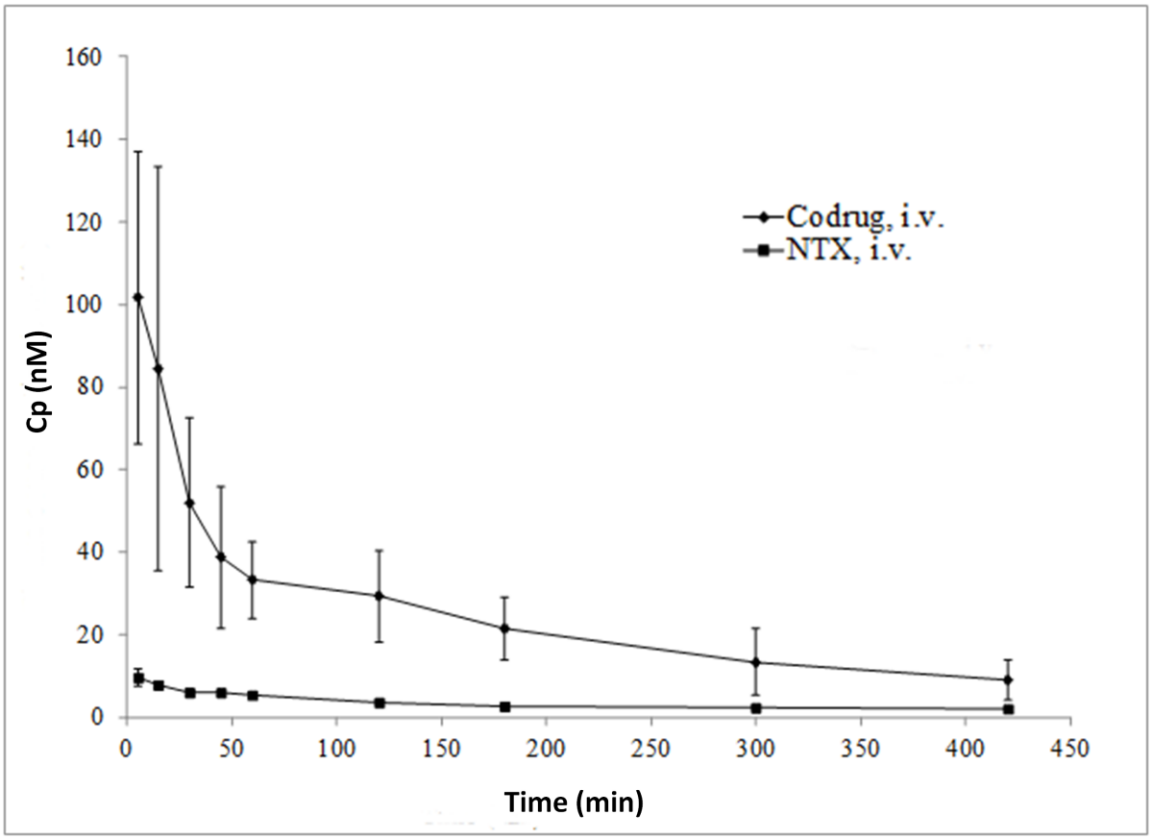

Figure 7.2 Plot of mean plasma concentration vs. time of the CYT-NTX codrug and NTX released from the codrug after a single intravenous dose of 1.79 x 10^3 nmol/kg. *Results are the mean of 3 rats ± SEM.*

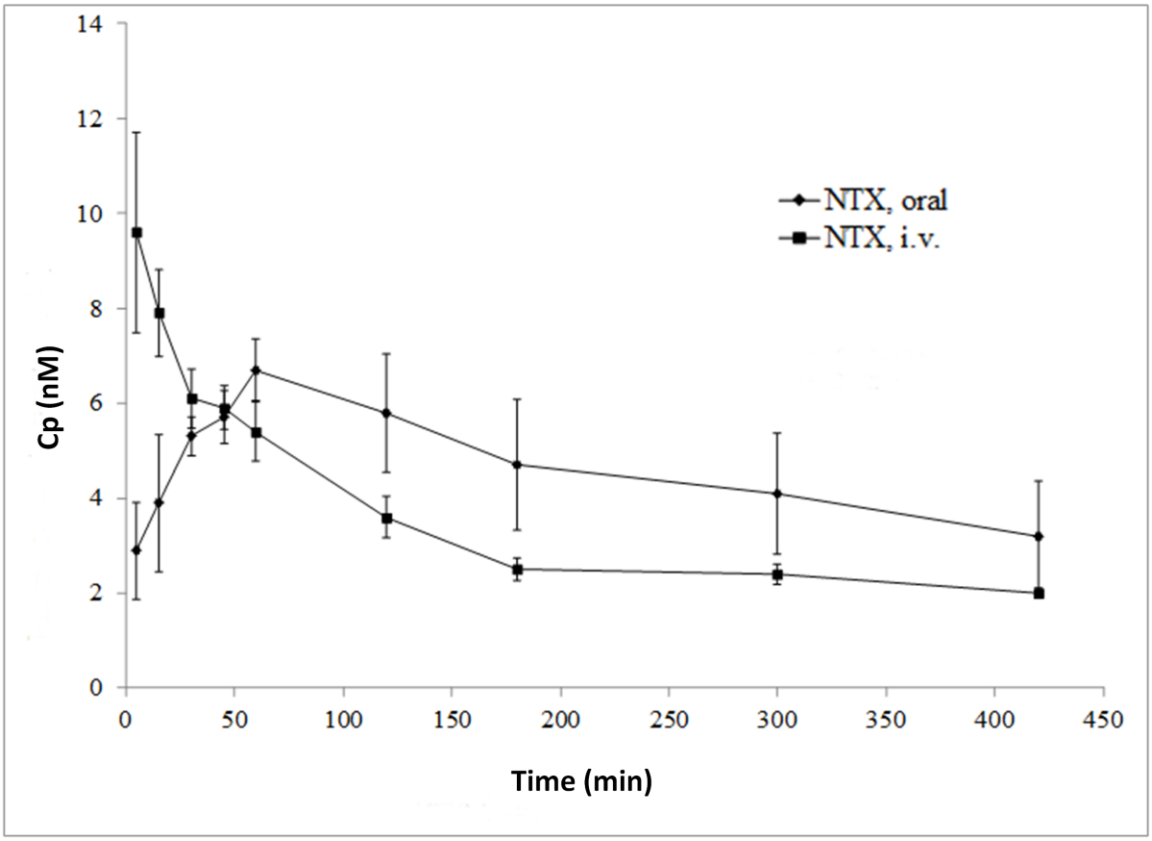

Figure 7.3 Plot of mean plasma concentration vs. time of NTX released from CYT-NTX codrug after oral and i.v. administration. *Results are the mean of 3 rats ± SEM.*

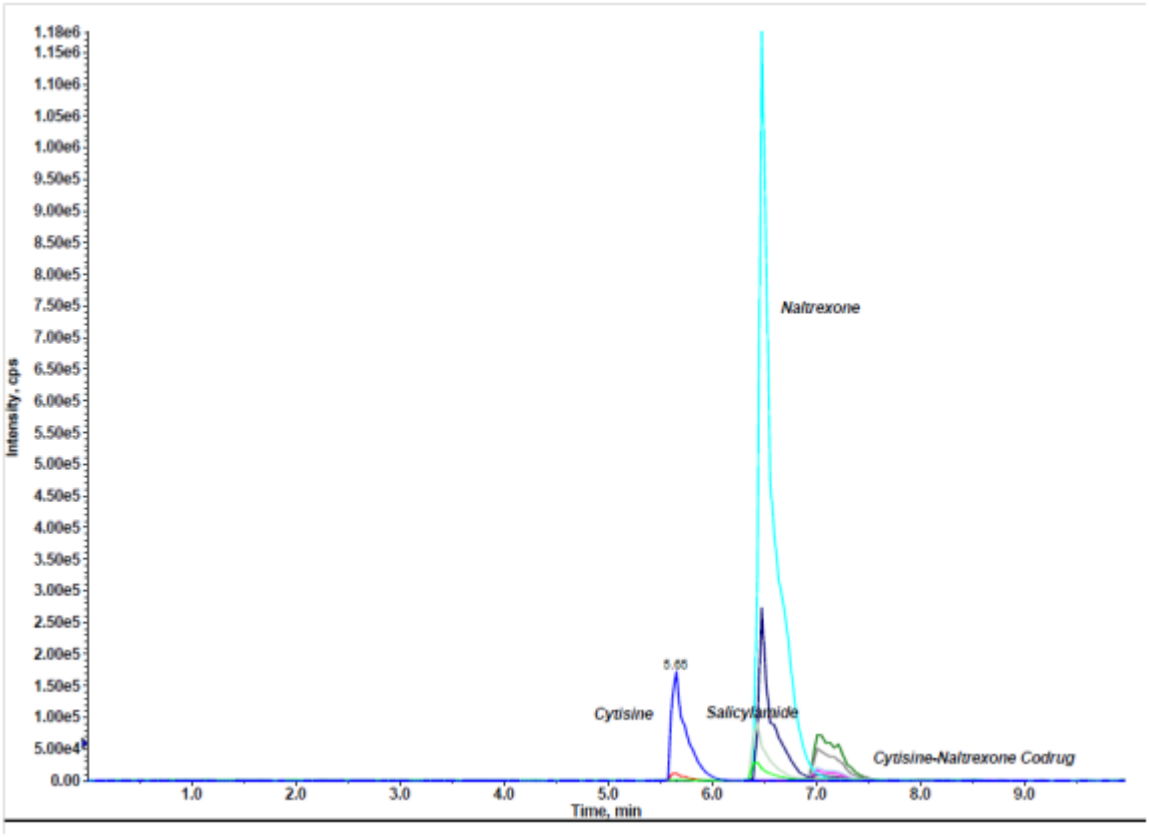

Figure 7.4A LC-MS/MS chromatogram of (-)-cytisine, salicylamide, NTX and the CYT-NTX codrug.

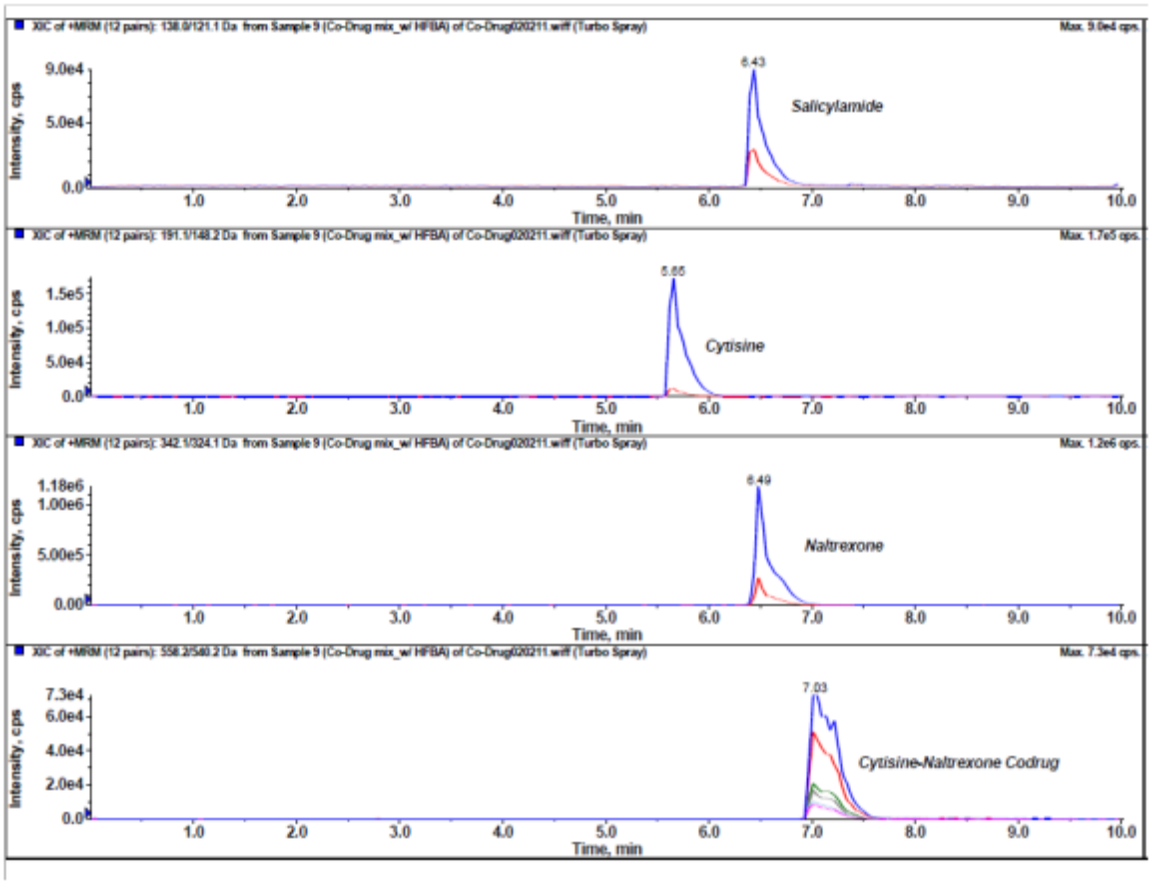

Figure 7.4B LC-MS/MS extracted ion chromatograms of (-)-cytisine, salicylamide, NTX and the CYT-NTX codrug.

Chapter 8

Summary

There exists an ongoing need for new medications that can provide efficacy in the treatment of alcohol abuse and nicotine addiction with minimal side effects. This project was designed to address two specific populations of drug-addicted individuals. The first target population was those individuals who abuse alcohol, but do not smoke cigarettes as well. The second target population was the group of individuals who smoke cigarettes and abuse alcohol simultaneously. For those who abuse alcohol but do not smoke, NTX is often a medication that is prescribed. However, NTX is not without its limitations, as it exhibits poor bioavailability and gastrointestinal side effects in addition to dose-dependent hepatotoxicity. In particular, patients who would need higher levels of NTX to achieve relief from craving, and who are also already hepatocompromised from their drug abuse behaviors, would be excluded from therapeutic outcomes of NTX oral dosage forms. Transdermal delivery is an attractive alternative to the oral route of drug administration; however, NTX does not possess the necessary physiochemical properties that would allow it to be dosed efficaciously by the percutaneous route. To solve this problem, it was envisioned that highly water soluble prodrugs of NTX or its active metabolite 6-β-naltrexol (NTXOL) could possibly serve as dosage forms for microneedle-enhanced transdermal delivery (MNTD). Accordingly, we designed synthetic strategies to afford phenolic amino acid esters of NTX using carbodiimide coupling techniques and BOC protecting groups. Deprotection of BOC from the prodrugs required multiple studies to find

conditions that preserved the ester linker moiety, and 4N HCl in dioxane proved to be the reagent of choice. Unfortunately, the phenolic prodrugs of NTX were triaged early in our stability studies due to rapid degradation at skin-relevant pHs. In subsequent efforts to stay with the popular amino acid prodrug theme, we designed regioselective synthetic strategies to afford aliphatic amino acid ester prodrugs of NTXOL. The chemistry was much more difficult to achieve our goal in the 6-*O*-NTXOL prodrugs series, due to design limitations that required orthogonal protecting groups and fairly unconventional deblocking strategies in synthetic procedures. For instance, problems arose when BOC methodology was applied to the 6-*O*-NTXOL series of prodrugs due to hygroscopic end products that could not be isolated in pure form. Likewise, solid phase peptide synthesis strategies failed to afford our desired prodrugs. Eventually, a combination of Fmoc and Allyl protecting groups proved to be the route to success in our synthesis efforts, although some of the most hydrophilic prodrugs suffered from apparent degradation during purification by column chromatography. Nonetheless, of the six 6-*O*-NTXOL amino acid prodrugs that were synthesized and tested, three of the compounds proved to be stable enough in pH 5.0 donor solution for further evaluation at pH 7.4 (enzymatic and non-enzymatic conditions). 6-*O*-Ile-NTXOL had the best pH 5.0 stability, but it was also very stable at pH 7.4, and showed evidence of protein binding in plasma with a longer half-life under conditions of enzymatic challenge as compared to blank buffer. The Ile prodrug was also crystalline in nature, and it easily crystallized out from solution at pH 7.4. 6-*O*-Val-NTXOL had similar

stability at pH 5.0 and pH 7.4 compared to 6-*O*-β-Ala-NTXOL, but the Val prodrug was also prone to precipitation at pH 7.4, and it too showed evidence of protein binding in plasma stability studies due to an increased half-life compared to that observed in blank buffer. In contrast, 6-*O*-β-Ala-NTXOL was established as the lead compound amongst the three MNTD candidates due to its faster rate of hydrolysis in human plasma. However, further skin diffusion and disposition studies would be needed to assess its rate of bioconversion and microchannel transport in skin. Unfortunately, MNTD analyses require multi-gram amounts of prodrug, and scale-up efforts to afford enough 6-*O*-β-Ala-NTXOL were unsuccessful. Thus, the 6-*O*-NTXOL amino acid esters were so difficult to synthesize that they were disqualified from further development. Indeed, scale-up problems are well known in the pharmaceutical industry, and they are often the reason for the termination of many promising clinical candidates.

In order to treat the second target population of individuals who abuse alcohol and smoke cigarettes simultaneously, a dual therapeutic strategy was indicated. This is true because consumption of either alcohol or tobacco alone serves as a cue for abuse of the other (comorbidity). In the case of patients belonging to this population, we envisioned that an oral codrug of NTX conjugated to (-)-cytisine (a smoking cessation agent used in Europe) could be a plausible therapeutic agent to approach the treatment of both addictions with a single drug molecule (i.e. a codrug).

In order to justify a codrug design, it should not be feasible to simply prepare a dosage form that contains a physical mixture of the two constituent drugs. Our

decision to prepare the CYT-NTX codrug as an oral drug delivery candidate was based on three critical design features. First, CYT and NTX are both known to exhibit poor oral bioavailability. Second, the pharmacokinetics of CYT and NTX are not amenable to dosing the two drugs as a physical mixture. Third, the therapeutic windows of CYT and NTX overlap. For instance, NTX dosed at 50-100 mg/day with a 5-40% bioavailability corresponds to 7-118 μmol/day while CYT dosed at 9 mg/day with 32.18% bioavailability corresponds to a 14.8 μmol/day dose. Therefore, we decided to pursue the CYT-NTX codrug design.

The CYT-NTX codrug was afforded in good yield using a novel and facile one-pot microwave chemistry procedure. The carbamate linker was found to be stable over the time course of 24 h in buffer systems held at pH 1.5, 5.0, 7.4 and 9.0, and in 80% rat plasma, 80% human plasma, simulated gastric fluid and simulated intestinal fluid. Such stability studies are conducted in the pharmaceutical industry to assay drug candidates for stability in the gastrointestinal tract. Thus, our *in vitro* stability work provided evidence that CYT-NTX would be expected to survive the rigors of oral dosing in a living animal.

In order to determine *in vivo* performance of CYT-NTX, we chose the adult male Sprague-Dawley rat as an animal model. Six (3 rats/group) S-D rats were dosed i.v. with 1.0 mg/kg CYT-NTX codrug, or 10.0 mg/kg, p.o. Plasma CYT-NTX codrug, NTX and CYT concentrations were quantitated with a sensitive LC-MS/MS method. The plasma PK parameters of CYT-NTX and NTX were calculated using a two-compartment open model. The oral route of administration

resulted in greater plasma levels of NTX than those observed following intravenous administration. Comparatively, the fraction of intravenously administered codrug that was converted to NTX was 11%, while the fraction of orally administered codrug converted to NTX was 13%. Furthermore, the oral delivery profile showed higher mean plasma levels of NTX compared to codrug at all time points after $t_{max(codrug)}$, while i.v. administration resulted in higher plasma levels of codrug compared to NTX at all time points up to the 7 hour end point of the study. Oral administration of the CYT-NTX codrug also resulted in rapid absorption and distribution (5 min) of the codrug, and NTX was released from codrug with a peak plasma concentration of 6.8 ± 0.9 nM reached at 1.08±0.36 hours. Unfortunately, plasma CYT was not detected at any time point for reasons that remain unclear. We suspect that elimination or metabolism events may have prevented our detection and quantitation of CYT, or the drug may have evaded detection under our assay conditions. The latter point is highly unlikely, because a one-to-one molar release of CYT from the codrug at the plasma concentrations we detected in our PK study would be well within the robust detection range of CYT based on our standard curves. This is especially true in the early time points of the Cp-t curve that represents iv administration of the codrug (**Figure 7.2**). Otherwise, CYT plasma levels may have dropped below the limit of quantitation of our LC-MS/MS assay due to substantial loss of CYT by biotransformation and/or sequestration into an unknown tissue compartment, or it is also possible that the ester side of the carbamate linker of CYT-NTX cleaves readily *in vivo* to release NTX while the amide side remains intact as a carbamic

acid intermediate following release of NTX. As mentioned previously, CYT has a short half-life *in vivo*, and CYT derivatives have also been designed, because CYT is known to have poor bioavailability (Canu Boido and Sparatore 1999, Tasso, Canu Boido et al. 2009). Whatever the case, it appears that CYT-NTX is stable under the conditions that are necessary for oral delivery, and the codrug absorbs and distributes rapidly. Once in the biophase, it appears that the hydrolysis is more efficient by the oral route, which suggests that hepatic metabolism is involved. Indeed, *in vitro* experiments revealed that the codrug is stable in rat plasma over a time course of 24 hours. Overall, CYT-NTX may show promise for further development. However, determination of the fate of CYT *in vivo* would be necessary to make any claim that the codrug can function as a promising clinical candidate for the treatment of comorbid alcohol and tobacco abuse, and it is quite likely that CYT-NTX needs further structural optimization to achieve therapeutic delivery of both CYT and NTX in an animal model or a human patient.

References

(2005). "ME Global Diethylene Glycol." Retrieved January 27, 2013, from http://www.meglobal.biz/literature/product_guides/MEGlobal_DEG.pdf.

Al-Ghananeem, A. M. and P. A. Crooks (2007). "Phase I and phase II ocular metabolic activities and the role of metabolism in ophthalmic prodrug and codrug design and delivery." Molecules **12**(3): 373-388.

Altomare, C., G. Trapani, et al. (2003). "Highly water-soluble derivatives of the anesthetic agent propofol: in vitro and in vivo evaluation of cyclic amino acid esters." Eur. J. Pharm. Sci. **20**(Copyright (C) 2012 American Chemical Society (ACS). All Rights Reserved.): 17-26.

Anand, B. S., S. Katragadda, et al. (2004). "Amino acid prodrugs of acyclovir as possible antiviral agents against ocular HSV-1 infections: interactions with the neutral and cationic amino acid transporter on the corneal epithelium." Curr. Eye Res. **29**(Copyright (C) 2012 American Chemical Society (ACS). All Rights Reserved.): 153-166.

Anand, B. S. and A. K. Mitra (2002). "Mechanism of Corneal Permeation of L-Valyl Ester of Acyclovir: Targeting the Oligopeptide Transporter on the Rabbit Cornea." Pharm. Res. **19**(Copyright (C) 2012 American Chemical Society (ACS). All Rights Reserved.): 1194-1202.

Balimane, P. V., I. Tamai, et al. (1998). "Direct evidence for peptide transporter (PepT1)-mediated uptake of a nonpeptide prodrug, valacyclovir." Biochem. Biophys. Res. Commun. **250**(Copyright (C) 2012 American Chemical Society (ACS). All Rights Reserved.): 246-251.

Baltzer, B., E. Binderup, et al. (1980). "Mutual pro-drugs of beta-lactam antibiotics and beta-lactamase inhibitors." J Antibiot (Tokyo) **33**(10): 1183-1192.

Banks, S. L., R. R. Pinninti, et al. (2008). "Flux Across Microneedle-treated Skin is Increased by Increasing Charge of Naltrexone and Naltrexol In Vitro." Pharm. Res. **25**(Copyright (C) 2012 American Chemical Society (ACS). All Rights Reserved.): 1677-1685.

Banks, S. L., R. R. Pinninti, et al. (2008). "Flux across microneedle-treated skin is increased by increasing charge of naltrexone and naltrexol in vitro. [Erratum to document cited in CA149:062101]." Pharm. Res. **25**(8): 1964.

Banks, S. L., R. R. Pinninti, et al. (2010). "Transdermal delivery of naltrexol and skin permeability lifetime after microneedle treatment in hairless guinea pigs." J. Pharm. Sci. **99**(Copyright (C) 2012 American Chemical Society (ACS). All Rights Reserved.): 3072-3080.

Beales, D. L., H. C. Burry, et al. (1972). "Comparison of aspirin and benorylate in the treatment of rheumatoid arthritis." Br Med J **2**(5812): 483-485.

Beauchamp, L. M., G. F. Orr, et al. (1992). "Amino acid ester prodrugs of acyclovir." Antiviral Chem. Chemother. **3**(Copyright (C) 2012 American Chemical Society (ACS). All Rights Reserved.): 157-164.

Biasutto, L., E. Marotta, et al. (2007). "Ester-Based Precursors to Increase the Bioavailability of Quercetin." J. Med. Chem. **50**(Copyright (C) 2012 American Chemical Society (ACS). All Rights Reserved.): 241-253.

Bjoernsson, E., H. Nordlinder, et al. (2006). "Clinical characteristics and prognostic markers in disulfiram-induced liver injury." J. Hepatol. **44**(Copyright (C) 2012 American Chemical Society (ACS). All Rights Reserved.): 791-797.

Blum, M. R. (1983). "Pharmacokinetics of acyclovir after intravenous and oral administration." J Antimicrob Chemother **12 Suppl B**(Copyright (C) 2012 U.S. National Library of Medicine.): 29-37.

Bos, J. D. and M. M. H. M. Meinardi (2000). "The 500 Dalton rule for the skin penetration of chemical compounds and drugs." Exp. Dermatol. **9**(3): 165-169.

Bradshaw, T. D., M. C. Bibby, et al. (2002). "Preclinical evaluation of amino acid prodrugs of novel antitumor 2-(4-amino-3-methylphenyl)benzothiazoles." Mol. Cancer Ther. **1**(Copyright (C) 2012 American Chemical Society (ACS). All Rights Reserved.): 239-246.

Bradshaw, T. D., M. S. Chua, et al. (2002). "In vitro evaluation of amino acid prodrugs of novel antitumour 2-(4-amino-3-methylphenyl)benzothiazoles." Br. J. Cancer **86**(Copyright (C) 2012 American Chemical Society (ACS). All Rights Reserved.): 1348-1354.

Bradshaw, T. D., S. Wrigley, et al. (1998). "2-(4-Aminophenyl)benzothiazoles: novel agents with selective profiles of in vitro antitumor activity." Br. J. Cancer **77**(Copyright (C) 2012 American Chemical Society (ACS). All Rights Reserved.): 745-752.

Bryskier, A. (1997). "Dual β-lactam-fluoroquinolone compounds: a novel approach to antibacterial treatment." Expert Opin. Invest. Drugs **6**(10): 1479-1499.

Bryskier, A. (2005). Codrugs, American Society for Microbiology.

Bundgaard, H. (1985). Design of Prodrugs, Elsevier.

Bundgaard, H., C. Larsen, et al. (1984). "Prodrugs as drug delivery systems XXVII. Chemical stability and bioavailability of a water-soluble prodrug of metronidazole for parenteral administration." International Journal of Pharmaceutics **18**(1–2): 79-87.

Bundgaard, H., C. Larsen, et al. (1984). "Prodrugs as drug delivery systems. XXVI. Preparation and enzymic hydrolysis of various water-soluble amino acid esters of metronidazole." Int. J. Pharm. **18**(Copyright (C) 2012 American Chemical Society (ACS). All Rights Reserved.): 67-77.

Canu Boido, C. and F. Sparatore (1999). "Synthesis and preliminary pharmacological evaluation of some cytisine derivatives." Il Farmaco **54**(7): 438-451.

Carvalho, E., J. Iley, et al. (1998). "Triazene drug metabolites: Part 15. Synthesis and plasma hydrolysis of anticancer triazenes containing amino acid carriers." Pharm. Res. **15**(Copyright (C) 2012 American Chemical Society (ACS). All Rights Reserved.): 931-935.

Carvalho, E., J. Iley, et al. (1998). "Triazene drug metabolites. Part 16. Kinetics and mechanism of the hydrolysis of aminoacyltriazenes." J. Chem. Soc., Perkin Trans. 2(Copyright (C) 2012 American Chemical Society (ACS). All Rights Reserved.): 2375-2380.

Carvalho, E., J. Iley, et al. (1993). "Triazene drug metabolites. Part 13. The decomposition of 3-acyl-3-alkyl-1-aryltriazenes in aqueous sulfuric acid." J. Chem. Soc., Perkin Trans. 2(Copyright (C) 2012 American Chemical Society (ACS). All Rights Reserved.): 865-870.

Chakraborty, U. (2011). Opioid Codrugs For Pain Management. Ph.D. Chemistry Doctoral Dissertation, University Of Kentucky.

Chandrasekhar, S., R. C. Raji, et al. (2001). "Facile and selective cleavage of allyl ethers, amines and esters using polymethylhydrosiloxane-ZnCl2/Pd(PPh3)4." Tetrahedron **57**(16): 3435-3438.

Chandrasekhar, S., Y. R. Reddy, et al. (1997). "Chemoselective reduction of carbonyl compounds with PMHS - ZnCl2." Synth. Commun. **27**(13): 2251-2254.

Colla, L., R. Busson, et al. (1983). "Synthesis and antiviral activity of water-soluble esters of acyclovir [9-[(2-hydroxyethoxy)methyl]guanine]." J Med Chem **26**(Copyright (C) 2012 U.S. National Library of Medicine.): 602-604.

Corey, E. J. and A. Venkateswarlu (1972). "Protection of hydroxyl groups as tert-butyldimethylsilyl derivatives." J. Amer. Chem. Soc. **94**(17): 6190-6191.

Covyeou, J. A., K. E. Atto, et al. (2011). "Case report of severe injection site reaction associated with intramuscular naltrexone." Am. J. Pharmacol. Toxicol. **6**(Copyright (C) 2012 American Chemical Society (ACS). All Rights Reserved.): 1-4.

Crooks, P. A., H. K. Dhooper, et al. (2011). "Improving the use of drug combinations through the codrug approach." Methods Princ. Med. Chem. **47**(Prodrugs and Targeted Delivery): 347-383.

Cynkowski, T., G. Cynkowska, et al. (2008). Codrugs: potential therapies for dermatological diseases, Informa Healthcare.

Das, K. M., J. R. Chowdhury, et al. (1979). "Small bowel absorption of sulfasalazine and its hepatic metabolism in human beings, cats, and rats." Gastroenterology **77**(Copyright (C) 2012 American Chemical Society (ACS). All Rights Reserved.): 280-284.

Das, K. M., M. A. Eastwood, et al. (1973). "Adverse reactions during salicylazosulfapyridine therapy and the relation with drug metabolism and acetylator phenotype." N Engl J Med **289**(Copyright (C) 2012 U.S. National Library of Medicine.): 491-495.

Das, N., M. Dhanawat, et al. (2010). "Codrug: An efficient approach for drug optimization." Eur. J. Pharm. Sci. **41**(5): 571-588.

Das, N., M. Dhanawat, et al. (2010). "Codrug: an efficient approach for drug optimization." Eur J Pharm Sci **41**(5): 571-588.

De, C. B. R., M. J. Iadarola, et al. (1992). "Probes for narcotic receptor mediated phenomena. 18. Epimeric 6α- and 6β-iodo-3,14-dihydroxy-17-(cyclopropylmethyl)-4,5α-epoxymorphinans as potential ligands for opioid receptor single photon emission computed tomography: synthesis, evaluation, and radiochemistry of [125I]-6β-iodo-3,14-dihydroxy-17-(cyclopropylmethyl)-4,5α-epoxymorphinan." J. Med. Chem. **35**(15): 2826-2835.

Di, L., E. H. Kerns, et al. (2005). "Development and application of high throughput plasma stability assay for drug discovery." International Journal of Pharmaceutics **297**(1–2): 110-119.

Dressman, B. A., L. A. Spangle, et al. (1996). "Solid phase synthesis of hydantoins using a carbamate linker and a novel cyclization / cleavage step." Tetrahedron Letters **37**(7): 937-940.

Duffel, M. W., I. S. Ing, et al. (1986). "N-Substituted sulfonamide carbonic anhydrase inhibitors with topical effects on intraocular pressure." J. Med. Chem. **29**(Copyright (C) 2012 American Chemical Society (ACS). All Rights Reserved.): 1488-1494.

Dwoskin, L. P., A. M. Smith, et al. (2009). "Nicotinic receptor-based therapeutics and candidates for smoking cessation." Biochem. Pharmacol. **78**(7): 732-743.

Etter, J.-F. (2006). "Cytisine for smoking cessation: a literature review and a meta-analysis." Arch Intern Med **166**(15): 1553-1559.

Etter, J.-F., R. J. Lukas, et al. (2008). "Cytisine for smoking cessation: A research agenda." Drug Alcohol Depend. **92**(1-3): 3-8.

Farese-Di, G. A., M. Rouquayrol, et al. (2000). "Synthesis and anti-HIV activity of prodrugs derived from saquinavir and indinavir." Antivir Chem Chemother **11**(Copyright (C) 2012 U.S. National Library of Medicine.): 97-110.

Forest. (2004, January 2012). "Campral® (acamprosate calcium) Delayed-Release Tablets. Highlights of Prescribing Information." Retrieved January 27, 2013, 2013, from http://www.frx.com/pi/campral_pi.pdf.

Frenk, H. and R. Dar (2011). "If the data contradict the theory, throw out the data: Nicotine addiction in the 2010 report of the Surgeon General." Harm Reduct J **8**: 12.

Frosch, D. L., S. Shoptaw, et al. (2000). "Associations between tobacco smoking and illicit drug use among methadone-maintained opiate-dependent individuals." Exp Clin Psychopharmacol **8**(1): 97-103.

Garbutt, J. C. (2006). "New therapeutic options for alcohol dependence: long-acting intramuscular formulations of naltrexone." J. Clin. Psychiatry (Memphis, TN, U. S.) **67**(Copyright (C) 2012 American Chemical Society (ACS). All Rights Reserved.): 30-34.

Gaucher, B., M. Rouquayrol, et al. (2004). "Prodrugs of HIV protease inhibitors-saquinavir, indinavir and nelfinavir-derived from diglycerides or amino acids: synthesis, stability and anti-HIV activity." Org. Biomol. Chem. **2**(Copyright (C) 2012 American Chemical Society (ACS). All Rights Reserved.): 345-357.

Gill, H. S. and M. R. Prausnitz (2007). "Coated microneedles for transdermal delivery." J. Controlled Release **117**(Copyright (C) 2012 American Chemical Society (ACS). All Rights Reserved.): 227-237.

Granero, G. E. and G. L. Amidon (2006). "Stability of valacyclovir: Implications for its oral bioavailability." Int. J. Pharm. **317**(Copyright (C) 2012 American Chemical Society (ACS). All Rights Reserved.): 14-18.

Hajek, P., H. McRobbie, et al. (2013). "Efficacy of cytisine in helping smokers quit: systematic review and meta-analysis." Thorax.

Hamad, M. O., P. K. Kiptoo, et al. (2006). "Synthesis and hydrolytic behavior of two novel tripartate codrugs of naltrexone and 6β-naltrexol with hydroxybupropion as potential alcohol abuse and smoking cessation agents." Bioorg. Med. Chem. **14**(20): 7051-7061.

Hammell, D. C., M. Hamad, et al. (2004). "A duplex "Gemini" prodrug of naltrexone for transdermal delivery." J. Controlled Release **97**(2): 283-290.

Hammell, D. C., E. I. Stolarczyk, et al. (2005). "Bioconversion of naltrexone and its 3-O-alkyl-ester prodrugs in a human skin equivalent." J. Pharm. Sci. **94**(4): 828-836.

Han, H. K., D. M. Oh, et al. (1998). "Cellular uptake mechanism of amino acid ester prodrugs in Caco-2/hPEPT1 cells overexpressing a human peptide transporter." Pharm Res **15**(Copyright (C) 2012 U.S. National Library of Medicine.): 1382-1386.

Harnden, M. R., R. L. Jarvest, et al. (1987). "Synthesis and antiviral activity of 9-[4-hydroxy-3-(hydroxymethyl)but-1-yl]purines." J Med Chem **30**(9): 1636-1642.

Harnden, M. R., R. L. Jarvest, et al. (1989). "Prodrugs of the selective antiherpesvirus agent 9-[4-hydroxy-3-(hydroxymethyl)but-1-yl]guanine (BRL 39123) with improved gastrointestinal absorption properties." J Med Chem **32**(Copyright (C) 2012 U.S. National Library of Medicine.): 1738-1743.

Hegarty, A. F. and L. N. Frost (1972). "Isocyanate intermediates in Elcb mechanism of carbamate hydrolysis." J. Chem. Soc., Chem. Commun.(9): 500-501.

Henry, S., D. V. McAllister, et al. (1998). "Microfabricated Microneedles: A Novel Approach to Transdermal Drug Delivery." J. Pharm. Sci. **87**(Copyright (C) 2012 American Chemical Society (ACS). All Rights Reserved.): 922-925.

Higuchi, T. and V. Stella (1975). ACS Symposium Series, Vol. 14: Pro-Drugs as Novel Drug Delivery Systems, ACS.

Holtman, J. R., P. A. Crooks, et al. (2009). Opioid-ketamine and norketamine codrug combinations for pain management, University of Kentucky Research Foundation, USA . 55pp.

Holtman, J. R., P. A. Crooks, et al. (2009). Opioid-nornicotine codrugs for pain management, University of Kentucky Research Foundation, USA . 78 pp.

Houston, J. B. (1981). "Drug metabolite kinetics." Pharmacology & Therapeutics **15**(3): 521-552.

Hutchinson, I., M.-S. Chua, et al. (2001). "Antitumor Benzothiazoles. 14. Synthesis and in Vitro Biological Properties of Fluorinated 2-(4-Aminophenyl)benzothiazoles." J. Med. Chem. **44**(Copyright (C) 2012 American Chemical Society (ACS). All Rights Reserved.): 1446-1455.

Hutchinson, I., S. A. Jennings, et al. (2002). "Antitumor Benzothiazoles. 16. Synthesis and Pharmaceutical Properties of Antitumor 2-(4-Aminophenyl)benzothiazole Amino Acid Prodrugs." J. Med. Chem. **45**(Copyright (C) 2012 American Chemical Society (ACS). All Rights Reserved.): 744-747.

Iley, J., G. Ruecroft, et al. (1989). "Triazene drug metabolites. Part 9. Base-catalyzed deacylation of 3-acyl-3-alkyl-1-aryltriazenes in ethanol." J. Chem. Res., Synop.(Copyright (C) 2012 American Chemical Society (ACS). All Rights Reserved.): 162-163.

Imai, T. (2012). "Esterase-targeted drug design. Prodrugs and antedrugs." Farumashia **48**(7): 668-672.

Jain-Vakkalagadda, B., S. Dey, et al. (2003). "Identification and functional characterization of a Na+-independent large neutral amino acid transporter, LAT1, in human and rabbit cornea." Invest Ophthalmol Vis Sci **44**(Copyright (C) 2012 U.S. National Library of Medicine.): 2919-2927.

Jain-Vakkalagadda, B., D. Pal, et al. (2004). "Identification of a Na+-Dependent Cationic and Neutral Amino Acid Transporter, B0,+, in Human and Rabbit Cornea." Mol. Pharm. **1**(Copyright (C) 2012 American Chemical Society (ACS). All Rights Reserved.): 338-346.

Jung, Y.-C. and K. Namkoong (2006). "Pharmacotherapy for alcohol dependence: anticraving medications for relapse prevention." Yonsei Med. J. **47**(2): 167-178.

Kai, E., K. Tapani, et al. (2009). "Fosphenytoin." Expert Opin. Drug Metab. Toxicol. **5**(6): 695-701.

Kashiyama, E., I. Hutchinson, et al. (1999). "Antitumor benzothiazoles. 8. Synthesis, metabolic formation, and biological properties of the C- and N-oxidation products of antitumor 2-(4-aminophenyl)benzothiazoles." J. Med. Chem. **42**(Copyright (C) 2012 American Chemical Society (ACS). All Rights Reserved.): 4172-4184.

Katragadda, S., R. Jain, et al. (2008). "Pharmacokinetics of amino acid ester prodrugs of acyclovir after oral administration: Interaction with the transporters on Caco-2 cells." Int. J. Pharm. **362**(Copyright (C) 2012 American Chemical Society (ACS). All Rights Reserved.): 93-101.

Katragadda, S., R. Talluri, et al. (2005). "Identification and Characterization of a Na+-Dependent Neutral Amino Acid Transporter, ASCT1, in Rabbit Corneal Epithelial Cell Culture and Rabbit Cornea." Curr. Eye Res. **30**(Copyright (C) 2012 American Chemical Society (ACS). All Rights Reserved.): 989-1002.

Keating, G. M. and K. A. Lyseng-Williamson (2010). "Pharmacoeconomic spotlight on varenicline as an aid to smoking cessation." CNS Drugs **24**(9): 797-800.

Kemeny, N., Y. Huang, et al. (1999). "Hepatic arterial infusion of chemotherapy after resection of hepatic metastases from colorectal cancer." N Engl J Med **341**(27): 2039-2048.

Kim, D.-K., N. Lee, et al. (1996). "Synthesis and evaluation of amino acid ester prodrugs of penciclovir." Bioorganic & Medicinal Chemistry Letters **6**(15): 1849-1854.

Kiptoo, P. K., M. O. Hamad, et al. (2006). "Enhancement of transdermal delivery of 6-beta-naltrexol via a codrug linked to hydroxybupropion." J Control Release **113**(2): 137-145.

Kiptoo, P. K., K. S. Paudel, et al. (2008). "In vivo evaluation of a transdermal codrug of 6-beta-naltrexol linked to hydroxybupropion in hairless guinea pigs." Eur J Pharm Sci **33**(4-5): 371-379.

Kiptoo, P. K., K. S. Paudel, et al. (2009). "Transdermal delivery of bupropion and its active metabolite, hydroxybupropion: a prodrug strategy as an alternative approach." J. Pharm. Sci. **98**(2): 583-594.

Krasny, H. C., D. A. Page, et al. (1981). "The disposition of acyclovir in different species." J Pharmacol Exp Ther **219**(Copyright (C) 2012 U.S. National Library of Medicine.): 309-315.

Lark, B. S., P. Patyar, et al. (2007). "Temperature effect on the viscosity and heat capacity behaviour of some amino acids in water and aqueous magnesium chloride solutions." J. Chem. Thermodyn. **39**(3): 344-360.

Larsen, J. D., H. Bundgaard, et al. (1988). "Prodrug forms for the sulfonamide group. II. Water-soluble amino acid derivatives of N-methylsulfonamides as possible prodrugs." Int. J. Pharm. **47**(Copyright (C) 2012 American Chemical Society (ACS). All Rights Reserved.): 103-110.

Lau, W. M., A. W. White, et al. (2008). "Scope and limitations of the co-drug approach to topical drug delivery." Curr. Pharm. Des. **14**(8): 794-802.

LeSage, M. G., D. Shelley, et al. (2009). "Effects of the nicotinic receptor partial agonists varenicline and cytisine on the discriminative stimulus effects of nicotine in rats." Pharmacol., Biochem. Behav. **91**(3): 461-467.

Li, W.-b., F.-h. Dong, et al. (2012). "Application of prodrug design in research and development of oral drugs." Yaoxue Jinzhan **36**(8): 347-355.

Lorenzi, P. L., C. P. Landowski, et al. (2006). "N-methylpurine DNA glycosylase and 8-oxoguanine DNA glycosylase metabolize the antiviral nucleoside 2-bromo-5,6-dichloro-1-(β-D-ribofuranosyl)benzimidazole." Drug Metab. Dispos. **34**(Copyright (C) 2012 American Chemical Society (ACS). All Rights Reserved.): 1070-1077.

Lorenzi, P. L., C. P. Landowski, et al. (2005). "Amino acid ester prodrugs of 2-bromo-5,6-dichloro-1-(beta-D-ribofuranosyl)benzimidazole enhance metabolic stability in vitro and in vivo." J Pharmacol Exp Ther **314**(2): 883-890.

Ludden, T. M., S. L. Beal, et al. (1994). "Comparison of the Akaike Information Criterion, the Schwarz criterion and the F test as guides to model selection." J Pharmacokinet Biopharm **22**(5): 431-445.

Lukas, R. J. (2007). Pharmacological effects of nicotine and nicotinic receptor subtype pharmacological profiles, CRC Press LLC.

Lupia, R. H., N. Ferencz, et al. (1993). "Comparative pharmacokinetics of two prodrugs of zidovudine in rabbits: enhanced levels of zidovudine in brain tissue." Antimicrob. Agents Chemother. **37**(Copyright (C) 2012 American Chemical Society (ACS). All Rights Reserved.): 818-824.

Mahdi, M. F. and H. N. Alsaad (2012). "Design, synthesis and hydrolytic behavior of mutual prodrugs of NSAIDs with gabapentin using glycol spacers." Pharmaceuticals **5**: 1080-1091.

Maren, T. H. (1956). "Carbonic anhydrase inhibition. V. N5-Substituted 2-acetamido-1,3,4-thiadiazole-5-sulfonamides; their metabolic conversion and use as control substances." J. Pharmacol. Exp. Ther. **117**(Copyright (C) 2012 American Chemical Society (ACS). All Rights Reserved.): 385-401.

McAllister, D. V., P. M. Wang, et al. (2003). "Microfabricated needles for transdermal delivery of macromolecules and nanoparticles: Fabrication methods and transport studies." Proc. Natl. Acad. Sci. U. S. A. **100**(Copyright (C) 2012 American Chemical Society (ACS). All Rights Reserved.): 13755-13760.

Mello, N. K., J. H. Mendelson, et al. (1987). "Cigarette smoking by women: interactions with alcohol use." Psychopharmacology (Berl) **93**(1): 8-15.

Milewski, M. (2011). MICRONEEDLE-ASSISTED TRANSDERMAL DELIVERY OF NALTREXONE SPECIES: IN VITRO PERMEATION AND IN VIVO PHARMACOKINETIC STUDIES. Ph.D. Pharmaceutical Sciences, University of Kentucky.

Milewski, M., N. K. Brogden, et al. (2010). "Current aspects of formulation efforts and pore lifetime related to microneedle treatment of skin." Expert Opin. Drug Delivery **7**(Copyright (C) 2012 American Chemical Society (ACS). All Rights Reserved.): 617-629.

Milewski, M. and A. L. Stinchcomb (2011). "Vehicle Composition Influence on the Microneedle-Enhanced Transdermal Flux of Naltrexone Hydrochloride." Pharm. Res. **28**(Copyright (C) 2012 American Chemical Society (ACS). All Rights Reserved.): 124-134.

Milewski, M., T. R. Yerramreddy, et al. (2010). "In vitro permeation of a pegylated naltrexone prodrug across microneedle-treated skin." J. Controlled Release **146**(1): 37-44.

Mineur, Y. S., O. Somenzi, et al. (2007). "Cytisine, a partial agonist of high-affinity nicotinic acetylcholine receptors, has antidepressant-like properties in male C57BL/6J mice." Neuropharmacology **52**(5): 1256-1262.

Misicka, A. (2012). General strategies of peptide synthesis, CRC Press.

O'Brien, J. J. and D. M. Campoli-Richards (1989). "Acyclovir. An updated review of its antiviral activity, pharmacokinetic properties and therapeutic efficacy." Drugs **37**(Copyright (C) 2012 U.S. National Library of Medicine.): 233-309.

Oksdath-Mansilla, G. and A. B. Penenory (2007). "Simple and efficient deprotection of 1,3-dithianes and 1,3-dithiolanes by copper(II) salts under solvent-free conditions." Tetrahedron Lett. **48**(35): 6150-6154.

Paudel, K. S., B. N. Nalluri, et al. (2005). "Transdermal delivery of naltrexone and its active metabolite 6-β-naltrexol in human skin in vitro and guinea pigs in vivo." J. Pharm. Sci. **94**(9): 1965-1975.

Pellicciari, R., A. Garzon-Aburbeh, et al. (1993). "Brush-border-enzyme-mediated intestine-specific drug delivery. Amino acid prodrugs of 5-aminosalicylic acid." J. Med. Chem. **36**(Copyright (C) 2012 American Chemical Society (ACS). All Rights Reserved.): 4201-4207.

Peppercorn, M. A. (1984). "Sulfasalazine. Pharmacology, clinical use, toxicity, and related new drug development." Ann Intern Med **101**(Copyright (C) 2012 U.S. National Library of Medicine.): 377-386.

Perry, M. d. J., E. Carvalho, et al. (2009). "Towards an efficient prodrug of the alkylating metabolite monomethyltriazene: Synthesis and stability of N-acylamino acid derivatives of triazenes." Eur. J. Med. Chem. **44**(Copyright (C) 2012 American Chemical Society (ACS). All Rights Reserved.): 1049-1056.

Pillai, O., M. O. Hamad, et al. (2004). "Physicochemical Evaluation, in Vitro Human Skin Diffusion, and Concurrent Biotransformation of 3-O-Alkyl Carbonate Prodrugs of Naltrexone." Pharm. Res. **21**(7): 1146-1152.

Prausnitz, M. R. (2004). "Microneedles for transdermal drug delivery." Adv. Drug Delivery Rev. **56**(Copyright (C) 2012 American Chemical Society (ACS). All Rights Reserved.): 581-587.

Pue, M. A. and L. Z. Benet (1993). "Pharmacokinetics of famciclovir in man." Antiviral Chem. Chemother. **4**(Copyright (C) 2012 American Chemical Society (ACS). All Rights Reserved.): 47-55.

Reeves, D., D. Speller, et al. (1989). FCE 22101, a New Penem Antibacterial and Its Oral Prodrug, FCE 22891. The 28th Interscience, Conference on Antimicrobial Agents and Chemotherapy, Los Angeles, Calif. 23-26, October, 1988. [In: J. Antimicrob. Chemother., 1989; 23 (Suppl. C)], Academic.

Robertson, A., J. P. Glynn, et al. (1972). "Absorption and metabolism in man of 4-acetamidophenyl-2-acetoxybenzoate (benorylate)." Xenobiotica **2**(4): 339-347.

Roche, E. B. (1977). Design of Biopharmaceutical Properties Through Prodrugs and Analogs, American Pharmaceutical Association.

Rodgman, A., C. J. Smith, et al. (2000). "The composition of cigarette smoke: a retrospective, with emphasis on polycyclic components." Hum Exp Toxicol **19**(10): 573-595.

Rouquayrol, M., B. Gaucher, et al. (2002). "Transepithelial Transport of Prodrugs of the HIV Protease Inhibitors Saquinavir, Indinavir, and Nelfinavir Across Caco-2 Cell Monolayers." Pharm. Res. **19**(Copyright (C) 2012 American Chemical Society (ACS). All Rights Reserved.): 1704-1712.

Roy, A., M. Chatterjee, et al. (2011). "Oral pre cancerous lesions (OPL) : a clinicopatholocgical and molecular assessment for risk categorization and treatment." PHARMBIT **23/24**(1/2): 5-10.

SAMHSA. (2011, June 25, 2012). "Results from the 2011 National Survey on Drug Use and Health: Summary of National Findings, NSDUH Series H-44, HHS Publication No. (SMA) 12-4713." Retrieved January 27, 2013, 2013, from http://www.samhsa.gov/data/NSDUH/2k11Results/NSDUHresults2011.htm.

Shao, Z. and A. K. Mitra (1994). "Bile salt-fatty acid mixed micelles as nasal absorption promoters. III. Effects on nasal transport and enzymic degradation of acyclovir prodrugs." Pharm. Res. **11**(Copyright (C) 2012 American Chemical Society (ACS). All Rights Reserved.): 243-250.

Sheppeck, J. E., H. Kar, et al. (2000). "A convenient and scaleable procedure for removing the Fmoc group in solution." Tetrahedron Lett. **41**(28): 5329-5333.

Simila, S., S. Keinanen, et al. (1975). "Oral antipyretic therapy: evaluation of benorylate, an ester of acetylsalicylic acid and paracetamol." Eur J Pediatr **121**(1): 15-20.

Simmons, D. M., G. A. Portmann, et al. (1995). "Danazol Amino Acid Prodrugs: In Vitro and In Situ Biopharmaceutical Evaluation." Drug Dev. Ind. Pharm. **21**(Copyright (C) 2012 American Chemical Society (ACS). All Rights Reserved.): 687-708.

Slojkowska, Z., H. J. Krasuska, et al. (1982). "Enzymic hydrolysis of amino acid derivatives of benzocaine." Xenobiotica **12**(Copyright (C) 2012 U.S. National Library of Medicine.): 359-364.

Smith, P. L. and C. P. Lee (1998). "Transport of L-valine-acyclovir via the oligopeptide transporter in the human intestinal cell line, Caco-2." J Pharmacol Exp Ther **286**(Copyright (C) 2012 U.S. National Library of Medicine.): 1166-1170.

Song, X., B. S. Vig, et al. (2005). "Amino acid ester prodrugs of the antiviral agent 2-bromo-5,6-dichloro-1-(beta-D-ribofuranosyl)benzimidazole as potential substrates of hPEPT1 transporter." J Med Chem **48**(4): 1274-1277.

Starek, A. and I. Podolak (2009). "Carcinogenic effect of tobacco smoke." Rocz Panstw Zakl Hig **60**(4): 299-310.

Stella, V. J., R. T. Borchardt, et al. (2007). Prodrugs: Challenges and Rewards. [In: Biotechnol.: Pharm. Aspects, 2007; 5(Pt.2)], Springer.

Stinchcomb, A. L., P. W. Swaan, et al. (2002). "Straight-chain naltrexone ester prodrugs: diffusion and concurrent esterase biotransformation in human skin." J. Pharm. Sci. **91**(12): 2571-2578.

Strasinger, C. L., N. N. Scheff, et al. (2008). "Prodrugs and codrugs as strategies for improving percutaneous absorption." Expert Rev. Dermatol. **3**(2): 221-233.

Suresh, K., X. Zhu, et al. (2010). "Small neutral amino acid ester prodrugs of acyclovir targeting amino acid transporters on the cornea: possible antiviral agents against ocular HSV-1 infections." Ophthalmol. Eye Dis. **2**(Copyright (C) 2012 American Chemical Society (ACS). All Rights Reserved.): 43-56.

Sureshbabu, V. V. and H. P. Hemantha (2008). "A facile synthesis of N-Fmoc protected amino/peptidyl Weinreb amides employing acid chlorides as key intermediates." ARKIVOC (Gainesville, FL, U. S.)(2): 243-249.

Swainston, H. T., G. L. Plosker, et al. (2006). "Extended-release intramuscular naltrexone." Drugs **66**(Copyright (C) 2012 American Chemical Society (ACS). All Rights Reserved.): 1741-1751.

Taffet, S. L. and K. M. Das (1983). "Sulfasalazine. Adverse effects and desensitization." Dig Dis Sci **28**(Copyright (C) 2012 U.S. National Library of Medicine.): 833-842.

Tasso, B., C. Canu Boido, et al. (2009). "Synthesis, Binding, and Modeling Studies of New Cytisine Derivatives, as Ligands for Neuronal Nicotinic Acetylcholine Receptor Subtypes." Journal of Medicinal Chemistry **52**(14): 4345-4357.

Thomas, J. D. and K. B. Sloan (2007). "Overcoming steric effects in the coupling reaction of alkyloxycarbonyloxymethyl (AOCOM) halides with phenols: an efficient synthesis of AOCOM phenolic prodrugs." Tetrahedron Letters **48**(1): 109-112.

Trapani, G., A. Latrofa, et al. (1998). "Water-soluble salts of amino acid esters of the anesthetic agent propofol." Int. J. Pharm. **175**(Copyright (C) 2012 American Chemical Society (ACS). All Rights Reserved.): 195-204.

Tsukamoto, H. and Y. Kondo (2003). "Facile and selective cleavage of allyl ethers based on palladium(0)-catalyzed allylic alkylation of N,N'-dimethylbarbituric acid." Synlett(7): 1061-1063.

Unterwald, E. M. (2008). "Naltrexone in the treatment of alcohol dependence." J Addict Med **2**(3): 121-127.

Vaddi, H. K., M. O. Hamad, et al. (2005). "Human Skin Permeation of Branched-Chain 3-O-Alkyl Ester and Carbonate Prodrugs of Naltrexone." Pharm. Res. **22**(5): 758-765.

Valiveti, S., D. C. Hammell, et al. (2005). "In vivo evaluation of 3-O-alkyl ester transdermal prodrugs of naltrexone in hairless guinea pigs." J. Controlled Release **102**(2): 509-520.

Verbaan, F. J., S. M. Bal, et al. (2007). "Assembled microneedle arrays enhance the transport of compounds varying over a large range of molecular weight across human dermatomed skin." J. Controlled Release **117**(Copyright (C) 2012 American Chemical Society (ACS). All Rights Reserved.): 238-245.

Vere, H. R. A., D. Sutton, et al. (1989). "Selection of an oral prodrug (BRL 42810; famciclovir) for the antiherpesvirus agent BRL 39123 [9-(4-hydroxy-3-hydroxymethylbut-l-yl)guanine; penciclovir]." Antimicrob Agents Chemother **33**(Copyright (C) 2012 U.S. National Library of Medicine.): 1765-1773.

Verebey, K. (1981). "The clinical pharmacology of naltrexone: pharmacology and pharmacodynamics." NIDA Res Monogr **28**(Copyright (C) 2012 U.S. National Library of Medicine.): 147-158.

Verebey, K., J. Volavka, et al. (1976). "Naltrexone: Disposition, metabolism, and effects after acute and chronic dosing." Clin. Pharmacol. Ther. **20**(3): 315-328.

Verebey, K. G. and S. J. Mule (1986). "Naltrexone (Trexan): a review of hepatotoxicity issues." NIDA Res Monogr **67**(Copyright (C) 2012 U.S. National Library of Medicine.): 73-81.

Vermeersch, H., J. P. Remon, et al. (1990). "In vitro antitrichomonal activity of water-soluble prodrug esters of metronidazole." International Journal of Pharmaceutics **60**(3): 253-260.

Vig, B. S., K. M. Huttunen, et al. (2012). "Amino acids as promoieties in prodrug design and development." Adv Drug Deliv Rev.

Vig, B. S., P. J. Lorenzi, et al. (2003). "Amino acid ester prodrugs of floxuridine: synthesis and effects of structure, stereochemistry, and site of esterification on the rate of hydrolysis." Pharm Res **20**(9): 1381-1388.

Volpicelli, J. R. (1995). "Naltrexone in alcohol dependence." Lancet **346**(8973): 456.

Volpicelli, J. R., K. C. Rhines, et al. (1997). "Naltrexone and alcohol dependence. Role of subject compliance." Arch. Gen. Psychiatry **54**(Copyright (C) 2012 American Chemical Society (ACS). All Rights Reserved.): 737-742.

Walker, I., D. Nicholls, et al. (1994). "Drug delivery via active transport at the blood-brain barrier: affinity of a prodrug of phosphonoformate for the large amino acid transporter." Int. J. Pharm. **104**(Copyright (C) 2012 American Chemical Society (ACS). All Rights Reserved.): 157-167.

Wermeling, D. P., S. L. Banks, et al. (2008). "Microneedles permit transdermal delivery of a skin-impermeant medication to humans." Proc. Natl. Acad. Sci. U. S. A. **105**(Copyright (C) 2012 American Chemical Society (ACS). All Rights Reserved.): 2058-2063.

Wermeling, D. P., S. L. Banks, et al. (2008). "Microneedles permit transdermal delivery of a skin-impermeant medication to humans." Proc. Natl. Acad. Sci. U. S. A. **105**(6): 2058-2063.

Wexselblatt, E. and D. Gibson (2012). "What do we know about the reduction of Pt(IV) pro-drugs?" J. Inorg. Biochem. **117**: 220-229.

Yamaoka, K., T. Nakagawa, et al. (1978). "Application of Akaike's information criterion (AIC) in the evaluation of linear pharmacokinetic equations." J. Pharmacokinet. Biopharm. **6**(2): 165-175.

Yang, C., H. Gao, et al. (2001). "Chemical stability, enzymatic hydrolysis, and nasal uptake of amino acid ester prodrugs of acyclovir." J. Pharm. Sci. **90**(Copyright (C) 2012 American Chemical Society (ACS). All Rights Reserved.): 617-624.

Yang, C. and A. K. Mitra (2001). "Nasal absorption of tyrosine-linked model compounds." J. Pharm. Sci. **90**(Copyright (C) 2012 American Chemical Society (ACS). All Rights Reserved.): 340-347.

Yang, Y.-H., H. Aloysius, et al. (2011). "Enzyme-mediated hydrolytic activation of prodrugs." Acta Pharm. Sin. B **1**(3): 143-159.

Yerramreddy, T. R., M. Milewski, et al. (2010). "Novel 3-O-pegylated carboxylate and 3-O-pegylated carbamate prodrugs of naltrexone for microneedle-enhanced transdermal delivery." Bioorg. Med. Chem. Lett. **20**(11): 3280-3283.

Zatonski, W., M. Cedzynska, et al. (2006). "An uncontrolled trial of cytisine (Tabex) for smoking cessation." Tob Control **15**(6): 481-484.

Zhang, Y., X. Qu, et al. (2012). "Research progress on curcumin prodrugs." Adv. Mater. Res. (Durnten-Zurich, Switz.) **554-556**(Pt. 3, Advances in Chemistry Research II): 1857-1860.

Zhou, J., D. S. Michaud, et al. "Smokeless tobacco and risk of head and neck cancer: Evidence from a case-control study in New England." Int. J. Cancer: Ahead of Print.

Vita

Joshua A. Eldridge

EDUCATION

Bachelor of Science in Chemistry, Kentucky State University, Frankfort, KY.

Overall GPA: 3.833 Graduation: May 2006

PROFESSIONAL POSITIONS

Instructor of Medicinal Chemistry, Midway College, Paintsville, KY.

Dates of Appointment: April 2012 – March 2013

SCHOLASTIC AWARDS AND FELLOWSHIPS

Delta Epsilon Iota Academic Honor Society (2012)

Center of Membrane Sciences Graduate Student Mentoring Fellow

University of Kentucky (2010 – 2011)

Departmental 300 MHz NMR Service Technician Fellowship

University of Kentucky (2010 – 2011)

Summer Undergraduate Research Fellow

University of Kentucky (2005)

Department of Mathematics and Sciences Scholarship

Kentucky State University (2005-2006)

Award for Academic Excellence in Chemistry

Kentucky State University (2005-2006).

PUBLICATIONS

Penthala NR, Eldridge JA, Reddy TRY, Parkin S, Crooks PA. **(***E*,*E*)-1-Methyl-2,6-distyrylpyridinium iodide. Acta Crystallographica Section E Structure Reports Online [Internet]. 2010 July 1 [cited 2011 May 15]; 66(Pt 7**)**: o1793. Available

from: http://www.ncbi.nlm.nih.gov/pmc/articles/PMC3006972/pdf/e-66-o1793.pdf

Lu X, Howard MD, Mazik M, Eldridge JA, Rinehart JJ, Jay M, Leggas M. Nanoparticles Containing Anti-inflammatory Agents as Chemotherapy Adjuvants: Optimization and In Vitro Characterization. The AAPS Journal. 2008 10(1):133-140.

Synthesis and *in vitro* stability of amino acid ester prodrugs of naltrexone and 6-β-naltrexol (in preparation)

In Vitro and *In Vivo* Characterization of a (-)-Cytisine-Naltrexone Codrug (in preparation)

PRESENTATIONS

Elidridge JA, Albayati Z A, Sunkara M, Morris A J, Crooks PA. *In Vitro* and *In Vivo* Characterization of a (-)-Cytisine-Naltrexone Codrug. Poster session presented at: 39th Annual MALTO Medicinal Chemistry-Pharmocognosy Meeting; 2012 May 20-22; ULM College of Pharmacy; Monroe, LA.

Eldridge JA, Milewski M, Stinchcomb AL, Crooks PA. Amino acid ester prodrugs of naltrexone and 6-β-naltrexol as candidates for microneedle-enhanced transdermal delivery. Poster session presented at: American Association of Pharmaceutical Scientists Annual Convention; 2010 Nov 14-18; New Orleans, LA.

Eldridge JA, Milewski M, Stinchcomb AL, Crooks PA. Synthesis of amino acid ester prodrugs of 6-β-naltrexol for microneedle-enhanced transdermal delivery. Poster session presented at: American Association of Pharmaceutical Scientists Annual Convention; 2009 Nov 8-12; Los Angeles, CA.

Eldridge JA, Milewski M, Stinchcomb AL, Crooks PA. Synthesis and hydrolysis studies of a (-)-cytisine-naltrexone carbamate codrug for transdermal drug delivery. Poster session presented at: American Association of Pharmaceutical Scientists Annual Convention; 2008 Nov 16-20; Atlanta, GA.